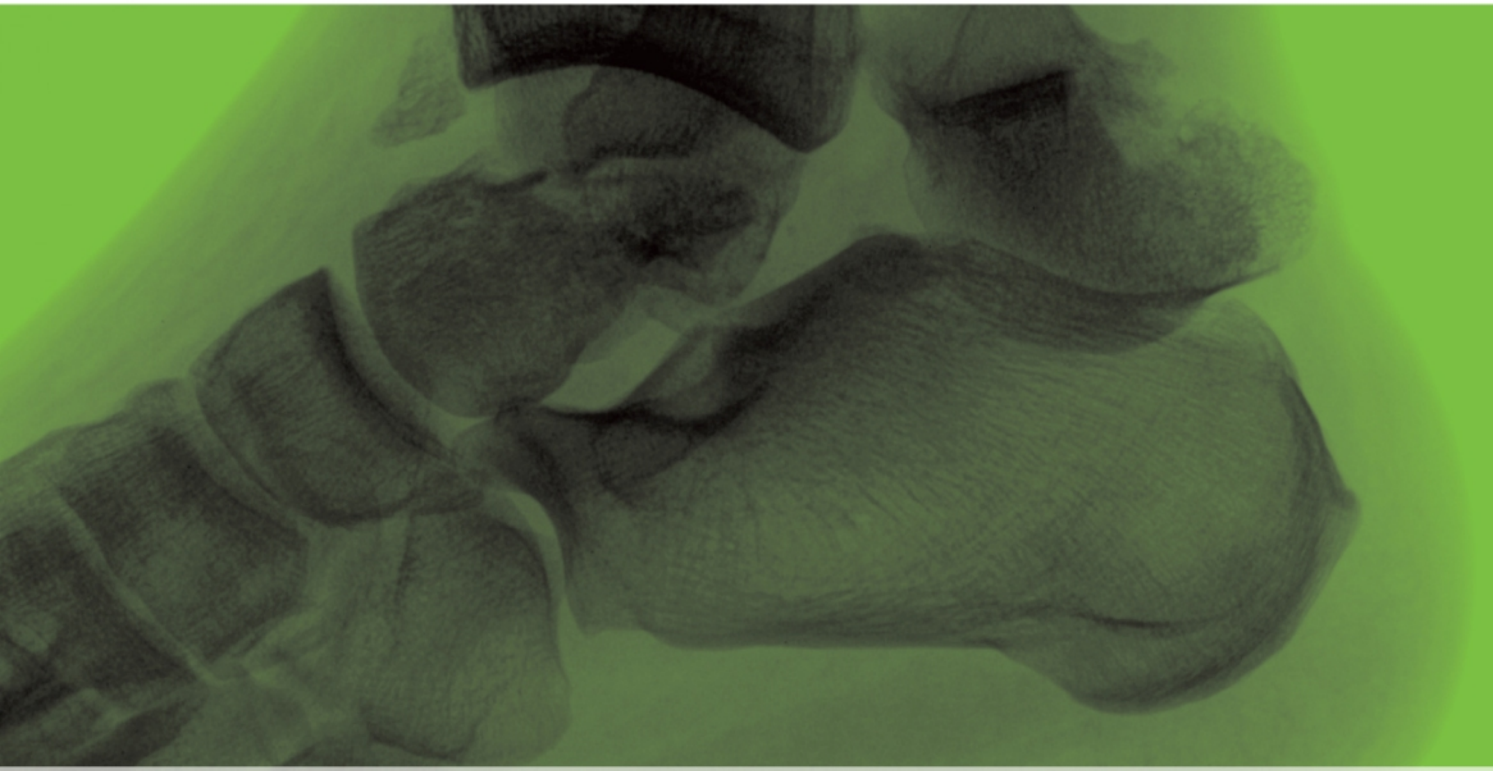
ABC of Emergency Radiology

THIRD EDITION

Edited by Otto Chan



WILEY-BLACKWELL www.abcbookseries.com BMJ|Books

ABC of

Emergency Radiology

Third Edition

ABC series

An outstanding collection of resources for everyone in primary care



The *ABC* series contains a wealth of indispensable resources for GPs, GP registrars, junior doctors, doctors in training and all those in primary care

- **Highly illustrated, informative and a practical source of knowledge**
- **An easy-to-use resource, covering the symptoms, investigations, treatment and management of conditions presenting in day-to-day practice and patient support**
- **Full colour photographs and illustrations aid diagnosis and patient understanding of a condition**

For more information on all books in the *ABC* series, including links to further information, references and links to the latest official guidelines, please visit:

www.abcbookseries.com

WILEY-BLACKWELL

BMJ | Books

ABC of

Emergency Radiology

Third Edition

EDITED BY

Otto Chan

Consultant Radiologist
The London Independent Hospital
London, UK

WILEY-BLACKWELL
A John Wiley & Sons, Ltd., Publication

BMJ Books

This edition first published 2013, © 2013 by Blackwell Publishing Ltd.

Previous editions 1995, 2007

BMJ Books is an imprint of BMJ Publishing Group Limited, used under licence by Blackwell Publishing which was acquired by John Wiley & Sons in February 2007. Blackwell's publishing programme has been merged with Wiley's global Scientific, Technical and Medical business to form Wiley-Blackwell.

Registered office: John Wiley & Sons, Ltd, The Atrium, Southern Gate, Chichester, West Sussex, PO19 8SQ, UK

Editorial offices: 9600 Garsington Road, Oxford, OX4 2DQ, UK
The Atrium, Southern Gate, Chichester, West Sussex, PO19 8SQ, UK
111 River Street, Hoboken, NJ 07030-5774, USA

For details of our global editorial offices, for customer services and for information about how to apply for permission to reuse the copyright material in this book please see our website at www.wiley.com/wiley-blackwell

The right of the author to be identified as the author of this work has been asserted in accordance with the UK Copyright, Designs and Patents Act 1988.

All rights reserved. No part of this publication may be reproduced, stored in a retrieval system, or transmitted, in any form or by any means, electronic, mechanical, photocopying, recording or otherwise, except as permitted by the UK Copyright, Designs and Patents Act 1988, without the prior permission of the publisher.

Designations used by companies to distinguish their products are often claimed as trademarks. All brand names and product names used in this book are trade names, service marks, trademarks or registered trademarks of their respective owners. The publisher is not associated with any product or vendor mentioned in this book. This publication is designed to provide accurate and authoritative information in regard to the subject matter covered. It is sold on the understanding that the publisher is not engaged in rendering professional services. If professional advice or other expert assistance is required, the services of a competent professional should be sought.

The contents of this work are intended to further general scientific research, understanding, and discussion only and are not intended and should not be relied upon as recommending or promoting a specific method, diagnosis, or treatment by physicians for any particular patient. The publisher and the author make no representations or warranties with respect to the accuracy or completeness of the contents of this work and specifically disclaim all warranties, including without limitation any implied warranties of fitness for a particular purpose. In view of ongoing research, equipment modifications, changes in governmental regulations, and the constant flow of information relating to the use of medicines, equipment, and devices, the reader is urged to review and evaluate the information provided in the package insert or instructions for each medicine, equipment, or device for, among other things, any changes in the instructions or indication of usage and for added warnings and precautions. Readers should consult with a specialist where appropriate. The fact that an organization or Website is referred to in this work as a citation and/or a potential source of further information does not mean that the author or the publisher endorses the information the organization or Website may provide or recommendations it may make. Further, readers should be aware that Internet Websites listed in this work may have changed or disappeared between when this work was written and when it is read. No warranty may be created or extended by any promotional statements for this work. Neither the publisher nor the author shall be liable for any damages arising herefrom.

Library of Congress Cataloging-in-Publication Data

ABC of emergency radiology. – 3rd ed. / edited by Otto Chan.
p. ; cm.
Includes bibliographical references and index.
ISBN 978-0-470-67093-4 (pbk. : alk. paper)
I. Chan, Otto.
[DNLM: 1. Radiography. 2. Emergencies. WN 200]
616.07′572–dc23
2012032717

A catalogue record for this book is available from the British Library.

Wiley also publishes its books in a variety of electronic formats. Some content that appears in print may not be available in electronic books.

Cover images: Courtesy of the editor
Cover design by Meaden Creative

Set in 9.25/12 Minion by Laserwords Private Limited, Chennai, India

1 2013

I would like to dedicate this book to my family, my parents, my brother Bob, my sisters Ana and Diana, my children Natalie, Oliver, Sophie, Julia, Marina, Charlie and George, my grandchildren Ella, Leo and Amber-Lily and to my loving wife Zaide.

Contents

Contributors, ix

Preface, xi

1 Introduction: ABCs and Rules of Two, 1
Otto Chan

2 Hand and Wrist, 11
Joe Coyle, Ali Naraghi and Otto Chan

3 Elbow, 22
Muaaze Ahmad

4 Shoulder, 30
Ahmed Daghir and James Teh

5 Pelvis and Hip, 38
Syed Babar, James A. S. Young, Jeremy W. R. Young and Otto Chan

6 Knee, 49
Lisa Meacock and David A. Elias

7 Ankle and Foot, 59
Tudor Hughes

8 Head, 71
Suki Thomson and Amrish Mehta

9 Face, 85
Simon Holmes, Ravikiran Pawar, Jimmy Makdissi and Otto Chan

10 Cervical Spine, 93
Leonard J. King

11 Thoracic and Lumbar Spine, 104
Leonard J. King, Andreas Koureas and Otto Chan

12 Chest, 111
Arjun Nair and Ioannis Vlahos

13 Abdomen, 123
Katie Planche and Niall Power

14 Computed Tomography in Emergency Radiology, 135
Anmol Malhotra and Jeremy Rabouhans

15 Emergency Ultrasound, 152
Tim Fotheringham, Otto Chan and Ian Renfrew

16 Emergency Paediatric Radiology, 159
R. J. Paul Smith, Rosy Jalan and Marina J. Easty

17 Major Trauma, 171
Dominic Barron, Sujit Vaidya and Otto Chan

Index, 177

Contributors

Muaaze Ahmad
Consultant Musculoskeletal Radiologist, Barts Health NHS Trust, The Royal London Hospital, London, UK

Syed Babar
Consultant Radiologist and Honorary Senior Lecturer, Hammersmith & Charing Cross Hospitals, Imperial College, London, UK

Dominic Barron
Consultant Musculoskeletal and Trauma Radiologist, Leeds Teaching Hospitals, Leeds, UK

Otto Chan
Consultant Radiologist, The London Independent Hospital, London, UK

Joe Coyle
Fellow, Joint Department of Medical Imaging, University of Toronto, Toronto, ON, Canada

Ahmed Daghir
Clinical Fellow in Musculoskeletal Radiology, Oxford University Hospitals NHS Trust, Nuffield Orthopaedic Centre, Oxford, UK

Marina J. Easty
Consultant Radiologist, Great Ormond Street Hospital, London, UK

David A. Elias
Consultant Radiologist, King's College Hospital, London, UK

Tim Fotheringham
Consultant Interventional Radiologist, Barts Health NHS Trust, The Royal London Hospital, London, UK

Simon Holmes
Consultant Oral and Maxillofacial Surgeon, Bart's Health NHS Trust, London, UK

Tudor Hughes
Associate Professor of Clinical Radiology, Department of Radiology, University of California, San Diego, CA, USA

Rosy Jalan
Consultant Musculoskeletal Radiologist, Barts Health NHS Trust, The Royal London Hospital, London, UK

Leonard J. King
Consultant Musculoskeletal Radiologist, Southampton University Hospitals, Southampton, UK

Andreas Koureas
Associate Professor of Radiology, University of Athens, Athens, Greece

Jimmy Makdissi
Senior Lecturer/ Honorary Consultant, Barts Health NHS Trust, Institute of Dentistry, The London Hospital School of Medicine and Dentistry, London, UK

Anmol Malhotra
Consultant Radiologist, Radiology Department, Royal Free London NHS Foundation Trust, London, UK

Lisa Meacock
Consultant Radiologist, King's College Hospital, London, UK

Amrish Mehta
Honorary Senior Lecturer in Neuroradiology, Imperial College London, London, UK

Arjun Nair
Specialist Registrar, Radiology, St Georges Hospital, London, UK

Ali Naraghi
Staff Radiologist, Joint Department of Medical Imaging, University of Toronto, Toronto, ON, Canada

Ravikiran Pawar
Clinical Lecturer in Dental and Maxillofacial Radiology, Barts Health NHS Trust, The London Hospital School of Medicine and Dentistry, London, UK

Katie Planche
Consultant Radiologist, Royal Free London NHS Foundation Trust, London, UK

Niall Power
Consultant Radiologist, Upper GI Cancer, Royal Free London NHS Foundation Trust, London, UK

Jeremy Rabouhans
Consultant Radiologist (Locum), Royal Free London NHS Foundation Trust, London, UK

Ian Renfrew
Consultant Interventional Radiologist, Barts Health NHS Trust, The Royal London Hospital, London, UK

R.J. Paul Smith
Radiology Specialist Registrar, Barts Health NHS Trust, The Royal London Hospital, London, UK

James Teh
Consultant Radiologist, Oxford University Hospitals NHS Trust, Nuffield Orthopaedic Centre, Oxford, UK

Suki Thomson
Clinical Fellow in Neuroradiology, Lysholm Department of Radiology, National Hospital for Neurology and Neurosurgery, London, UK

Sujit Vaidya
Consultant Musculoskeletal Radiologist, Barts Health NHS Trust, The Royal London Hospital, London, UK

Ioannis Vlahos
Honorary Senior Lecturer, St George's, University of London, London, UK

James A.S. Young
Specialist Registrar in Trauma & Orthopaedics, St. Georges Hospital, London, UK

Jeremy W.R. Young
The Regional Medical Center, Orangeburg, SC, USA

Preface

Emergency medicine is under scrutiny as never before, with daily newspaper reports highlighting the inadequacies for the provision of a 24/7 medical service. Reduced 'out-of-hours' survival rates for virtually all forms of acute medicine – not least trauma, strokes and heart attacks – have led to a rethink in strategy for emergency care in the UK.

Specific recommendations to address recognized deficiencies such as reorganisation of trauma care into regional systems has been shown to improve outcome and this relies on optimising all aspects of pre-hospital and hospital care and using a multidisciplinary approach to optimise patient care in polytrauma.

There have been dramatic technological advances in the past decade in diagnostic radiology that are central to the provision of a 24/7 service, in particular digital radiography (DR), picture archiving and communication systems (PACS), portable ultrasound (US), interventional radiology, magnetic resonance imaging (MRI) and multidetector computed tomography (MDCT).

Rapid acquisition and interpretation of DR, portable US and immediate availability of MDCT are now the mainstay of initial successful management of sick and traumatised patients admitted to Accident and Emergency departments (A&E).

Virtually any condition can present to A&E and so the volume of medical knowledge needed to manage these patients satisfactorily is enormous. Despite the reorganisation of acute medical services, unfortunately these patients are still initially seen and often treated by relatively inexperienced staff, most if not all with little or no training in radiology, in particular the interpretation of DR and CT. Although safety nets exist – in particular now that PACS is widely available in the UK – specialist radiological advice is still often not available at the time of presentation, when it is most needed.

Therefore, it is essential that all staff should be able to interpret DR and basic CT for fast, accurate and effective initial treatment, in order to avoid errors in interpretation, inappropriate treatment and the medicolegal consequences that may result from these errors.

This new edition of the *ABC of Emergency Radiology* has incorporated the latest technological advances (in particular replacing plain radiographs with digital radiographs) and changes in imaging protocols (in particular the use of MDCT).

Myself and the contributors have produced a simple and logical step-by-step approach on how to interpret DR and basic CT. The book is divided into anatomical chapters, followed by chapters in US, CT, paediatrics and major trauma. Each chapter starts with radiological anatomy, then recommended standard views, then a systematic approach to basic interpretation followed by a review of common abnormalities and finally a summary chart.

This book provides an up-to-date, simple, concise and systematic approach to the interpretation of DR and CT that should be very helpful to medical students, young trainee doctors, consultants in all specialties including radiologists and other health professionals working in A&E, not least radiographers and nurses.

Otto Chan

CHAPTER 1

Introduction: ABCs and Rules of Two

Otto Chan

The London Independent Hospital, London, UK

OVERVIEW

- Request the correct investigation
- Use a systematic approach to interpretation – ABCs
- Fundamental principles to avoid errors – Rules of two
- Always ASK for help – if in doubt!

Emergency medicine often brings together critically ill patients and inexperienced and tired doctors – a dangerous combination at the best of times with potentially serious clinical and medicolegal consequences. Virtually any medical condition can present in the emergency department (ED) and so the volume of medical knowledge needed to manage these patients satisfactorily is enormous.

There have been major technological advances in the past decade which have had a major impact on the management of patients in the ED, not least picture archiving and communication systems (PACS), digital radiography (replacing conventional plain to X rays), portable ultrasound (US; which is now readily available and often, but not often enough, performed by clinicians in the ED) and multidetector computed tomography (MDCT) in the ED. Despite all these advances, plain to X rays (whether conventional or digital) remain the mainstay of initial and successful management of most sick and traumatised patients in the ED.

Radiological investigations

- Plain to X rays (conventional or digital)
- Portable US
- MDCT
- MRI

The correct selection of imaging modality, rapid acquisition and the accurate interpretation of these investigations is often the key to quick and successful management of patients in the ED. Unfortunately these investigations are often done and interpreted by medical staff who have little, if any, training in radiology and the usual safety net of a specialist radiological service is not available at the time of presentation, when it is most needed. This leads to delays and invariably results in increased morbidity and mortality! The selection of the correct imaging modality on admission saves time and saving time, saves lives! Ideally there should be a seamless 24/7 service.

MDCT – initial imaging modality of choice in the ED

Head injuries/headaches or epilepsy	Skull X-ray (SXR) no longer done. CT head ± contrast
Facial injuries	MDCT with multiplanar reconstructions (MPR) and 3D are essential
Chest pain (suspected aortic aneurysm (AA), myocardial infarction (MI), pulmonary embolus (PE) or pneumothorax (Px))	Triple rule out CT scan
Severe abdominal pain (obstruction)	CT has replaced abdominal X-ray (AXR)
Renal/ureteric colic	CT kidneys, ureters and bladder (KUB) has replaced Intravenous urogram (IVU) in ED
Suspected leaking abdominal aortic aneurysm (AAA)	CT has replaced US and AXR
Suspected gastrointestinal (GI) bleeding	Initially CT angiography instead of angiography
Major trauma (adults)	Whole body CT instead of chest X-ray (CXR), AXR and US

The Rules of Two (Ro2) is a helpful, simple set of guidelines, which relate to who, what, when and how to radiograph and how to get help or get out of trouble and therefore minimise the chances and the consequences of errors.

The ABCs systematic assessment is a simple systematic approach, which starts with basic essential normal radiographic anatomy, common normal variants, which may mimic pathology and in

ABC of Emergency Radiology, Third Edition. Edited by Otto Chan.
© 2013 John Wiley & Sons, Ltd. Published 2013 by John Wiley & Sons, Ltd.

particular how to interpret imaging using a systematic approach, which is logical and easy to remember and therefore hopefully helps to minimise interpretive errors.

Rules of Two

These rules represent a simple set of guidelines, most are obvious, some relate to specific clinical problems, but most are common sense useful general principles which should help in avoiding errors in interpretation and management of patients in the ED.

Rules of Twos

- Two views – one view is always one view too few
- Two abnormalities – if you see one abnormality, always look for a second
- Two joints – image the joint above
- Two sides – if not sure or difficult X ray, compare with other side
- Two views too many – CT (and rarely US) has replaced plain X rays in many clinical situations
- Two occasions – always compare with old films IF available
- Two visits – bring patient back for repeat examination
- Two opinions and two records – always ask a colleague if not sure and record findings
- Two specialists – always get your ED specialist and also a radiologist's opinion
- Two investigations – always consider whether US, CT or MRI would help in diagnosis

Rule 1 – two views ('One view is always one view too few')

Two views should be taken, preferably perpendicular to each other (Figure 1.1). This applies to all radiographs except the chest, abdomen and pelvis. It is not uncommon for a fracture or an abnormality to be visible only on one view (Figure 1.2).



(a) (b)

Figure 1.2 (a) Anteroposterior shows no obvious abnormality; (b) lateral shows oblique fracture of fibula.



(a) (b)

Figure 1.1 (a) Anteroposterior shows minimal overlap of proximal interphalangeal joint (PIPJ) of little finger; (b) lateral shows obvious dislocation of PIPJ.



Figure 1.3 Lateral elbow: anterior (arrow) and posterior fat pads (arrowhead). Anteroposterior view was normal so additional views of radial head were requested.

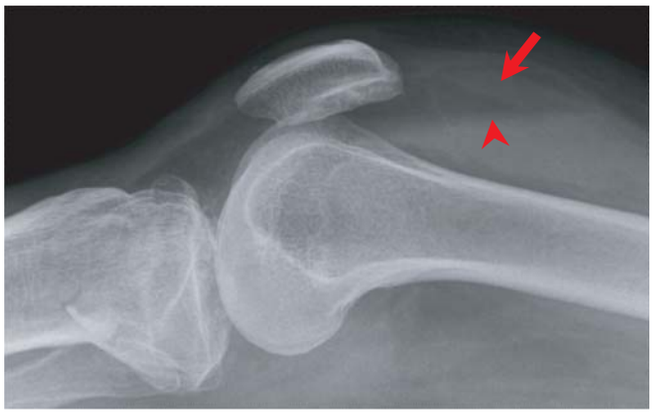


Figure 1.4 Lateral horizontal beam: lipohaemoarthrosis fat above (arrow); blood below (arrowhead).

In addition, if the two views fail to show an injury when there is a radiological suspicion of an injury (such as the presence of a fat pad sign (Figure 1.3) in the elbow or a lipohaemoarthrosis (Figure 1.4) of the knee or if the findings don't fit in with the clinical presentation, then further views are warranted.

Rule 2 – two abnormalities

Do not stop looking after detecting one abnormality; always keep looking for a second abnormality. There may be more than one fracture (Figure 1.5) or there may be an underlying predisposing abnormality, such as metastases (Figure 1.6). In addition, if there is a fracture in a ring-like structure such as the pelvis (Figure 1.7),



Figure 1.5 Salter–Harris II of proximal tibia (large arrow for fracture of proximal tibial metaphysis, arrowhead for separation of epiphyseal growth plate) and fracture of shaft of proximal fibula (small arrow).

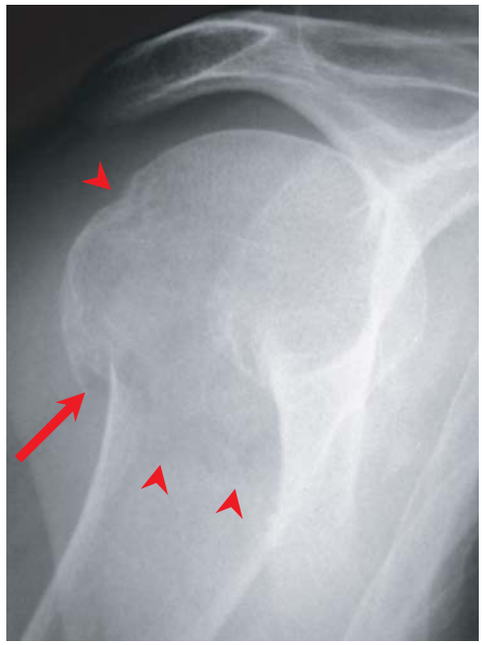


Figure 1.6 Fracture of proximal humerus (arrow) with subtle lytic metastases (arrowheads).

mandible (Figure 1.8), radius/ulna or tibia/fibula, there will usually be a second fracture (a polo mint will always break in two places; see Figure 1.9).

Rule 3 – two joints

In the forearm (Figure 1.10) and in the lower leg (Figure 1.11), always image the joint above and below the injury.

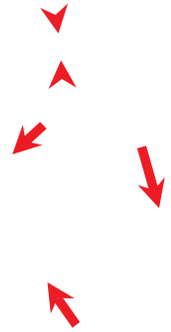
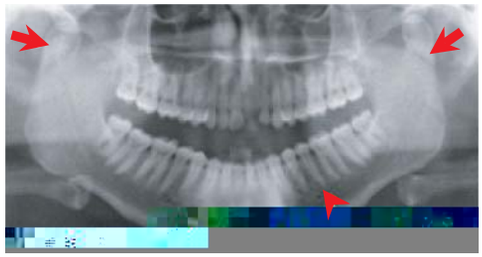


Figure 1.7 Numerous pelvic fractures (arrows), several in each ring with subtle right sacral foramina fractures (arrowheads – compare with intact left side).



(a)



(b)

Figure 1.8 (a) Left mandibular fracture with bilateral displaced condylar neck fractures, better seen on CT (b).

(a) (b)

Figure 1.9 (a) Intact Polo mint and (b) broken mint shows there are at least two fractures in a ring.



Figure 1.10 Monteggia fracture-dislocation: fractured proximal ulnar shaft (arrow) with dislocated radial head (arrowhead).



(a)



(b)

Figure 1.11 Maisonneuve fracture: (a) right ankle anteroposterior shows minimal widening of the medial joint margin (arrow); (b) this is associated with a proximal fibula fracture (arrow).

Rule 4 – two sides

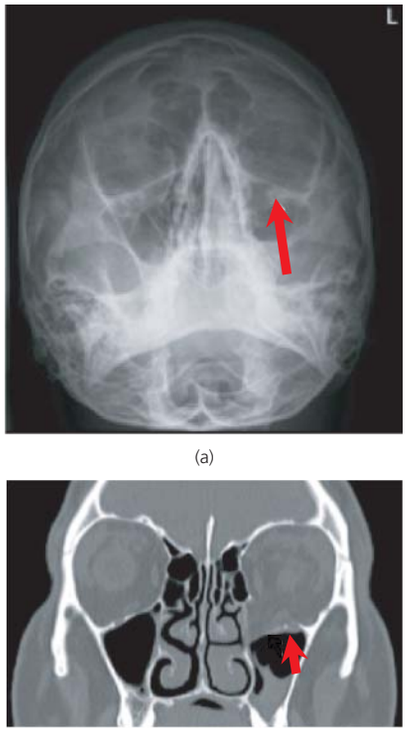
There are certain circumstances, where it is difficult to ascertain whether something is normal (Figures 1.12 and 1.13), or abnormal (Figures 1.14–1.16), in particular in children and on these occasions it is worth imaging the asymptomatic side for comparison.

Rule 5 – two views too many

The advent of MDCT and the siting of MDCT scanners in the ED, has made MDCT the INITIAL imaging modality of choice in many



Figure 1.16 Completely displaced avulsion of left medial epicondyle ossification centre (arrow).



(a)

(b)

Figure 1.18 (a) OM view with left tear drop – classic blow-out fracture; (b) Cor CT shows orbital floor fracture with inferior rectus muscle displaced.

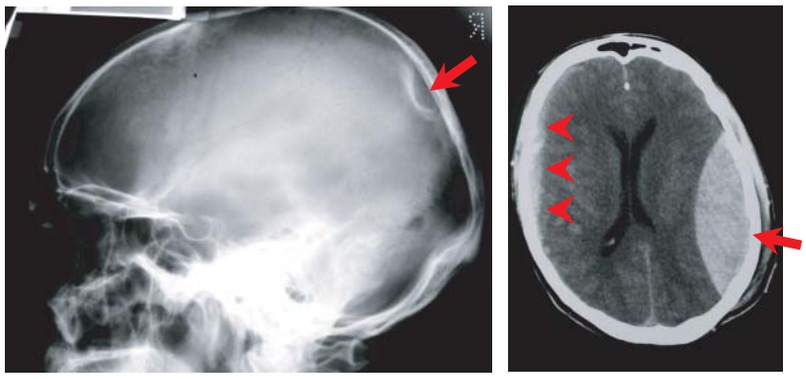
who clearly needs an immediate open thorocotomy and instead the clinical team request a multiple X-rays! The other extreme is when a patient has an open bleeding wound, which just needs dressings and compression initially and instead the clinical team request plain X-rays to look for a fracture! Sadly, both of these examples occur commonly!

Rule 6 – two occasions

ALWAYS look for old films for comparison, in particular if there is an abnormality. Old films are the cheapest and best investigation, in particular CXRs (Figure 1.19). Similarly, if there is a bony abnormality, an old film will not only confirm whether this is an old or new finding, but also the speed of change will help in the diagnosis (Figure 1.20).

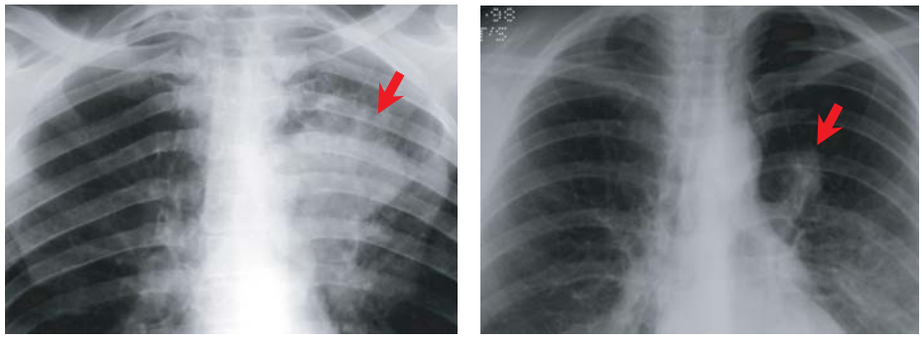
Rule 7 – two visits

ALWAYS repeat the X ray after a patient has undergone an intervention, in particular after insertion of a line or tube (central lines, endotracheal (ET) tubes, chest drains, etc.), reduction of a dislocation, putting a plaster of Paris (POP) (Figure 1.21) or cast or removal of a foreign body (FB).



(a) (b)

Figure 1.17 (a) Depressed fracture seen on SXR (arrow); (b) Large left extradural haematoma (arrow) and subtle right subdural collection (arrowhead) and numerous right intraparenchymal contusions seen on CT.



(a) (b)

Figure 1.19 (a) CXR showing large left hilar mass. (b) CXR one year earlier shows much smaller mass, so a confident diagnosis of a primary bronchogenic carcinoma can be made with old CXR available.



(a) (b) (c)

Figure 1.20 (b) Initial film showed loss of joint space a large erosion (arrow) and a huge amount of soft tissue swelling, which was not present on X ray taken (arrow) 1 week earlier (a) or after treatment 1 month later (c). Confident diagnosis of a septic arthritis was made with old film available showing rapid progression.

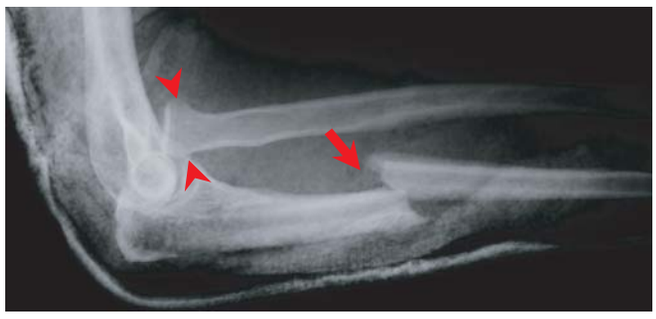
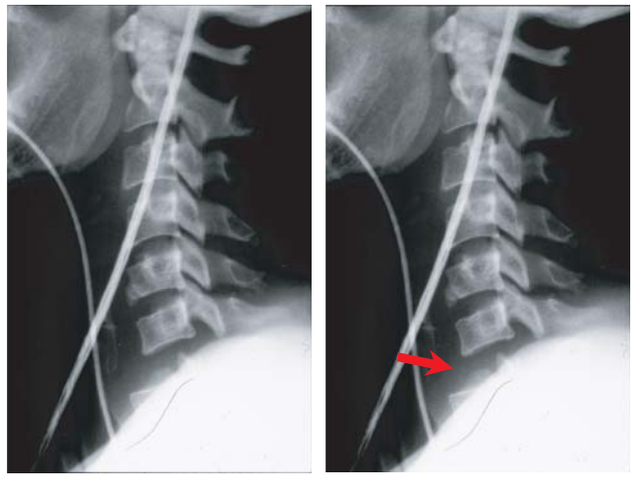


Figure 1.21 Patient with fractured ulna (arrow) put in plaster of Paris, but follow-up check X-ray reveals a dislocated radial head (arrowhead) – a Monteggia fracture dislocation.



(a) (b)

Figure 1.22 (a) Lateral CS reported normal initially! (b) Lat CS clearly shows a hugely displaced C6 on C7 with marked separation.

Rule 8 – two opinions and two records

If you are not sure, get a second opinion from a colleague or the radiographers (who are extremely knowledgeable). The red dot system is a form of a second opinion.

There are particular X-rays which are more challenging (children with unfused epiphyses and AXRs) or where missing an abnormality may have serious consequences (cervical spine X-rays (Figure 1.22) and suspected non-accidental injury (NAI) (Figure 1.23)). Under these circumstances, you should ALWAYS get a second opinion and record both your interpretations, both in the notes and also in the radiology information system (RIS). If at a later date, a major abnormality has been missed or overlooked, it means that you

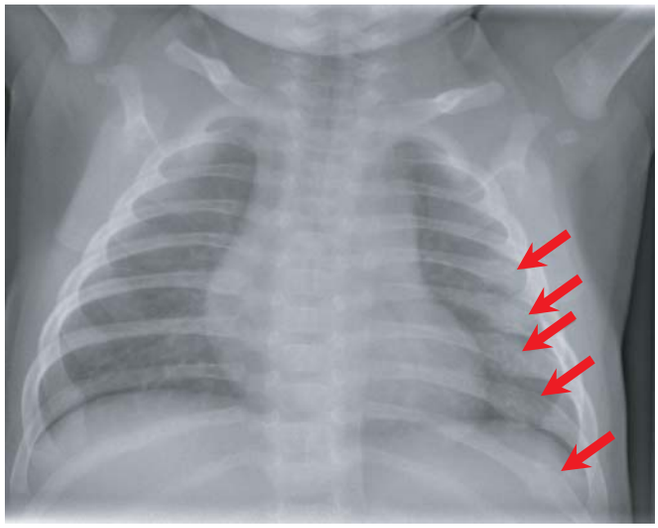


Figure 1.23 CXR thought initially to be 'normal'; review shows clearly at least 5 left rib fractures consistent with NAI – referred immediately to paediatricians as suspected NAI.

can share the blame! The mere fact that you sought out a second opinion and recorded it, shows common sense and insight (even if it's not the case!).

Rule 9 – two specialists

The report and the X-rays should be checked (Figure 1.23) both by your seniors (first specialist) and also a formal report should ALWAYS be sought from the radiologists (second specialist). If two specialists have missed the abnormality, the likelihood of the case of ending up in court in the UK is virtually zero!

Rule 10 – two investigations

There are times when the initial X-ray has helped to exclude an obvious abnormality, but the history or clinical findings warrant further investigations (Figure 1.24). These investigations should be done as soon as possible but often are done the following day on a routine list. The problem is that delaying these investigations often leads to the investigation not being done or the team that looks after the patient forgetting about it!

Patients with head injuries and with suspected facial injuries often have a CT scan of the head but the facial injuries are not scanned at the time. Similarly, major trauma patients often have multiple intra-articular fractures detected on the plain X-rays and then have whole body CT, but the intra-articular fractures are not included in the CT scanning protocol. In both these groups of patients, the patient has to be brought back to the CT room. This is clearly not efficient use of CT and it is dangerous to move the 'stable' polytraumatised patient!

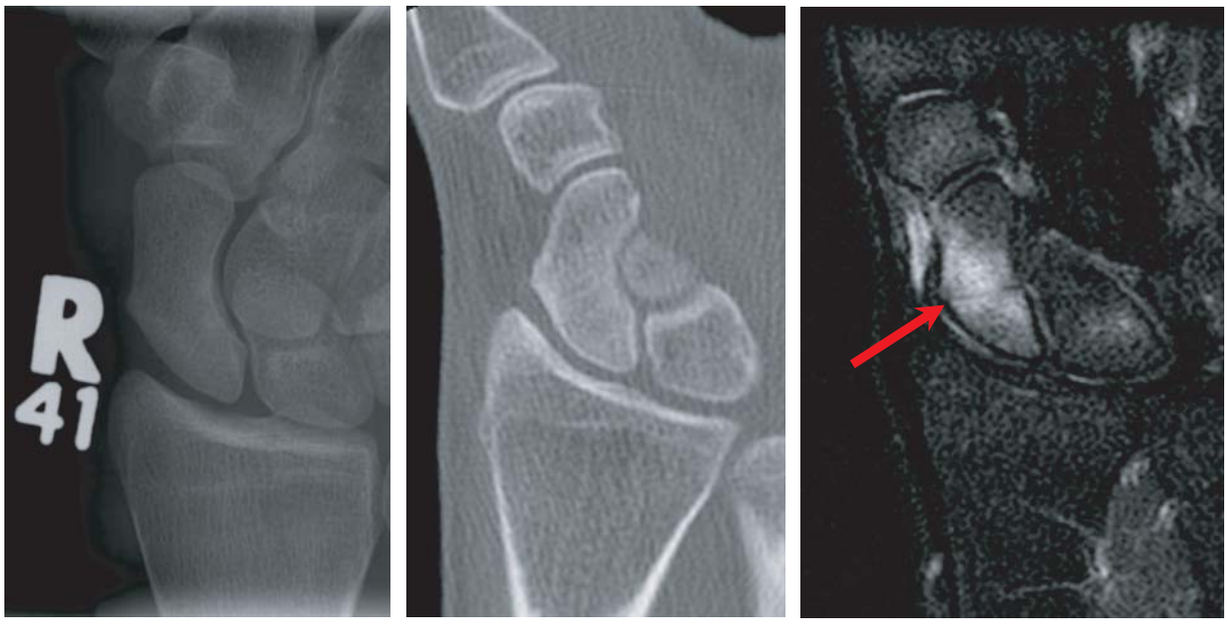
ABCs systematic assessment

The ABCs systematic approach is without doubt the simplest and worldwide the most popular and widely used system for the assessment of plain X-rays. However, in the context of patients in the ED, the ABCs systematic approach is equally effective for the interpretation and assessment of whole body CT and seamlessly incorporates an advanced trauma life support (ATLS) approach in trauma.

Its as simple as ABC!

Anatomy

The ABCs starts in ALL the chapters with a short section on 'basic' radiological anatomy, which is the 'bread and butter' of radiology!



(a) (b) (c)

Figure 1.24 (a) Initial X ray reported normal, but patient symptomatic, so (b) CT performed which was also normal and (c) an MRI was then performed confirming fracture though the waist of the scaphoid.

The images are colour coded, so that ALL "normal" anatomy diagrams, lines and annotations are shown in white or shades of blue.

> Know your anatomy and you know radiology!

Adequacy

Anatomy is followed in ALL the chapters by adequacy. Under adequacy, we have included the imaging investigation of choice and either basic knowledge necessary to understand the modality and the 'standard views' and also the other views available.

Peripheral and axial skeleton

The ABCs for the bony skeleton are the same, although from an interpretive point of view, the order should be changed so that soft tissues are looked at first in the elbow (looking for the displaced fat pad sign) and the knee (looking for fat-fluid levels indicating a lipohaemoarthosis). Both these signs are easy to detect and immediately alert the clinician to the presence of a probable fracture.

Alignment

- Exclude subluxations and dislocations

Bone

- Follow the bony contour very carefully and exclude a fracture
- Check for disruption of the trabecular pattern, linear sclerosis or lucency indicating a fracture

Cartilage and joints

- Check for even joint spaces and uneven loss of joint width

Soft tissues

- Bright light X-rays or change 'window setting and contrast on The PACS system
- Look for FBs

Head CT scan

Airspaces

- Sphenoid sinus – look for fluid level
- Frontal sinus/mastoids/middle ear – look for fracture or infection
- Pneumocephalus – look for sinus or vault fracture

Bones

- Look on bone windows and thin sections
- Look carefully over areas with soft tissue swelling

Brain parenchyma

- Look for low density lesions
- Look for high density lesions
- Blood density and implications
- Look for signs of brain swelling

CSF spaces

- Look for blood
- Look for mass effect
- Look for hydrocephalus

Dura

- Look for subdural and extradural collections

Eyes

- Globe injuries
- Optic nerve injuries
- Fractures
- Extraconal spaces

Face

- Fractures
- Foreign body

Survey (review areas)

- Scout
- Symmetry
- SAH
- Subtle
- Skull vault

Face

Alignment

- Check Dolan's, McGrigor's and Campbell's lines

Bones

- Check all bones in the mid face and upper and lower third of the face.

Cartilage and joints

- Check the ZF sutures and TMJs

Sinuses and soft tissues

- Check for local swelling of the soft tissue
- Surgical/orbital emphysema
- Air-fluid levels and opaque sinuses
- Teardrop injuries
- FBs such as glass and metal

Chest – CXR

Airways

- Check endotracheal tube (ETT)
- Exclude FB in airway
- Position of trachea

All lines

- ETT position
- Nasogastric (NG) tube position
- Venous catheters
- Chest drains

Breathing

- Check lungs are clear

Circulation

- Cardiac silhouette size
- Mediastinal position and contour
- Widening of mediastinum
- Hila: evaluate size, shape, and position

Diaphragm

- Position
- Below the diaphragm

Edges (pleura)

- Pneumothorax
- Effusion
- Empyema

Skeleton

- Fractures
- Paraspinal lines
- Spine

Soft tissues

- FB
- Emphysema
- Swelling/asymmetry

Abdomen

Air

- Exclude free intraperitoneal or abnormally sited air

Bowel gas

- Check size, distribution and pattern

Calcification

- Check for normal and abnormal calcification

Densities

- Check for inserted or ingested foreign bodies

Edges

- Check the hernial orifices
- Check the lung bases and pleural spaces

Fat planes

- Check presence and symmetry of psoas shadows
- Check presence of perivesical fat plane
- Check that properitoneal fat planes are present

Soft tissues

- Check for enlarged or absent organs. Confirm with US

Skeleton

- In trauma, check that there are no obvious fractures
- If malignancy is suspected, exclude bony metastases

Further reading

Krishnam MS, *Curtis J (eds)*. *Emergency Radiology*. Cambridge University Press, 2009.

Marincek B, Dondelinger RF (eds). *Emergency Radiology: Imaging and Intervention*. Springer, 2006.

Mirvis SE, Shanmuganathan K, Miller LA. *Emergency Radiology: Case Review*. Mosby, 2009.

Raby N, Berman L, De Lacey G. *Accident and Emergency Radiology: A Survival Guide*, 2nd edn. Saunders, 2005.

Rogers LF. *Radiology of Skeletal Trauma*. Churchill Livingstone, 2001.

CHAPTER 2

Hand and Wrist

Joe Coyle[1], *Ali Naraghi*[1] *and Otto Chan*[2]

[1]University of Toronto, Toronto, ON, Canada
[2]The London Independent Hospital, London, UK

OVERVIEW

- Hands and wrist fractures account for 20% of acute fractures
- Age alone can accurately predict most injuries
- Plain radiographs remain the mainstay of imaging
- MRI (and CT) are developing increasing roles
- Aim is to restore function and avoid chronic disability

Injuries to the hand and wrist are very common, accounting for 20% of acute fractures presenting to emergency departments. The hand is the most active part of the body, is the least well protected and thus is often injured.

Most injuries to the wrist occur following a fall onto an outstretched hand (FOOSH). Mechanism of injury in these patients can accurately predict injury pattern. Age alone also can accurately predict likely fracture pattern (Table 2.1).

Clinical exam is usually accurate in this scenario and strong clinical suspicion for fracture can often direct close radiologic evaluation for subtle abnormalities.

The goal of treatment is rapid restoration of function with attention given to the prevention of chronic disability. Plain radiographs are the mainstay of imaging. Computed tomography (CT) and magnetic resonance imaging (MRI) are developing increasing roles, particularly as their availability increases.

Anatomy

Hand

Each ray, apart from the thumb, consists of a metacarpal and proximal, middle and distal phalanges. The thumb has a metacarpal and proximal and distal phalanges. At each metacarpophalangeal (MCP) joint and interphalangeal (IP) joint, lateral stability is provided by the collateral ligaments. The joint capsule at the MCP and IP joints also demonstrate on the volar aspect areas of dense fibrous thickening, known as the volar plate, which provide further strength. Each finger has two flexor tendons on the volar (palmar) surface and an extensor tendon complex on the dorsal surface.

Table 2.1 Age as a predictor of distal radial fractures following FOOSH.

Age	Fracture pattern
<10	Transverse metaphyseal (often incomplete)
10–16	Epiphyseal plate (Salter–Harris type injury)
17–40	Scaphoid and triquetral fractures
>40	Transverse distal radial fractures

Wrist

The wrist (Figure 2.1a–c, e and f) consists of eight carpal bones arranged in two rows. The proximal row (scaphoid, lunate, triquetrum and pisiform) articulates wth the radius and ulna and the distal row (trapezium, trapezoid, capitate and hamate) articulates with the bases of the metacarpals. The distal row is more rigid and stable than the proximal. These bones are held together by a complex arrangement of strong ligaments. The radiocarpal joint has a 4–15° volar tilt and the hand is usually held in slight flexion and ulnar deviation. The radial styloid is distal to the ulnar styloid. Radial inclination to the ulna is assessed on the PA view and should be 20–25°.

In children the carpal bones first appear at the age of 3 months and all of the carpal bones are visible by 12 years. The age of a child can be estimated by counting the number of epiphyses minus one (see Chapter 16).

ABCs systematic assessment

- **A**dequacy – check correct views have been obtained
- **A**lignment – check the relationship of the individual bones to each other
- **B**one – trace the contours of all the bones
- **C**artilage and joints – joint spaces should be uniform in width
- **S**oft tissues – change windows to look for soft tissue swelling and foreign bodies (FBs)

Recommended radiological views

- Hands – anteroposterior (AP), lateral or oblique
- Fingers – AP, lateral or oblique
- Wrist – AP, lateral ± oblique
- Scaphoid – coned scaphoid series (× 4)

ABC of Emergency Radiology, Third Edition. Edited by Otto Chan.
© 2013 John Wiley & Sons, Ltd. Published 2013 by John Wiley & Sons, Ltd.

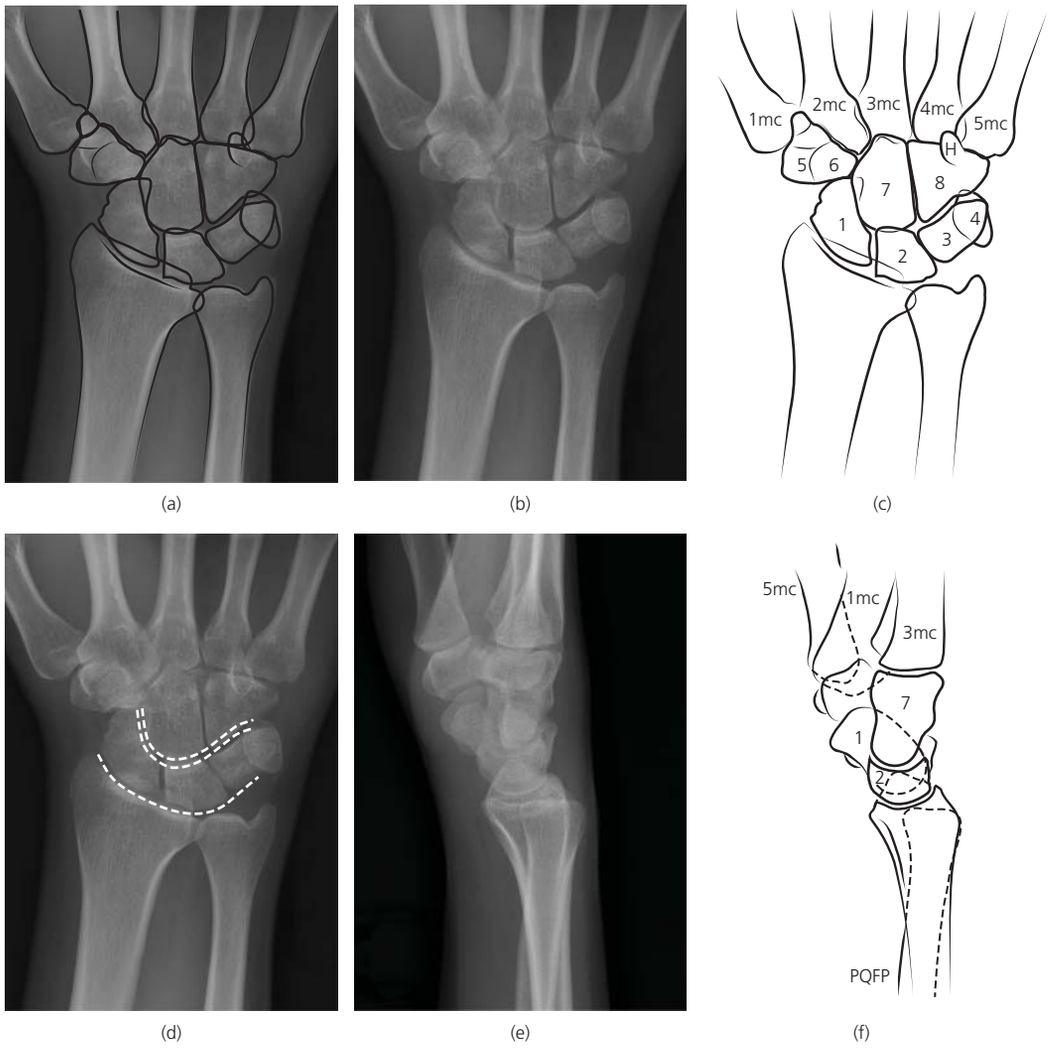


Figure 2.1 (a) Normal AP view with line drawing; (b) normal AP view; (c) AP view of right wrist: scaphoid (1), lunate (2), triquetrum (3), pisiform (4), trapezium (5), trapezoid (6), capitate (7), hamate (8), hook of hamate (H), metacarpal (mc); (d) Gilula's three carpal arcs; (e) normal lateral view; (f) line drawing lateral view.

Adequacy

The clinical findings should guide the radiologic views to be obtained. At least two views are mandatory and additional views may be necessary for specific injuries, such as scaphoid injuries, where coned views with an AP, lateral, oblique and a dedicated scaphoid view are indicated. MRI and CT are becoming increasingly available and are being used even in the acute setting.

Hand

AP, lateral and oblique views are recommended for finger and hand injuries.

On the lateral views the fingers should be flexed to varying degrees to avoid overlap and confusing composite shadows.

Wrist

In general a minimum of posteroanterior (PA) and lateral views are recommended, but in addition some centres advocate external oblique views whereby the radial side of the wrist is elevated. If a scaphoid fracture is suspected, a PA view with ulnar deviation and also a dedicated scaphoid view with 20–30° of tube angulation are recommended in addition to a lateral and an oblique view (Figure 2.2).

On a true lateral wrist view, the palmar surface of the pisiform bone should overly between the palmar surfaces of the distal scaphoid pole and the capitate head.

CT is typically reserved for suspected fractures with negative initial and follow-up radiographs or for preoperative planning in cases with significant comminution and intra-articular extension. MRI is rarely indicated acutely, although some centres are doing MRIs on patient's with anatomical snuff box tenderness who have normal plain X rays (XRs) to exclude scaphoid fractures.

Alignment

In alignment we look at bones and their relationship to each other.



Figure 2.2 Scaphoid coned PA view in ulnar deviation allows for visualisation of the full length of the scaphoid.



Figure 2.3 Normal lateral view of the wrist outlining the normal relationship of the lunate and capitate bones and normal anatomy.

Hand

Bony surfaces should be congruent along each ray from the metacarpals to distal phalanges. Alignment should always be assessed on at least two views. On AP views, overlap of joint margins may be the only indication of subluxation/dislocation. The carpometacarpal articulations in particular, where some degree of overlap is unavoidable, should be carefully scrutinised. Dislocations here may be overlooked.

Wrist – AP view (see Figure 2.1a)

The intercarpal joint spaces should be uniform and <2 mm wide. Widening following injury, seen most commonly at the scapholunate articulation resulting in the Terry Thomas or Madonna sign, may be indicative of joint dissociation and ligamentous injury. The proximal and distal carpal rows form three arcs (Gilula's three carpal arcs). Arc 1 outlines the proximal surface of the scaphoid, lunate and triquetrium. Arc 2 outlines the distal surface of these same bones. Arc 3 outlines the proximal surface of the capitate and hamate bones. Disruption of one of these arcs suggests pathology at that site (Figure 2.1c).

The lunate should have a square (quadrilangular) shape. A 'pie-shaped' (triangular) lunate indicates a perilunate or lunate dislocation.

Wrist – lateral view (Figure 2.3)

This can be daunting as there is significant overlap of many of the carpal bones! It is crucial to assess the alignment of the distal radius, lunate, capitate and 3rd metacarpal. The lunate is moon shaped (lunar = moon) and lies on its back on the distal radius (saucer on table). The proximal pole of the capitate sits into the concave distal surface of the lunate (cup in the saucer) and the third metacarpal should line up with the distal pole of the capitate. Interruption of this alignment is usually secondary to a perilunate or lunate dislocation (and should result in careful assessment for associated carpal and distal radial fractures).

Bone

Trace the cortical contour of each bone on each projection. Fractures typically consist of a cortical step deformity, which may be visible on only one view. In more subtle cases there may be a subtle intramedullary lucency without significant visible cortical breach at initial presentation. Impacted or healing fractures may be manifested as an ill-defined sclerotic or dense band. As with all fractures, the location, direction, displacement, angulation and comminution of the fracture as well as the involvement of the articular surfaces should be assessed.

On the AP view, the normal fused distal radial epiphysis may present a slight irregularity on the radial aspect and may mimic a fracture. The dorsal surface of the distal radius typically shows a small area of irregularity representing Lister's tubercle, a normal anatomic landmark. Similarly vascular grooves in the mid shaft of the phalanges may mimic a fracture. Remember to use the digital 'windows' to look for soft tissue swelling associated with subtle fractures and to help with tricky calls.

Cartilage

Joint spaces should be uniform in width. Narrowing may be due to technical factors (rotation, flexion, tilting) or disease (arthritis).

Soft tissues

Careful attention should be paid to the cortical margins in regions of soft tissue swelling. Digital windowing of a radiograph may be required to adequately assess for soft tissue swelling particularly if the radiograph is overexposed. There is a fat plane volar to the distal radial metaphysis, along the volar aspect of the pronator quadratus muscle. This may be displaced (convex anterior surface) or obliterated in distal radial fractures. In the hand and wrist, soft tissue swelling often also spreads distal to the point of injury.

Injuries

Hand

Phalanges

Shaft fractures

These may be transverse or spiral and may show angulation, shortening or rotational deformity. Angulation is particularly common in fractures through the proximal metaphysis of the proximal phalanx and should be carefully evaluated on the lateral view as there is often some overlap. The PA view often underestimates the degree of angulation. Rotation is often difficult to assess on plain radiographs and clinical examination, whereby rotation is more apparent on flexion, is important.

Crush fractures

Crush injuries to the terminal tuft are common and most often occur in the thumb or middle finger. These are generally stable but if associated with a significant soft tissue or nail bed injury may be treated as compound or open fractures (Figure 2.4).



Figure 2.4 Crush fracture distal phalanx, AP view.



(a) (b)

Figure 2.5 Proximal interphalangeal joint dislocation. This injury is subtle on the AP view (a) and becomes obvious on the lateral view (b).

Dislocations/coach's finger

Interphalangeal joint dislocations are common. Most are dorsal and as well as significant ligamentous and soft tissue injury, there can be associated fractures. In sports, rapid reduction usually occurs at the pitchside, hence the term 'coach's finger' (Figure 2.5).

Boutonniere deformity

This is a less common acute injury, seen more often in the setting of rheumatoid arthritis, where there is rupture of the central slip of the extensor tendon at its insertion on the base of the middle phalanx. This produces a characteristic deformity with the proximal IP (PIP) held in flexion, and the distal IP (DIP) in extension. There is usually no other radiographic abnormality.

Tendon and capsular avulsions

Mallet finger

This is caused by an acute flexion force on the distal phalanx of the finger such as by a direct blow from a ball in sport on the tip of the extended finger. The force results in avulsion of the extensor tendon at its insertion at the dorsal lip of the base of the distal phalanx. Clinically active extension is lost and the DIP is held in partial flexion. There may or may not be a small avulsed bony fragment. If greater than one-third of the bony articular surface of the DIP joint is avulsed, operative fixation may be indicated (Figure 2.6).

Jersey finger/volar plate avulsion

Both these injuries involve the volar aspect of the digits and occur as a result of a hyperextension injury. Jersey finger involves the base of the distal phalanx at the attachment of the flexor digitorum profundus tendon and the classic volar plate avulsion occurs at the base of the middle phalanx at the site of attachment of the



Figure 2.6 Mallet finger, lateral view.

volar plate, an area of fibrous thickening of the volar capsule. Radiographically there is a small avulsed bony fragment. This can be very subtle and is often best seen on the lateral view. In subtle cases it may be missed on the lateral view but may be seen on the oblique view (Figure 2.7).

Metacarpals

Metacarpal fractures account for at least a third of all hand fractures. The fifth metacarpal is the most commonly injured.

Boxer's

This is a fracture of the neck of the fifth metacarpal. This results from a direct axial force as sustained in punching a solid object. The fracture typically occurs at the neck and angulates in a volar direction. Some degree of volar angulation is typically well tolerated. As with the phalangeal fractures, rotational abnormality is also of concern.

An axial load may also result in fracture dislocations through the bases of the metacrapals and at the carpometacarpal joints. This is most commonly seen through the base of the fourth and fifth metacarpals and may be associated with hamate fractures.



(a) (b)

Figure 2.7 Volar plate avulsion: (a) lateral and (b) oblique views. Occasionally these fractures are only visible on the oblique view.



(a) (b)

Figure 2.8 Boxer's fracture: (a) AP and (b) oblique views showing the typical radial and volar angulation.

Following a punch injury occasionally a fracture is also seen through the base of the fifth metacarpal. Localised soft tissue swelling is often a clue to the site of injury (Figures 2.8 and 2.9).

Carpometacarpal joint dislocations

An axial load may result in fractures or dislocations through the bases of the metacarpals. These are most commonly seen at the first and fifth carpometacarpal joints (Figures 2.10 and 2.11).

Bennett's fracture

This is an intra-articular fracture dislocation involving the base of the first metacarpal along its palmar and ulnar aspect. The shaft



Figure 2.9 Fracture of base of fifth metacarpal, oblique view.



Figure 2.11 Fracture dislocation of fifth carpometacarpal joint, PA view. Note the ulnar subluxation of the shaft of the fifth metacarpal with a longitudinal intra-articular fracture.



Figure 2.10 Dislocation of first carpometacarpal joint, PA view.



Figure 2.12 Bennett's fracture, AP view. Note the radial subluxation of the distal fragment.

(distal fracture fragment) is typically displaced radially and dorsally by abductor pollicus longus. This an unstable injury at a very important articulation often requiring surgical fixation. Closed reduction is often complicated by redisplacement of the fracture fragments (Figure 2.12).

Rolandos

This is a comminuted intra-articular fracture through the base of the first metacarpal, often with Y or T configuration. It has a worse prognosis than a Bennett's fracture.

Skier's (gamekeeper's) thumb
This involves disruption of the ulnar collateral ligament at the first MCP joint from an acute stress such a fall with a ski pole causing forced abduction and extension. Injury typically occurs at the distal attachment of the ligament. A small avulsion fracture may be seen adjacent to the base of the proximal phalanx. In the absence of an osseous avulsion, integrity of the ligament is best assessed by MRI or ultrasound (Figure 2.13).

Wrist

Distal radius and ulna

Fractures here can be divided by age group and mechanism.

Children/skeletaly immature (see Chapter 16)
Childrens' bones are more pliable than those of adults and thus can bend a little. Fracture patterns reflect applied bending forces. Treatment of all these fractures is cast immobilisation.

Torus—This is a buckle fracture of the cortex from a longitudinal compression injury in a child. The cortex fractures on the compressive side. These occur most typically on the dorsal distal radius and may be seen on only one view (Figure 2.14).

Greenstick—This an incomplete transverse fracture from a longitudinal distraction injury in a child. The bone bends away from the injury and the distraction force causes a break in the cortex, like in immature fresh wood, 'greenstick'. This extends a variable distance across the bone but the opposite cortex is normal.

Salter–Harris—This is an injury to the physeal growth plate in an immature skeleton typically aged between 11 and 17 years. At this stage the bones are more rigid than those of the child and the point of inherent weakness is at the cartilaginous growth plate. There are five fracture patterns (Table 2.2). At the distal radius, type 2 injuries are most common. This type involves the growth plate and the metaphysis, sparing the epiphysis. Treatment is usually cast immobilisation. If the epiphysis is fractured (type 3 and 4), surgery may be indicated (Figure 2.15).



(a) (b)

Figure 2.13 Skier's thumb (gamekeeper). UCL tear with avulsion fracture: (a) AP oblique radiograph demonstrating an avulsed fragment adjacent to the sesamoid bone; (b) coronal STIR MRI of same injury. The MRI shows the tear gap but the osseous fragment is not well seen.



Figure 2.14 Torus fracture, lateral view.

Table 2.2 Salter–Harris type fractures.[a]

Type	Pneumonic SALTE. . .R	Description
1	S	Slip of the physis
2	A	Above the physis (spares the epiphysis)
3	L	BeLow the physis (involves the epiphysis)
4	T	Through the physis (involves both epiphysis and metaphysis)
5	EveRything	Everything (crush injury to the physis)

[a] See Chapter 16.

Adults/skeletally mature
Colles' fracture—This is the most common fracture of the wrist. This is a transverse fracture of the distal radius with dorsal angulation and displacement of the fracture fragment. These typically occur in middle-aged and elderly patients following a FOOSH. Important to assess on the radiograph are radial length, dorsal tilt, radial inclination and possible intra-articular extension to the radiocarpal and distal radioulnar joints. Intra-articular extension is typically seen along the lunate fossa of the distal radius and is particularly well appreciated on the external oblique view. CT may be of value for evaluation of the degree of step deformity at the articular surface. Associated ulnar styloid fractures are common. Absence of an ulnar styloid fracture may suggest injury to the triangular



Figure 2.15 Salter–Harris type 1 injury (arrow), with associated distal ulnar fracture (arrowhead). Lateral shoot through view. The entire distal radial epiphysis has slipped dorsally.



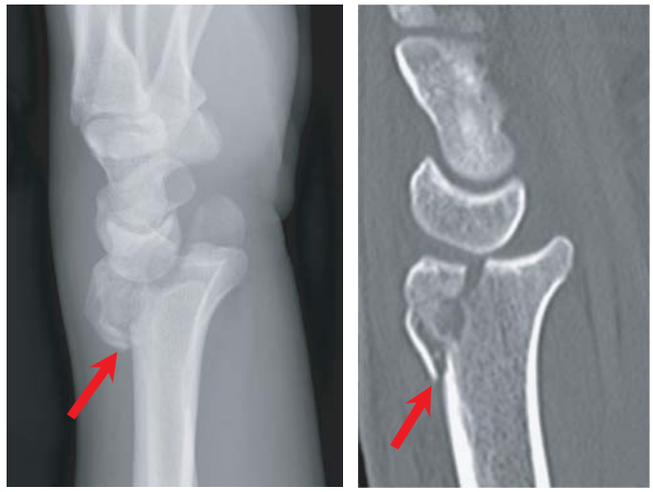
(a) (b)

Figure 2.16 Colles' fracture: (a) AP and (b) lateral views with shortening, dorsal displacement and dorsal angulation.

fibrocartilage complex (TFCC). Associated scaphoid fractures are less common but of major importance. Treatment is generally closed reduction and cast immobilisation. Comminution and intra-articular involvement is common and may complicate attempts at achieving adequate closed reduction. In these cases open reduction and internal fixation may be warranted (Figure 2.16).

Smith's fracture—This is a reversed Colles' fracture where there is volar angulation and displacement of the distal fracture fragment. Volar comminution is commonly seen with this fracture. This is a less common injury than the Colles' fracture. This pattern typically occurs in younger patients with higher energy injuries.

Barton's fracture—This is secondary to a shear injury to the radiocarpal articulation. In the original description there is an intra-articular fracture of the dorsal rim of the radius with dorsal subluxation of the carpus (dorsal Barton's fracture). Subsequently an intra-articular fracture of the volar rim of the radius with volar subluxation of the carpus was also described (volar Barton's fracture). Closed reduction is rarely successful and these injuries are treated with open reduction and internal fixation (IF) (Figure 2.17).



(a) (b)

Figure 2.17 Dorsal Barton's fracture: (a) lateral view with (b) corresponding sagittal CT bony reconstruction.

Die punch—This is an injury where an axial load is transmitted through the lunate onto the distal radius resulting in the 'punching out' of a depressed fracture of the articular surface of the distal radius. Closed reduction may be attempted; however, any intra-articular incongruity post-reduction may require CT evaluation and percutaneous pinning.

Chauffeur (Hutchinson) fracture—This is an oblique intra-articular fracture of the distal radius involving the base of the radial styloid. The fracture fragment may vary considerably in size (Figure 2.18).

Galeazzi and Monteggia fractures—A Galeazzi fracture is a fracture of the shaft of the radius, usually at the junction of middle and distal thirds, with associated dislocation of the distal radio-ulnar joint (Figure 2.19). The distal ulna typically dislocates dorsally.

A Monteggia fracture is a fracture of the ulna, often at the proximal or mid shaft with disruption of the radiocapitellar joint and dislocation of the radial head at the elbow. The radial head typically dislocates anteriorly. Both of these injuries disrupt the radioulnar fibro-osseous ring. Treatment of both these fractures is with open reduction and IF.

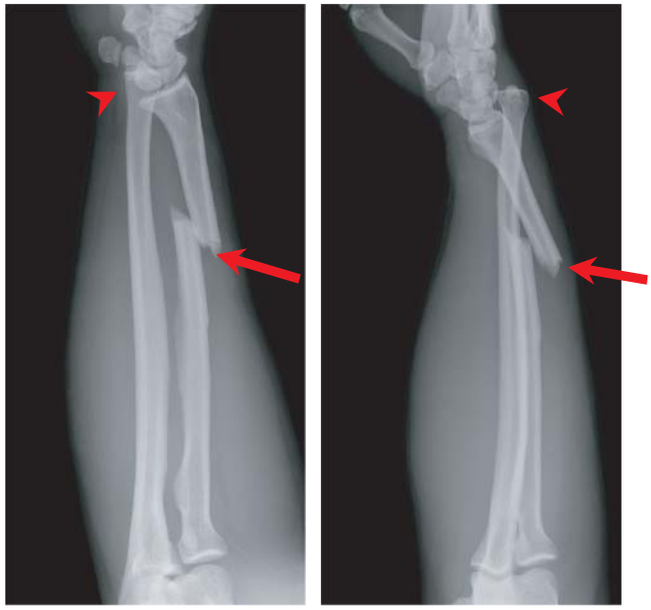
Carpal bones

Scaphoid

Scaphoid fractures comprise 80% of all carpal bone fractures. The majority tend to be subtle on initial radiographic examination.



Figure 2.18 Chauffeur's (radial styloid) fracture, AP oblique view.



(a) (b)

Figure 2.19 Galeazzi fracture: (a) AP and (b) lateral views. Fracture of the distal radius (arrow) and dorsal dislocation of the distal radioulnar joint (arrowhead).

Despite adequate radiographic projections, 30% of these fractures remain occult initially. Most (70%) fractures occur at the waist. A second set of radiographs 10 days after an initial negative assessment are often necessary if there is clinical concern regarding a scaphoid fracture with snuffbox tenderness and negative initial radiographs. CT or MRI are very sensitive for detecting subtle fractures.

The distal to proximal blood supply of the scaphoid, leaves the proximal pole at risk of avascular necrosis in fractures of the waist or proximal pole. Diagnosis is therefore crucial to avoid this outcome. A more common complication is fracture non-union. This is more common with displaced fractures (>1 mm) or fractures demonstrating a hump back deformity with palmar flexion of the distal fracture fragment. Immobilization alone may suffice for treatment unless there is displacement in which case surgical fixation may be warranted to avoid non-union (Figure 2.20 and 2.21).

Triquetral fractures

This is the second most common carpal bone fracture. This results from a ligamentous avulsion or a dorsal impaction from the ulnar styloid. Any small flake of bone on the dorsal aspect of the carpus seen on the lateral view following an acute injury likely represents a triquetral fracture. Treatment is cast immobilisation (Figure 2.22).

Others

Carpal dislocations

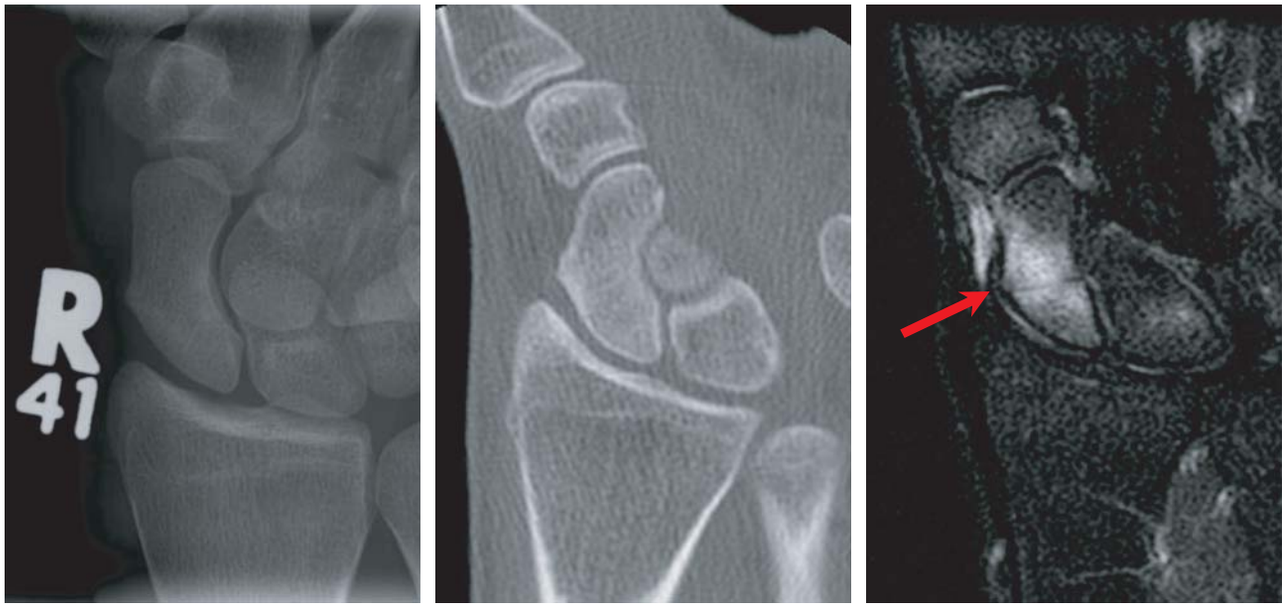
These are a spectrum of injuries comprising ligamentous injuries with or without associated fractures. The mechanism is often high-energy trauma in young males. These injuries occur in a sequence as ligaments around the lunate fail in a radial to ulnar direction. The least severe type of injury consists of a tear of the scapholunate ligament with scapholunate dissociation. Progressive injury results in perilunate and lunate dislocations.

On the AP view, interruption of Gilula's arcs, widening of the scapholunate distance (Figure 2.23) or a pie-shaped lunate may be seen. On the lateral view, the position of the lunate relative to radius and capitate is crucial. In perilunate dislocations (Figure 2.24a and b), the lunate articulates normally with the radius but the capitate is displaced, typically in a dorsal direction, resulting in an empty distal articular surface of the lunate. In lunate dislocations (Figure 2.25), the lunate articulation with distal



(a) (b)

Figure 2.20 Scaphoid waist fracture seen on ulnar deviation radiograph (a) and on corresponding CT bony reconstruction (b) performed 2 weeks later.



(a) (b) (c)

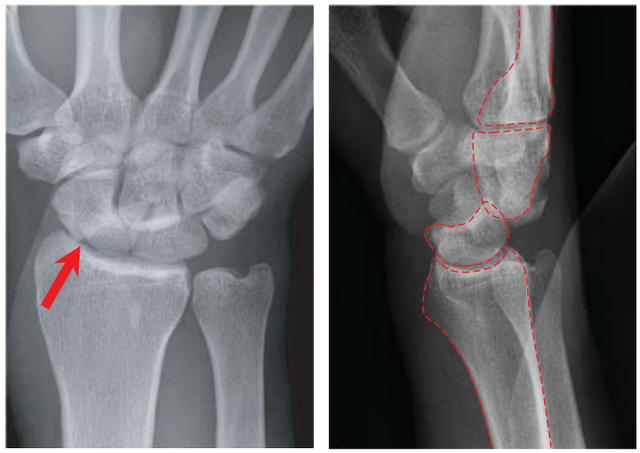
Figure 2.21 Scaphoid fracture. Coned ulnar deviation view of the scaphoid (a) in a young male with a suspected scaphoid fracture is unremarkable. Subsequent CT bony reconstruction (b) performed the same day, did not demonstrate a fracture. Coronal STIR MRI (c) performed 4 days later due to ongoing pain reveals extensive bone oedema and a subtle linear fracture.



Figure 2.22 Triquetral fracture.

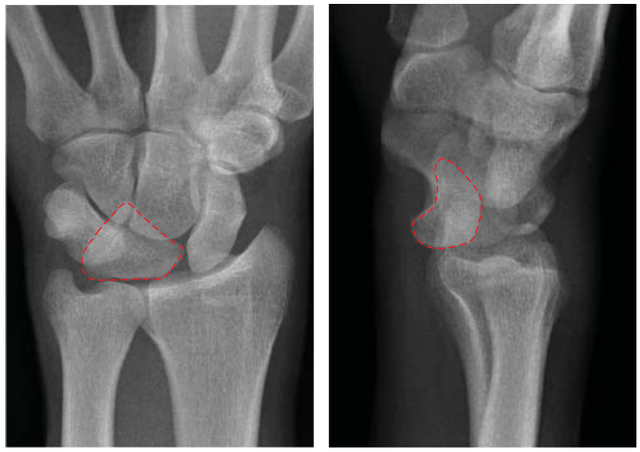


Figure 2.23 Scapholunate dissociation. AP radiograph showing widening of the scapholunate distance in comparison with the other intercarpal spaces.



(a) (b)

Figure 2.24 Transscaphoid perilunate dislocation. (a) AP view. Note the disruption of Gilula's arcs. (b) Lateral view. Note the loss of normal lunocapitate alignment, with the capitate displaced dorsally.



(a) (b)

Figure 2.25 Lunate dislocation. (a) AP view showing pie-shaped lunate and (b) lateral view showing a volarly displaced and tilted lunate.

radius is lost and the lunate is displaced volarly. Often in lunate dislocation the capitate will maintain an alignment with the distal radius. Carpal dislocations may be associated with carpal fractures as well as fractures of the distal radius and ulnar styloid.

ABCs systematic assessment

Alignment

- There should be a uniform carpal joint space measuring 2 mm
- Check Gilula's three arcs
- The base of third MC, capitate, lunate and distal radius should lie in a line

Bone

- Check each bone separately
- Check shape of the lunate and exclude an 'empty' lunate
- Check contour of distal radius
- Check there is no flake fracture on the dorsal aspect of the carpal bones
- Check scaphoid views VERY carefully

Cartilage and joints

- Joint spaces should be uniform
- If joint spaces are wide, it suggests carpal instability

Soft tissues

- Swelling indicates site of injury
- A displaced pronator quadratus fat pad may indicate a subtle distal radius fracture

Further reading

Goldfarb CA, Yin Y, Gilula LA, Boyer M. Wrist fractures: What the clinician wants to know. *Radiology* April 2001;219:11–28.

Kaewlai R, Avery L, Novelline RA. Multidetector CT of carpal injuries: Anatomy, fractures, and dislocations. *Radiographics* October 2008;28: 1771–1784.

Peterson JJ, Bancroft LW. Injuries of the fingers and thumb in the athlete. *Clin Sports Med* 2006;25:527–542.

Rogers LF. *Radiology of Skeletal Trauma*, 3rd edn. Churchill Livingstone/ Harcourt Health Sciences, 2001. ISBN 0–443–06563–2.

CHAPTER 3

Elbow

Muaaze Ahmad

Barts Health NHS Trust, The Royal London Hospital, London, UK

OVERVIEW

- Commonly present following a FOOSH
- Injury patterns in children differ from adults due to the epiphyseal and apophyseal centres
- An understanding of age of ossification of these centres is important
- A methodical review, including lines and congruity of the joint spaces, is important to avoid missing injuries

Elbow injuries are common and usually result from a fall onto an outstretched hand (FOOSH). Detecting and interpreting abnormal features on radiographs can be difficult and challenging – particularly in children because they have multiple epiphyseal and apophyseal growth centres. An understanding of normal anatomy and adoption of a systematic approach when assessing the radiographs is essential. MRI, CT and US are not necessary in the acute presentation.

Anatomy

The elbow (Figures 3.1a–c and 3.2a,b) is a hinge joint that consists of three articulations within a single synovial space. The lower end of the humerus is composed of two different shapes. On the lateral side, a partly spherical contour (capitellum) articulates with the concave articular surface of the head of the radius. On the medial side, a notched medial contour (trochlea) articulates with the ulna.

The stability of the radioulnar articulation is maintained by the annular ligament. This is a sling that holds the head of the radius against the ulna. The radial head is free to rotate within this sling.

The joint capsule comprises an inner layer of synovium, a layer of fat and an outer layer of fibrous tissue. The layer of fat results in anterior and posterior fat pads. These lie outside the synovial lining of the joint, but within the joint capsule. The anterior fat pad is radiographically visible in almost all normal elbows. The posterior fat pad lies deep in the olecranon fossa and is never visible in the flexed position unless a large effusion or haemarthrosis displaces it out of the fossa.

ABC of Emergency Radiology, Third Edition. Edited by Otto Chan.
© 2013 John Wiley & Sons, Ltd. Published 2013 by John Wiley & Sons, Ltd.

Table 3.1 Particular problems in children.

Potential traps	Helpful hints
Ossifying secondary centres can cause confusion, particularly when a centre shows multicentric ossification An incompletely fused growth plate can mimic a fracture A fracture involving the lateral condyle can be dismissed erroneously as the normal apophyseal growth plate	Doubt or confusion can usually be resolved with the help of a comparison radiograph of the opposite uninjured elbow
A pulled off medial epicondyle may be trapped in the joint. It can be mistaken for the normal trochlea ossification centre. This lesion is rare but is a recognised complication of a dislocated elbow – even one that has reduced spontaneously	Suspect this injury if there is slight widening of the medial joint space on the anteroposterior projection Remember CRITOE . . . and the ossified trochlea never appears before the ossified internal epicondyle

Children

Unfused ossification centres in children (Figures 3.3a,b and 3.4a,b) lead to a particular set of injuries (Table 3.1). Children have three epiphyseal ossification centres (capitellum, trochlea and radius) and three apophyseal centres (internal epicondyle, external epicondyle and olecranon). These appear (begin to ossify) at different ages. The trochlear and olecranon centres are often multicentric and should not be mistaken for fracture fragments. If the appearance is confusing, refer to a textbook of normal variants or seek a specialist opinion. If necessary, radiograph the opposite uninjured elbow for comparison.

The acronym CRITOE (or CRITOL) (capitellum, radial head, internal epicondyle, trochlea, olecranon, external or lateral epicondyle) lists the most common sequence in which the secondary ossification centres appear on the radiograph (Table 3.2). Although the CRITOE order is the most common sequence, individual variation does occur. Nevertheless, one part of the sequence never varies: the internal epicondyle always ossifies before the trochlea. This has particular diagnostic relevance to an uncommon, but clinically important, injury involving major displacement of the internal epicondyle ossification centre.

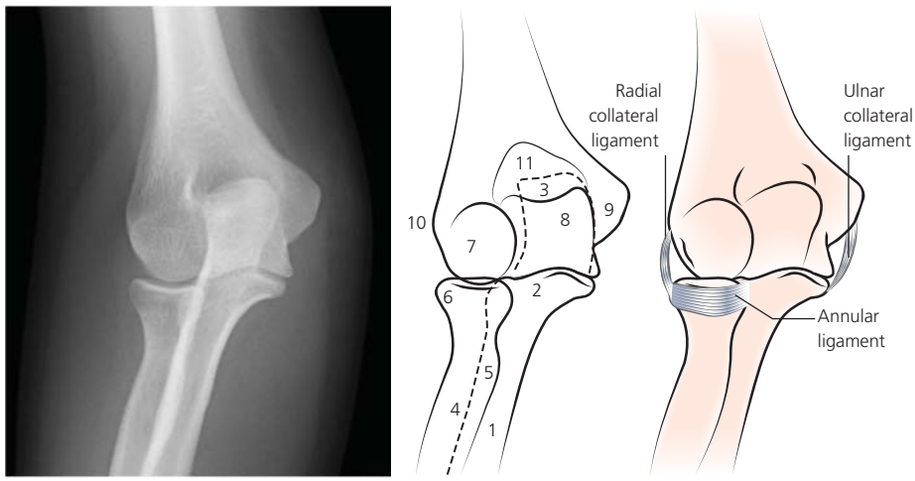


Figure 3.1 (a)–(c) Normal anteroposterior view of right elbow and ligaments. 1, Ulna; 2, coronoid process; 3, olecranon; 4, proximal radius; 5, radial tuberosity; 6, radial head; 7, capitellum; 8, trochlea; 9, medial epicondyle; 10, lateral epicondyle; 11, coronoid fossa; 12, olecranon fossa.

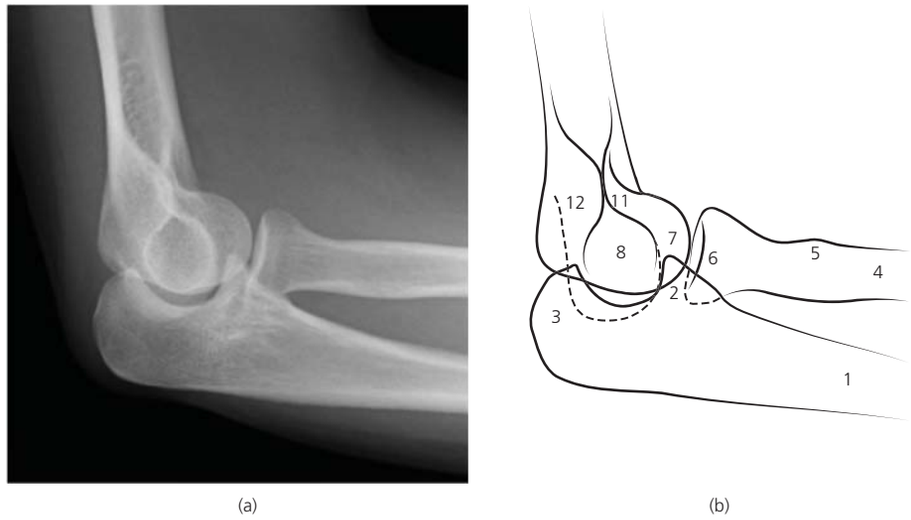


Figure 3.2 (a),(b) Normal lateral elbow (for explanation of numbers see legend for Figure 3.1).

Table 3.2 Approximate age at which secondary ossification centres appear on radiographs (CRITOE).

Centre	Appears[a]	Age (years)
Capitellum	First	1
Radial head	Second	3–6
Internal epicondyle *always before the* . . .	Third	4–7
Trochlea	Fourth	7–10
Olecranon	Fifth	6–10
External epicondyle	Sixth	11–14

[a]NB The sequence in which the secondary centres appear (above) is the most common sequence. There are occasional individual variations.

ABCs systematic assessment

- Adequacy
- Alignment
- Bones
- Congruity
- Soft tissues

Recommended radiological views

- AP and lateral
- Additional radial head views rarely required
- CT necessary only for preoperative assessment
- US and MRI not necessary in acute setting

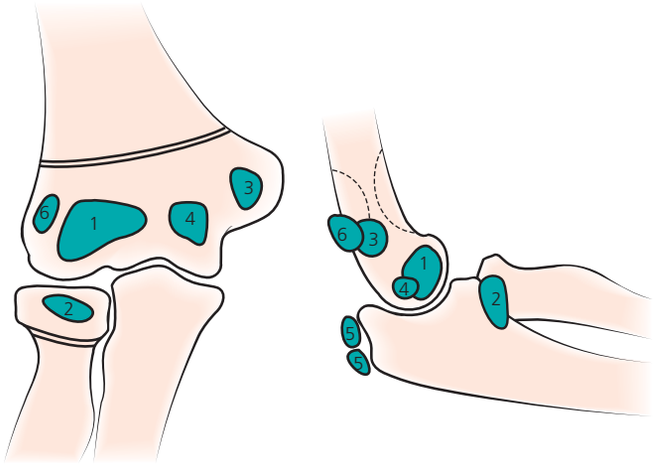
Adequacy (Figures 3.1 and 3.2)

The standard radiographic projections are anteroposterior (AP) and lateral (lat). A severe injury will often make perfect positioning impossible. Other additional projections to show the head and neck of the radius are only necessary if the routine views are normal and there is a strong suspicion of a fracture (e.g. positive 'fat pad sign').

Alignment

Lateral radiograph

The olecranon articulates with the trochlea, and the radial head articulates with the capitellum. Note that the trochlea and



(a) (b)

Figure 3.3 (a),(b) Diagram of ossification centres. 1, Capitellum; 2, radial head; 3, medial or internal epicondyle; 4, trochlea; 5, olecranon; 6, lateral or external epicondyle.



(a) (b)

Figure 3.4 (a),(b) Normal AP and lateral elbow in a 12-year-old boy.

capitellum are superimposed on each other on the lateral view. Two lines need to be assessed on the lateral view:

Radiocapitellar line (RCL) (Figure 3.5a,b) – The shaft of a normal radius, as seen on the AP and lat projections, is not always a perfectly straight line. Its proximal 2–4 cm may be set at an angle to the long axis of the rest of the bone. A line drawn along the centre of the long axis of this proximal 2–4 cm of the radius should pass through the capitellum. If it doesn't on either view, then a dislocated head of the radius is present (Figures 3.6 and 3.7).

Anterior humeral line (AHL) (Figure 3.5b) – There is a range of normal condylar shapes. Nevertheless, all normal elbows show a hockey stick or J-shaped contour. Loss of the hockey stick contour suggests a displaced supracondylar fracture.

A line drawn along the anterior cortex of the humerus should have a third or more of the blade of the hockey stick (the capitellum) laying anterior to it. If this rule is broken, there will probably be a supracondylar fracture with posterior displacement of the distal fragment. The AHL is also useful to assess the degree of posterior displacement when a fracture is obvious.

Anteroposterior radiograph

In normal adults, and in children, check the RCL to exclude a radial head dislocation.

Bones

Lateral radiograph (Figure 3.5b)

Examine the cortical surfaces of the humerus, radius and ulna. A subtle break in the anterior humerus from a supracondylar fracture can be hard to detect, especially in a child. Check the X appearance (X-sign or hour glass sign) made up of the deep bone margins of the olecranon and coronoid fossae). A disrupted X appearance is indicative of a supracondylar fracture.



(a) (b)

Figure 3.5 (a) Radiocapitellar line (RCL) – white line; (b) anterior humeral line (AHL) – white dotted line.

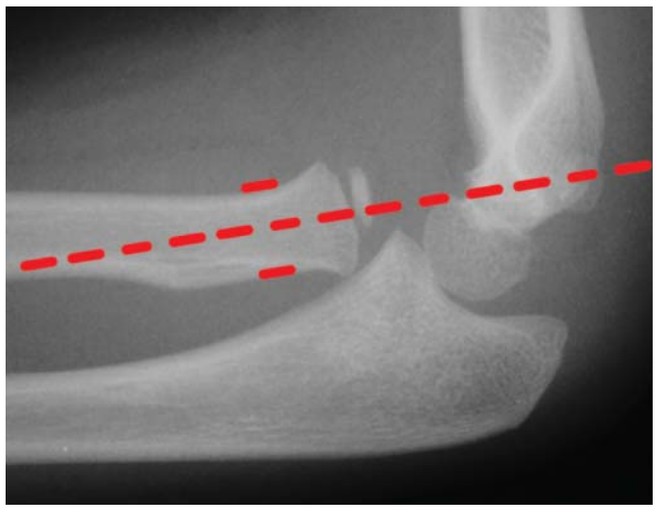


Figure 3.6 Dislocated radial head with abnormal RCL as red dashed line.

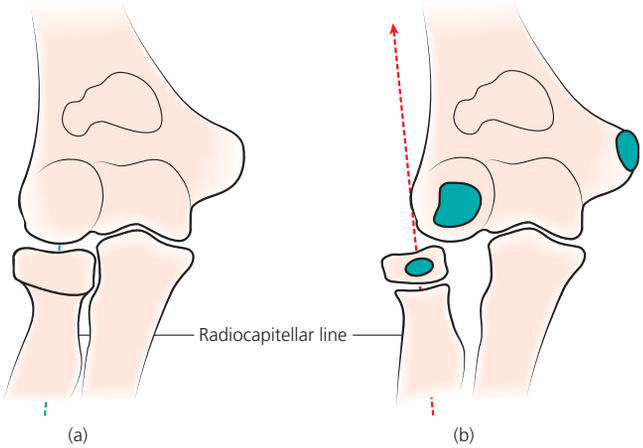


Figure 3.7 (a) Normal and (b) abnormal RCL.

Examine the internal trabecular pattern of the bones for bands of increased density. An impacted radial neck fracture may be visible only as a faint transverse band of increased density at the junction of the head and the neck. Bruising or damage to cartilage does occur, but it will not show on a radiograph.

Anteroposterior radiograph

About half of all radial head fractures are undisplaced, and a radiographic abnormality can be subtle. Slight cortical disruption, faint depression, and/or slight angulation should be looked for.

In addition, in children:

- Check for a faint lucent line crossing the distal humerus – this is often the only evidence of either an undisplaced supracondylar fracture or a fracture of the lateral condyle of the humerus.
- Check the medical epicondyle is in a normal position. Specifically, make sure that it is not trapped in the joint and masquerading as a trochlear ossification centre. This is a rare injury. Children with a dislocation of the elbow joint that reduces spontaneously are the group most at risk.

If the medial epicondyle is trapped within the joint, minor but detectable widening of the medial part of the joint will occur. Consequently, the joint's normal congruity is altered. The trapped epicondyle is rarely seen on an AP projection – it will be seen more clearly on a lateral radiograph.

Cartilage and joint

The radiocapitellar and coronoidtrochlear joint spaces should be parallel and spaced equally.

Congruity of articular surfaces should be confirmed:

- The trochlea is congruous with the ulna.
- The capitellum is congruous with or parallels the articular surface of the radial head.

Loss of congruity or parallelism will be seen with some radial head fractures.

Soft tissues

Lateral radiograph

The normal anterior fat pad appears as a thin elongated radiolucency lying parallel and adjacent to the distal cortex of the humerus. A posterior fat pad is not identified in a normal elbow held in flexion. Displacement of these fat pads occurs when there is an intraarticular effusion (for example, a haemarthrosis) displacing the synovial lining (Figure 3.8).

- A displaced anterior fat pad appears as a triangular shaped black lucency anterior to the cortex of the humerus – but elevated off the bone. Sometimes this displacement is referred to as the '*sail sign*'.
- The posterior fat pad requires a large effusion to push it out of the deep olecranon fossa. It is then visualised as a black line just posterior to the cortex of the humerus.



Figure 3.8 (a) Lateral elbow with prominent anterior and posterior fat pads. (b) Sagittal fat-suppressed MRI showing haemoarthrosis causing fat pad displacement. The fracture of the radial head is seen on the MRI, but not on the X ray.

Rule of fat pad sign

- Positive anterior fat pad sign: an intra-articular fracture is likely
- Positive posterior fat pad sign: an intra-articular fracture is even more likely

Some authors refer to a supinator fat stripe. Claims that the appearance of this lucent line is helpful in diagnosing a bone injury have been shown to be over-optimistic. The supinator fat stripe can be ignored.

Anteroposterior radiograph

If an injury has occurred to the medial or lateral epicondyles, adjacent soft tissue swelling will be present.

Injuries

Fractures

Supracondylar fracture

Supracondylar fractures (Figure 3.9) are commonly seen in children accounting for the majority (60%) of injuries around the elbow. The fracture line extends transversely across the condyles and through the coronoid and olecranon fossae. The majority (75%) of injuries are complete fractures with posterior displacement and occasionally anterior. However up to 25% are incomplete fractures without displacement that can be subtle.

Lateral condylar fracture

Lateral condylar fractures (Figure 3.10) are the second most common injuries in children. Injuries of the lateral condyle are either incomplete or complete. Complete injuries are type 4 Salter Harris injuries.



(a) (b)

Figure 3.9 (a),(b) Supracondylar fracture with disrupted X-sign.



(a) (b)

Figure 3.10 (a),(b) Lateral condylar fracture.

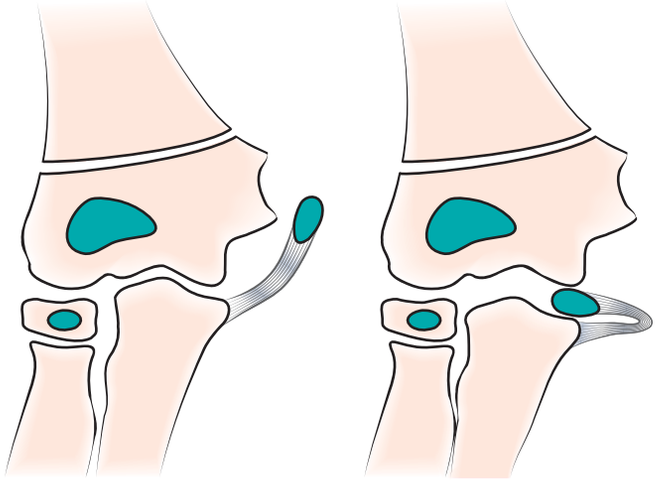


Figure 3.11 Avulsion and displaced medial epicondyle.

Medial epicondylar avulsion

This injury is only seen in children. If there is major separation the apophysis is displaced in to the medial joint space (Figures 3.11 and 3.12). This injury is often overlooked. It is important to identify the different ossification centres depending on age to ensure the medial epicondyle is correctly located.

Olecranon fracture

Olecranon fractures (Figures 3.13) are usually well identified, however it is important not interpret an epiphyseal growth plate as a fracture in children.

Radial head fracture

This is a common injury in adults accounting for 50% of injuries around the elbow (Figure 3.14). Often difficult to detect fracture



(a) (b)

Figure 3.12 (a) AP and lateral showing avulsed and displaced medial epicondyle; (b) lateral of a different patient.



Figure 3.13 Fracture of olecranon.

line however diagnosis often inferred in the presence of injury and a joint effusion.

Dislocations

Elbow dislocation are seen commonly in adults and clearly identified on the lat view. It can be difficult to appreciate on the AP view (Figure 3.15).

Radial head

Anterior radial head dislocations are occasionally seen in isolation.



Figure 3.14 Fracture of radial head.

Fracture dislocation of the capitellum

A capitellar fracture may be associated with anterior displacement of the capitellum (Figure 3.16). This may present as an additional bony fragment seen only on the lateral view.



(a) (b)

Figure 3.15 (a),(b) Dislocated elbow.

Pulled elbow

Common injury in 2–6 year olds. Rare injury, with the diagnosis made on clinical examination rather than radiography which can often be normal. The annular ligament is stretched and there is slight radial head subluxation (Figure 3.17).

Fracture-dislocations

A Monteggia fracture (Figure 3.18) is a fracture of the ulna, often at the proximal or mid shaft with disruption of the radiocapitellar joint and dislocation of the radial head at the elbow. The radial head typically dislocates anteriorly. Both of these injuries disrupt the radioulnar fibroosseous ring. Treatment of both these fractures is with open reduction and IF.

A Galeazzi fracture (Figure 3.19) is a fracture of the shaft of the radius, usually at the junction of middle and distal thirds, with associated dislocation of the distal radio-ulnar joint. The distal ulna typically dislocates dorsally.

ABCs systematic assessment

Alignment

- Radio-capitellar line – dislocated radial head
- Anterior humeral line – displaced supracondylar fracture

Bones

- Wrinkles of the cortex – fracture
- Faint depression of the cortex – fracture
- Slight angulation of the cortex – fracture
- Disrupted X sign – supracondylar fracture
- Additional fragment on lateral view. In adults suspect a radio-capitellar fracture or dislocation. In children suspect an avulsed medical epicondyle

Cartilage and joints

- Joint spaces not equidistant – dislocated elbow

Soft tissues

- Positive anterior or posterior fat pads – search for a fracture
- No visible fracture but both fat pads displaced. In adults – fracture of the radial head. In children – undisplaced supracondylar fracture



(a) (b)

Figure 3.16 (a),(b) Fracture-dislocation of the capitellum. There is an additional rounded bone fragment on the lateral, which should not be there (arrow) and represents the fracture-dislocation of the capitellum. AP looks almost normal but careful inspection confirms a subtle fracture.



Figure 3.17 Pulled elbow.



Figure 3.18 Monteggia fracture dislocation: fractured ulna (arrow) with dislocated radial head (arrowhead).



(a) (b)

Figure 3.19 Galeazzi fracture: (a) AP and (b) lateral fracture of the distal radius (arrow) and dorsal dislocation of the distal radioulnar joint (arrowhead).

Further reading

Chessare JW, Rogers LF, White H. Injuries of the medial epicondylar ossification center of the humerus. *Am J Roentgenol* 1977;129:49–55.

Donnelly LF, Klostermeier TT, Klosterman LA. Traumatic elbow effusions in pediatric patients: are occult fractures the rule? *Am J Roentgenol* 1998;171:243–5.

Raby N, Berman L, de Lacey G. *Accident and Emergency Radiology: A Survival Guide*, 2nd edn. Philadelphia: Saunders, 2005.

Rogers LF. *Radiology of Skeletal Trauma*, 3rd edn. London: Churchill Livingstone, 2004.

Rogers LF, Malave S, White H, Tachdijan MO. Plastic bowing, torus and greenstick supracondylar fracture of the humerus: radiographic clues to obscure fractures of the elbow in children. *Radiology* 1978;128:145–50.

CHAPTER 4

Shoulder

Ahmed Daghir and James Teh

Oxford University Hospitals NHS Trust, Nuffield Orthopaedic Centre, Oxford, UK

OVERVIEW

- The shoulder is very mobile and prone to dislocation
- Different patterns of injury in different age groups
- Plain radiographs remain the mainstay of imaging
- Anterior dislocations are obvious but posterior dislocations are subtle
- MRI, US, and CT are rarely necessary in the acute setting

Traumatic injury to the shoulder is a common presenting complaint to the emergency department. The shoulder girdle is highly mobile and it is particularly prone to dislocation (Box 4.1). There are different patterns of injury in different age groups. Plain radiographs are the initial investigation of choice for suspected fractures and dislocations. A variety of radiographic views of the shoulder may be obtained. The anatomy shown on each of these will be described. The radiological signs of pathology may be subtle so it is important to be familiar with the specific findings associated with certain injuries.

Box 4.1 **Shoulder girdle**

Three joints

- Glenohumeral
- Acromioclavicular
- Sternoclavicular

Three bones

- Scapula
- Humerus
- Clavicle

Anatomy

The shoulder girdle (Figures 4.1–4.3) is made up of three bones – the scapula, clavicle, and proximal humerus – and three joints – the glenohumeral (GHJ), acromioclavicular (ACJ) and sternoclavicular (SCJ) joints. The highly mobile GHJ is formed by the articular surfaces of the humeral head and the glenoid fossa. The glenoid cavity is deepened by a fibrocartilaginous ring – the glenoid labrum. The humeral head also includes the greater and lesser tuberosities, the sites of attachment of the rotator cuff tendons. The rotator cuff muscles and tendons are important dynamic stabilisers of the joint; the glenohumeral and coracohumeral ligaments also contribute to joint stability. The bicipital groove lies between the lesser and greater tuberosities and accommodates the long head of the biceps tendon. The ACJ is stabilised by ligaments around the joint itself as well as the strong coracoclavicular ligament, which anchors the clavicle to the scapula.

Important related neurovascular structures include the subclavian vessels and brachial plexus, which lie posterior to the clavicle, and the axillary neurovascular bundle passing inferior to the glenoid.

ABCs systematic assessment

- Adequacy – check correct views have been obtained
- Alignment – check joint spaces are the same
- Bone – trace the contours of all the bones
- Cartilage and joints – joint spaces should be uniform in width
- Soft tissues – change windows to look for soft tissue swelling and FB.

Recommended radiological views

- Shoulder (GHJ) – AP and either a Y view or an axial view
- ACJ – AP and weight-bearing views

Adequacy

Two projections should always be performed. The AP view is routinely obtained and is the most useful for identifying pathology. There are three alternative second views. The axial view is taken with the arm abducted; this view will show dislocation clearly and is particularly useful for demonstrating small, avulsed fracture fragments. When it is painful to abduct the arm, the 'Y' view is a useful alternative, as it requires no shoulder movement. A less commonly used second view is the axial oblique; this also requires

ABC of Emergency Radiology, Third Edition. Edited by Otto Chan.
© 2013 John Wiley & Sons, Ltd. Published 2013 by John Wiley & Sons, Ltd.



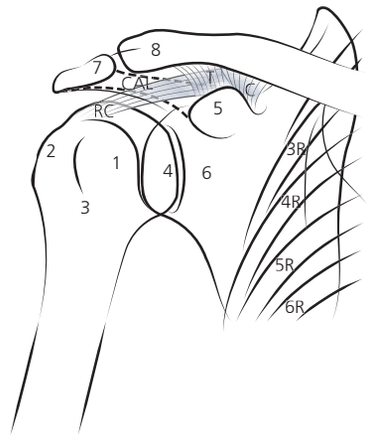
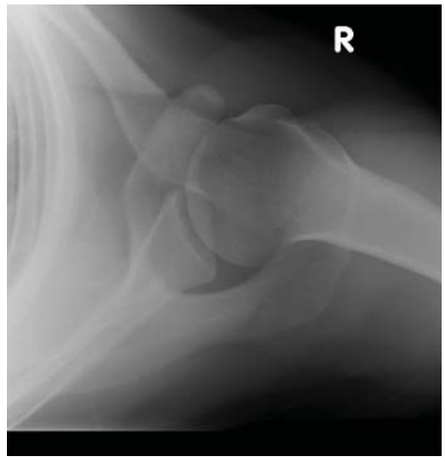


Figure 4.1 Normal AP right shoulder. 1, Humeral head; 2, greater tuberosity; 3, lesser tuberosity; 4, glenoid fossa; 5, coracoid process; 6, neck of scapula; 7, acromion; 8, lateral end of clavicle.



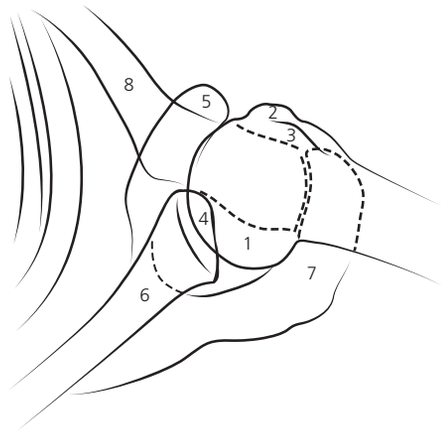


Figure 4.2 Normal axial shoulder. Note the coracoid process and acromion both project anteriorly. 1, Humeral head; 2, greater tuberosity; 3, lesser tuberosity; 4, glenoid fossa; 5, coracoid process; 6, neck of scapula; 7, acromion; 8, lateral end of clavicle.

no shoulder movement and demonstrates the relation of the humeral head to the glenoid clearly. The AP view shows the ACJ well but an additional weight-bearing view may be requested if subluxation or dislocation is suspected.

Alignment

Box 4.2 shows alignment and normal measurements.

Box 4.2 **Alignment and normal measurements (Figure 4.4)**

- GHJ space less than 6 mm
- Inferior margin of the clavicle and acromion should be level
- ACJ should be no greater than 7 mm
- Coracoclavicular distance no greater than 13 mm
- AHD of <7 mm is highly suggestive of a large rotator cuff tear

Assess the GHJ alignment on the AP view by checking there is an even joint space between the humeral head and glenoid. There should be an equal distance between the margins of their articular surfaces. The normal GHJ space is no greater than 6 mm. The axial view shows the humeral head normally aligned with the glenoid fossa like 'a golf ball sitting on a tee'. On the 'Y' view check that the humeral head is positioned over the junction of the 'Y' shape, which indicates the position of the glenoid fossa.

The ACJ alignment is assessed on the AP view. The inferior margins of the acromion and lateral clavicle should be level with each other. This rule holds true in most instances but due to normal variation between individuals there is slight misalignment at this inferior margin in up to 20%. ACJ injury may result in widening of the joint space (normally no greater than 7 mm) or the coracoclavicular distance (normally no greater than 13 mm).

Check the space between the superior margin of the humeral head and the undersurface of the acromion. This acromiohumeral space accommodates part of the rotator cuff and if it is narrowed to less than 7 mm, it indicates the presence of a large rotator cuff tear.

Bone

The contour of each bone should be carefully assessed to ensure it is smooth. Check there is no step or buckle of the cortex that may indicate a fracture. Other subtle signs of a fracture include disruption of the trabecular pattern and linear sclerosis that may indicate impaction. Each view needs to be systematically evaluated. The AP and axial views are particularly useful for identifying small

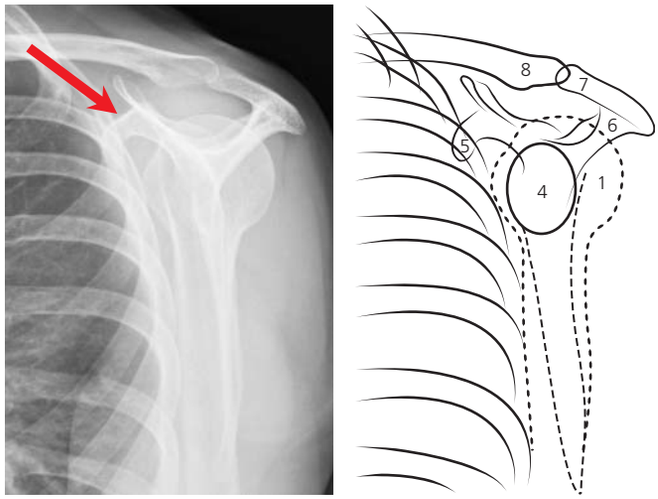


Figure 4.3 Normal Y view of shoulder. The coracoid process projects anteriorly and may be used as a landmark to determine the direction of humeral head dislocation. The glenoid fossa has been outlined.

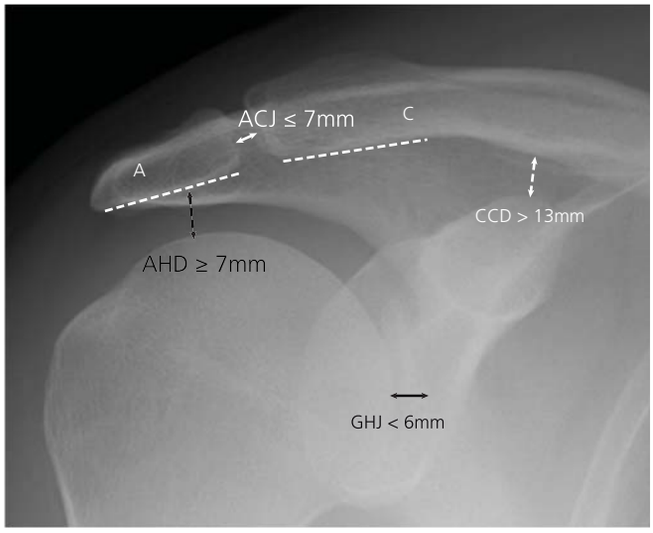


Figure 4.4 Normal measurements in the shoulder.

fracture fragments. Anterior dislocation is commonly associated with a Hill–Sachs fracture in the posterosuperior humeral head and/or a Bankart fracture of the anteroinferior bony glenoid. Ribs shown on the AP view also need to be checked to exclude a fracture.

Cartilage and joints

Ensure the joint spaces are preserved. The borders of the humeral head and glenoid should appear as two parallel lines. The GHJ space may appear reduced for technical reasons as well as true cartilage loss. Where there is true cartilage loss, there may be secondary findings including subarticular sclerosis and osteophytes. As primary degeneration of the GHJ is uncommon, cartilage loss due to another condition such as rheumatoid arthritis, haemophilia or, rarely, infection should be considered.

Soft tissues

In the presence of ACJ disruption there is often marked overlying soft tissue swelling which may be apparent on the AP view. With intra-articular fractures of the humeral head there may be a lipohaemarthrosis visible on the AP view, seen as a sharp horizontal line. If there is a large haemarthrosis of the GHJ, this may displace the humeral head laterally and inferiorly giving the appearance of a 'pseudo-dislocation'. Calcification of the rotator cuff tendons is a common finding, which indicates calcific tendonitis. This condition is often painful in the acute phase and may become asymptomatic in the long term. The visible lung on the AP view needs to be carefully checked for pathology including a pneumothorax or unsuspected lung cancer.

Injuries

Dislocations

The GHJ is the most commonly dislocated joint in the body. The dislocation is described by the position of the humeral head with respect to the glenoid.

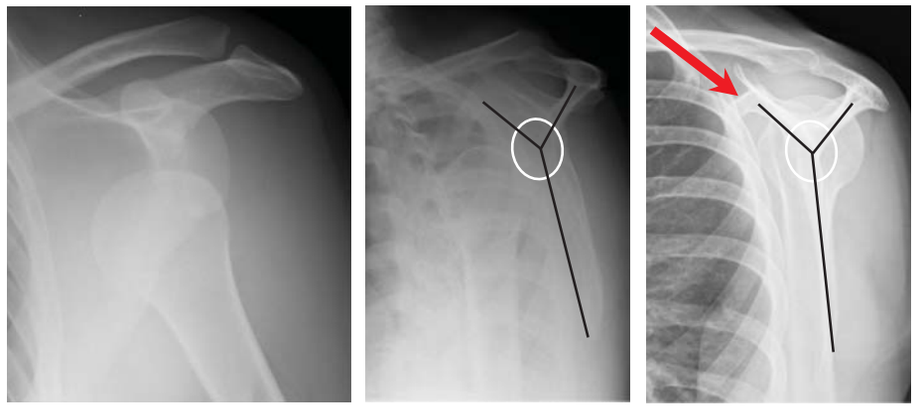
Anterior dislocation

Anterior dislocations account for over 90% of shoulder dislocations. This occurs when a posteriorly directed force is applied to the arm held in abduction and external rotation. Anterior dislocations are usually clinically apparent as there is a squared appearance of the shoulder with a prominent lateral tip of the acromion. On an AP view, the diagnosis is usually obvious. The humeral head is shown displaced inferiorly and medially, frequently lying below the coracoid process. A second view confirms the humeral head is displaced anterior to the glenoid fossa, and more importantly helps to identify associated fractures. A Hill–Sachs fracture may be found in up to 50% of cases. This follows impaction of the posterosuperior humeral head on the anterior rim of the glenoid, and it usually appears as a hatchet-shaped indentation of the cortex. A Hill–Sachs fracture may be difficult to detect on the AP view unless the arm is held in internal rotation thereby showing the posterior humeral head in profile. The fracture may be better shown on the axial or 'Y' views (Figure 4.5). Greater tuberosity fractures are found in approximately 15% of anterior dislocations. Bankart fractures of the ferior antero-inferior glenoid occur in up to 10% (Figures 4.6 and 4.7).

Anterior dislocations may be further classified according to the humeral head position as subcoracoid, subclavicular, subglenoid and intrathoracic. A repeat radiograph following manipulation should be obtained to show successful reduction of the dislocation. Approximately 40% of anterior dislocations will recur, especially in younger age groups. Soft tissue injuries of the capsulolabral complex and associated ligaments – not shown on radiographs – may lead to chronic pain and instability and are best evaluated with dedicated MR arthrography.

Posterior dislocation

Posterior dislocations (Figures 4.8 and 4.9) are uncommon and represent less than 10% of all shoulder dislocations. The clinical



(a) (b) (c)

Figure 4.5 (a) Anterior dislocation. On the AP view the humeral head is shown lying inferior to the coracoid process. (b) Y view: the humeral head is dislocated anterior to the glenoid fossa, which is sited at the centre of the Y shape. (c) Y view: normal for comparison.

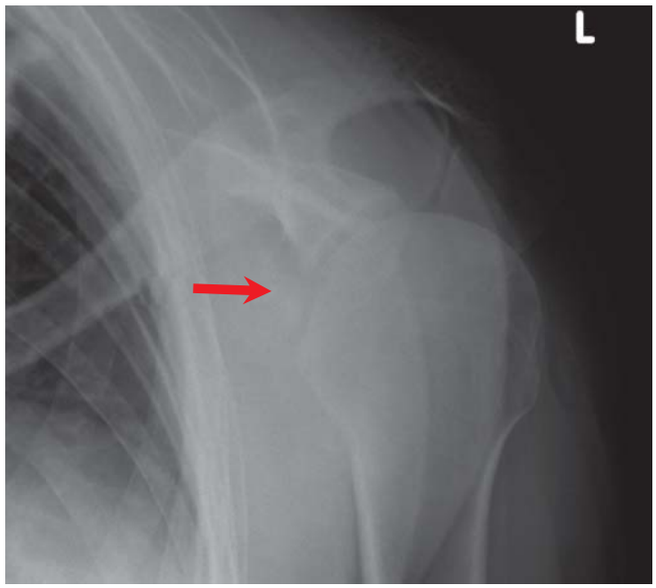


Figure 4.6 Bankart fracture. A small fracture fragment (arrow) has become displaced from the anteroinferior glenoid.

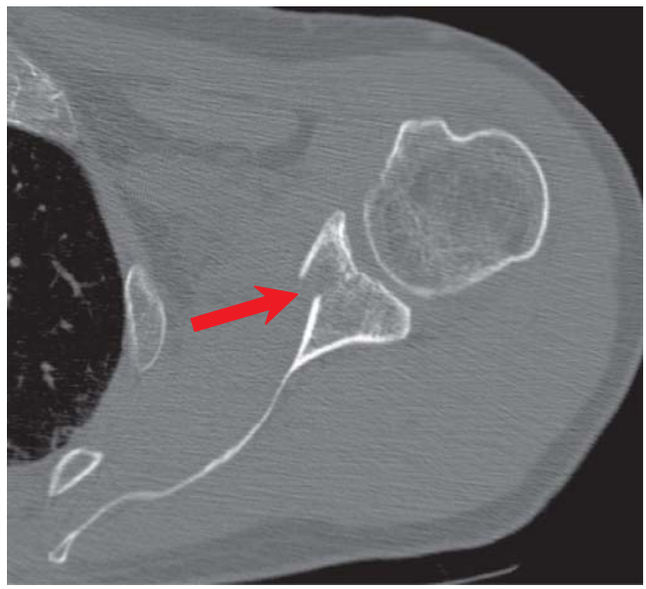
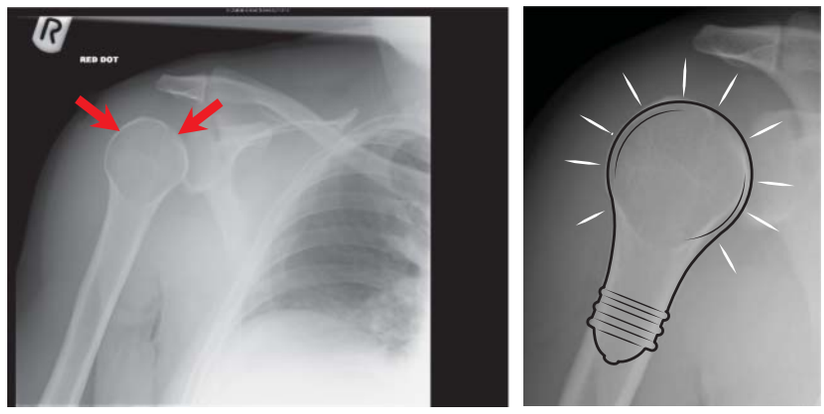


Figure 4.7 The same fracture as in Figure 4.6 (arrow) is demonstrated more clearly on this axial CT image.



(a) (b)

Figure 4.8 (a) Posterior dislocation. (b) The humeral head is internally rotated resulting in a symmetric 'lightbulb' appearance. The glenohumeral joint space is increased, and there is loss of the normal parallelism of the articular surfaces.



Figure 4.9 Posterior dislocation on an axial radiograph. The humeral head is clearly displaced posteriorly and there is a hatchet-type impaction fraction of the humeral head ('reversed' Hill–Sachs fracture).



Figure 4.10 Luxatio erecta. The arm is held in abduction. Note the articular surfaces of the glenohumeral joint do not overlap indicating dislocation.

and radiological signs may be subtle such that up to half of cases may be missed at the time of presentation. Posterior dislocation occurs when a posteriorly directed force is exerted on the humeral head with the arm held in internal rotation. Severe muscle spasm resulting from seizures or electrocution is a typical cause, and dislocation may be bilateral. Associated fractures are common, including a 'reversed' Hill–Sachs impaction of the anterior humeral head. There are three signs to look for on the AP view (Box 4.3): the 'lightbulb' sign describes a symmetrical appearance of the humeral head and neck due to internal rotation of the arm. This sign is not specific for posterior dislocation as internal rotation for any reason (e.g. pain) will give rise to this appearance. Secondly an increase in the normal glenohumeral joint space (greater than 6 mm) may be seen with associated loss of parallelism of the articular surfaces. Thirdly there may be a 'trough line', which is seen as a vertically orientated sclerotic line just lateral to the humeral head articular surface; this results from an impaction of the humeral head onto the glenoid. Posterior dislocations are more easily diagnosed on the second view, which shows the humeral head displaced posteriorly relative to the glenoid fossa. The coracoid process points anteriorly and is a useful landmark when evaluating the second view.

Box 4.3 **Signs of a posterior dislocation on an AP view**

- 'Lightbulb' sign
- Increase in GHJ space >6 mm
- 'Trough' line

Luxatio erecta

Luxatio erecta is a very rare inferior dislocation, which classically results from a fall down an open manhole cover. The patient presents with the affected arm in the air (Figure 4.10).

Table 4.1 Rockwood classification.

Classification	Injury	Radiological findings
I	ACJ injury without complete tear of AC or CC ligaments	Normal appearance
II	Complete tears of AC ligaments	Widening of AC joint
III	Complete tears of AC and CC ligaments	Widening of AC joint and CC distance
IV	As in III but with posterior displacement of lateral clavicle through trapezius	Posterior displacement of lateral clavicle on axial view
V	As in III but with upward displacement of the lateral clavicle	Widening of AC joint and CC distance with elevation of lateral clavicle
VI	As in III but with inferior displacement of the lateral clavicle	Inferior displacement of lateral clavicle below coracoid process

Acromioclavicular joint injury

Injury of the ACJ is common in young adults. The degree of injury is quite variable and may be described using the Rockwood classification (Table 4.1). On the AP view the important features to look for are loss of alignment of the inferior margins of the acromion and clavicle, an increase in the ACJ space >7 mm and an increased coracoclavicluar distance >13 mm (Figure 4.11). If there is uncertainty, a weight-bearing AP view may be obtained to exaggerate any displacement resulting from injury. Also, when comparing with the contralateral side, there should be no more than 5 mm difference in the coracoclavicular distance.

Sternoclavicular joint injury

Dislocation of the SCJ may be difficult to assess radiographically due to overlapping structures. The medial end of the clavicle usually



Figure 4.11 Type III ACJ injury with widening of the ACJ distance and coracoclavicular distance. Note the fracture fragment (arrow) avulsed off the coracoid process by the coracoclavicular ligament.

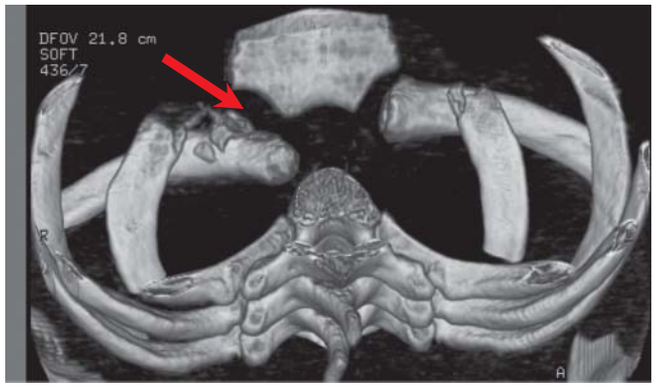


Figure 4.12 Dislocation of the right sternoclavicular joint (arrow). Three-dimension axial CT reconstruction shows posterior displacement of the medial end of the clavicle.

dislocates anterosuperiorly. On a frontal view of the chest, the medial ends of the clavicles are shown lying at different levels. An oblique AP view may show the dislocation more clearly. Rarely the medial end of the clavicle dislocates posteriorly, thus potentially injuring adjacent mediastinal structures. A CT scan should be considered if there is clinical uncertainty about the diagnosis or for evaluation of suspected intrathoracic injury (Figure 4.12).

Fractures

Clavicle

Clavicular fractures are common and usually result from falls onto the shoulder or outstretched hand. The AP view is usually sufficient to make the diagnosis, but if a second view is required an AP view with cranial angulation may be obtained. The middle third of the clavicle is involved in 80% of fractures, the lateral third in 15% and the medial third in 5%. Middle third fractures often result in overriding of the two fragments with inferior displacement of the distal end. The subclavian vessels or brachial plexus may be injured with posterior displacement of the fractured bone. Lateral clavicular fractures are usually more stable due to ligamentous support (Figure 4.13). Medial third fractures are easy to miss due to overlapping structures on the AP radiograph.



Figure 4.13 There is a minimally displaced fracture of the lateral third of the clavicle (arrow).

Scapula

Scapula fractures account for 5% of shoulder girdle injuries. Most scapular fractures are associated with injury to the head, thorax or spine. Fractures of the body of the scapula (Figures 4.14 and 4.15)

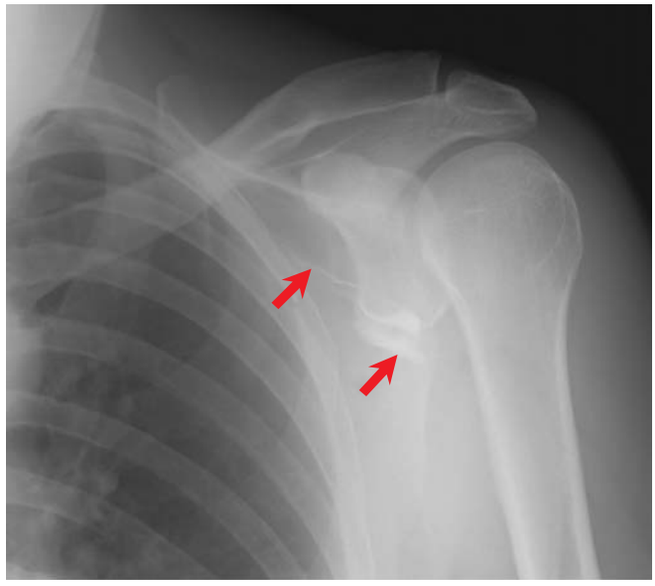


Figure 4.14 A fracture of the body of the scapula. There is linear sclerosis (arrows) indicating the site of fracture.



Figure 4.15 A 3D CT reconstruction shows the extent of the scapular body fracture which is comminuted.

usually occur with severe trauma whereas fractures of the acromion typically result from a direct blow, for example a fall. A fracture of the coracoid process may occur with shoulder dislocations. If a scapular fracture is identified on a screening chest radiograph, dedicated shoulder views should also be obtained for better evaluation. Most scapula fractures can be managed conservatively but those involving the glenoid fossa or neck or the superior shoulder suspensory complex (SSSC) may require surgery.

The SSSC is a bone and soft-tissue ring attached to the trunk by a superior strut (middle third of the clavicle) and inferior strut (lateral scapular body and spine) from which the upper limb is suspended. The ring is comprised of the glenoid, coracoid process, coracoclavicular ligament, distal clavicle, ACJ and acromion.

Traumatic disruptions of a single component of the SSSC are common (e.g. simple clavicle fracture). If the ring is injured in two or more places (double disruption), this may result in altered shoulder biomechanics and instability, which may necessitate surgery.

The floating shoulder is an important injury to recognise consisting of ipsilateral fractures of the clavicle and scapular neck (Figure 4.16). Ligament disruption associated with isolated scapular neck fractures may result in the functional equivalent of this injury.

Scapulothoracic dissociation is a rare and potentially life-threatening injury. The scapula is distracted from the thoracic cage resulting in the equivalent of a closed forequarter amputation. Associated rib fractures are common and there is often neurovascular injury necessitating angiography. Plain radiographs demonstrate lateral displacement of the scapula with marked soft tissue swelling and a clavicle fracture or ACJ separation. On a well-centred chest radiograph the distance from the midline of the spine to the tips of both scapulae is unequal.

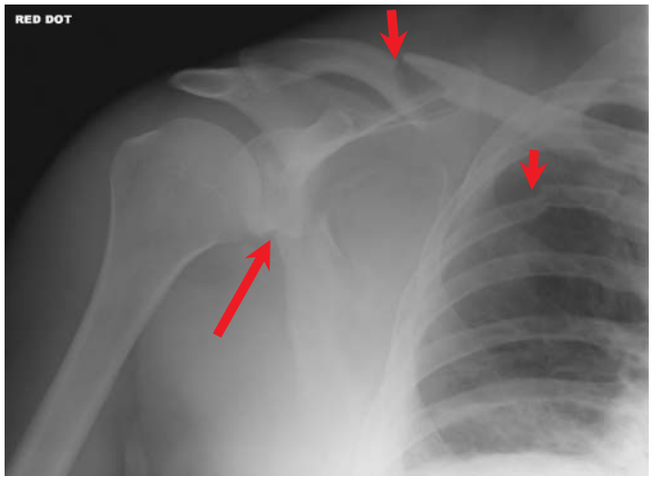


Figure 4.16 Floating shoulder. The arrows show a scapular neck fracture, clavicle fracture and rib fracture.

Proximal humerus fractures

Proximal humeral fractures are common following falls in the elderly, who may have coexisting osteoporosis. Adolescents with injuries of the proximal humerus may present with epiphyseal separation. The commonest site of fracture in adults is the surgical neck. Comminution of the fracture and involvement of the tuberosities is common (Figure 4.17). The Neer classification describes the displacement or angulation related to four parts of the proximal humerus – the articular surface, greater tuberosity, lesser tuberosity, and shaft. More than 80% are one-part fractures (without substantial displacement). Three-part and four-part fractures often require surgery. A CT scan is frequently necessary for



Figure 4.17 A three-part fracture of the proximal humerus involving the surgical neck, greater and lesser tuberosities with displacement.

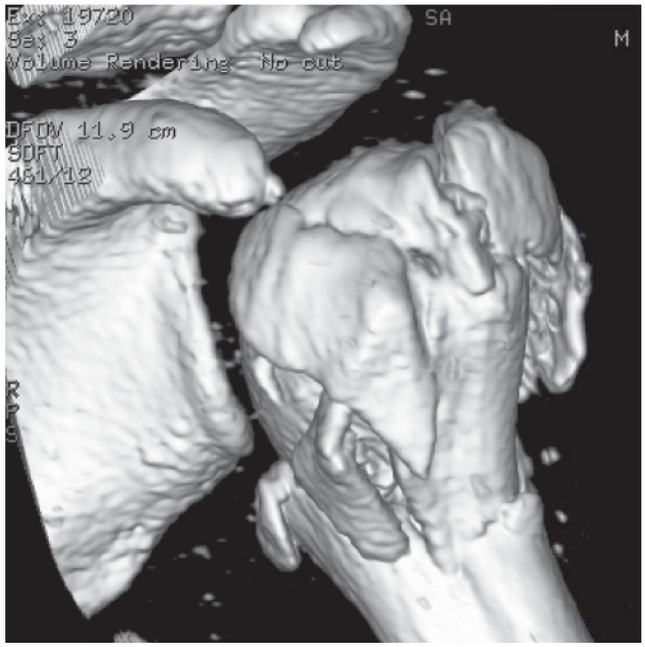


Figure 4.18 A 3D CT reconstruction of the same injury AS IN Figure 4.17 demonstrates the relations of the fracture fragments and aids surgical planning.

surgical planning (Figure 4.18). Complications include neurovascular injury – including radial nerve damage – which is found in up to 17% of fractures involving the humeral shaft.

ABCs systematic assessment

Alignment

- GHJ space should be even and no greater than 6 mm
- On the axial view the GHJ appears as a 'golf ball on a tee'
- On the 'Y' view the humeral head should be centred over the junction of the Y shape
- ACJ alignment – the inferior margins of the acromion and clavicle should be level
- Check for widening of the ACJ and coracoclavicular distance

Bone

- The contours of the humeral head and scapula should be smooth
- Check for disruption of the trabecular pattern or linear sclerosis indicating impaction
- Small fracture fragments should be identified
- Anterior dislocation is frequently associated with a Hill–Sachs and/or Bankart fracture

Cartilage and joints

- Check for even joint spaces and loss of joint width
- Loss of GHJ space may be degenerative secondary to other causes

Soft tissues

- Check for a horizontal line indicating lipohaemarthrosis of the glenohumeral joint. There may associated lateral and inferior 'pseudo-dislocation' of the humeral head
- Calcification of the rotator cuff tendons is often painful in the acute phase
- Marked loss of acromiohumeral space indicates a large rotator cuff tear

Further reading

Brucker PU, Gruen GS, Kaufmann RA. Scapulothoracic dissociation: evaluation and management. *Injury* 2005;36(10):1147–55.

Edelson G, Saffuri H, Obid E, Vigder F. The three-dimensional anatomy of proximal humeral fractures. *J Shoulder Elbow Surg* 2009;18(4):535–44.

Melenevsky Y, Yablon CM, Ramappa A, Hochman MG. Clavicle and acromioclavicular joint injuries: a review of imaging, treatment, and complications. *Skeletal Radiol* 2011;40(7):831–42.

Owens BD, Goss TP. The floating shoulder. *J Bone Joint Surg Br* 2006; 88(11):1419–24.

Robinson CM, Shur N, Sharpe T, Ray A, Murray IR. Injuries associated with traumatic anterior glenohumeral dislocations. *J Bone Joint Surg Am* 2012;94(1):18–26.

CHAPTER 5

Pelvis and Hip

Syed Babar[1], *James A. S. Young*[2], *Jeremy W. R. Young*[3] *and Otto Chan*[4]

[1]Hammersmith & Charing Cross Hospitals, Imperial College, London, UK
[2]St Georges Hospital, London, UK
[3]The Regional Medical Center, Orangeburg, SC, USA
[4]The London Independent Hospital, London, UK

OVERVIEW

- Pelvic fractures in major trauma may be life-threatening (NB suspect vascular and pelvic organ injuries in these patients)
- If one fracture is detected, always look for a second one
- Hip fractures may occur after minor trauma in elderly patients
- Plain radiographs are difficult to interpret and provide limited information. There should be a low threshold for use of CT and MRI

Pelvic and hip fractures are seen in the elderly population with trivial trauma whilst the mechanism in young patients generally involves high-impact injuries including road traffic accidents (RTAs). There is high morbidity and mortality associated with pelvic fractures. This results from internal visceral injuries (commonly bladder and urethra and rarely uterus, cervix, vagina and rectum) and bleeding due to high impact in RTAs, falls in young patients and associated underlying co-morbidities in elderly population. Prognosis is poor if the injuries are not detected and treated promptly. Pelvic fractures can be open or closed. The mortality rate for closed pelvic fractures is 27% and that for open fractures is 55%.

In contrast, hip fractures may occur after relatively minor trauma in elderly patients and are suspected from the clinical history and examination. The fractures may be subtle on plain radiographs and may be overlooked in particular in obese and elderly osteopenic patients.

ANATOMY

Bony anatomy

Pelvis

The pelvis is the connection between lower limb and trunk and hence it is inherently unstable. It comprises three separate bones (the sacrum and two iliac/innominate bones) which are held together by a series of strong ligaments. The integrity of this pelvic bony ring can be compromised by disruption of these ligaments (Figures 5.1 and 5.2).

The ligaments are the anterior and posterior sacroiliac ligaments, the sacrotuberous ligament, sacrospinous ligaments and the ligaments of the symphysis pubis. The posterior group is strong and complex and attaches the spine to the pelvis. They resist posterior deformation. The anterior group in contrast is weak and prevents distraction and anteroposterior displacement. The anterior ligaments are the first to disrupt.

Hip

The femoral head and the acetabulum form the hip joint. The acetabulum is formed by the anterior and posterior columns and connected by the supra-acetabular region. The anterior and posterior columns are connected to the axial skeleton through the sciatic buttress. Hip fractures are not commonly associated with dislocations because of the strong joint capsule. Hip fractures may be associated with avascular necrosis of the femoral head. This is more commonly seen in intracapsular rather than extracapsular fractures. There are various muscle attachments around the pelvis and hip region, which may be avulsed in traction injuries.

In children, the proximal capital femoral epiphysis is present from the age of 3 months until 18–20 years. There can be asymmetry of the epiphysis with irregularity and notching, which can be a normal finding. However, flattening is generally considered abnormal.

ABCs systematic assessment

- Adequacy
- Alignment
- Bone
- Cartilage and joints
- Soft tissues

Radiographic projections of pelvis and hip

Pelvis

Standard

- AP view of hips
- Lateral

ABC of Emergency Radiology, Third Edition. Edited by Otto Chan.
© 2013 John Wiley & Sons, Ltd. Published 2013 by John Wiley & Sons, Ltd.

Additional

- Oblique view
- Inlet view
- Outlet view

Hip

Standard

- AP view of both hips

Additional

- Frog leg lateral view

Pelvis

Plain X-rays

Adequacy

The routine view is a single AP view of the pelvis. The x-ray is generally done along with the AP CXR in the trauma protocol series. It is difficult to assess the stability of the pelvis on the AP view. In a comparative study between MDCT and plain X ray of the patients with blunt trauma, CT demonstrated 629 fractures in contrast to 405 fractures in a total of 226 patients. This gives an overall sensitivity of only 55% stressing the importance of pelvic CT in evaluation of patients with pelvic trauma.

Ideally the AP view has to cover the pelvis from the level of the iliac crests to the ischial tuberosity and laterally to include both greater trochanters.

Penetration should be adequate and is assessed by looking at the soft tissue structures. The soft tissue shadows which should be seen include the bladder with its perivesical fat, iliopsoas shadows and the rectum and bowel gas. It is important to note that the adequacy criteria may be difficult to meet due to reasons mentioned earlier. In addition elderly patients may have a large belly with thin proximal thighs and hence the exposure may vary significantly. The pelvic AP view is generally considered sensitive for the anteroinferior part of the pelvis, reasonable in the region of the acetabulum and Ilium and poor in the region of the posterior ring.

Pelvic centring also needs to be assessed. This can be done by aligning the symphysis with the sacrum and checking for the symmetry of the obturator foramina.

The AP view of the pelvis gives important information about the initial assessment of the traumatised patient so as to assess for other more significant underlying injuries. These significant injuries may be fractures of the acetabulum, obturator ring, injury to the bladder and urethra.

The AP view can be supplemented by inlet and outlet views of the pelvis in addition to the oblique (Judet) views especially in cases of suspected acetabular injury. However, nowadays these views have been replaced by CT with MPR and 3D reconstructions.

Alignment and bones

The bony alignment is assessed by dividing the pelvis into three circles, one large circle and two smaller circles (Figure 5.3). The larger circle is the pelvic brim whilst the smaller circles are made by the obturator rings. The larger circle of the pelvic brim should be visualised as a continuous line around the margins of the brim

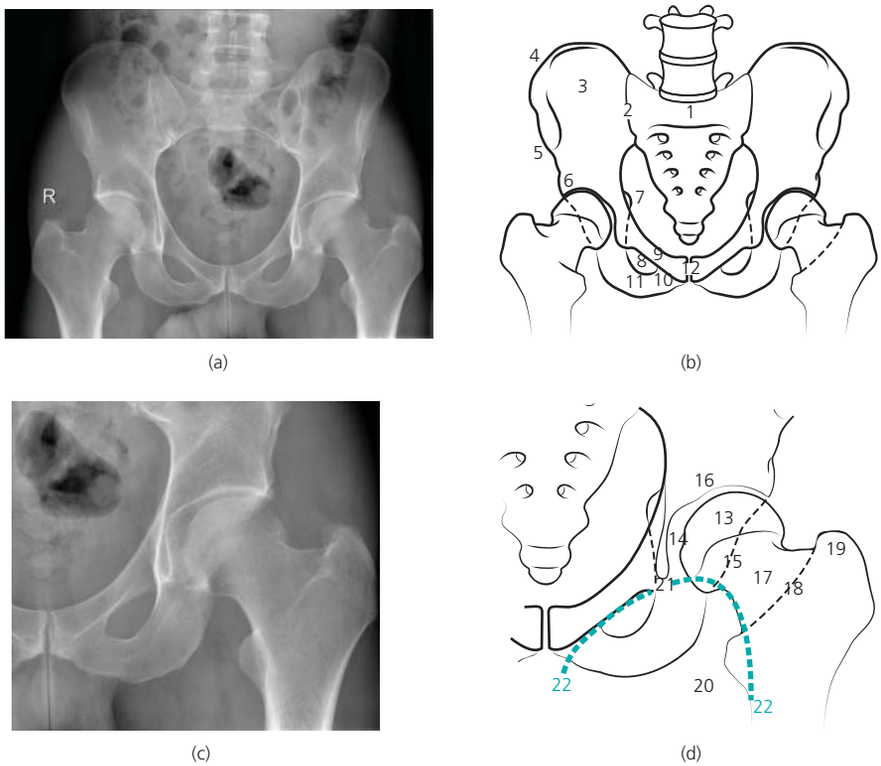


Figure 5.1 (a)–(d) Normal pelvic and hip anatomy: 1, sacrum; 2, sacro-iliac joint; 3, ilium; 4, iliac crest; 5, anterior superior iliac spine; 6, anterior inferior iliac spine; 7, ischial spine; 8, obturator foramen; 9, superior pubic ramus; 10, inferior pubic ramus; 11, ischial tuberosity; 12, symphysis pubis; 13, femoral head; 14, fovea centralis; 15, posterior acetabular rim; 16, acetabulum; 17, neck of femur; 18, inter-trochanteric line; 19, greater trochanter; 20, lesser trochanter; 21, Kohler's tear drop; 22, Shenton's line.

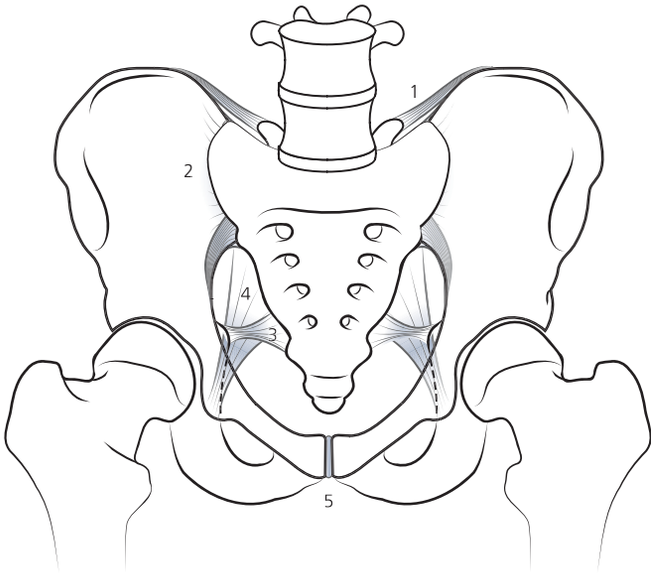


Figure 5.2 Normal pelvic ligamentous anatomy: 1, left posterior sacro-iliac ligament; 2, right anterior sacro-iliac ligament; 3, right sacrospinous ligament; 4, sacrotuberus ligament; 5, symphysis pubis.

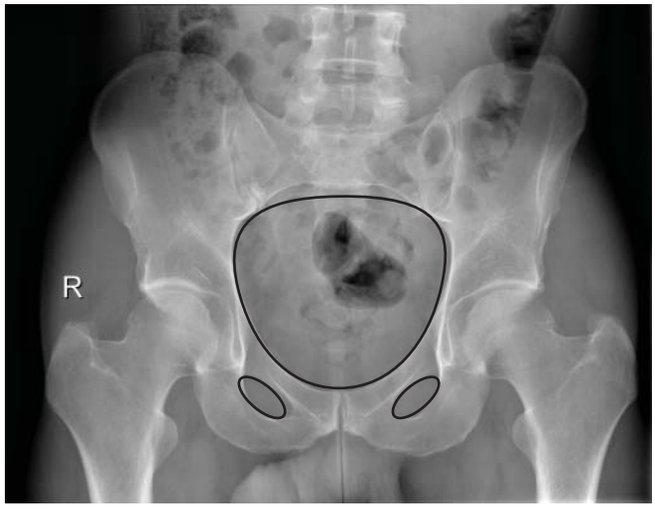


Figure 5.3 Normal three bony pelvic rings.

and continuing across the sacroiliac joints (SIJs) posteriorly and symphysis pubis anteriorly.

If a fracture is detected, always check for a second fracture or disruption/diastasis in the same ring (imagine trying to break a polo mint in one place!).

The smaller rings are formed by the two obturator foramina. (The same rule applies to the obturator foramina, if a fracture is detected, there is almost always a second fracture in the same ring or diastasis of the pubic symphysis.) There is a smooth uniform arc formed by drawing a line along the inner margin of the femoral neck and extending continuously to the superior margin of the obturator foramen. This continuous line is called Shenton's line. Disruption of this line indicates a femoral neck fracture. The only exception to this is if the fracture is non-displaced.

There are certain other important lines, which can be assessed. These include the iliopectineal line, which assesses the anterior column, the ilioischial line, which assesses the posterior column, the anterior acetabular line and the posterior acetabular line. The latter two form the anterior and posterior margins of the acetabulum respectively. The teardrop line is seen at the medial margin of the acetabulum and hip joint, which indicates damage to the medial wall of the acetabulum.

In addition it is vital to follow the lines of the sacral foramina as a discontinuity of the sacral foramina line indicates a fracture, which can involve the sacral nerve roots.

Avulsion injuries tend to occur at the site of the attachment of the strong anterior and posterior hip and thigh muscles. The sites to look for avulsion injuries are the ischial tuberosity for hamstring tendons, anterior inferior iliac spine for rectus femoris muscle, anterior superior iliac crest for the sartorial muscle and also the sacral spines for sacrospinous and sacrotuberous ligaments.

In children, the pubis, ischium and ilium remain separated by a Y-shaped cartilage (called the triradiate cartilage) which fuses in puberty to form the acetabulum. In addition, there are other small accessory ossification centres, which should not be mistaken for fractures.

Cartilage and joints

The pubic symphysis is well visualised and should be checked for alignment, widening, asymmetry or overlapping bones. The symphysis pubis shows widening of the joint space in AP compression injuries. In vertical shear or injury to the pelvis from a fall, superior displacement of the symphysis can be seen.

The anterior margins of the SIJs are well visualised and should be checked for alignment, widening, asymmetry and overlapping. These changes tend to be more subtle and can be easily overlooked, in particular as there is often overlying bowel gas.

Soft tissues

Check for loss or displacement of soft tissue outlines, in particular displacement or asymmetry of the perivesical fat plane (surrounding the bladder) or the obturator internus fat plane (medial edge of the obturator internus muscle), which are strongly suggestive of a pelvic sidewall haematoma secondary to a fracture.

Computed tomography (CT)

In major trauma, the pelvic CT is covered as part of the whole body CT protocol. However, if a CT has not been performed, then pelvic CT should be carried out with intravenous contrast enhancement and is viewed on soft tissue and bone algorithm windows, in addition to MPR and 3D. CT angiography (CTA) should also be performed to look for vascular injuries. CT cystography (contrast is instilled into the bladder) can be performed to look for and assess bladder injuries.

MPRs and 3D reconstructions give detailed characterisation of simple and complex pelvic fractures and are now considered essential for preoperative planning for major pelvic reconstructions.

CT is also used to exclude and to assess injuries to the pelvic organs including the bladder, urethra, rectum, uterus and the

cervix and vagina. Pelvic haematomas can be detected and active contrast extravasation at the time of the CT, indicates active ongoing bleeding.

Patterns of injury to the pelvis

There are numerous classifications for pelvic fractures. However, the two most commonly used are the Tile classification based on the integrity of the posterior sacroiliac complex and the Young classification based on the mechanism of injury. Young's classification divides the pelvic fractures into three main categories. These are AP compression, lateral compression and vertical shear and combinations of the three.

Lateral compression (LC)

This is the most common form. The direction of force is side to side. As a result the typical fractures are seen in the pubic rami in the horizontal direction (Figure 5.4). This common form of injury results from broadside traffic accidents or from fall on to the side. This is also associated with sacral impaction injury, fractures through the sacral foramina and rotational instability (Figure 5.5). Lateral compression causes an effect opposite to the AP directed force and causes a closed book phenomenon with internal rotation of the hemipelvis (Figure 5.6). There may also be an avulsion fracture from the posterior iliac bone. Further increase in the lateral compression force can cause the external rotation of the contralateral hemipelvis resulting in a windswept pelvis. This will cause both rotational and vertical instability. Lateral force can cause central dislocation of the femoral head and crush fracture of the femoral neck.

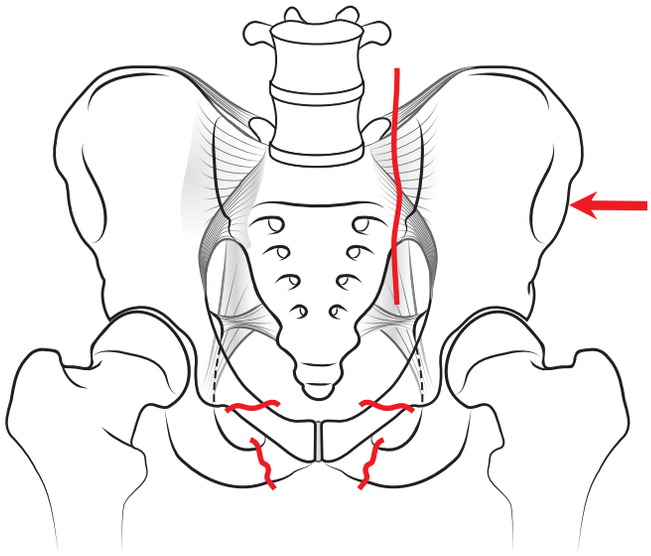


Figure 5.4 Lateral compression injury with horizontal fracture of the pubic rami and through the neural foramina.

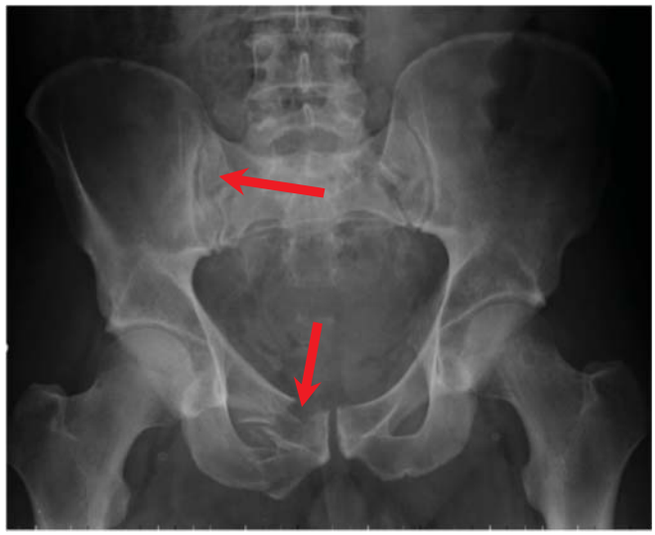
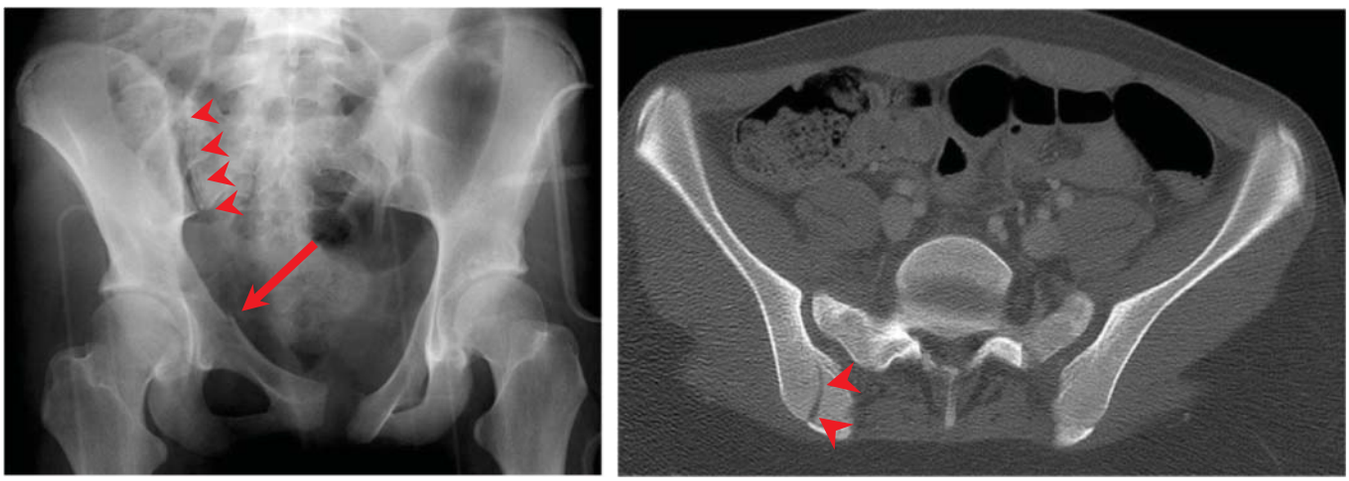
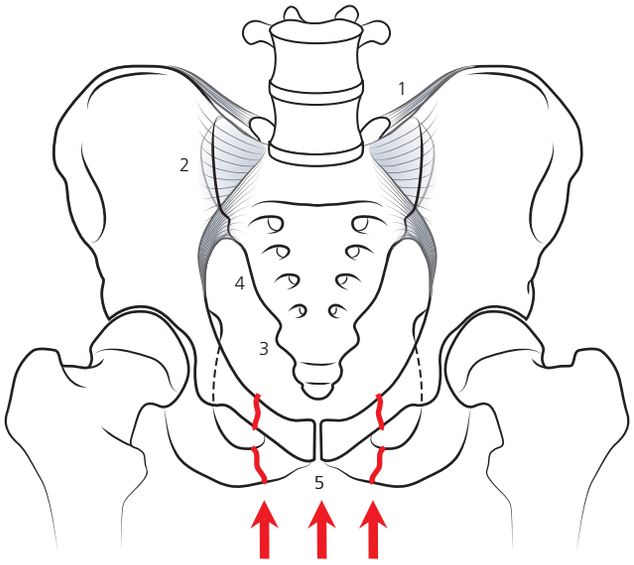


Figure 5.5 Lateral compression injury with horizontal fractures through the pubic rami (arrowed).

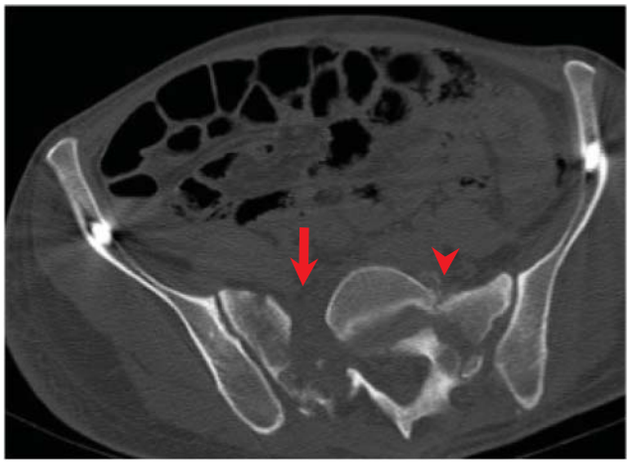


(a) (b)

Figure 5.6 (a) Lateral compression injury with an impacted horizontal fracture of the right superior pubic ramus (arrow) and diastases of the right sacro-iliac joint (arrowheads). (b) CT pelvis showing the vertical fracture (arrowheads) through the Ilium at the level of the right SIJ.



(a)



(b)

Figure 5.7 (a) AP compression pelvic injury; (b) CT in pelvic trauma.

AP compression (APC)

The direction of the force is in the anteroposterior direction usually from the front (or behind). As a result the typical fractures are seen in the pubic rami in a vertical orientation (Figure 5.7). This causes the ligaments of the symphysis pubis to disrupt. The distance between the symphysis pubis is normally less than 5 mm. A measurement of greater than 1 cm is considered abnormal. Disruption of the symphyseal ligaments does not lead to instability. However, excessive force in the AP direction results in opening up of the hemipelvis like a book if the anterior sacroiliac ligaments are also torn. This results in rotational instability and is generally seen if the symphyseal diastasis is greater than 2.5 cm. Further increase in the force vector will result in disruption of the posterior sacroiliac ligaments and hence cause not only rotational instability but also vertical instability (Figure 5.8.). This results in the loss of the tamponade effect on any underlying pelvic haematoma. In addition this sort of force vector may cause posterior dislocation of the femoral head with resultant posterior acetabular rim fracture.

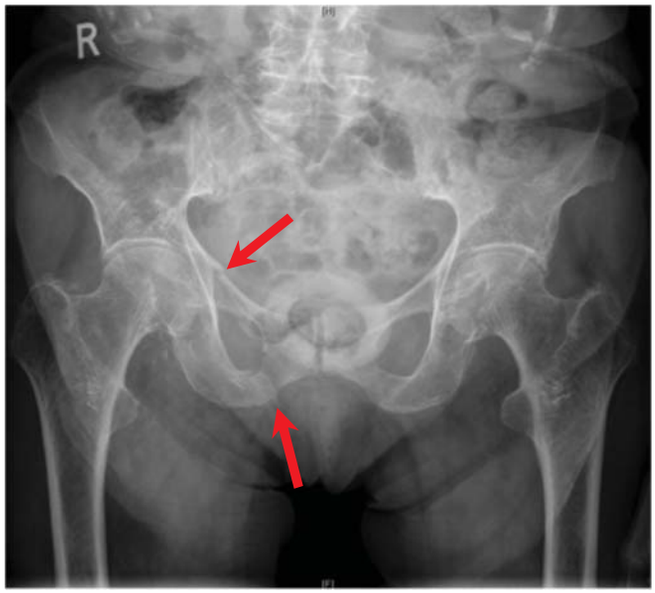


Figure 5.8 AP compression injury with vertical fractures of the right superior and inferior pubic rami (arrowed).

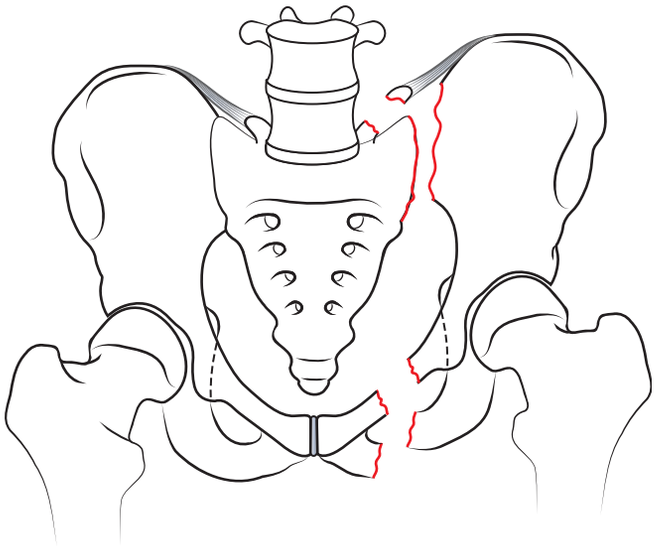


Figure 5.9 Left vertical compression injury with vertical fractures through the pubic rami and the Ilium close to the SIJ.

Vertical shear (VS)

The direction of the force is in the vertical direction (up and down), such as a fall from a height. The typical fractures of the pubic rami and the iliac bones are in the vertical plane with disruption of the anterior and posterior sacroiliac ligaments and resultant superior displacement of the hemipelvis (Figure 5.9). The symphyseal ligaments are also disrupted. There is severe vertical pelvic instability and soft tissue injuries and haematoma formation (Figure 5.10). The normal distance between the SI joint is about 2–4 mm. If there is only disruption of the anterior SI ligaments the vertical stability of the pelvis is preserved. If however the posterior SI ligaments are disrupted as well, then the pelvis becomes vertically unstable (Figure 5.10). Displaced vertical fractures through the

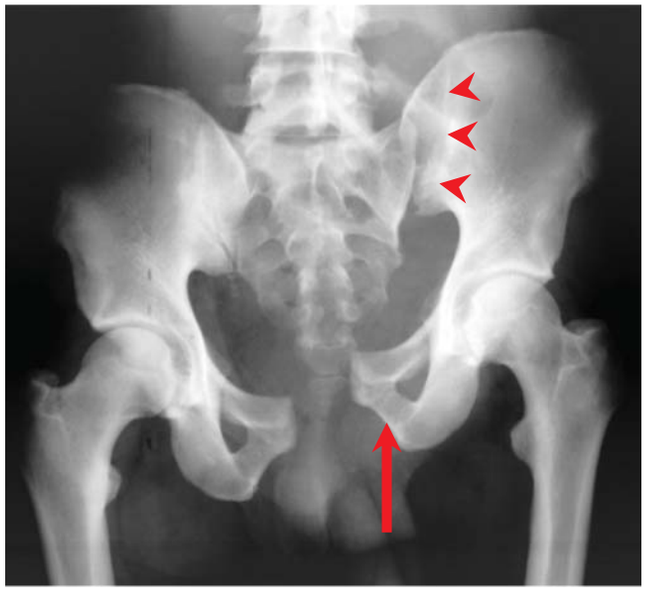


Figure 5.10 Left vertical fracture with cranial displacement of the hemi-pelvis, pubic symphysis diastases (arrow) and SIJ displacement (arrowhead).

sacrum and the ilium adjacent to the SIJs have the same implications as fractures through the joint. The iliolumbar ligament is attached to the tip of the L5 transverse process. Fracture of the tip of the L5 may cause disruption of the posterior SI ligament and hence may cause vertical instability. So a fracture of the transverse process of L5 should not be dismissed lightly as this may be the only sign of pelvic instability.

Complex combined injury

This is the result of a combination of force vectors ending in a pattern of injuries with complex orientation (Figure 5.11). The

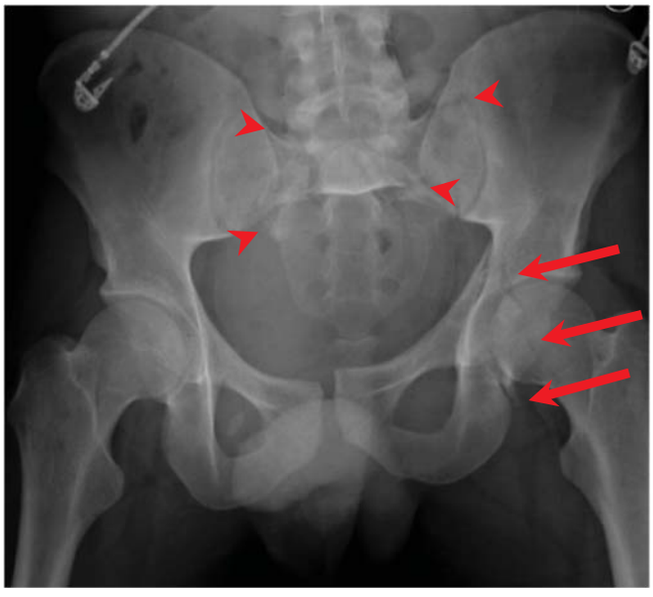


Figure 5.11 Combined complex injury of the pelvis with PS diastasis, subtle left acetabular fracture (arrows) and multiple sacral fractures (arrowheads).

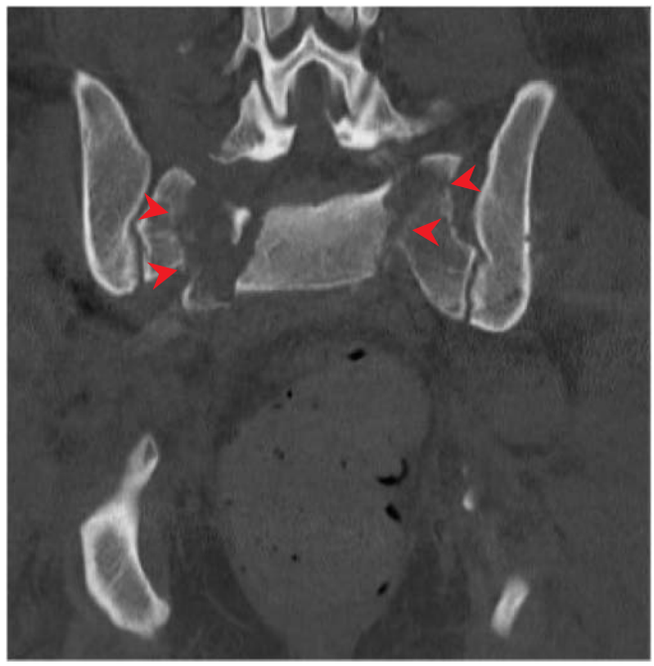


Figure 5.12 CT with coronal reformats showing the vertical orientation of the sacral fractures.

basic principles of force vector however still hold true and the same mechanistic approach should be used to deal with these fractures, which are inherently unstable (Figure 5.12).

Bleeding

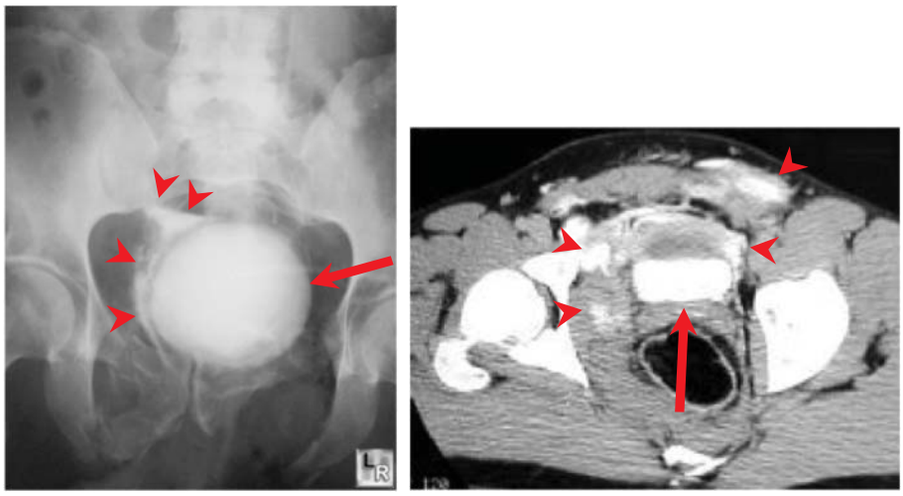
The bony pelvis is extremely vascular and hence it can bleed from the fractures. The mortality from pelvic haemorrhage is about 10–20%. Venous bleeding accounts for 90% of the bleeds. Superior gluteal artery is a large vessel and is commonly injured in posterior pelvic fractures. The obturator and pudendal arteries are injured in fractures involving the pubic rami. The retroperitoneum is a large space and can hold up to about 4 litres of blood. Diastasis of the pubic bone by more than 3 cm can double the pelvic volume.

There is morbidity and mortality associated with all the above mentioned injuries. The mortality rate is about 70% for VS, 20% for APC and about 7% for LC injuries. Haematomas are generally more commonly seen in VS and APC injuries.

Soft tissue injuries

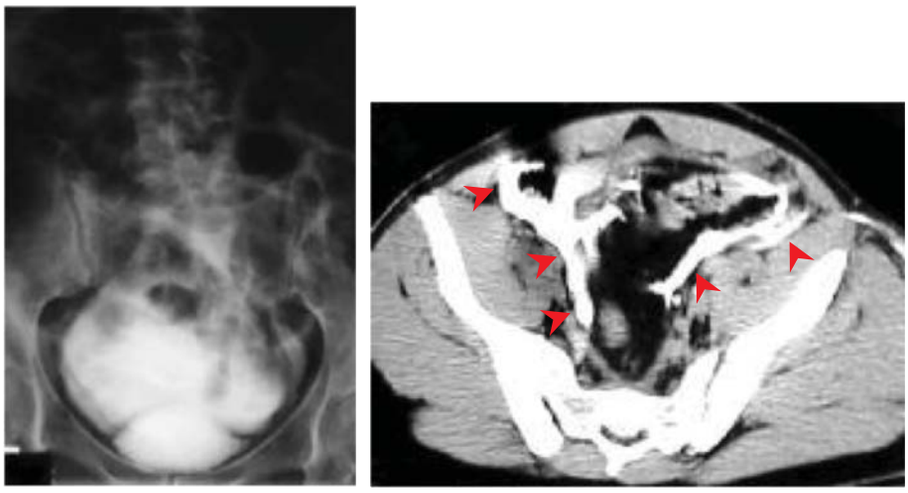
The bony pelvis protects the internal pelvic organs and therefore if there is a fracture,then internal pelvic viscera may be damaged. Pelvic arch fractures have an incidence of about 20% for bladder and urethral injuries. Urethral injuries are more common in males and are seen in about 5–10% of all pelvic fractures. These injuries are seen with diastasis of the symphysis pubis and result from fractures of the inferomedial pubic bone. This may manifest as blood at the tip of the penis.

Extraperitoneal bladder rupture accounts for 80% of bladder injuries and is seen to involve the anterolateral aspect of the bladder



(a) (b)

Figure 5.13 (a, b) Plain X ray with intravesical contrast and corresponding CT showing extraperitoneal bladder rupture.



(a) (b)

Figure 5.14 (a, b) Plain abdominal X ray with intravesical contrast and corresponding CT demonstrates intraperitoneal bladder rupture.

base and is treated conservatively (Figure 5.13). The intraperitoneal rupture (20%) is seen more commonly in children and involves the weaker bladder dome (Figure 5.14). This results in contrast leak into the paracolic regions and is treated surgically.

Hip

AP view of the hip

Adequacy

AP and lateral are the standard views, which are requested when evaluating a patient with a suspected hip fracture. The AP view of the hip is very similar to the AP view of the pelvis except that it is centred lower and includes both hip joints. The reason for this is that similar symptoms may be caused by an injury to the pubic ring on the same or opposite side.

In children additional views like the frog leg lateral view may also be performed as a routine. This is useful for assessing the femoral capital epiphysis on both sides and will show the femoral head and neck in a position in between the AP and lateral views.

Alignment and bones

Check Shenton's line initially. AP view should be analysed in detail for both obvious and more subtle signs of fracture. If no obvious cortical breach is seen, then careful inspection of the bony trabecular pattern should be done. Disruption of bony trabeculae may be the only sign of fracture. Impacted fractures may present as sclerotic lines in the hip and hence should not be disregarded. Rarely, an undisplaced fracture can look completely normal and if the patient is in severe pain and cannot weight bear, then initially a CT or preferably an MRI is indicated.

In early childhood, the trabecula of the femoral neck may produce a striated pattern or unusual lucencies that simulate osteoporosis. If the plain film shows no abnormality in children who present with an irritable hip, other imaging is indicated, and orthopaedic referral is mandatory.

Cartilage and joints

In children, widening of the joint space between the teardrop and the cortex of the femoral head may be seen in joint effusions. A

difference of more than 2 mm between the two sides is important clinically. Check that the physis (growth plate) is symmetrical in appearance and not widened or compressed (Salter-Harris types I and V fractures). Clearly ultrasound is advantageous in children to detect joint effusion, which in a trauma setting would suggest an underlying injury.

Soft tissues

Plain X-rays are usually not very good in assessing the soft tissues around the hip joint. This is due to the large muscle mass around the hip. However, a displaced gluteus medius fat plane is a reliably indicator of an effusion.

Lateral view of the hip

Adequacy

The cross table lateral film should include the acetabulum, ischial spine and tuberosity, and proximal femur. The trochanters should overlap. The lateral view may be difficult to evaluate and is of limited value.

In the frog leg lateral film, the greater trochanter should project over the neck of the femur.

Computed tomography is often the preferred choice if the clinical diagnosis is difficult and initial imaging is equivocal.

Anteroposterior and lateral views of the femoral shaft and knee are indicated in patients with a history of severe trauma or when the clinical findings suggest more than one site of fracture. Gonad protection should always be used in children and adults of reproductive age, as long as it will not obscure a fracture.

Alignment

Femoral neck lies anteverted about 30° to the femoral shaft. Check that the entire metaphysis is covered by the epiphysis in children and adolescents. In a slipped upper femoral epiphysis, the centre of the femoral metaphysis lies anterior to its normal position over the central epiphysis. In patients with dislocated hips, the cross table lateral film will define whether dislocation is anterior or posterior.

Bones

Trace around the margins of the femur and then the acetabulum and ischium. If a dislocation is present, look for acetabular fragments. These are usually displaced in the same direction as the femoral head.

Cartilage and joints

Accessory ossification centres, recognised by their corticated margins, are commonly seen around the acetabular margins and may simulate fractures when partially fused in adolescence. They may persist into adult life. Acetabular roof notches and roof asymmetry are recognised normal variants. Symmetrical protrusion of the acetabular roofs medially is common in children aged 4–12 years.

Hypertrophic changes of the femoral head or inferior aspect of the neck may simulate fractures.

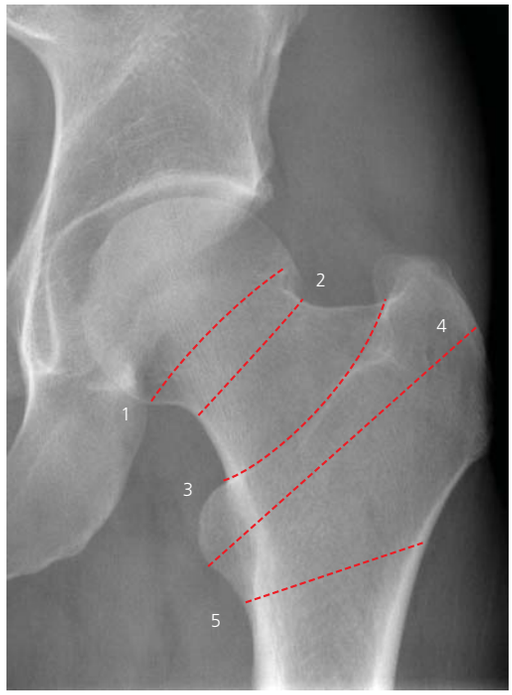


Figure 5.15 Classification of hip fractures. Intracapsular: 1, subcapital; 2, transcervical; 3, basal or basicervical. Extracapsular: 4, transtrochanteric; 5, subtrochanteric.

Soft tissues

Skin folds superimposed over the intertrochanteric region extend past the outer cortical margins, and this differentiates them from fractures.

Femoral neck fractures

Hip fractures are associated with a high morbidity and mortality especially in the elderly population. Mortality in the 1st year after a fracture is 25% and only 25% return to preinjury level of activity. Femoral neck fractures are most often seen after a fall in older women with osteopenia, although they also are seen in younger patients who have sustained major pelvic trauma.

Femoral neck fractures occur at four sites. Fractures may be intracapsular or extracapsular (Box 5.1; Figure 5.15).

Box 5.1 **Hip fractures**

Intracapsular – based on level of neck fracture

- Subcapital
- Transcervical
- Basicervical

Extracapsular – trochanteric fractures

- Intertrochanteric
- Subtrochanteric

Intracapsular fractures are subdivided depending on the level of the fracture in the neck of femur. Extracapsular fractures are also

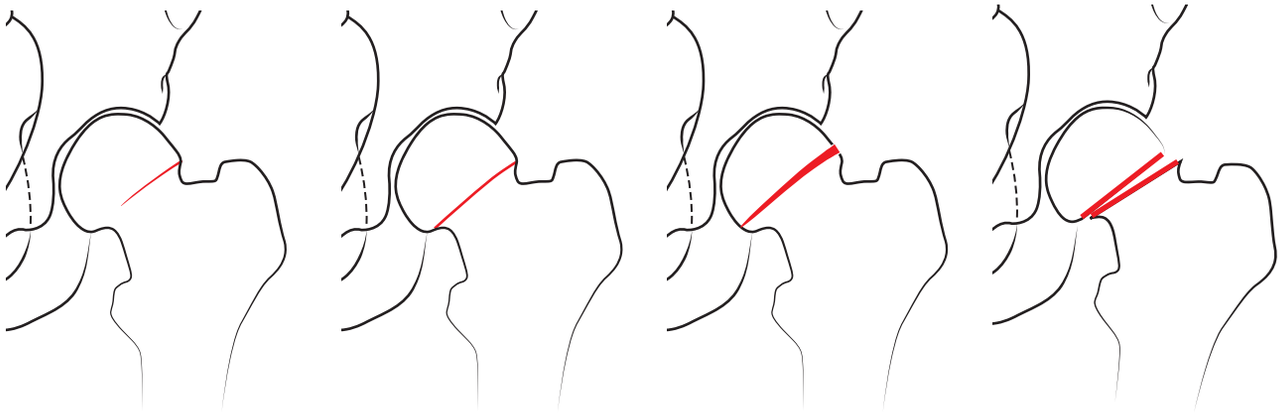


Figure 5.16 Garden classification.

subdivided depending on whether they go through both trochanters (transtrochanteric, intertrochanteric or pertrochanteric) and below the trochanters (subtrochanteric). Transtrochanteric fractures are often comminuted and the lesser trochanter is often displaced.

The fractures are usually visible in the anteroposterior view as a lucent line. The fracture line may be sclerotic if some impaction of the trabeculae has occurred.

The subcapital fractures, which are the most common type of intracapsular fractures are also classified by the severity and extent of the injury (Figure 5.16). This is important because the classification will decide the management of the fracture (Box 5.2).

Box 5.2 **Garden's classification of subcapital fractures**

- Grade I – incomplete fracture (Figure 5.17)
- Grade II – complete fracture but no displacement (Figure 5.18)
- Grade III – some separation of fracture (Figure 5.19)
- Grade IV – complete separation of fracture (Figure 5.20)

In children, considerable violence is needed to fracture the neck of the femur. In transepiphyseal fractures, the femoral capital epiphysis is separated from the metaphysis and dislocated out of the acetabulum; this often results in avascular necrosis (Box 5.3).

Box 5.3 **Delbet classification of femoral neck fractures in children**

- Type 1 – transepiphyseal (avascular necrosis usually follows)
- Type 2 – transcervical (avascular necrosis common if displaced)
- Type 3 – cervicotrochanteric
- Type 4 – pertrochanteric

Acetabular fractures

Acetabular fractures may occur because of injury to the pelvic ring or they may occur separately. Fractures of the posterior rim are usually caused by posterior dislocation of the femur and are



Figure 5.17 Garden type 1 incomplete left NOF fracture.

therefore often seen in APC fractures of the pelvis (Figure 5.21). Less common anterior pillar fractures are seen in APC fractures of the pelvis, usually as a result of direct trauma to the anterior pelvis. Fractures of the quadrilateral plate, however, generally occur after LC fractures and are often part of a more complex pattern of acetabular injury that usually involves the posterior pillar or anterior pillar, or both. Acetabular fractures may be complicated by sciatic nerve palsy and by severe intrapelvic haemorrhage.

It is important to accurately classify the acetabular fractures as it has a direct bearing on the type of surgery to be performed (Box 5.4). Although there are various classification schemes for acetabular fractures, the most commonly used is that by Judet–Letournel. CT is the imaging modality of choice in classifying the acetabular



Figure 5.18 Garden type 2 complete fracture of left NOF.



Figure 5.19 Garden type 3 complete fracture of left NOF with some displacement.

injuries. Although the Judet and Letournel classification includes 10 different types of fractures, there are five fractures which account for 90% of these injuries. These fractures may or may not involve the obturator rings. The detailed explanation of these fractures is beyond the scope of this chapter.

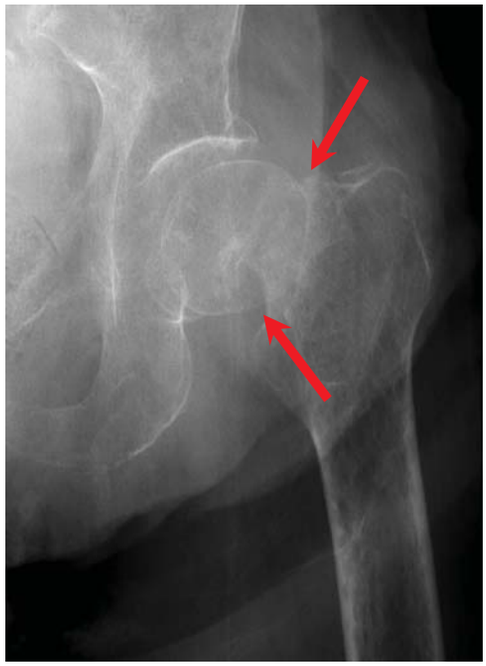


Figure 5.20 Garden type 4 complete fracture of left NOF with complete displacement.

Box 5.4 **Acetabular fractures**

Judet–Letournel Classification of the five common acetabular fractures

- Both column
- T-shaped fracture
- Transverse fracture
- Transverse with posterior wall fracture
- Isolated posterior wall fracture

Dislocation

The femoral head can dislocate anteriorly, posteriorly or centrally (Box 5.5). Central dislocation occurs when the femoral head impacts through the acetabulum because of lateral compression injury from a sideways fall or a blow to the greater trochanter. Falling onto the feet is often associated with a vertical fracture of the anterior or posterior pelvic columns. Posterior dislocation may result from a blow to the lumbar spine with the hip flexed – for example, from falling masonry. Dashboard injury in motor vehicle accidents

Box 5.5 **Complications of hip dislocation**

- Slipped femoral epiphysis (unfused skeleton)
- Sciatic nerve palsy
- Femoral nerve or artery compression (anterior dislocation)
- Failed reduction and recurrent dislocation
- Avascular necrosis of the femoral head
- Osteoarthritis
- Myositis ossificans
- Femoral head, neck or shaft fractures in major trauma



(a) (b)

Figure 5.21 (a, b) AP and oblique view demonstrating a right acetabular fracture with involvement of roof posteriorly.

results in posterior dislocation of the hip and is often associated with fracture of the femoral shaft or patella.

Congenital dislocation of the hip

Successful treatment depends on correct and early recognition of congenital dislocation of the hip (CDH). Ultrasonography is the imaging modality of choice in diagnosis of CDH; however, diagnosis can be made from plain radiographs. At birth, the femoral epiphysis is not ossified, but the acetabular roof is often abnormal, with notching laterally and an increased acetabular angle. Once the epiphysis is ossified, the disorder becomes obvious from radiography.

Idiopathic coxa vara

Idiopathic coxa vara is part of a spectrum of conditions known as proximal femoral focal deficiency (PFFD) of which two types exist: congenital and infantile. Lesions are usually bilateral and present with coxa vara with epiphysis that are low lying and look 'woolly', and there is epiphyseal or metaphyseal lucency.

Slipped capital femoral epiphysis (adolescent coxa vara)

In this condition, the femoral neck moves proximally and externally rotates on the unfused epiphysis. In 20% of cases the condition is bilateral, and it occurs in overweight, hypogonadal, or tall but thin adolescents. Pain sometimes referred to the knee, or limp is a common presenting symptom. Both hips should be evaluated. Early slip is best assessed in the frog leg lateral film. The plain X-ray findings of this condition include indistinct epiphysis with associated widening; a line drawn along the lateral margin of the neck of the femur does not intersect the femoral head epiphysis. These patients are prone to avascular necrosis and degenerative arthritis.

ABCs systematic assessment

Adequacy

- Use one view for the pelvis and two views for the hips
- Ensure that all the pelvis and hips are visible
- Use a bright light to look at radiographs or
- Adjust windows on PACS

Alignment

- Check three rings
- Check SIJs and pubis
- Check Shenton's line
- Bone
- Check each bone carefully
- Check the trabecular lines
- If there is one pelvic ring fracture, look for a second

Cartilage and joints

- Check the pubic symphysis
- Check the sacroiliac joints
- Check the hip joints and acetabulum

Soft tissues

- Check the obturator internus fat planes inside the pelvis
- Check the perivesical fat plane
- Check the gluteus medius fat plane
- Check the femoral pulses and sciatic nerve

Further reading

Judet R, Judet J, Letournel E. Fractures of the acetabulum: classification and surgical approaches for open reduction – preliminary report. *J Bone Joint Surg Am* 1964;46:1615–1646.

Letournel E, Judet R. *Fractures of the Acetabulum*, 2nd edn. Heidelberg, Germany: Springer-Verlag, 1993.

Lloyd E, Stambaugh, CC Blackmore. Pelvic ring disruption in emergency radiology. *Eur J Radiol* October 2003;48: 1:71–87.

Lyons AR. Clinical outcomes and treatment of hip fractures. *Am J Med* 1997;103:S51–S63.

Their, M.E, Bensch, F.V, Koskien, S. K, Handolin, L, Kiuru, M.J. Diagnostic value of pelvic radiography in the initial trauma series in blunt trauma. *Eur Radiol* 2005 Aug;15(8):1533–1537.

CHAPTER 6

Knee

Lisa Meacock and David A. Elias

King's College Hospital, London, UK

OVERVIEW

- Conventional radiographs are useful in the acute setting
- Significant internal derangement can occur with normal XRs
- A lipohaemoarthrosis indicates an intra-articular fracture
- Popliteal artery injuries have to be excluded in supracondylar fractures and femorotibial dislocations
- CT should be performed for intra-articular fractures and in pre-operative planning
- If internal derangement is suspected, then MRI should be performed
- Ultrasound is rarely indicated in acute trauma except in suspected extensor injuries

Conventional radiographs (XRs) are initially performed for knee trauma but severe injuries may be present with little or no abnormality on XRs. If XRs show a lipohaemarthrosis, then CT or MRI is indicated to confirm the intra-articular fracture and potential associated injuries. If internal knee derangement is suspected, then MRI should be requested. MRI allows comprehensive assessment of soft tissue and bony injuries. CT is indicated for suspected intra-articular fractures and in pre-operative planning of complex bony injuries. In supracondylar fractures and knee dislocations, popliteal artery injuries need to be excluded, generally using CT angiography.

Anatomy

The knee is a hinge-type synovial joint formed by the articulation between the femoral condyles and tibial plateau. The two bones are separated by two C-shaped fibrocartilaginous structures: the medial and lateral menisci. The patella is a large sesamoid bone in the knee extensor mechanism. The quadriceps muscles form the quadriceps tendon, which inserts into the superior pole of the patella. The patella ligament extends from the inferior patella pole to insert onto the tibial tuberosity. The posterior surface of the patella articulates with the trochlear groove on the anterior surface of the femoral condyles and forms the patellofemoral joint (PFJ). The fibular head and posterolateral proximal tibia articulate at the proximal tibiofibular joint (Table 6.1).

Ligaments and musculotendinous structures provide the knee with stability (Table 6.2; Figure 6.1). The knee is surrounded by multiple bursae. The suprapatellar bursa is continuous with the knee joint and distends in the presence of a joint effusion. It lies between the suprapatellar fat and prefemoral fat above the level of the patella (Figure 6.3).

Table 6.1 Timing of appearance and fusion of the secondary ossification centres about the knee.

Bone	Secondary ossification centre	Age (years)	
		At formation	At fusion
Femur	Distal femoral epiphysis	Birth–2 months	15–17
Tibia	Proximal tibial epiphysis	Birth–2 months	15–17
	Tibial tuberosity apophysis	8–14	15 (with metaphysis)
Patella	May have multiple centres	3–6	

Table 6.2 Main supporting ligaments and musculotendinous structures of the knee.

Structure	Origin	Insertion	Primary function
Anterior cruciate ligament (ACL)	Posterolateral aspect of roof of intercondylar notch of femur	Anterior intercondylar eminence of tibia	Resists anterior translation and internal rotation of tibia
Posterior cruciate ligament (PCL)	Anteromedial intercondylar notch of femur	Posterior tibial eminence	Resists posterior translation and external rotation of tibia
Medial collateral ligament (MCL)	Medial epicondyle of femur	Medial proximal tibial metaphysis	Resists valgus stress
Lateral collateral ligament	Lateral epicondyle of femur	Fibular head	Resists varus stress
Quadriceps mechanism	Anterior pelvis and proximal femur	Tibial tuberosity (via patellar)	Knee extension and patellar stabilisation

ABC of Emergency Radiology, Third Edition. Edited by Otto Chan.
© 2013 John Wiley & Sons, Ltd. Published 2013 by John Wiley & Sons, Ltd.

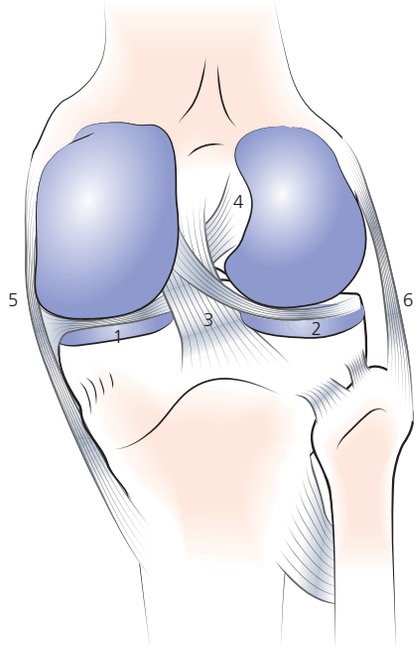


Figure 6.1 The posterior knee demonstrating normal ligaments and menisci: 1, medial meniscus; 2, lateral meniscus; 3, posterior cruciate ligament; 4, anterior cruciate ligament; 5, medial collateral ligament; 6, lateral collateral ligament.

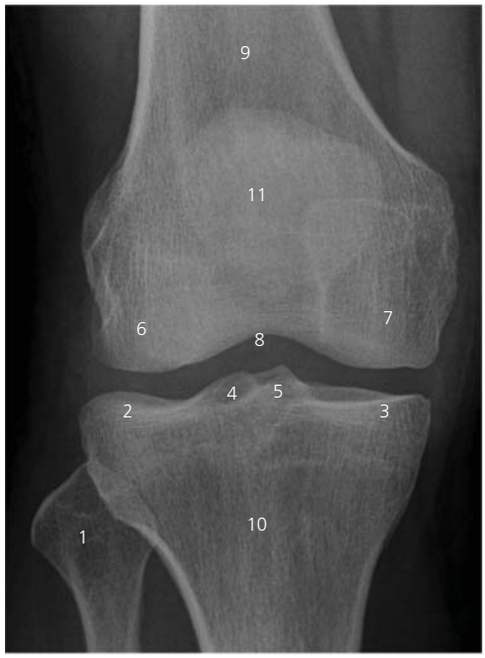


Figure 6.2 Normal anteroposterior radiograph of the right knee in an adult: 1, fibular head; 2 lateral tibial plateau; 3, medial tibial plateau; 4 and 5, lateral and medial tibial spines; 6, lateral femoral condyle; 7, medial femoral condyle; 8, intercondylar notch; 9, femur; 10, tibia; 11, patella.

Radiographic views

- Anteroposterior (AP) (Figure 6.2) and lateral (lat) (Figure 6.3) projections are standard
- A skyline view (Figure 6.4) allows assessment of the patellofemoral articulation
- A tunnel or notch view is valuable to look at the intercondylar notch and to identify osteochondral fractures or intra-articular bodies
- Oblique views in internal and external rotation allow further evaluation of tibial plateau fractures and of the proximal tibiofibular joint

ABCs systematic assessment

- Adequacy – check correct views have been obtained
- Alignment – check femorotibial alignment and patellar height
- Bones – trace the contours of all the bones
- Cartilage and joints – joint spaces should be uniform in width
- Soft tissues – change windows to look for soft tissue swelling, effusion, and fat/fluid level

Adequacy

Routine AP and lat views should be obtained. Following acute trauma, the lat view should be performed with a horizontal beam so that a fat-fluid level can be identified. View the lat view first.

Lateral view

Soft tissues (on this occasion, S before ABC!)

Separation of the suprapatellar and prefemoral fat pads (>5 mm) indicates an effusion (Figure 6.5). The presence of a fat-fluid level (lipohaemathrosis) within the joint is pathognomonic of an intra-articular fracture (causing bleeding and therefore a haemoarthrosis), with leakage of marrow fat into the joint (hence the lipohaemoarthosis) (Figure 6.6).

Alignment

On a lateral view, anterior tibial displacement indicates rupture of the anterior cruciate ligament, while posterior displacement indicates rupture of the posterior cruciate ligament.

On a lateral view with the knee in 20–30° flexion, the ratio of the patella tendon length to patella length should be in the range 0.8–1.2 (Figure 6.7). A high riding patella (patella alta) may be a congenital variant or the result of rupture of the patella tendon (Figure 6.8). A low riding patella (patella baja) may be a congenital variant or the result of rupture of the quadriceps tendon.

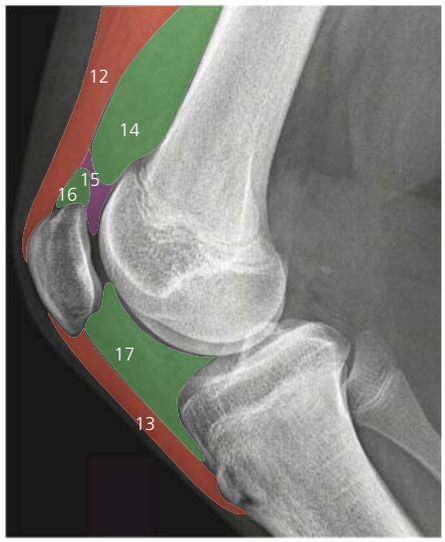
On the AP view, a line through the lateral edge of the lateral femoral condyle (lateral tibial line) should run to the lateral edge of the lateral tibial plateau. A significant step usually indicates a tibial plateau fracture (Figure 6.9).

Bone

The cortices of the femur, tibia, patella, and fibula should be smooth, with no disruption of the trabecular pattern within the



(a)



(b)

Figure 6.3 Normal lateral knee radiograph of an adolescent. (a) 1, Fibula; 2 and 3, tibial spines; 4 and 5, lateral and medial femoral condyles (overlapping); 6, roof of intercondylar notch; 7, femur; 8, distal femoral growth plate; 9, patella; 10, tibial tuberosity; 11, fabella (sesamoid bone in the lateral head of gastrocnemius); (b) 12, quadriceps tendon (and distal muscle belly); 13, patellar ligament; 14, prefemoral fat pad; 15, suprapatella bursa; 16, suprapatella fat pad; 17, Hoffa's fat pad.

bones. Tibial plateau fractures may be identifiable as a subtle sclerotic line or subtle step defect only. A careful search should be made for intra-articular bodies, and for certain bony avulsions which may indicate significant ligamentous injuries.

Cartilage and joints

The joint spaces in the medial and lateral compartments may be assessed on the AP view for height (reduced height may be the result of knee flexion or cartilage loss or arthritis) and for chondrocalcinosis (linear calcification within the cartilage, which may occur in numerous conditions).



Figure 6.4 Normal skyline view of the right knee in an adult: 1, lateral patellar facet; 2, lateral trochlear facet (anterior lateral femoral condyle; 3, medial patellar facet; 4, medial trochlear facet (anterior medial femoral condyle).



Figure 6.5 Lateral radiograph of the knee in a 13-year-old boy following acute knee injury. There is a large effusion (arrows). Note how the effusion separates the suprapatellar (P) from the prefemoral fat pad (F).

Injuries

Distal femur

Femoral shaft fractures occur with considerable force. Anteroposterior and lateral views of the whole femur are essential to identify displacement and rotation.

Supracondylar fractures

These fractures may have a variety of configurations. Evidence of intra-articular extension of the fracture line should be sought, as



Figure 6.6 Horizontal beam lateral radiograph of the knee in a patient with a tibial plateau fracture following a road traffic accident. Note the lipohaemarthrosis (fat-fluid level – arrows), which indicates the presence of an intra-articular fracture. The comminuted tibial plateau and associated fibular head fracture are also identified.



Figure 6.7 Lateral view of a normal knee demonstrating measurement of the Insall Salvati ratio for patellar height. The ratio is measured as the patellar ligament length divided by the maximum patellar length and the ratio normally lies in the range 0.8–1.2.

this necessitates open reduction and internal fixation. The distal fragment may be angulated by the pull of gastrocnemius, and displacement can result in popliteal artery injury. Occasionally, supracondylar fractures are associated with fracture dislocations of the hip or tibial shaft (Figure 6.10).

Femoral condylar fractures

These fractures may show displacement or comminution and are often seen best with computed tomography. Shearing or rotatory

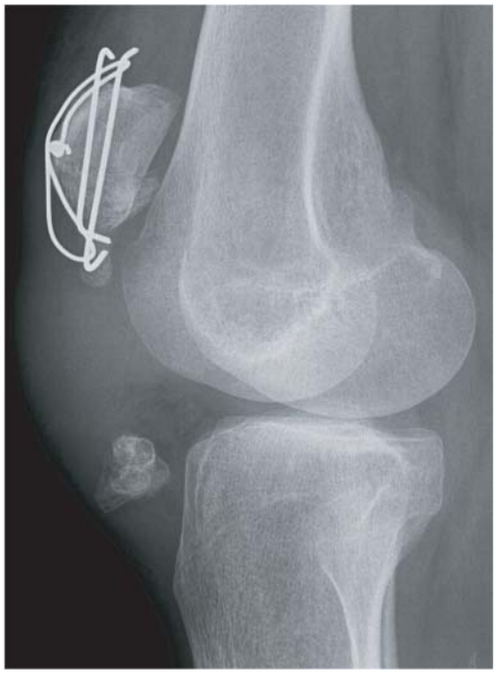


Figure 6.8 Lateral radiograph of the knee in a patient with an old patellar fracture which was fixed with two K-wires and a tension band wire. Following a recurrent injury, the patellar ligament ruptured resulting in patellar alta with ossific fragments in the disrupted ligament.



Figure 6.9 AP radiograph of the knee in a patient showing a comminuted tibial plateau fracture following a road traffic accident. Note the malalignment with a large step between the lateral margin of the lateral femoral and the lateral margin of the tibial plateau.



(a) (b)

Figure 6.10 Coronal plane reformatted CT image of the knee (a) and 3D volume rendered CT arteriogram (b) in a patient with a supracondylar fracture following a motorcycle accident. There is a traumatic avulsion of the origin of the anterior tibial artery (arrow) in association with the fracture.

forces directed at the articular surface of a femoral condyle may produce fractures, known as osteochondral fractures, through the cartilage and subchondral bone. These are often occult on conventional radiographs, but irregularity in the articular surface may be present and intra-articular fragments of bone may be seen (Figure 6.11).

Acute osteochondral fractures should be distinguished from osteochondritis dissecans.

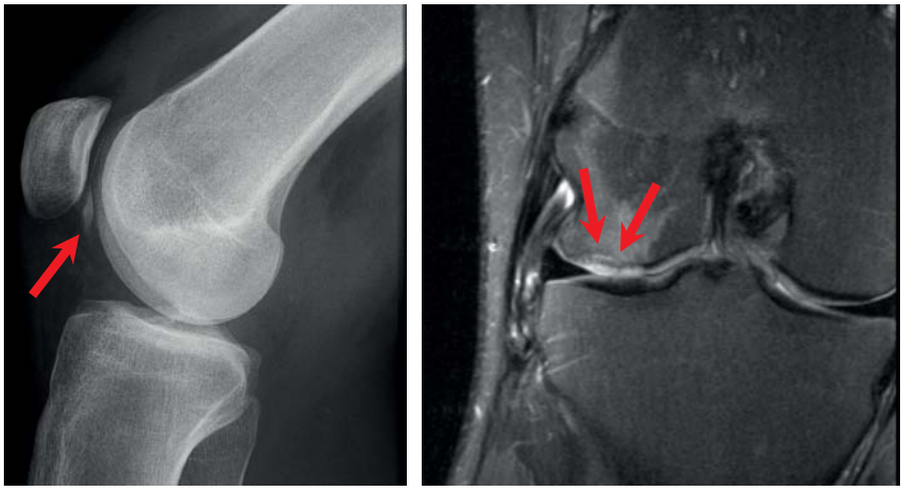
Osteochondritis dissecans

This occurs in adolescents at the lateral margin of the medial femoral condyle, and there may be a separated osteochondral fragment with sclerotic margins. The aetiology of this condition is controversial, but it may involve trauma (Figure 6.12).

Proximal tibia and fibula

Tibial plateau fractures

These fractures occur most often in women >50 years, usually after twisting falls (Figure 6.13). Typically, valgus force is encountered, with impaction of the femoral condyle on the plateau, and involvement is confined to the lateral plateau in 75–80% of cases. Less than 25% of cases are the result of RTA and these typically result from the bumper of a car striking the knee. These fractures are often subtle, and AP and lat radiographs need careful examination.



(a) (b)

Figure 6.11 (a) Lateral knee radiograph and (b) coronal intermediate density fat saturated MR image of a patient with an acute osteochondral fracture. Note the ossific body in the knee joint on the lateral radiograph with a joint small effusion. On the MRI the corresponding osteochondral defect is seen in the lateral femoral condyle (arrows) with underlying marrow oedema.



Figure 6.12 Notch view of a 13-year-old boy with osteochondritis dissecans. Note the typical osteochondral defect at the lateral aspect of the medial femoral condyle.

Computed tomography is valuable, as the degree of depression of the fracture determines the need for surgery, and this is difficult to assess on conventional radiographs. Alternatively, magnetic resonance imaging may be used to assess these injuries; it also shows associated ligamentous and meniscal injuries, which are reported in 68–97% of cases.

Tibial stress fractures

These fractures may be seen as transversely orientated sclerotic or lucent lines, with adjacent sclerosis in the medulla of the medial proximal tibial metaphysis extending to the cortex (Figure 6.14). The patient may show evidence of osteoporosis.

Proximal fibular fractures

Fibula head fractures may be isolated injuries that result from a direct blow, but they are associated most often with tibial plateau fractures. A fracture of the fibula neck or proximal shaft may suggest the presence of an associated ankle joint injury (Maisonneuve). Proximal fibular fractures may be associated with common peroneal nerve injury.

Patella

Fractures

These fractures may be caused by a direct blow or by excessive quadriceps contraction during forced knee flexion. Fractures may be transverse, vertical, or comminuted, with or without displacement. A bipartite patella is a normal variant, which lies at the superolateral aspect of the patella, and which can be confused with a fracture (Figure 6.15).

Patella dislocation

Dislocation of the patella is almost always in the lateral direction and classically occurs in teenage girls. Dislocation is usually transient



(a) (b) (c) (d)

Figure 6.13 Lateral tibial plateau fracture following a fall. The lateral radiograph demonstrates a large effusion with a lipohaemarthrosis but the fracture is relatively occult on both the lateral and AP radiographs (a and b). Subtle lucency is present on the AP radiograph at the site of fracture. The sagittal CT reformat (c) and 3D volume rendered CT image (d) demonstrate the lateral tibial plateau fracture and the extent of its depression.



Figure 6.14 Lateral radiograph of the tibia in a runner with a chronic tibial stress fracture. A typical horizontal lucency is seen in the anterior cortex.



Figure 6.15 AP radiograph of a normal knee which shows a normal variant of a bipartite patella. There is a separated ossific fragment at the superolateral aspect of the patella and this should not be confused with a fracture.



Figure 6.16 AP radiograph of the knee in a patient with acute lateral patellar dislocation. Generally dislocations are transient and it is unusual to present with a persistent dislocation in this way.



Figure 6.17 Axial CT image through the knee in a patient with previous transient lateral patellar dislocation. The patellar is laterally subluxed and there is a separated avulsion fracture off the medial patellar margin.



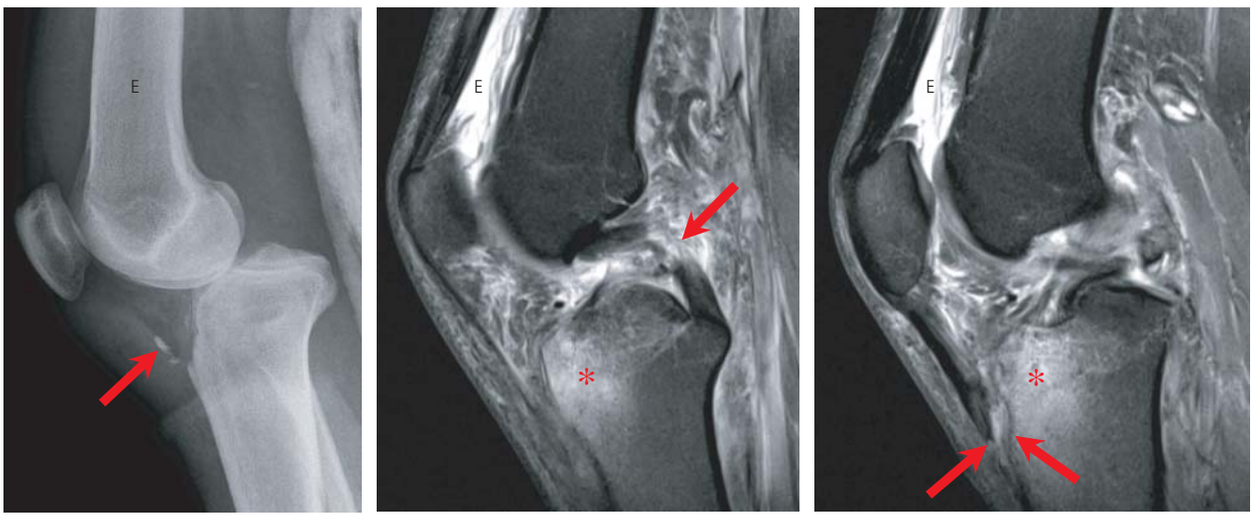
Figure 6.18 AP radiograph of a knee dislocation following a road traffic accident. Such injuries have a significant association with popliteal arterial injury.

and presents with non-specific acute haemarthrosis (Figure 6.16). In many patients dislocation becomes recurrent. Radiographs after injury rarely show a dislocated patella, as the patella has usually been reduced by the time the radiograph has been taken. Usually, plain radiographs are normal apart from a joint effusion. A skyline view occasionally shows osteochondral injury, with fragments separated from the medial aspect of the patella or the anterior tip of the lateral femoral condyle, or both, as a result of impaction of the cortices at the time of transient dislocation (Figure 6.17).

Table 6.3 Some signs of ligamentous injury visible on conventional radiographs of knee.

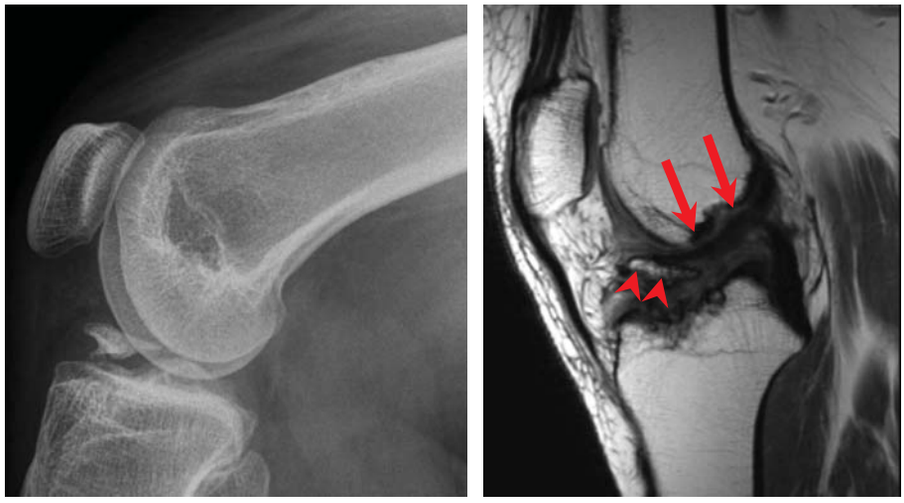
Ligament	Sign of injury	Cause
ACL	Avulsion of anterior tibial eminence	Avulsion of anterior cruciate ligament
	Segond fracture	Lateral capsular ligament avulsion producing a small avulsion fragment at the lateral tibial plateau (>75% associated with injuries of anterior cruciate ligament)
	Deep notch	Impaction of notch of lateral femoral condyle against posterior tibial plateau during injury of anterior cruciate ligament
PCL	Avulsion of posterior tibial eminence	Avulsion of tibial attachment of PCL
MCL	Pellegrini-Stieda lesion	Chronic recurrent injury of medial collateral ligament: shows linear calcification over the medial supracondylar edge
LCL	Avulsion of lateral epicondyle	Avulsion of lateral collateral ligament
QT	Avulsion of superior or inferior patella pole	Quadriceps contraction causing avulsion of distal quadriceps or proximal patella tendon
	Avulsion of tibial tuberosity[a]	Quadriceps contraction causing avulsion of distal patella tendon

[a]This should be distinguished from Osgood-Schlatter's disease, a chronic condition occurring in adolescents characterised by anterior knee pain and fragmentation of the tibial tuberosity, with overlying soft tissue swelling.



(a) (b) (c)

Figure 6.19 Lateral radiograph of the knee (a) of a patient with knee dislocation following a road traffic accident. The tibia is posteriorly dislocated. Note the bony fragments (arrow) which indicate bony avulsion of the patellar ligament from the tibial tuberosity. There is a joint effusion ('E'). The corresponding sagittal intermediate density fat saturated MR images (b, c) demonstrate a mid substance tear of the posterior cruciate ligament (arrows) and bony avulsion of the distal patellar ligament (arrowheads), as well as extensive marrow contusion at the tibial tuberosity (asterisk).



(a) (b)

Figure 6.20 Lateral radiograph of the knee (a) in a patient with a chronic anterior cruciate ligament (ACL) avulsion. The tibial bony footplate is avulsed and lies in the anterior intercondylar notch. The corresponding sagittal proton density MR image (b) demonstrates the bony avulsion fragment (arrowheads) with the attached ACL fibres (arrows).



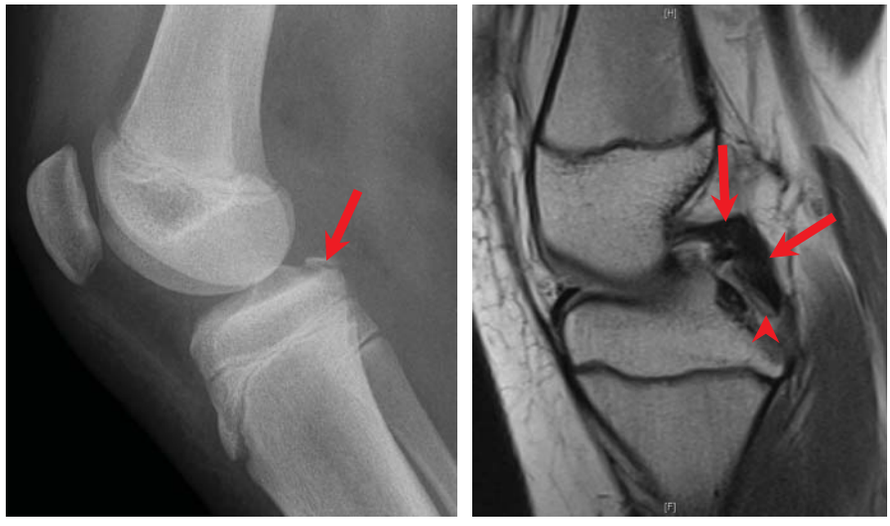
Figure 6.21 AP radiograph of the knee in a patient with an acute anterior cruciate ligament (ACL) tear demonstrating a Segond fracture (arrow) of the lateral tibial plateau which is typically associated with ACL injury.

Knee dislocation

Dislocation of the knee is rare. Most commonly, anterior translation of the tibia on the femur is present, and the risk of popliteal artery and peroneal nerve injury is considerable (Figure 6.18). True knee dislocation is invariably associated with rupture of multiple ligaments, but plain radiographs are often misleading, with little or no abnormality visible, apart from a joint effusion (Figure 6.19). Magnetic resonance imaging should be performed to evaluate associated injuries.

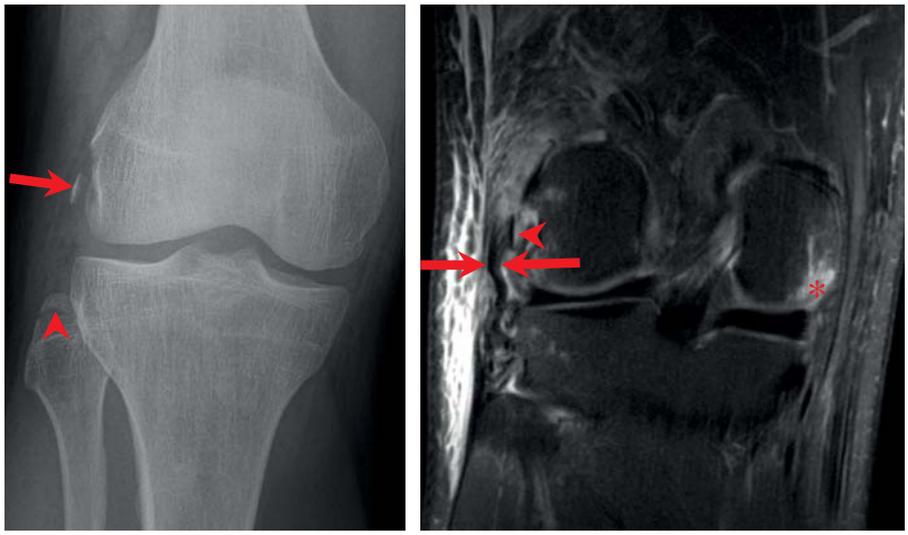
Avulsion fractures and signs of ligamentous injury

Injury to ligamentous structures about the knee usually shows clinical signs of instability and a knee effusion. Avulsion fractures occasionally provide relatively specific evidence of particular ligamentous injuries (Figures 6.19–6.23; Table 6.3).



(a) (b)

Figure 6.22 Lateral radiograph of a knee (a) with bony avulsion of the posterior cruciate ligament (PCL). Note the typical elevated bony fragment (arrow) from the posterior margin of the intercondylar region of the tibia. The corresponding sagittal proton density MR image (b) demonstrates the bony fragment (arrowhead) with the attached PCL fibres (arrows).



(a) (b)

Figure 6.23 AP radiograph of the knee (a) in a patient with lateral collateral ligament avulsion following a fall from a height. Note the bony avulsion fragment from the lateral epicondyle (arrow) there is also a fibular head fracture due to posterolateral corner injury (arrowhead). The corresponding coronal intermediate density fat saturated MR image (b) shows the bony fragment (arrowhead) with the attached retracted lateral collateral ligament (arrows). Medial femoral condylar marrow contusion (asterisk) and lateral soft tissue bruising is also seen.

ABCs systematic assessment

Easy 'AS ABC'!

Adequacy

- Minimum of lateral and AP views; lateral should be horizontal beam in acute trauma

Soft tissues

- Lipohaemarthrosis (fat-fluid level) indicates intra-articular fracture

Alignment

- Tibiofemoral alignment – anterior tibial displacement indicates ACL disruption; posterior tibial displacement indicates PCL disruption
- Patellar height – high riding patella ('alta') may indicate a congenital variant or patellar ligament disruption; low riding patella ('baja') may be a congenital variant or indicate quadriceps disruption

Bones

- Tibial plateau fractures may appear as subtle linear lucency or sclerosis
- Small bony fragments may represent significant ligamentous avulsions

Cartilage

- Joint space loss may be due to meniscal or hyaline cartilage injury.

Further reading

Gottsegen CJ, Eyer BA, White EA, Learch TJ, Forrester D. Avulsion fractures of the knee: imaging findings and clinical significance. *Radiographics* 2008;28:1755–70.

Kapur S, Wissman RD, Robertson M, Verma S, Kreeger MC, Oostveen RJ. Acute knee dislocation: review of an elusive entity. *Curr Probl Diagn Radiol* 2009;38:237–50.

Miller LS, Yu JS. Radiographic indicators of acute ligament injuries of the knee: a mechanistic approach. *Emerg Radiol* 2010 Nov;17:435–44.

Rogers LF (Ed.). The Knee in: *Radiology of Skeletal Trauma*, 3rd edn. New York: Churchill Livingstone, 2002.

CHAPTER 7

Ankle and Foot

Tudor Hughes

University of California, San Diego, CA, USA

OVERVIEW

- Ankle and foot injuries are very common – use OTTAWA rules
- Meticulous assessment essential to avoid disastrous consequences
- Remember 7 review areas in a 'normal' radiograph
- CT, MRI or US should be requested where appropriate

Trauma to the ankle and foot is one of the most common reasons that people attend emergency departments. A spectrum of injuries can occur; from sprains through fractures to dislocations. The decision to obtain radiographs is made by careful clinical examination and knowledge of the mechanism of injury. The use of certain guidelines (such as the Ottawa rules, Box 7.1) will exclude serious injuries while reducing unnecessary exposure of the patient to radiation. A higher index of suspicion is needed in elderly.

Box 7.1 **Ottawa rules**

- Bone tenderness along the distal 6 cm of the posterior edge of the tibia or fibula
- Bone tenderness of the medial or lateral malleoli
- Bone tenderness at the base of the fifth metatarsal or the navicular
- An inability to bear weight immediately or in the emergency department

Injuries of the feet often result in a request for radiographs of the ankle and foot. Clinically, it should be possible to distinguish which area has been injured, and imaging of both is rarely needed. Injuries to the feet, however, often masquerade as ankle injuries.

Anatomy

The ankle (Figure 7.1a–f) is a virtual hinge joint shaped as a mortice. The tibia and fibula form a ring with the proximal and distal tibiofibular joints.

ABC of Emergency Radiology, Third Edition. Edited by Otto Chan.
© 2013 John Wiley & Sons, Ltd. Published 2013 by John Wiley & Sons, Ltd.

The bony structure of the ankle is stabilised by three main groups of ligaments:

- Medial collateral ligament complex (deltoid ligament)
- Lateral collateral ligament, which includes anterior talofibular, posterior talofibular and calcaneofibular ligaments
- Tibiofibular syndesmotic complex.

The talus articulates inferiorly with the calcaneus and anteriorly with the navicular. It is made up of a body, neck, and anterior process and has a fragile blood supply that extends through the ankle joint capsule, which means that fractures of the talar neck may result in avascular necrosis of the body.

The foot (Figure 7.2a,b) is a complex structure of interdependent bones designed for weight bearing and movement. It can be divided into the forefoot, midfoot, and hindfoot. The joints are complex, but the articular surfaces are parallel and the joint spaces equidistant and symmetrical. Loss of articular parallelism and alteration of joint space width is always abnormal.

Normal variants

Radiographs may show variation from the normal anatomy because of the presence of sesamoids, fused or partly fused bones, or accessory ossification centres (Figure 7.3a,b). Although these are normal variants, they can also be the sites of pathology. Commonly occurring ossicles are the os tibiale externum (medial to the navicular), os trigonum (posterior to the talus), and os peroneum (adjacent to the cuboid).

ABCs systematic assessment

- Adequacy
- Alignment
- Bone
- Cartilage and joints
- Soft tissues

Adequacy

Standard imaging of the ankle in the emergency department should include anteroposterior (AP), mortice and lateral projections and for the foot AP, oblique and lateral. Weight-bearing views are

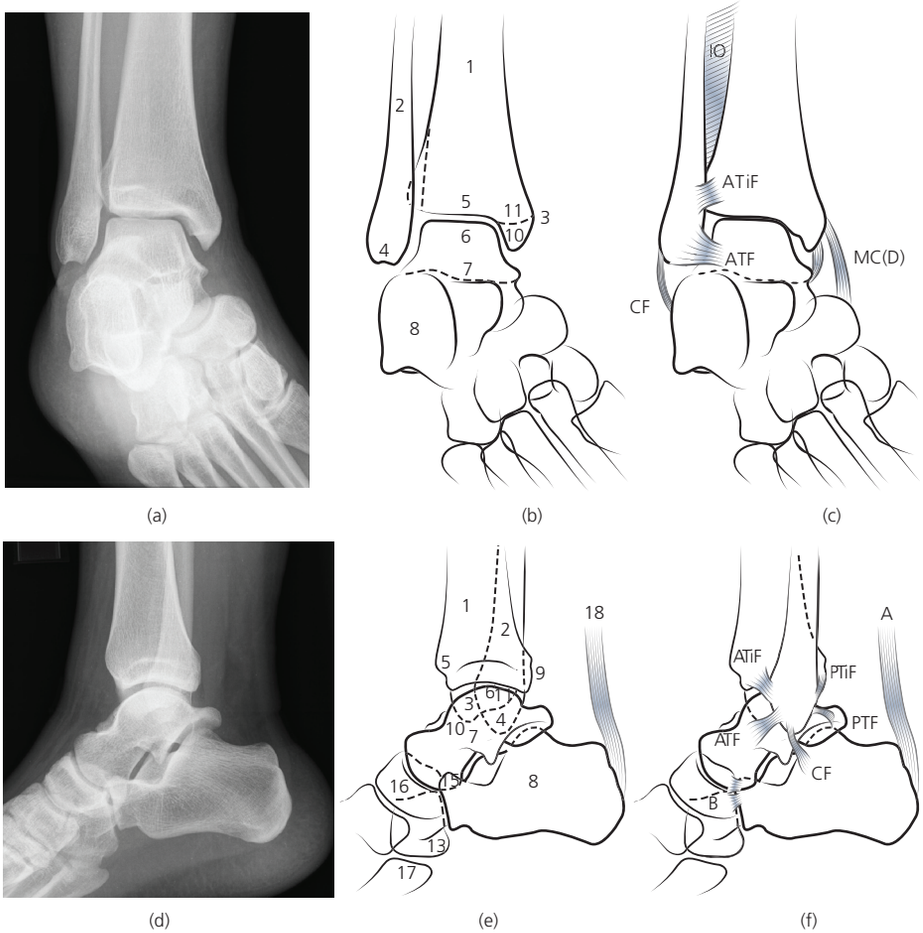


Figure 7.1 (a),(b) AP view of ankle and drawing: (1), Tibia; (2), fibula; 3, medial malleolus; 4, lateral malleolus; 5, plafond; 6, dome; 7, talus; 8, calcaneum; 9, posterior malleolus; 10, anterior colliculus; 11, posterior colliculus. (c) AP ankle ligaments: A, Achilles tendon; ATiF, anterior tibiofibular; ATF, anterior talofibular; B, bifurcate; CF, calcaneofibular; D, deltoid; IO, interosseous; MC, medial collateral; PTiF, posterior tibiofibular; PTF, posterior talofibular. (d),(e) Lat view of ankle and drawing: 1, tibia; 2, fibula; 3, medial malleolus; 4, lateral malleolus; 5, plafond; 6, dome; 7, talus; 8, calcaneum; 9, posterior malleolus; 10, anterior colliculus; 11, posterior colliculus; 12, anterior tubercle; 13, peroneal groove; 14, cuboid; 15, anterior process; 16, navicular; 17, base of fifth metatarsal; 18, Achilles tendon. (f) Lat ankle ligaments.

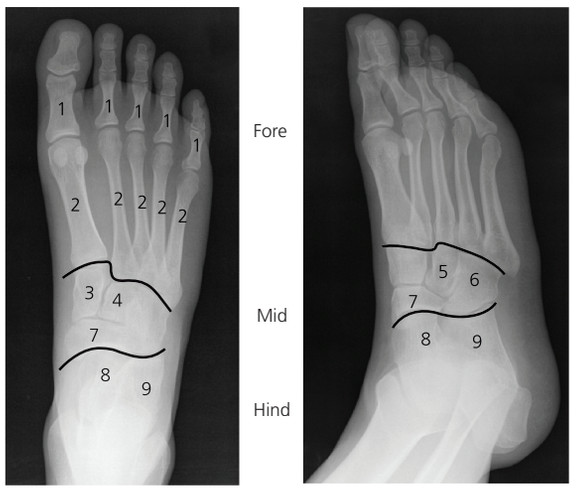


Figure 7.2 (a) AP view and (b) oblique view of foot. Forefoot: 1, phalanges; 2, Metatarsals. Midfoot: cuneiforms – 3, medial; 4, middle; 5, lateral; 6, cuboid; 7, navicula. Hindfoot: 8, talus; 9, calcaneum.

better when tolerable. If the pain is in the heel, lateral and axial (Harris) views of the heel are indicated. Advanced imaging should be performed only after consultation with a radiologist.

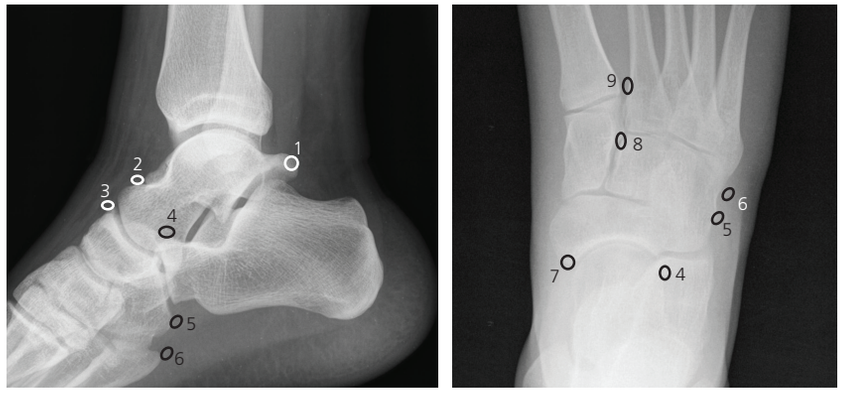
Not all bones and joints will be seen clearly on one view, so multiple views will be needed (Figure 7.4a,b). Some injuries are visualised poorly on radiography, and computed tomography or other types of imaging may be needed (Box 7.2).

Box 7.2

- US – Used to assess soft tissues, muscles, tendons and ligaments and for intervention; very operator dependent
- CT – Axial slices obtained with multiplanar reconstruction; good for looking at bones, bone bars and fractures
- MRI – Highly sensitive and specific; shows pathology in bones, joints, and soft tissues; multiplanar imaging, usually axial, sagittal and coronal
- Isotopes – Increase of isotope uptake in bones is a non-specific, highly sensitive indicator of disease

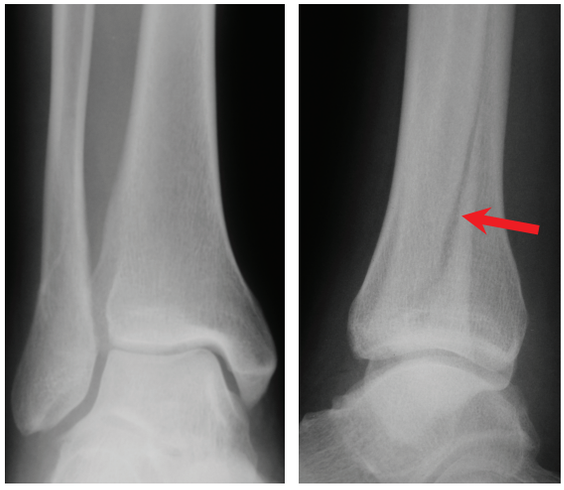
Alignment

On the anteroposterior view, the uniform distance between the tibiotalar and fibulotalar joints should be <4 mm in adults. On the lateral view, the long axis of the tibia and fibula should overlap.



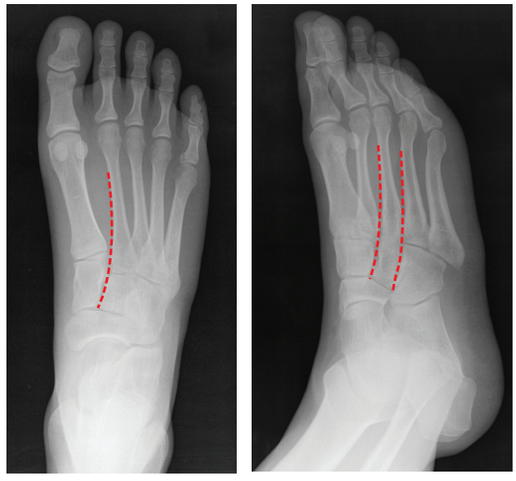
(a) (b)

Figure 7.3 (a),(b) Common accessory ossicles: 1, os trigonum; 2, os supratalare; 3, os supranaviculare; 4, os calcaneum secundarius; 5, os perineum; 6, os vesalaneum; 7, os tibiale externum; 8, os intercuneiforme; 9, os intermetatarseum.



(a) (b)

Figure 7.4 (a) AP view (right) 'normal'; (b) lat view – there is clearly an oblique fracture of the fibular shaft only seen in this view (arrow).



(a) (b)

Figure 7.5 The alignment of the midfoot is best assessed on standing views. On the AP (dorsoplantar) view (a) the medial side of the 2nd metatarsal should always align with the medial side of the middle cuneiform. On the AP pronation oblique view (b) the medial side of the 3rd and 4th metatarsal should align with the medial side of the lateral cuneiform and cuboid respectively.

On weight-bearing lateral view radiographs, the superior surfaces of the talus, navicular, medial cuneiform, and first metatarsal lie in a straight line. Böhler's angle (see Figure 7.18a) lies between the plane of the posterosuperior and anterosuperior surfaces of the calcaneus and measures 28–40° in normal feet. Flattening of the angle (<28°) follows calcaneal compression with trauma.

The midtarsal joint separates the talus and calcaneus from the navicular and cuboid and resembles a wave (cyma) on all 3 views of the foot (Figure 7.3a,b). An intact cyma line shows integrity of the midtarsal joints.

The midfoot articulates with the forefoot at the tarsometatarsal joint and must be evaluated carefully, as subluxations of this region can be subtle, and lead to disastrous consequences. In the anteroposterior view of the foot (Figure 7.5a), the medial aspect of the second metatarsal should align with the medial aspect of the middle cuneiform and on the oblique view (Figure 7.5b) the medial aspect of the third metatarsal should align with the medial aspect of the lateral cuneiform and the medial aspect of the fourth metatarsal should align with the medial aspect of the cuboid.

Bone

Trace the cortical margins of the bones. Abnormal steps in the cortex, lucent, or sclerotic lines sometimes indicate the presence of fractures. If no abnormality is seen, check these review areas:

Talar dome – Look at the corners on the AP and mortice ankle views.

Lateral process of talus – Look carefully on the AP ankle view.

Lateral malleolus – Oblique fractures can look normal on the antero-posterior view, so look through the tibia on the lateral.

Anterior margin of the tibial plafond – Small flake fractures can be easily overlooked on the lateral view.

Posterior malleolus – Small and even large fractures can be difficult to detect and represent an unstable ankle injury.

Superior surface of the talus or navicula – Small capsular avulsion flake fractures should be sought.

Calcaneus – fractures *usually* occur as a result of a fall from a height. Compression fractures of the body of the calcaneus may extend to the subtalar joint. Stress fractures of the calcaneus usually

occur in runners and may appear as a sclerotic linear band. Also anterolateral flake avulsion injuries by extensor digitorum brevis are common.

Anterior process of the calcaneus – These small avulsion or shear fractures may be seen on the lateral ankle view, but are best seen on the oblique view of the foot.

Base of fifth metatarsal – look carefully on the ankle films, unless foot views are available.

Cartilage and joints

The joint surface should be smooth, with no discontinuity. Small fractures, particularly of the talar dome, can have important consequences for a patient if missed.

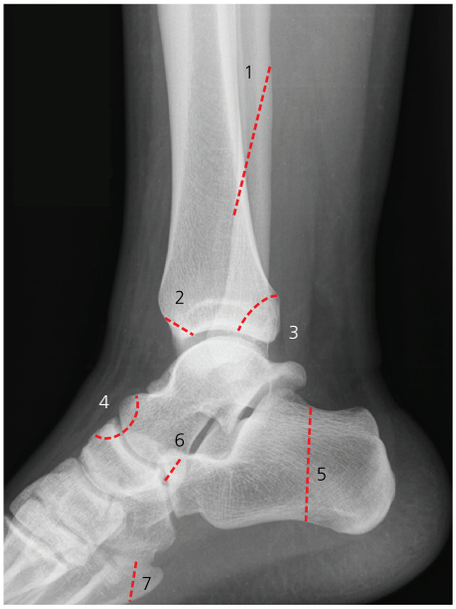


Figure 7.6 The normal ankle X-ray (*see box* Review areas).



Figure 7.7 Dorsal talar avulsion.

Review areas – 'The normal ankle X-ray' (Figure 7.6)

- Talar dome fractures – AP and lat
- Fibula fracture – look through tibia on lat (1)
- Tibial plafond – lat (2)
- Posterior malleolus – lat (3)
- Flake fractures of navicula or talus (Figure 7.7) – lat (4)
- Calcaneal fractures (Figure 7.8) – lat (5)
- Anterior process of calcaneum – lat (6)
- Base of fifth MT – lat (7)

In the feet, subluxations can be very subtle on radiographs, and it is critical that they are not missed. Displacement can be made apparent with weight-bearing views.

Soft tissues

The absence of soft tissue swelling usually rules out underlying pathology; conversely, soft tissue swelling may indicate local underlying disease. On the lateral view, look anteriorly for the tear-shaped sign of an ankle joint effusion and posteriorly for Achilles tendinosis as a fusiform swelling.

Mechanisms of injury

Ankle sprains

Sprains usually occur after supination or inversion injuries. They most commonly involve the sinus tarsi and the anterior talofibular ligament. Sinus tarsi syndrome occurs usually due to inversion injuries and the patient complains of very localised pain just inferior and anterior to the tip of the lateral malleolus, with instability in particular on uneven surfaces. Symptoms resolve rapidly with an US or CT guided injection with local anaesthetic and steroid. Severe ligamentous injuries may clinically simulate fractures, which radiographs exclude, or show joint incongruity. Ultrasonography or magnetic resonance imaging may be useful for further assessment of ligaments in selected patients.

Ankle fractures

Fractures of the ankle follow distinct patterns that depend on the mechanism of injury. This helps in the planning of surgical management. The Weber classification of ankle fractures is based on the position of the fibular fracture in relation to the inferior tibiofibular joint. The classification helps identify injuries that are most likely to involve the syndesmosis, cause instability of the ankle and are more likely to require surgical intervention. Type A injuries are below the syndesmosis and stable. Type C injuries are above the syndesmosis and unstable. Type B injuries are at the level of the syndesmosis and stability is variable.

Maisonneuve fracture

This is a variant of the pronation-external rotation fracture with a transverse medial malleolus fracture seen in the anteroposterior view; however, the fibular fracture is proximal and if is suspected, a full length radiograph of the fibula should be obtained (Figure 7.9a,b).

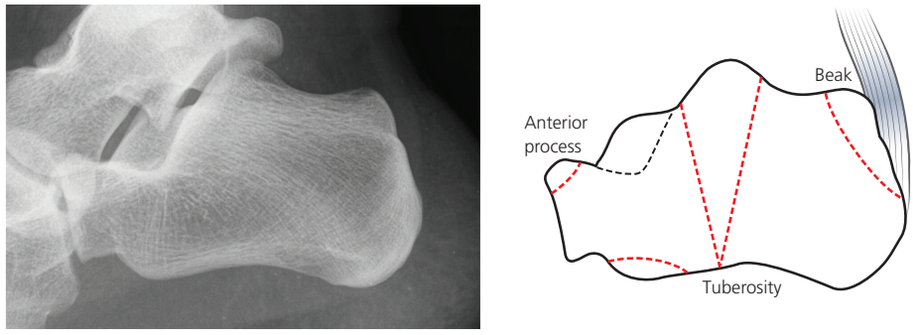
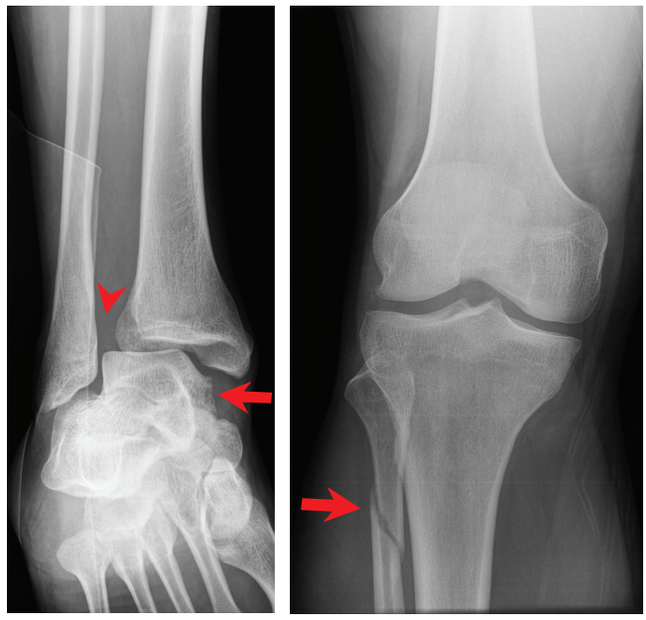


Figure 7.8 Site of calcaneal fractures.



Figure 7.9 Trimalleolar fracture.



(a) (b)

Figure 7.10 (a) Maisonneuve: AP shows gross disruption of the mortice and distal tibiofibular syndesmosis; (b) Maisonneuve, AP of the knee shows the proximal fibula spiral fracture.

Trimalleolar

These fractures are caused by severe forces of abduction or external rotation and involve all three malleoli. The fracture is often associated with an unstable ankle and may need surgical fixation, particularly if more than one-third of the articular surface of the tibia is involved by the posterior fracture (Figure 7.10a,b).

Pilon – French for 'pestle'

These fractures occur after axial compression injuries (Figure 7.11a,b). The talus is driven upwards into the mortice with enough force to cause comminution of the tibial plafond and a fracture of the distal tibia above the ankle joint. Computed tomography is often used to assess the degree of comminution and the relation of fragments to the articulating surface for surgical planning.

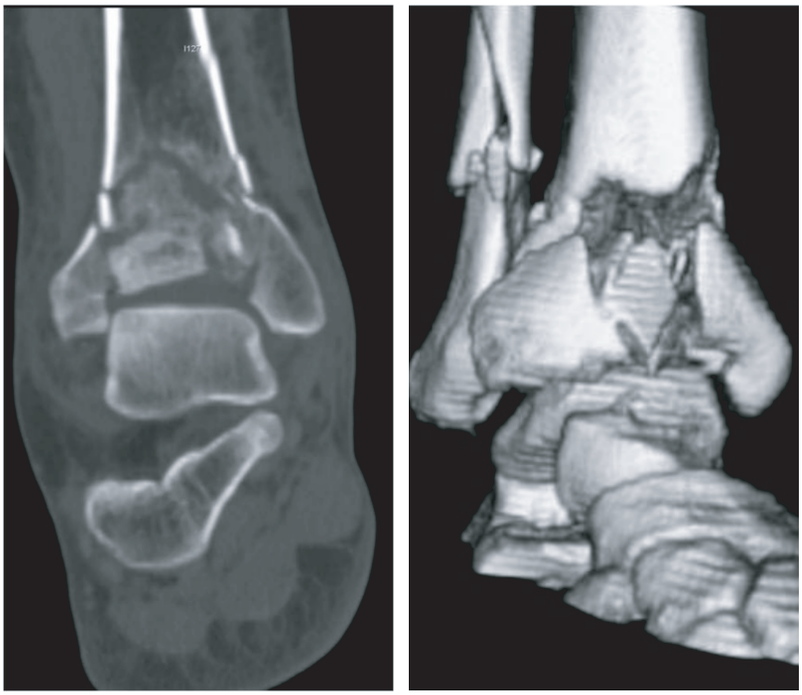
Ankle dislocation

Ankle dislocation (Figure 7.12) occurs as a result of substantial force and invariably there are associated fractures. The most common pattern of injury is posterior talar dislocation, often accompanied by a disruption of the tibiofibular syndesmosis or a fracture of the lateral malleolus. Lateral dislocations may occur in association with fractures of the malleoli. As with any dislocation, neurovascular injury is the main concern. Avascular necrosis of the talus may occur if joint reduction is delayed.

Fractures involving the growth plate

Juvenile Tillaux – This fracture is characterised by avulsion of the medial distal epiphysis of the tibia by the anterior inferior tibiofibular ligament and constitutes a Salter–Harris III fracture.

Triplane (Figure 7.13a–d) – This complex fracture is similar to a juvenile Tillaux, but with an additional coronal plane fracture of the distal tibial metaphysis. These fractures can be subtle, but suspicion should be raised if the anteroposterior view shows a vertical fracture of the epiphysis. Computed tomography imaging of these fractures is invaluable in surgical planning.



(a) (b)

Figure 7.11 (a),(b) Cor and 3D images (right) of a comminuted displaced tibial plafond pilon fracture.



Figure 7.12 AP view shows medial fracture dislocation of the left ankle, which needs to be reduced to prevent avascular necrosis.

Talar fractures

Fractures of the talus mainly occur in adults and are uncommon. Chip or avulsion fractures are the most frequent fractures (50%) and fractures of the talar neck are the next most common (30%).

Osteochondral fractures of the talus (Figure 7.14) occur as the result of impaction of the talar dome against the tibial plafond. They typically occur on the anterolateral and posteromedial aspects of the talar dome. Usually seen on radiographs but best visualised with computed tomography or magnetic resonance imaging. If they are unstable, they may result in an intra-articular body.

Talar neck fractures (Figure 7.15a,b) are important because of the serious risk of ischaemic necrosis of the body of talus. The more displaced, the more likely this serious complication. Hawkins classification, relates displacement of the fracture with risk of ischaemic necrosis (Box 7.3). Radiographs and computed tomographic images show changes of avascular necrosis (talar dome flattening and sclerosis) at 6–8 weeks. Magnetic resonance imaging is much more sensitive at detecting such fractures.

Box 7.3 **Hawkins classification of talar neck fractures and risk of AVN**

- I – undisplaced fracture (0–10% risk)
- II – displaced with subtalar joint subluxation (about a 30% risk)
- III – as II with tibiotalar disruption (>90%)
- IV – as III with talonavicular disruption (very high risk)

Talar and subtalar dislocations

Most talar dislocations (Figure 7.16a,b) are associated with talar fractures. Pure talar dislocation is seen rarely but is very disabling and involves the ankle, subtalar, and talonavicular joints. Most subtalar dislocations are reduced easily and should be reduced if detected clinically. Subluxations (Figure 7.17a-b)can be very subtle

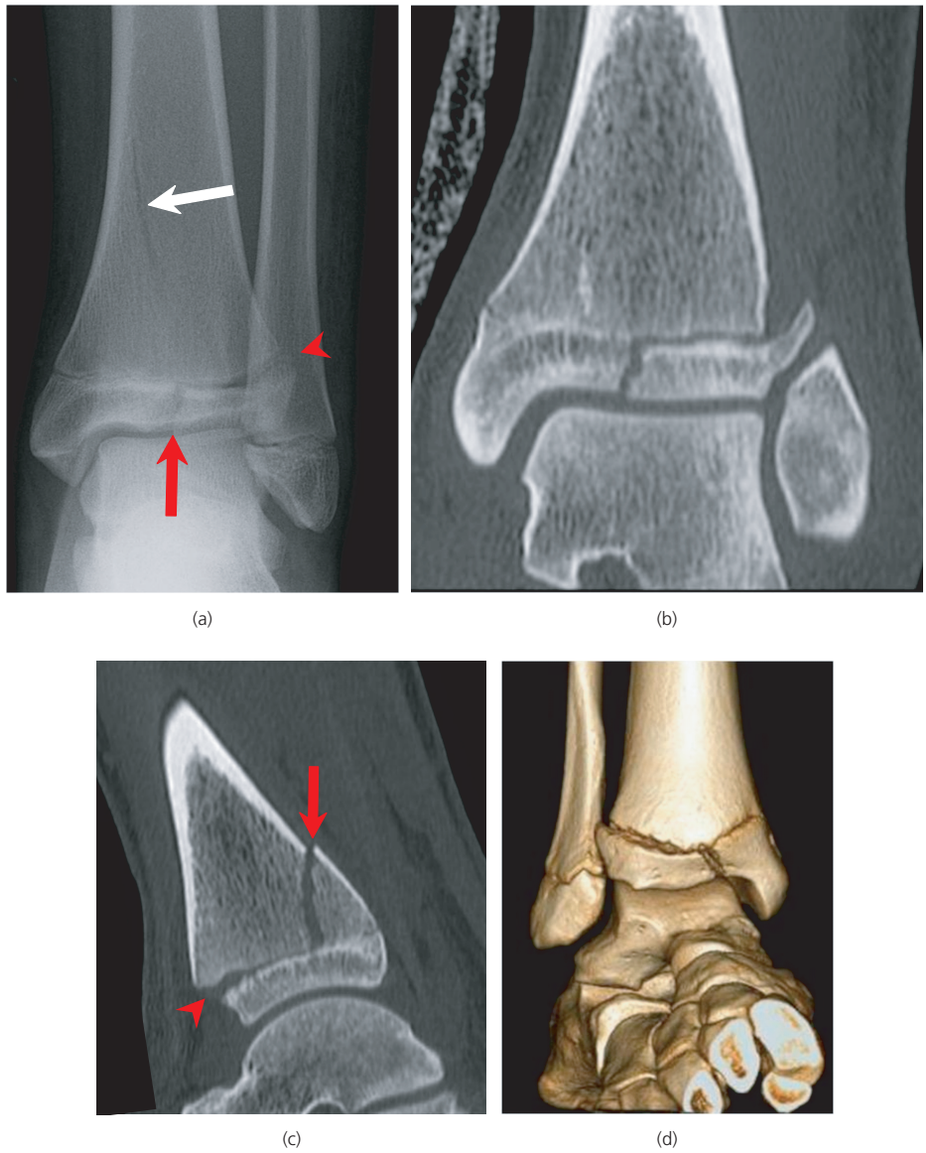


Figure 7.13 (a)–(d) Triplane Fracture: AP view shows a sagittal plane fracture through the epiphysis, widening of the lateral physis, with an already partly fused medial physis, and a third fracture line extending up through the metaphysis in a different plane (Triplane fracture). The coronal, sagittal and 3D images of the right ankle confirm findings.

and unless there is meticulous evaluation of the subtalar joint, these are often missed. The key is to evaluate the alignment of the talonavicular and calcaneocuboid joints by confirming an intact cyma line.

Computed tomographic scanning should always be done as osteochondral fractures are common. These fractures may prevent reduction and may lie within the joints, resulting in premature osteoarthritis.

Calcaneal injuries

Fractures in adults usually result from falls from a height and may be associated with lumbar vertebral body compression fractures (Figure 7.18a–c). In such patients the threshold for taking radiographs of the spine, pelvis, whole limb and the opposite calcaneum should be low.

Seventy-five per cent of adult calcaneal fractures involve the main part of the body and the subtalar joints and are often comminuted. About half show serious displacement. In children, most calcaneal fractures are peripheral or extra-articular.

Multiplanar and 3D CT scanning should always be done to assess the true extent of injury and to plan surgery. CT images show the direction of fracture lines and the involvement of subtalar joint facets. Vertical compression is associated with mediolateral bursting of the fracture parts.

Fractures of the subtalar joints may result in articular incongruity and subsequent osteoarthritis. Compression of the superior surface of the calcaneus leads to a diminution of Böhler's angle.

Twenty-five per cent of calcaneal fractures in adults are extra-articular, involving the anterior process (Figure 7.19), tuberosity, or posterosuperior aspect (Figure 7.20) of the bone ('beak fracture'). The Achilles tendon may avulse the bone at its insertion.

Fractures of the apophysis occur in children, but the normal apophysis may have a fragmented or sclerotic appearance before fusion. Trauma will be associated with local soft tissue swelling and pain.

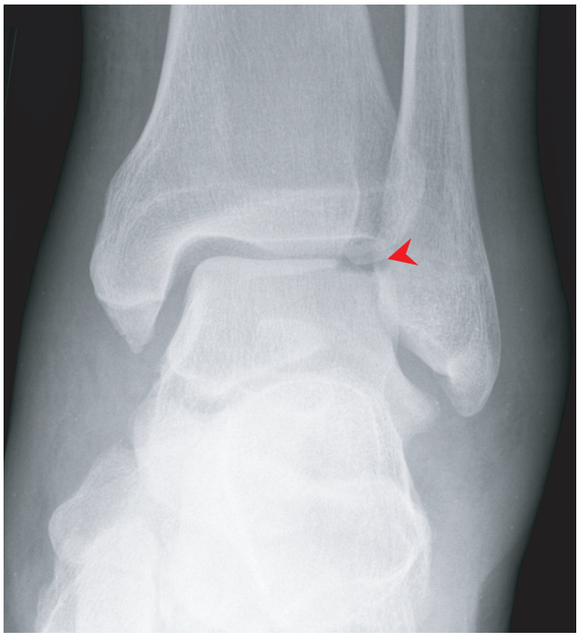


Figure 7.14 AP view shows a rotated superolateral osteochondral fracture of the talar dome.

Stress fractures of the calcaneus and foot

These fractures (Figure 7.21) appear as subtle (MRI may be required) sclerotic lines that usually parallel the posterior subtalar joint on radiographs. They are relatively common and may be due to fatigue in the young or insufficiency in the sick or elderly (Figure 7.22). Patients have pain and tenderness in the foot, which is worse on exercise and relieved with rest.

Navicular, cuboid and cuneiform fractures

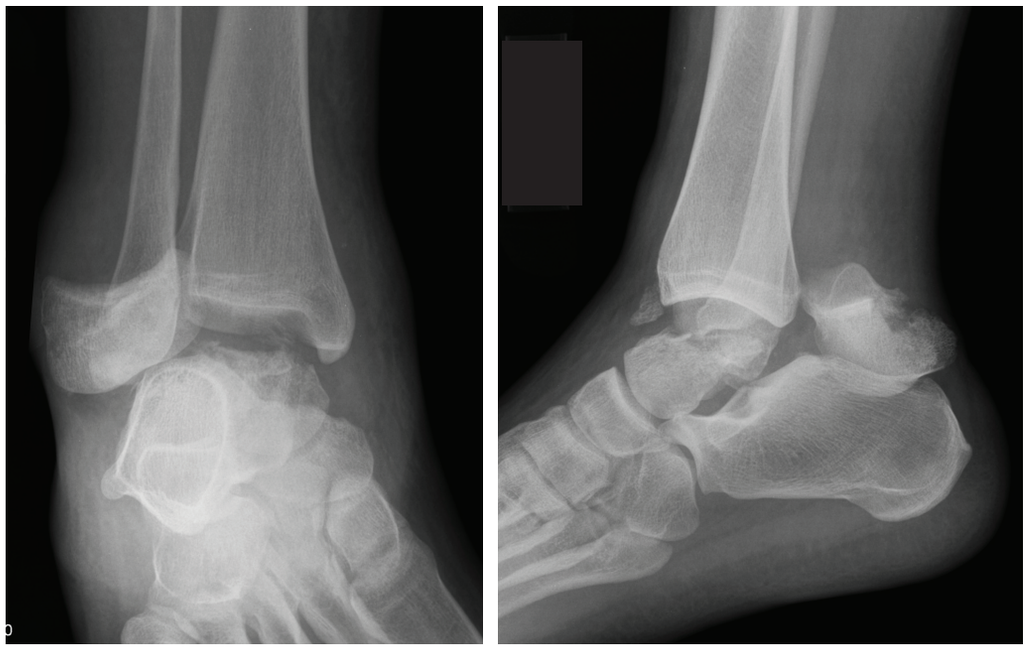
Isolated fractures of these bones are relatively rare. Avulsion fractures of the navicular, at the talonavicular joint superiorly or the medial aspect by the posterior tibialis tendon, are the most common.

Tarsometatarsal joints, Lisfranc fracture-dislocation

This is a not uncommon and important injury, in which the foot is forced into plantar flexion alone or is also rotated (Figure 7.23 and 7.24a,b). Different patterns of dislocation are seen at the tarsometatarsal joints, and these are best seen with radiographs. See alignment above. CT is useful to show the full extent of fractures and to plan surgery.

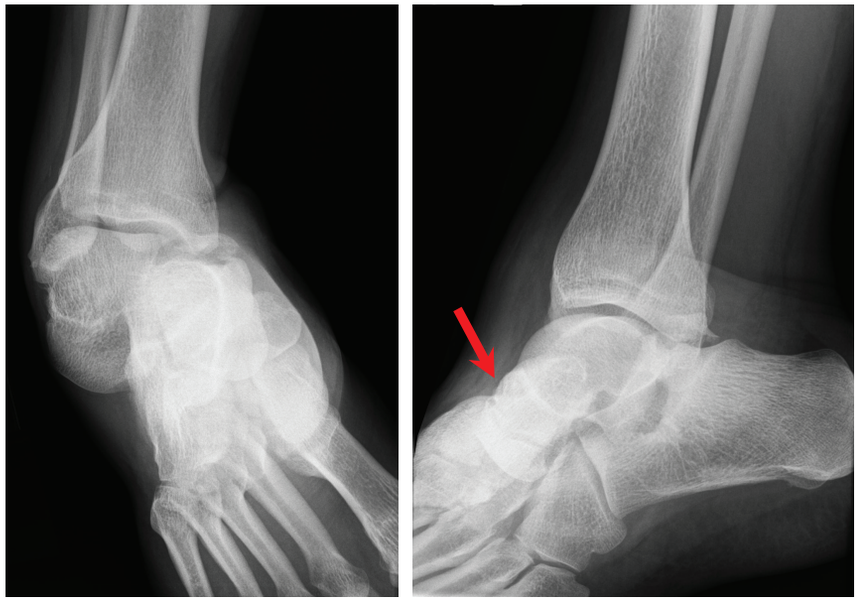
Metatarsals

Fractures may result from crush injuries (Figure 7.25), which produce a comminuted or transverse fracture, while indirect trauma from a twist can result in spiral fractures. Stress fractures (Figure 7.26) often occur at the second and third metatarsal shafts and are seen in new army recruits, joggers, and dancers. The normal sagittal plane well corticated apophysis at the base of the fifth metatarsal may remain unfused and should not be confused with a fracture. Transverse fractures of the proximal few centimetres, especially in young athletic people, have a high incidence of non-union.



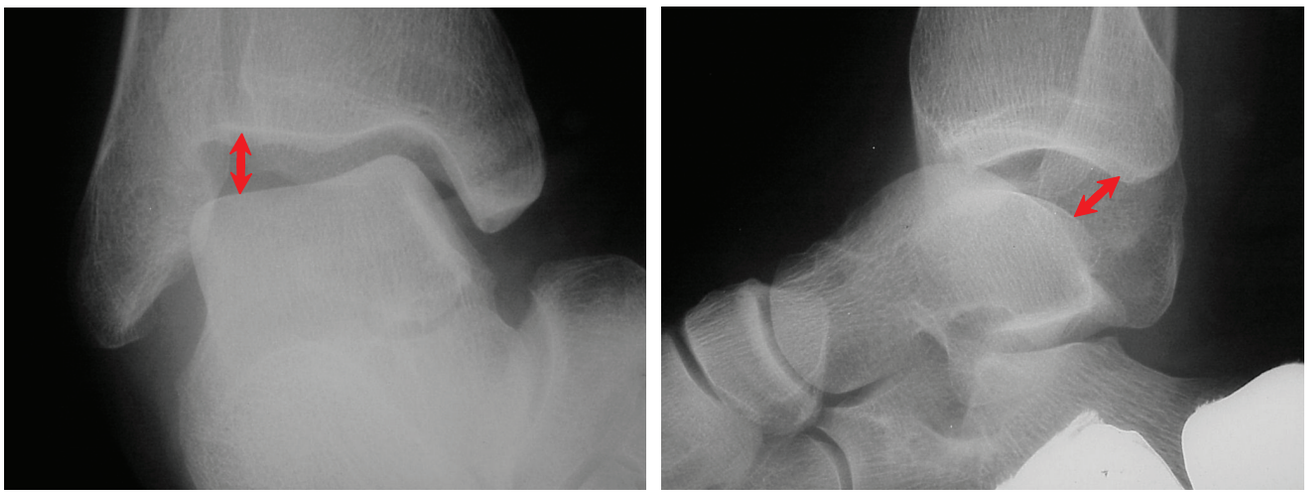
(a) (b)

Figure 7.15 (a), (b) AP and lat views of the right ankle show a displaced fracture of the talar neck (aviator's astragalus) with disruption of the tibiotalar and subtalar joints (Hawkins III). Note the talonavicular joint is still articulating.



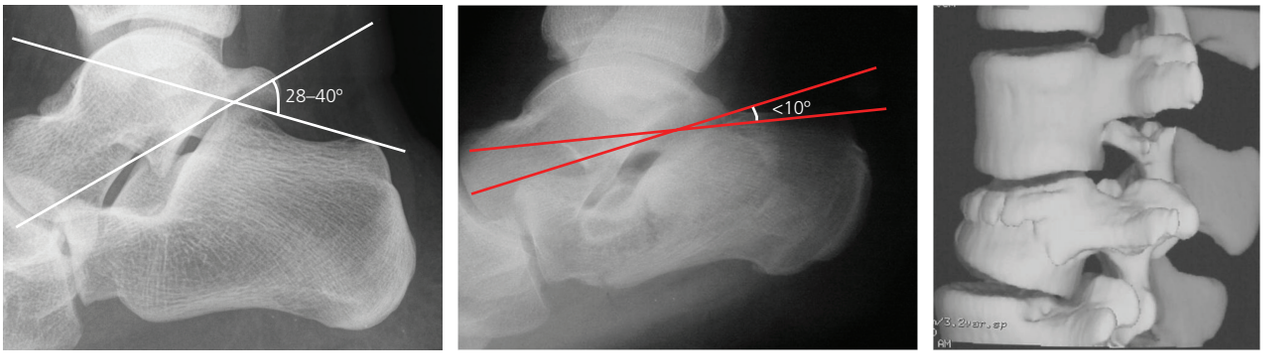
(a) (b)

Figure 7.16 (a), (b) The oblique and lateral radiographs of the ankle show the subtalar joints; talonavicular and posterior subtalar are dislocated, but the calcaneus maintains alignment with the midfoot.



(a) (b)

Figure 7.17 (a), (b) AP and lat views show the value of stress views which can show ligamentous insufficiency with varus and anterior draw stress, showing subluxation.



(a) (b) (c)

Figure 7.18 (a) Normal Böhler's angle 28–40°. (b) Lat view shows a depressed intra-articular calcaneal fracture with abnormal Böhler's angle <10°. (c) 3D surface CT of the lumbar spine shows a L2–3 flexion distraction fracture.



Figure 7.19 Lat view shows an anterior process calcaneal fracture.



Figure 7.20 Lat view shows a calcaneal beak fracture.

Phalanges

Fractures to the phalanges usually result from direct trauma – for example, from crush injuries. Always look at adjacent phalanges and toes.

Catches to avoid

Accessory ossicles can often be mistaken for avulsion injuries. They are usually rounded, with a well-corticated margin, whereas avulsion injuries have a sharp margin, and fit like pieces in a jigsaw puzzle to the adjacent bone.

Normal ankle movements

- Dorsiflexion or plantar flexion – ankle joint
- Inversion or eversion – subtalar join

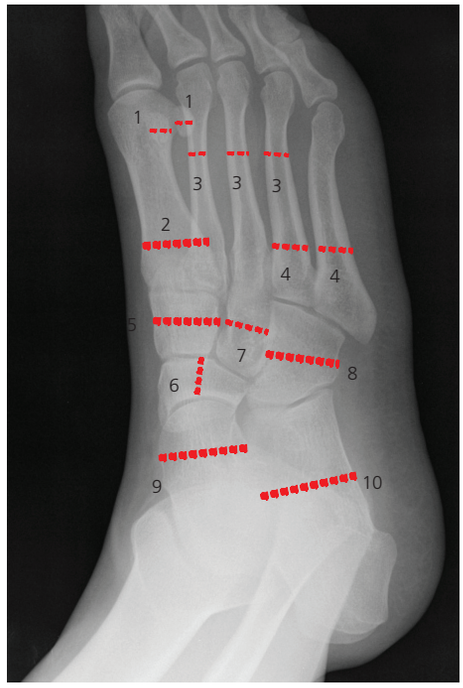


Figure 7.21 Sites of stress fractures of the foot. 1, Sesamoids; 2, first metatarsal; 3, neck of second to fourth metatarsals; 4, base of fourth and fifth metatarsal; 5, medial cuneiform; 6, navicula; 7, lateral cuneiform; 8, cuboid; 9, talus; 10, calcaneum.

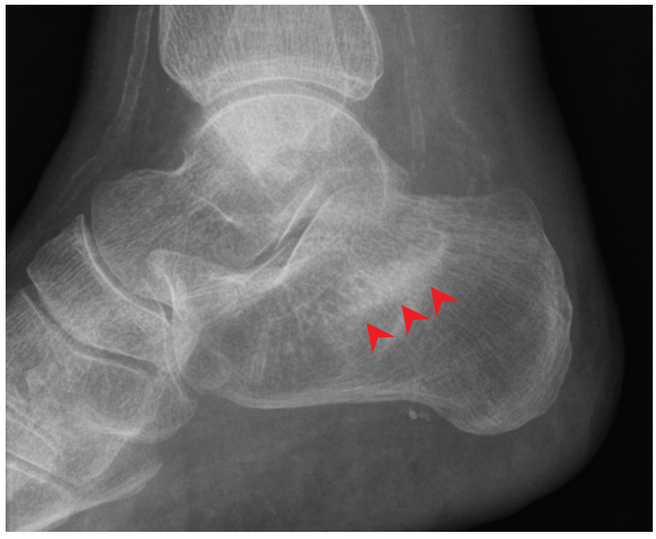


Figure 7.22 Calcaneal insufficiency fracture in a patient with renal failure.

Radiography

- Hindfoot – lateral, axial (Harris)
- Forefoot and midfoot – anteroposterior, oblique, lateral
- Phalanges – anteroposterior, oblique, elevated lateral of toe



Figure 7.23 AP view shows a first ray separation medially; isolated type of Lisfranc injury.

Mechanism of injury

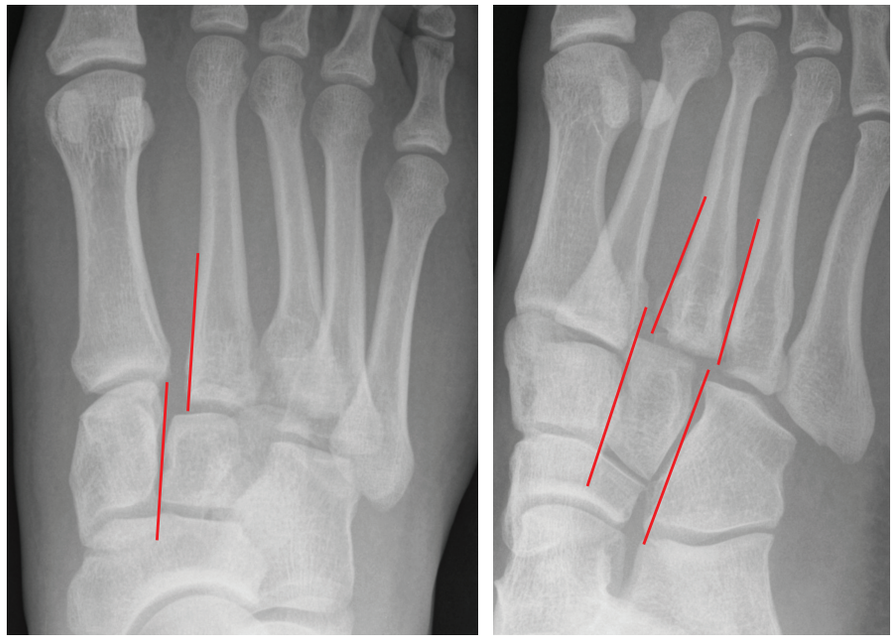
- Objects falling onto feet – forefoot injuries
- Kicking objects – big toe injuries
- Hitting objects barefoot – little toe fractures and dislocations
- Landing from a height (falls) – calcaneal fractures
- Twisting ankle – base of fifth metatarsal avulsion fractures
- Overuse – stress fractures

Calcaneal fractures

- Calcaneus (60% of fractures of the foot)
- Intra-articular – Body and subtalar joint
- Extra-articular – Anterior process, tuberosity, posterior aspect (beak)

Patterns of Lisfranc fracture-dislocation

- Hallux metatarsal may dislocate medially (divergent)
- Four lateral metatarsals may dislocate laterally (divergent)
- Associated with fracture of base of second metatarsal, which is proximal to the other metatarsal bases
- Laterally subluxed fourth and fifth metatarsal bases lie lateral to cuboid
- Dorsal and lateral dislocation of the lateral four, or all, metatarsals (homolateral)
- Proximal separation of the medial and middle cuneiforms



(a) (b)

Figure 7.24 AP (a) and oblique (b) views show a divergent Lisfranc fracture dislocation. Compare to image 7.5.

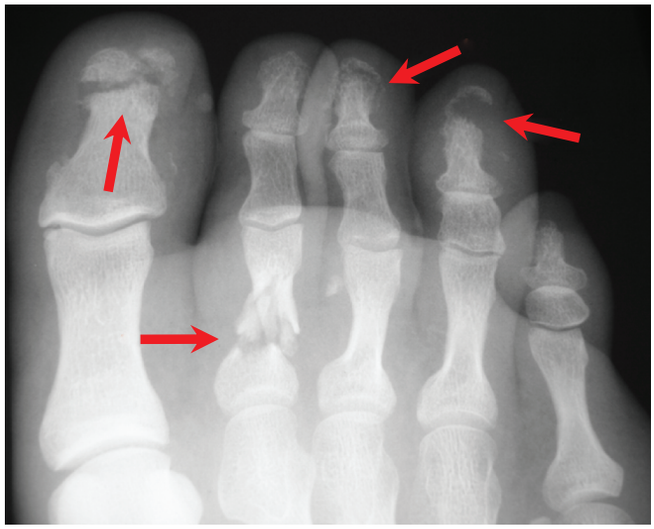


Figure 7.25 Multiple crush fractures of toes (arrows).



Figure 7.26 Stress fracture of third metatarsal (arrow).

ABCs systematic assessment

Alignment

- There should be a uniform ankle joint.
- The fibula should overlap the tibia on the lateral view
- Check talonavicular joint is intact to exclude a pure talus dislocation
- Make sure the cyma line is intact to exclude a midtarsal dislocation
- Carefully check tarsometatarsal alignment to exclude a Lisfranc injury

Bone

- Check distal fibula for an avulsion
- Check the cortical outline of the tibia and fibula
- Check the fibular shaft is intact on the lateral view
- Check the talar dome for fractures
- Check that the posterior malleolus is intact
- Follow contour of talar dome on mortice view to exclude an osteochondral fracture
- Fractures of the calcaneum can be subtle. Look for a disruption of the trabeculae and subtle sclerotic or lucent lines
- Check the anterior and posterior processes of the calcaneus
- Check for flake fractures of the superior surface of the navicular and talus on the lateral ankle view
- Isolated fractures of the cuboid and cuneiform are uncommon
- Do not confuse apophysis with fracture of fifth metatarsal

Cartilage and joints

- Joint space should be uniform
- Check cyma sign and Lisfranc joint

Soft tissues

- Swelling indicates site of injury
- Displacement of the fat pad at the anterior joint line on the lateral view may indicate an effusion which should prompt a search for a fracture

Further reading

Fox JC. *Clinical Emergency Radiology*. Cambridge University Press, 2008.

Kelikan AS, Sarrafian S (eds). *Sarrafian's Anatomy of the Foot and Ankle: Descriptive, Topographic, Functional*, 3rd edn. Lippincott, Williams & Wilkin, 2011.

Rogers LF. Radiology of Skeletal Trauma, 3rd edn. Churchill Livingstone, 2002.

CHAPTER 8

Head

Suki Thomson[1] *and Amrish Mehta*[2]

[1]National Hospital for Neurology and Neurosurgery, London, UK
[2]Imperial College London, London, UK

OVERVIEW

- CT is the investigation of choice in the ER (NB Skull XRs are NOT indicated in head injuries)
- Delayed management of head injuries is a major cause of preventable death
- Have a low threshold to CT or repeat a CT
- MRI is rarely necessary in the acute setting

Computed tomography (CT) is the investigation of choice for cranial imaging in the emergency setting. The main reasons for CT scanning in emergency setting are for trauma, stroke or TIA, suspected subarachnoid haemorrhage or meningitis. Intravenous (IV) contrast is used in perfusion imaging following stroke and if space occupying lesions are detected. Other than in stroke, magnetic resonance imaging does not feature in the acute setting.

Plain skull radiographs (SXRs) have no role in the emergency setting in adults.

CT technique

MDCT allows the spiral acquisition of data through the head with multiplanar reconstruction (MPR). Using different algorithms and altering window settings and MPR software has allowed more detailed analysis depending on which structures are being analysed. Most systems will have automatic selection for window levels to optimise viewing of different structures (Figure 8.1a–c)

Initially a scout image (scanogram) is obtained and then axial images are obtained without IV contrast (non-enhanced CT). These images are then reviewed and a decision is made whether to give intravenous contrast (contrast enhanced CT) (Box 8.1).

Box 8.1 **Indications for CT of the head**

- Non-contrast CT
- Trauma
- Stroke
- Subarachnoid haemorrhage
- Other intracranial haemorrhage
- Hypoxia
- Anoxia

Consider contrast if suspect:

- Meningitis
- Encephalitis (acute confusion)
- Raised intracranial pressure
- Obstructive hydrocephalus
- Following neurosurgery

Give contrast if suspect:

- Focal mass lesion
- Encephalitis
- Subdural empyema
- Venous sinus thrombosis
- Known primary malignancy
- HIV infection

ABCs systematic assessment

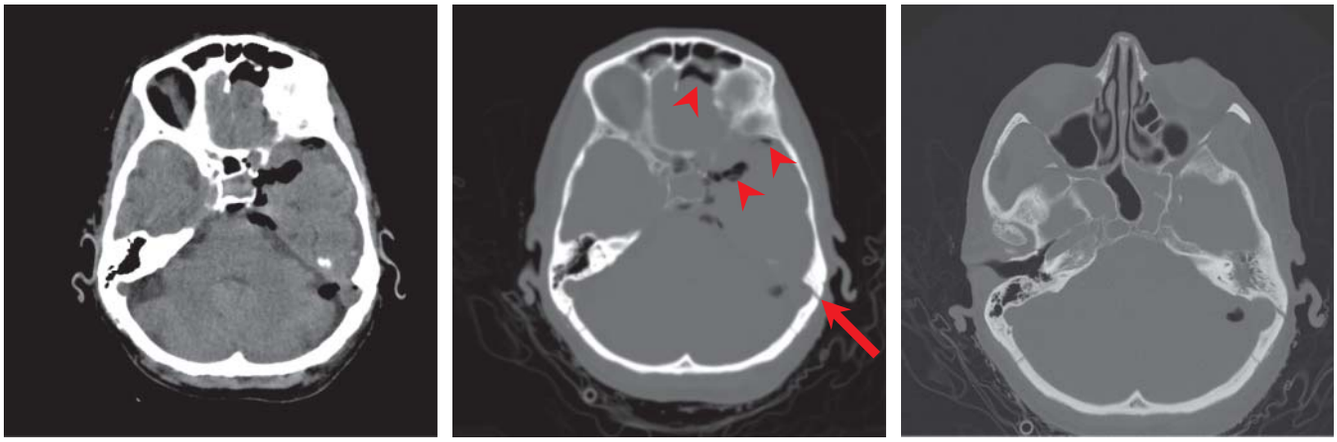
- Adequacy
- Airspaces
- Bones
- Brain
- CSF
- Dura
- Eyes
- Face/ Foreign body
- Survey (review areas)

The ABC assessment is a simple systematic approach, which is easy to remember. It is important to review key areas, analogous to the secondary survey.

The key to diagnosis is knowledge of basic anatomy. Understanding and determining if a lesion is within the brain parenchyma (intra-axial) or in the dural or cerebrospinal fluid spaces (extra-axial) is crucial.

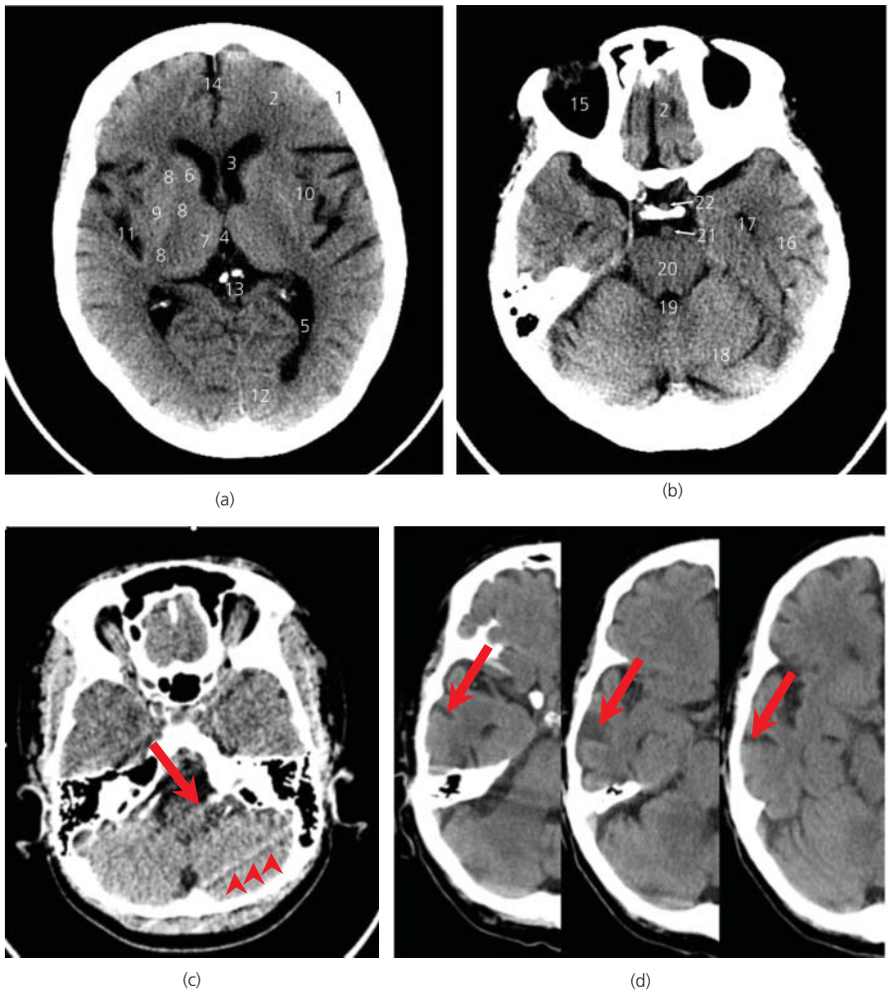
It is important to be able to recognise typical common imaging artefacts such as 'beam hardening' in the posterior cranial fossa and 'partial voluming' in the frontal lobes. Beam hardening can

ABC of Emergency Radiology, Third Edition. Edited by Otto Chan.
© 2013 John Wiley & Sons, Ltd. Published 2013 by John Wiley & Sons, Ltd.



(a) (b) (c)

Figure 8.1 (a) Soft-tissue settings; (b) bone window settings demonstrates pneumocephalus with pockets of air (arrow head) and a fracture through the left petrous temporal bone (arrow); (c) bony algorithm and bone windows makes images sharper for bony structures.

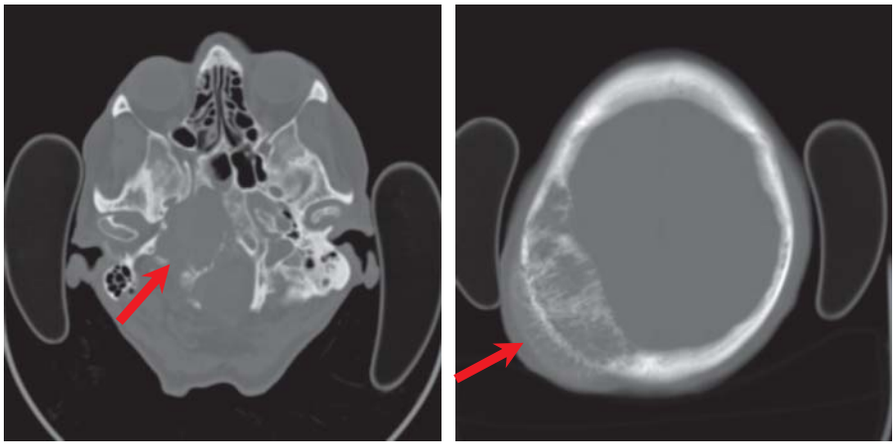


(a) (b) (c) (d)

Figure 8.2 (a),(b) 1, Skull left; 2, frontal lobe; 3, anterior horn of left lateral ventricle; 4, third ventricle; 5, occipital horn of the left lateral ventricle; 6, head of caudate nucleus; 7, thalamus; 8, internal capsule; 9, lentiform nuclei; 10, insular; 11, sylvian fissure; 12, occipital lobe; 13, pineal gland – typically calcified; 14, interhemispheric fissure; 15, orbit; 16, temporal lobe; 17, temporal horn of the left lateral ventricle; 18, left cerebellar hemisphere; 19, fourth ventricle; 20, brain stem; 21, basilar artery; 22, pituitary stalk. (c) Beam hardening artefacts – linear black streaks (arrow heads). (d) Partial voluming – the brain parenchyma appears of lower density in the middle scan.

be caused by a lot of bone, as present in the base of the skull vault, or by metal, where the XRs do not penetrate as well. The data manipulation of these areas can be spurious and cause straight high density lines to run across parts of the image. (Figure 8.2c arrow)

Conversely in areas of low density, such as CSF within sulci, if the data is not acquired in thin enough slices, part of the low density of the CSF can be included in the data manipulation, giving a false lower density in the brain parenchyma. (Figure 8.2d)



(a) (b)

Figure 8.3 (a) Large lytic metastasis of the right skull base. (b) Haemangioma of the right skull vault with coarse trabeculae and hair-on-end appearance.

Adequacy

- Has the patient moved excessively?
- Is repeating the scan going to improve the image?
- Has the top of the skull vault been included?
- Has the foramen magnum and all the intracranial contents been included?
- Would contrast be helpful?

Airspaces/bones (Figure 8.3a,b)

Look for:

- Sphenoid sinuses – an air-fluid level may indicate a base of skull fracture.
- Opacification of the paranasal sinuses – may be due to sinusitis, which may be the cause of a subdural empyema (infected subdural collection).
- Maxillary and ethmoid opacification – may be seen in facial fractures.
- Mastoid air cells – Fracture or infection leading to venous sinus thrombosis or abscess collection.
- Skull vault fractures (depressed or complex) – check for scalp soft tissue swelling as a marker of an acute injury.
- Focal bone lesions- primary bone tumour or metastases, myeloma
- Erosions at the skull base – foramina or pituitary fossa can be eroded in mass lesions
- Generalised skull vault thickening – Paget's, sickle cell, anticonvulsant therapy, long term ventricular shunting, diffuse metastatic disease.

Brain

Examination of the brain parenchyma on every slice is necessary for evidence of low or high density lesions or for mass effect (Figure 8.4).

Low density lesions

In the trauma setting, low density lesions such as non-haemorrhagic contusions or 'shear' injuries are typical. The latter include diffuse axonal injury which often occurs at the grey-white matter junction in the frontal and temporal lobes and in the corpus callosum, usually posteriorly.

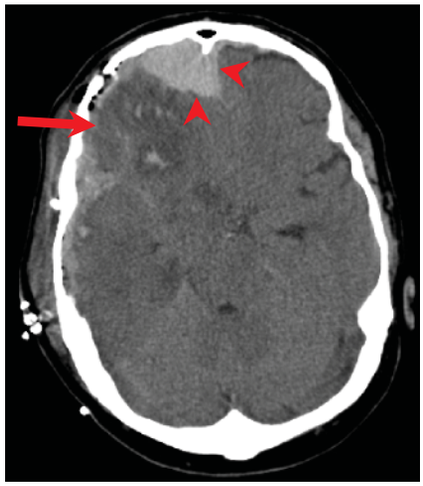


Figure 8.4 Head trauma with mixed density in the right frontal and temporal lobes with non-haemorrhagic contusions (low density areas) and haemorrhagic contusions (high density areas). Note also the right frontal extra-axial haematoma underlying the right frontal fracture (arrow heads).

In non-trauma cases, low density lesions may involve grey and white matter (such as infarcts, encephalitis and low grade gliomas) or white matter only. Demyelination and small vessel ischaemic disease in hypertension are common causes of white matter low density lesions.

Vasogenic oedema (Figure 8.5) is an area of low density around an abscess or tumour, which has finger like projections in to the white matter.

Diffuse low attenuation changes with reduced grey-white matter differentiation and associated generalised swelling usually indicates hypoxic brain injury – for example after cardiac arrest (Figure 8.6).

Other causes of focal low attenuation may be due to cystic lesions, for example, cystic tumours, such as pilocytic astrocytoma, or to



Figure 8.5 Vasogenic oedema. Finger-like areas of low attenuation involving white matter is typical in the presence of peripherally enhancing (arrow head) metastases.

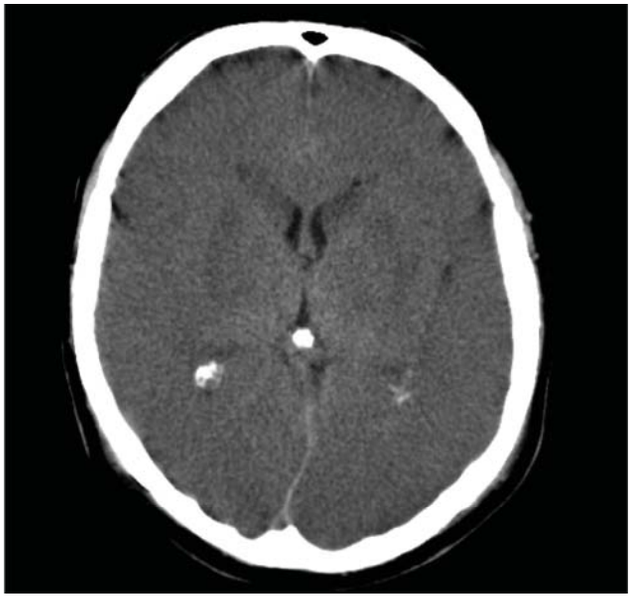


Figure 8.6 Severe hypoxic brain injury with generalised cerebral oedema. Symmetric low attenuation involving the basal ganglia, associated with cerebral swelling and global loss of the differentiation of grey and white matter.

areas of necrosis in more aggressive tumours such as glioblastoma multiforme. Similarly, an abscess has a low density core with a thin enhancing wall.

High density lesions

High density lesions usually represent acute haemorrhage (Figure 8.7). Certainly from day 1 to 7, a haemorrhage will

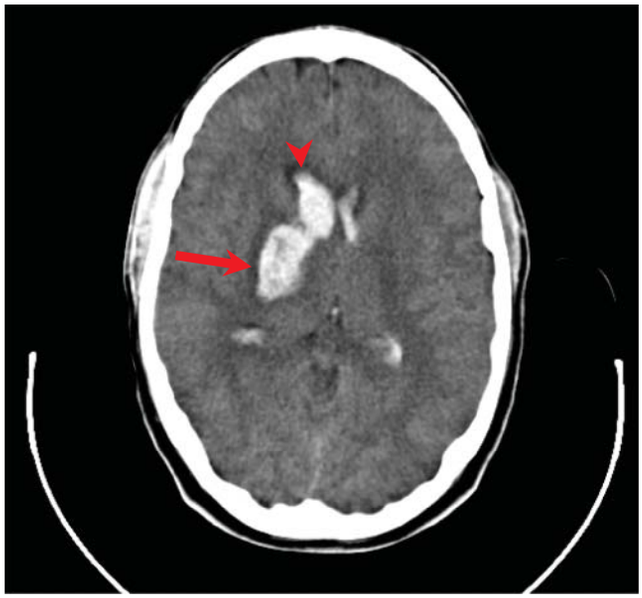


Figure 8.7 Acute parenchymal haemorrhage. High density acute haematoma in the right basal ganglia (arrow) but with intraventricular extension.

be of high attenuation. In the acute setting, there may be surrounding low density, for example, non-haemorrhagic contusion, venous infarction or haemorrhagic tumour. The density of the haemorrhage progressively reduces with time, such that it may not be conspicuous at three- four weeks. In cases of ongoing parenchymal bleeding or in the presence of a coagulopathy, hyperacute haemorrhage can be of low density and may form fluid levels and 'swirls'. An acute haemorrhage may also be less dense than expected in the context of anaemia.

Alternatively, very high density areas may reflect calcification, possibly from congenital infection, or they could be related to tumour.

Lesions with high cellular density (Figure 8.8) (for example lymphoma) are often mildly hyperdense, and they usually have mass effect.

Mass effect

Deciding if a lesion has mass effect or if there is evidence of mass effect (without necessarily appreciating the causative lesion) is crucial. If a lesion has mass effect it causes distortion of adjacent structures, initially locally, but when more severe there is a more widespread effect.

Signs of mass effect

- Gyral expansion
- Cerebrospinal fluid space effacement (local or generalised effect on sulci, basal cistern and ventricles)
- Subfalcine herniation
- Crowding of the foramen magnum
- Temporal uncal herniation, which may result in a posterior cerebral artery infarct.

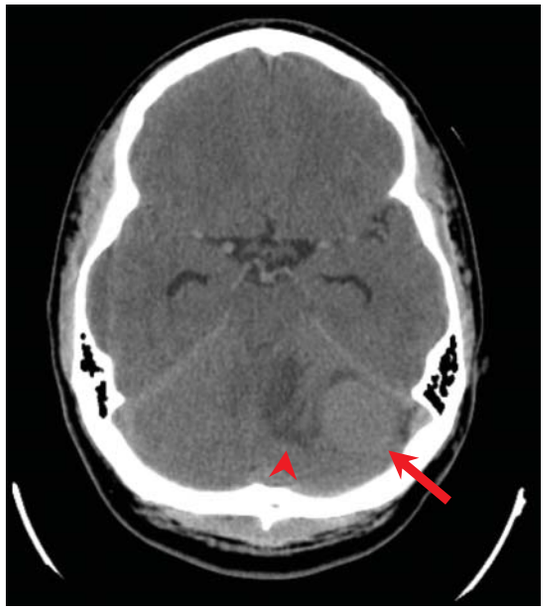


Figure 8.8 Mildly hyperdense mass (arrow) in the left cerebellar hemisphere with surrounding vasogenic oedema and mass effect (with effacement of the fourth ventricle) consistent with a highly cellular haemangioblastoma.

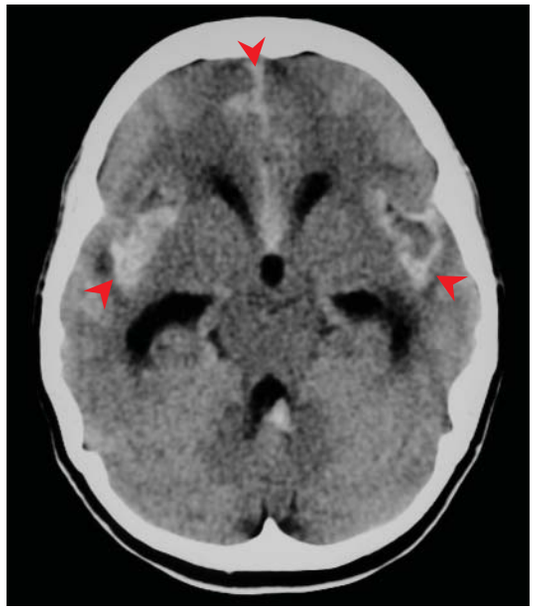


Figure 8.9 Communicating hydrocephalus with dilatation of all the ventricles in subarachnoid haemorrhage (extensive high density acute blood in the subarachnoid spaces).

CSF

The ventricles, basal cisterns and sulci contain cerebrospinal fluid. All components should be assessed for signs of acute haemorrhage (high density) or mass effect. Acute haemorrhage in the basal cisterns, sulci with or without ventricles is a subarachnoid haemorrhage, the most common causes of which are trauma and cerebral aneurysm rupture (Figure 8.9). Take care to look in the dependent locations, particularly in the occipital horns of the lateral ventricles and the interpeduncular fossa.

Haemorrhage in the sulci results in high density linear lesions between the cortical gyri. Mass effect on the cerebrospinal fluid spaces usually results in the loss of symmetry, for example of the ventricular system or sulci. The spaces are relatively small in normal young patients, so changes may be subtle.

Hydrocephalus

In general, enlargement of the ventricular system may be a compensatory effect related to reduced volume of brain parenchyma seen in old age and certain degenerative conditions, or hydrocephalus. Acute hydrocephalus is usually associated with signs of mass effect such as effacement of sulci and periventricular oedema (low attenuation), and may be caused by obstruction to the flow of CSF somewhere along its pathway, for example at the foramen of Monro by a colloid cyst (Figure 8.10). In this case only the ventricles upstream from the obstruction will be dilated, and in this example only the lateral ventricles.

Obstruction to the absorption of CSF at the arachnoid granulation, mainly on the cerebral convexity surfaces can result in dilatation of the ventricles. This is known as communicating hydrocephalus. Typical causes of communicating hydrocephalus include subarachnoid haemorrhage and meningitis. It can be confused with hydrocephalus which is caused by obstruction to the outflow from the fourth ventricle.

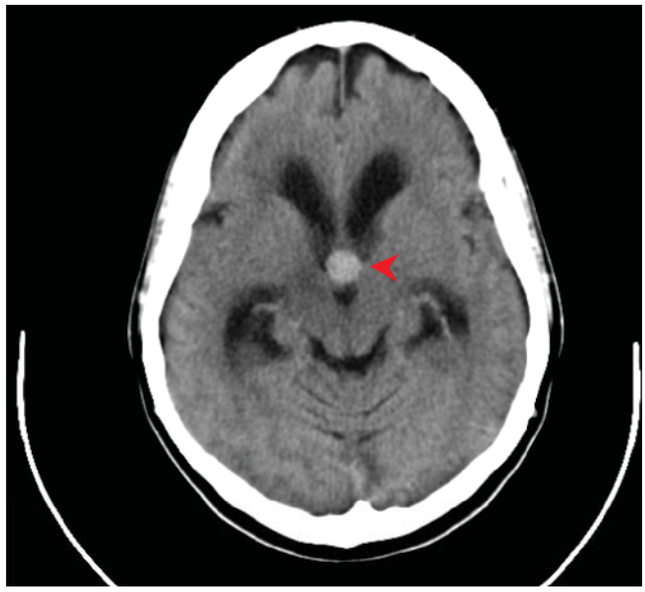


Figure 8.10 Third ventricular colloid cyst (high density round mass) with an obstructive hydrocephalus.

Dural spaces

Extra-axial compartment

1. Subarachnoid space (between the arachnoid/pia mater & the basal cisterns/sulci)
2. Subdural space (between the dura & arachnoid layer
3. Extradural space (between the dura & inner table of the skull)

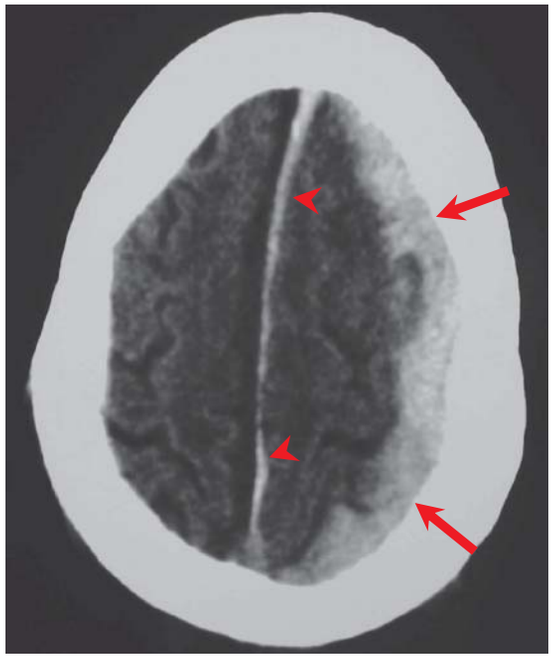


Figure 8.11 Subdural haematoma: large acute high-density crescent-shaped collection extending into the interhemispheric fissure (arrow heads).



Figure 8.12 Extradural haemorrhage: large left acute lentiform shaped collection with a shallow crescentic right sided subdural haematoma and associated right cerebral contusions. Note mild left to right subfalcine shift of the midline.

The principal abnormality to be identified is an extra-axial haemorrhage.

Subdural haematoma (Figure 8.11) is usually over the cerebral convexity but may be located in the interhemispheric fissure or related to the tentorium. Subdural haematomas are usually crescentic and often distant to the site of impact ('non-direct' or 'contre-coup').

Extradural haematomas (Figure 8.12) are typically related to the site of impact, often a skull vault fracture. They are biconvex and limited by the vault bone sutures.

The density of and extra-axial haemorrhage decreases over time. After about 12–15 days it may become isodense to brain and difficult to identify. Beyond three weeks, subdural haematomas are predominantly low density, occurring most often in elderly patients after minor trauma. In hyperacute haemorrhage or in patients with coagulopathy the subdural may be low density, but it usually contains swirls of mixed density.

Non-haemorrhagic, low density collections of subdural fluid are important. If present acutely after trauma, they may represent CSF effusion where there is a local arachnoid tear. They may have mass effect but are usually self limiting.

In the unwell, feverish patient, identifying a subdural empyema (Figure 8.13) (infected subdural effusion) is critical. Its margins are usually thickened and enhance after administration of intravenous contrast. Often they may present with sinusitis.

It is advisable to examine the dural venous sinuses for signs of thrombosis. In the acute setting a thrombosed venous sinus will be expanded and hyperdense on a plain CT scan. After contrast, a filing defect denoting the thrombus may be visible.

Deciding if a lesion is intra-axial or extra-axial is an important step in the interpretation of cranial CT. The differential diagnosis is quite different for the two compartments. An extra-axial lesion will displace inwardly the underlying cerebral cortex and pial blood vessels. A CSF cleft may be produced at the margin of the lesion. An extra-axial lesion will often have a broad based dural base or attachment and may be associated with overlying bony changes. Meningioma, which is an extradural tumour (benign tumour of the meninges) is typically well defined, hyperdense, enhancing and may cause calcification. Skull vault metastases may have an extradural soft tissue component.

Eyes

- Orbital fracture (exclude muscle entrapment in blow out fracture)
- Orbital haematoma
- Globe injury
- Optic nerve injury
- Face (see Chapter 9)
- Check maxilla, mandible, zygoma or pterygoid plates for fractures.
- Foreign bodies

Survey (key areas for review)

If the CT scan appears normal initially, survey key areas before calling it normal.

Check:

- Scout (scanogram) – it may show an area that has not been scanned but has an abnormality
- Sides (extra-axial haemorrhage) – check the periphery of the brain and along the falx and tentorium

- Sulci and ventricular – effacement and symmetry
- Sinuses – examine the dural venous sinus for hyperdensity and expansion on the non-enhanced CT to indicate acute thrombosis
- Skull vault – bones again

Head injury

Blunt trauma (non-penetrating) remains the most common cause of traumatic brain injury in the United Kingdom. Delay in diagnosis and treatment of head injuries is recognised as a major cause of preventable morbidity and mortality. Every effort should be made to accelerate the pathway to the management of these patients. Early recognition and suspicion of an intracranial injury and definitive surgery is essential and therefore there should be a low threshold for requesting CT head scans.

Trauma accounts for most cranial CTs performed as an emergency. In general, MRI is not used acutely although it does have long term applications in the investigation of cognitive or neurological deficits after head trauma.

Early CT, while maintaining a low threshold for re-imaging, is critical in the management of head injury patients to prevent or limit the extent of secondary brain injury.



Figure 8.13 Subdural empyema: loculated CSF density subdural collections over the right cerebral surface and in the interhemispheric fissure with enhancement of their dural margins.

Primary brain injury

Primary brain injury results directly from the traumatic event, the mechanism of which may be penetrating or non-penetrating (blunt) (Box 8.2). In the UK, blunt trauma to the head is far more common and, depending on the mechanism, it can injure the brain at the point of impact (direct local coup) or distant from the point of impact (non-direct or contre-coup). Non-direct injuries are produced by shear-strain forced, which are mechanical stresses on brain tissue generated by sudden deceleration or angular rotation. Indeed, such injuries can also be produced with no direct cranial impact (Figure 8.14 and 8.15).

Box 8.2 **Primary brain injury – non-penetrating (blunt)**

Direct (local impact = coup)

- Skull fracture/scalp laceration
- Contusion
- Parenchymal haemorrhage
- Extradural haematoma
- Subdural; haematoma less commonly
- Traumatic subarachnoid haemorrhage

Non-direct – Extra-axial

- Traumatic subarachnoid haemorrhage, subdural haematoma

Non-direct – Intra-axial

- Cortical contusions – often called 'contre coup' injuries. They are caused by the impact of brain against rough bone or dura. The anterior temporal lobes are involved in 50% of cases with cortical contusions and the anteroinferior frontal lobes are involved in 35%. They are multiple and bilateral in 90% of cases. Parasagittal and dorsolateral brainstem lesions are less common
- Diffuse axonal injury: second most common lesion in closed head injury – 45% of cases. Typically patients present with immediate loss of consciousness. Diffuse axonal injury is a common cause of post-traumatic persistent coma. Multiple, usually small, white matter lesions are seen at the grey-white matter interface (mainly frontotemporal), corpus callosum (mainly posteriorly), internal capsule and brainstem. The initial CT is normal in 50–80% of patients. Later petechial haemorrhage may develop at these sites
- Deep cerebral and brain stem injury: associated with severe injury and a poor prognosis. Shearing of perforating arteries can lead to haemorrhaging into the basal ganglia or brainstem. CT shows hyperdense lesions of varying size with oedema

The manifestations of the primary brain injury are extra-axial haemorrhage and a range of intrinsic lesions. Typically, multiple coexisting lesions are induced by direct and non-direct means (Figure 8.16).

In general, the management of head injuries aims to prevent or limit the degree of secondary brain injury. These injuries include ischaemia, infarction, diffuse cerebral oedema, brain herniation and vascular complications and contribute to and result from cyclical deterioration in local or generalised cerebral perfusion and intracranial pressure (Figure 8.17).

NICE publish guidelines for the indications for non-enhanced CT in trauma which include Glasgow coma score (GCS) less than 15 at 2 hours after the injury, GCS less than 13 on initial assessment,

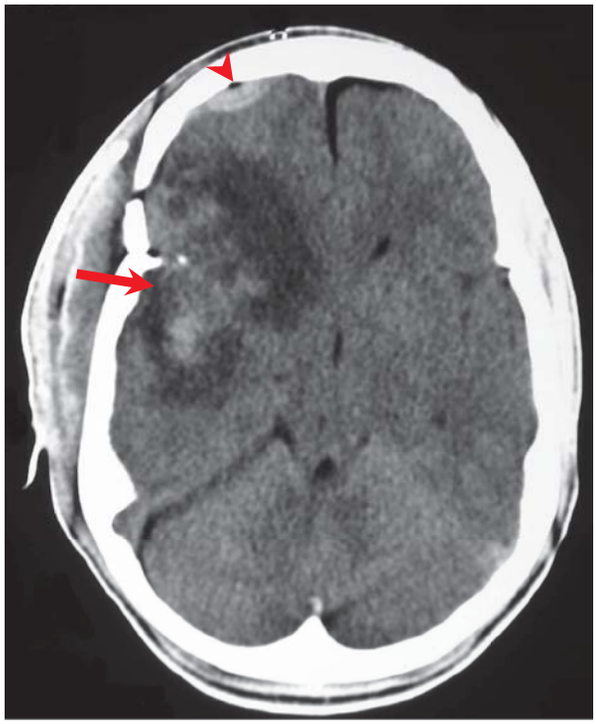


Figure 8.14 Haemorrhagic contusions in the right frontal and temporal lobes directly beneath a right frontal fracture at the site of impact. Note also a small and shallow right frontal extradural haematoma containing a tiny locule of air (arrow head).

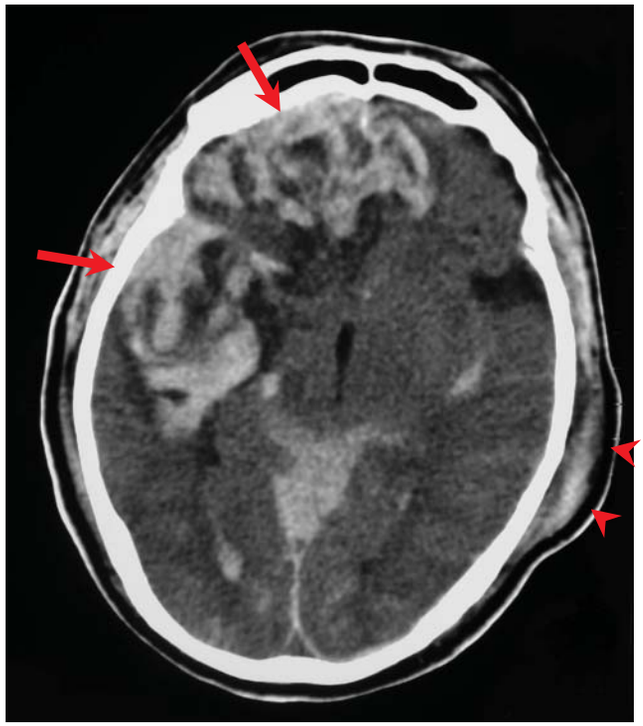


Figure 8.15 Contrecoup haemorrhagic contusions in the right frontal and temporal lobes following impact to the left parietal region as shown by soft tissue swelling. Associated subdural haemorrhage layering on the tentorium and some intraventricular blood.

focal neurological deficit and post-traumatic seizure. Full guidance is available online.

Stroke

The term stroke refers to a cerebrovascular event which may be ischaemic or haemorrhagic in aetiology (Box 8.3).

Box 8.3 **Causes of ischaemic stroke**

- Embolic phenomena from cardiac source – for example, atrial fibrillation and extracranial arterial source (typically atheroma in carotid bulb)
- Narrowing of extracranial carotid arteries leading to hypoperfusion and watershed or borderzone ischaemia
- Thrombosis or narrowing of major intracranial arteries (for example acute middle cerebral artery thrombosis
- Small vessel vasculopathy (secondary to ageing, diabetes, hypertension or vasculitis

In the UK, stroke is the third largest cause of death and the largest single cause of severe disability. The estimated cost to the NHS is over £2.8 billion per year. In 2008 the national stroke strategy was formed to try and improve the outcome for patients with stroke and a public awareness campaign was launched in 2009. Hyperacute stroke units across the UK were set up to provide rapid treatment to these patients to salvage brain at risk from infarction.

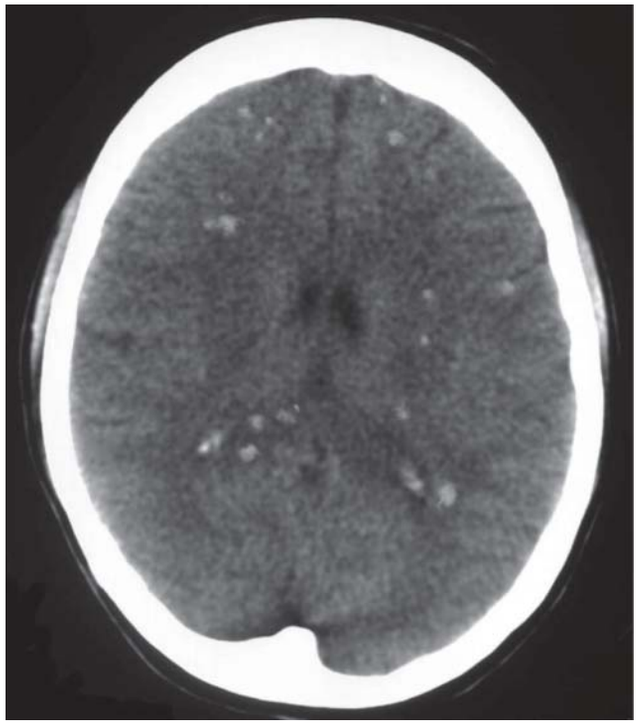


Figure 8.16 Typical multiple foci of petechial haemorrhage at the grey-white interface and also in the posterior corpus callosum, in diffuse axonal injury (DAI).

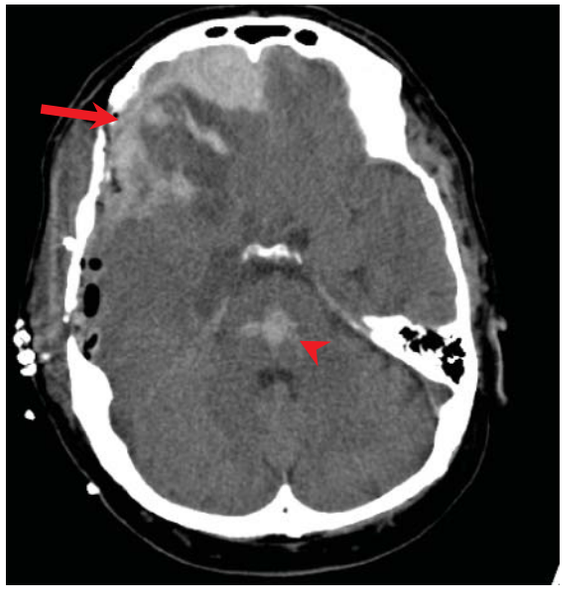


Figure 8.17 Severe right frontal and temporal traumatic injuries. There is focal haemorrhage within the pons which is a poor prognostic sign.



Figure 8.19 Acute left MCA territory infarct. Note the decreased density of the left insula cortex compared to the other side.

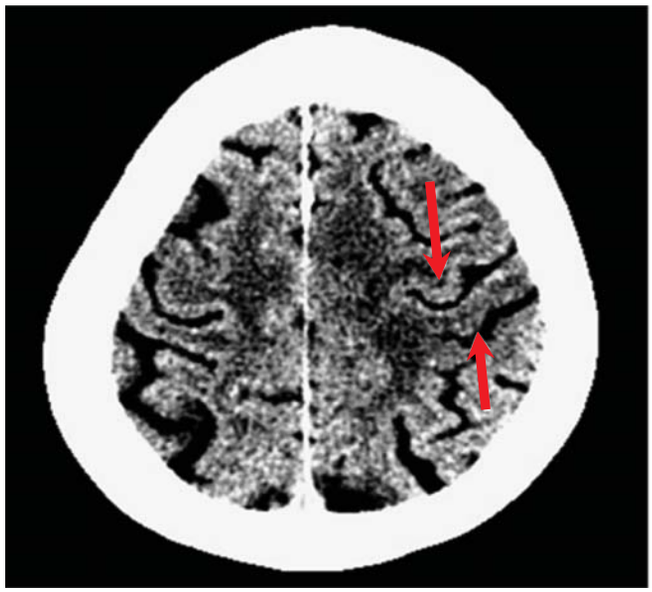


Figure 8.18 There is loss of the cortical density in the left frontal lobe, up-pointing arrow, compared to the down-pointing arrow. This is seen in hyper-acute stroke.

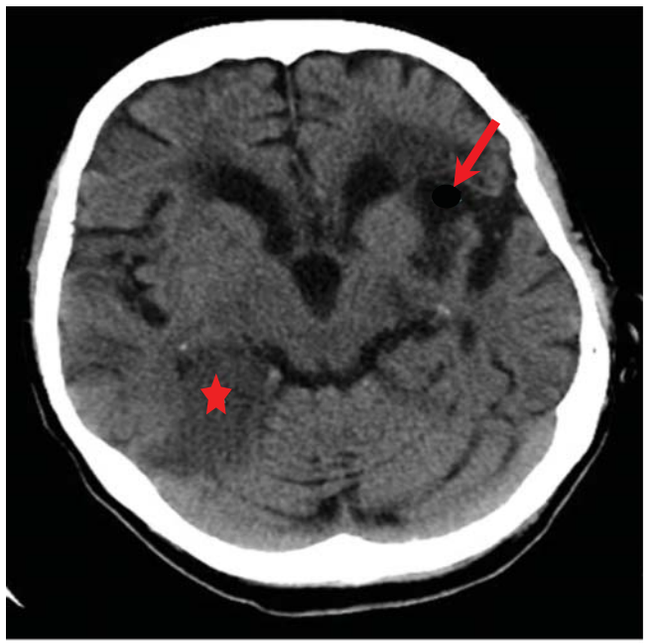


Figure 8.20 Old stroke: in the left insular (triangle) where the brain has become gliotic and now looks like CSF. A recent stroke is seen in the right posterior temporal lobe (star) where there is loss of the normal grey-white differentiation and swelling. Note there are no sulci when compared to the same position on the other side.

A non-contrast CT is the first investigation to exclude acute intracranial haemorrhage or any other contraindication for thrombolysis. At present in the UK, emergency access to MRI for the assessment of stroke is generally not available. CT is also more sensitive at detecting acute haemorrhage.

Once acute haemorrhage has been excluded, the CT scan should be assessed for signs of acute stroke. A decrease in cortical density similar to white matter, is what is often seen in acute infarct (Figures 8.18 and 8.19). Once this has occurred the brain is not salvageable. As time passes the density will decrease further until the point where it reaches that of CSF and is gliotic/encephalomalacia (Figure 8.20).

The vessels should also be analysed on thin slices, for increased density which may represent acute thrombus or occasionally calcification.

Swelling is also present in acute and subacute infarcts (Figure 8.21). Loss of sulci, in addition to the loss of cortical



Figure 8.21 Subacute right middle cerebral artery territory infarct with low attenuation involving grey and white matter and associated with local mass effect.

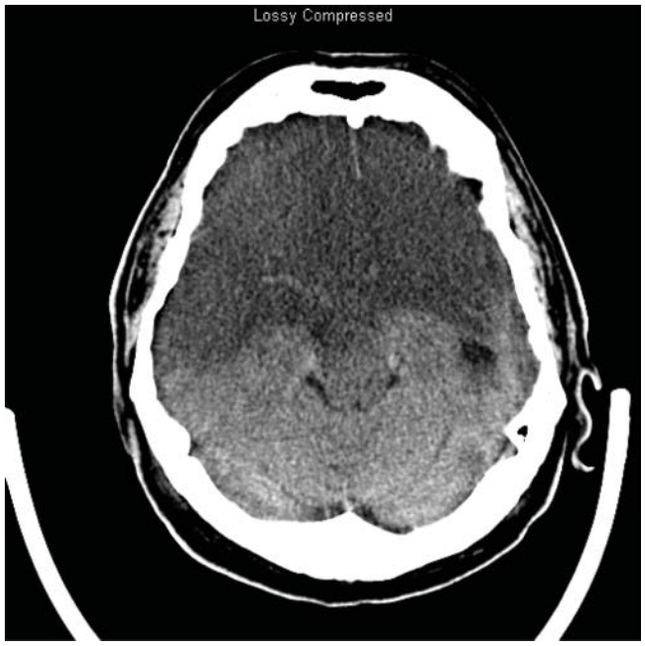


Figure 8.22 Bilateral anterior circulation territory stroke due to strangulation.

density is a good indicator that there is an ongoing underlying process. In cases of large territory infarct this can cause significant mass effect and lead to midline shift, effacement of ventricles and herniation. In these cases the patients should be urgently referred to neurosurgery for consideration of a decompressive craniectomy (Figures 8.22 and 8.23).

In cases where it is unclear from the history when the onset of symptoms started, a CT perfusion scan can help to determine

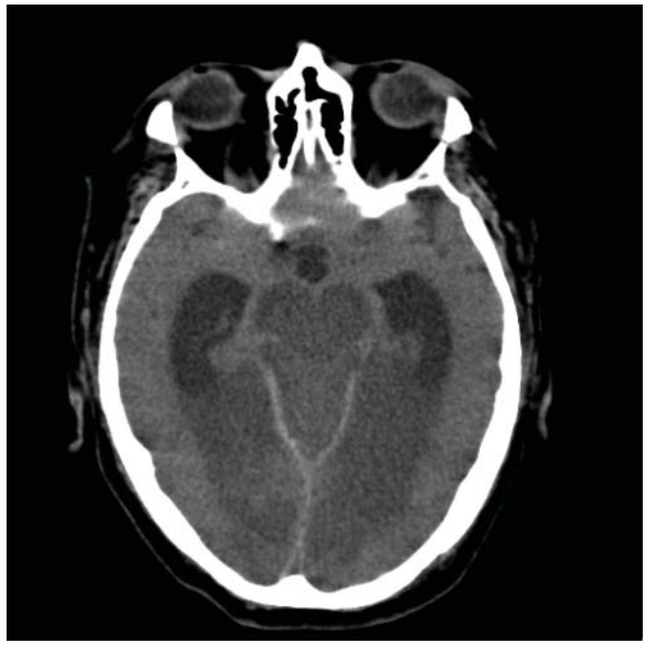


Figure 8.23 Bilateral and complete posterior circulation infarct following hanging and bilateral vertebral artery occlusion.

if there any salvageable brain. By injecting a contrast agent into the vein and then measuring the changes in the intracranial blood vessel opacification, a series of measurements and calculations can be made to determine the blood flow and blood volume. The time it takes to reach peak opacification, also known as time to peak (TTP), and the mean time taken for the contrast to enter and leave the various areas of the brain, also known as mean transit time (MTT), can also be measured. Using maps of these data it is possible to determine if an area has infarcted or is oligaemic and potentially salvageable if the blood flow to that area is improved.

A matched decrease in blood flow and blood volume is seen in areas of infarction, with prolonged MTT and decrease TTP. In areas of oligaemia, the blood flow is reduced, but the compensatory mechanisms mean the blood volume is maintained, thereby creating a mismatch. If the mismatch is moderate to large, these patients are more likely to benefit from thrombolysis (Figures 8.24 and 8.25).

Intraparenchymal haemorrhage

It is important to differentiate a primary haemorrhage from a haemorrhage that is caused by an underlying lesion, in particular a tumour or an underlying vascular malformation. Trauma remains the most common cause of parenchymal haemorrhage, and in non-traumatic cases, often the patient has a history of hypertension. Haemorrhage within a primary or secondary brain tumour usually evolves in a different pattern where there is persistent mass effect and surrounding oedema, possibly recurrent or multifocal haemorrhage and areas of contrast enhancement after contrast administration. A delayed CT before and after contrast or MRI is often necessary after 2 months when the acute haemorrhage has resolved. CT or catheter angiography may be indicated acutely if an underlying vascular malformation is suspected and surgery is planned immediately (Figure 8.26).

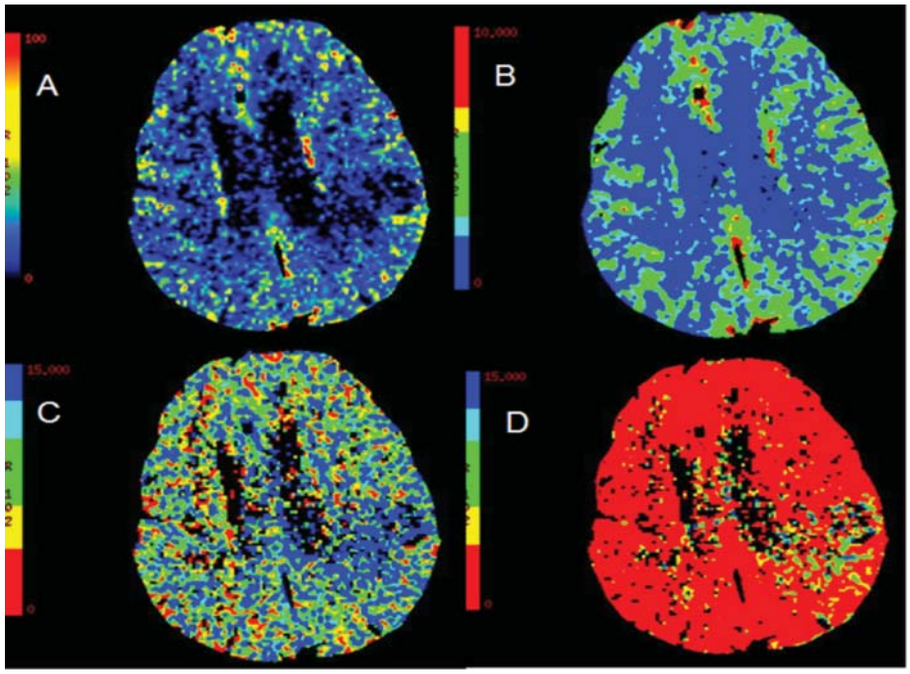


Figure 8.24 Match perfusion deficit: A, blood volume; B, blood flow; C, mean transit time; D, time to peak. There is decreased blood flow and volume with increased mean transit time and time to peak which match in territory and size. This is consistent with an area of infarcted, non-salvageable brain.

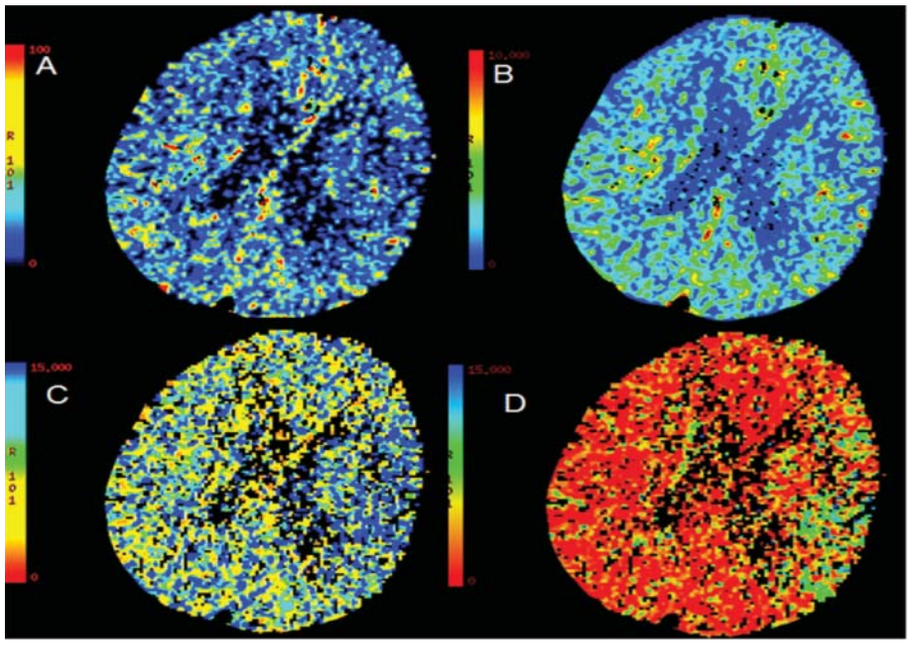
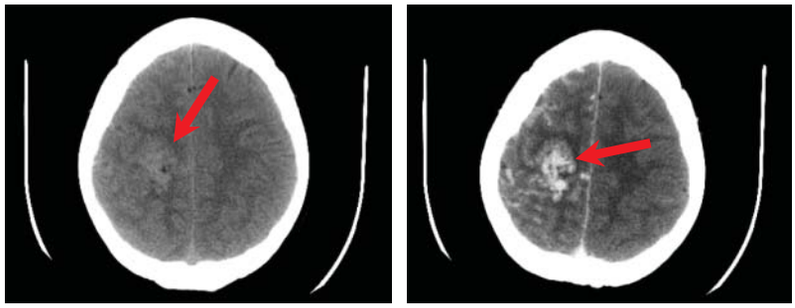


Figure 8.25 Mismatch perfusion deficit. There is decreased blood flow and increased mean transit time and time to peak but the blood volume is virtually normal. This is consistent with a small area of infarction with a larger area of oligaemia or 'penumbra' which is the potentially salvageable brain.

Box 8.4 **Causes of intraparenchymal haemorrhage**

- Trauma
- Non-trauma
- Elderly patient: hypertension, amyloid angiopathy, haemorrhagic transformation in an infarct, haemorrhagic tumour, coagulopathy
- Younger adults: aneurysms and atrioventricular malformations
- Venous sinus thrombosis, vasculitis, haemorrhagic encephalitis, cavernoma
- Tumours
- Infection

On non-contrast enhanced CT, the typical appearance is of a high density mass in the striatocapsular region (in 65% of presentations). Haemorrhage in the thalamus occurs in 20%, although the brain stem, cerebellum and periphery of the cerebral hemispheres are other potential sites. There is often an intraventricular extension



(a) (b)

Figure 8.26 Arteriovenous malformation in the right fronto-parietal region: (a) ill-defined high-density lesion with little mass effect on unenhanced images; (b) enhances avidly following contrast with serpiginous tubular structures in keeping with abnormal vessels.

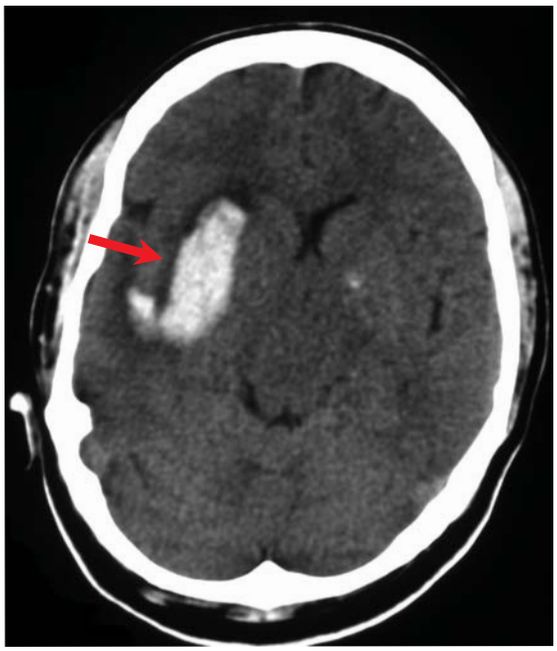


Figure 8.27 Acute hypertensive haemorrhage in the right basal ganglia.

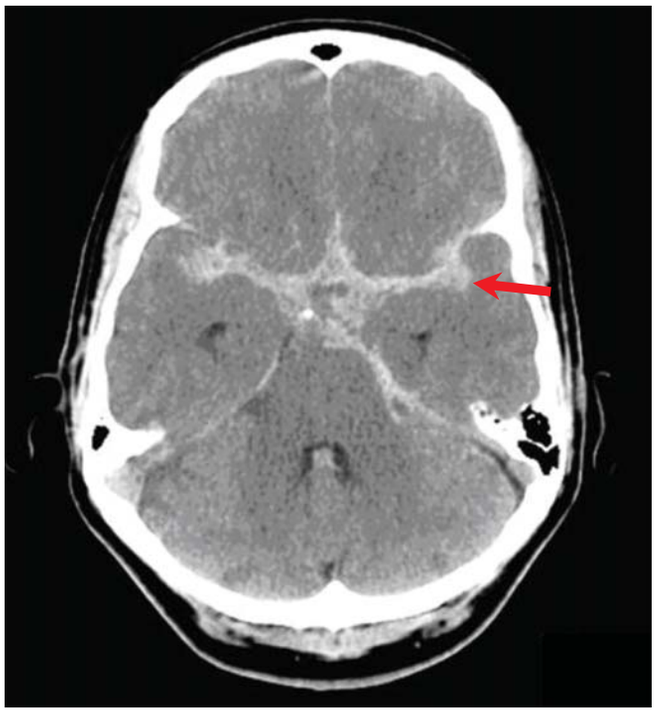


Figure 8.28 Acute subarachnoid haemorrhage secondary to aneurysmal rupture with blood in the basal cisterns.

and evidence of a background of hypertension. In particular there may be evidence of small vessel disease with low attenuation lesions in the cerebral white matter, brainstem, basal ganglia, thalami and cerebellum.

Imaging signs of hypertensive haemorrhage

- Non-enhanced CT – high density mass
- Typically striato capsular (60–65% of hypertensive patients)
- Thalamus (20% of hypertensive patients), lobar (5–10% of hypertensive patients)
- With or without intraventricular extension
- Mass effect
- Hydrocephalus due to mass effect
- Evidence of hypertensive small vessel disease with low attenuation areas

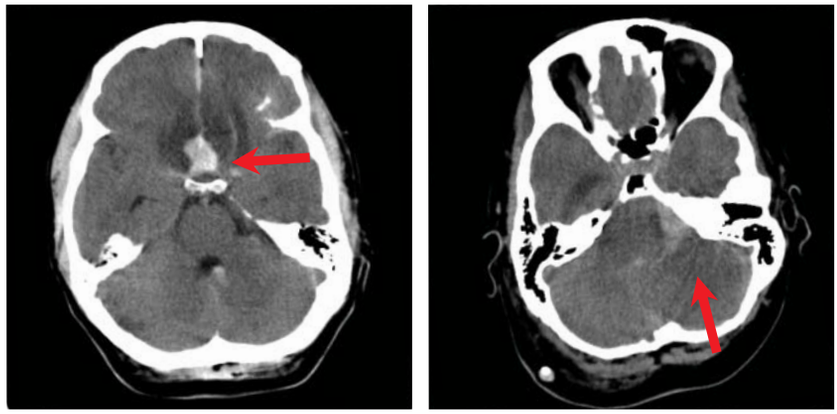
Subarachnoid haemorrhage (SAH)

SAH is defined as haemorrhage into the subarachnoid space. This space includes the basal cisterns, Sylvian fissures and cerebral sulci (Figure 8.28). It can involve the ventricular system and (rarely) the interhemispheric fissure. Usually SAH is caused by trauma. The most common non-traumatic cause in adults is a ruptured cerebral aneurysm.

Non-enhanced CT is the imaging modality of choice showing high density (acute haemorrhage) in the subarachnoid space. In aneurysmal subarachnoid haemorrhage, the distribution of blood may indicate the site of aneurysm (Figure 8.29).

Other causes of subarachnoid haemorrhage

- Aneurysm
- Atrioventricular malformations
- Venous thrombosis
- Cavernoma



(a) (b)

Figure 8.29 Acute subarachnoid haemorrhage: (a) acute inferior anterior interhemispheric clot from an anterior communicating artery aneurysm; (b) acute haemorrhage in the left cerebello-pontine angle, fourth ventricle and lateral aspect of the medulla from an aneurysm at the origin of the posterior inferior cerebellar artery.

Non-enhanced CT is highly sensitive in the detection of acute haemorrhage in the first 24 hours (approximately 98% and this may be higher if the scan is performed within 6 hours of the first presentation), but decreases with time to around 50% 1 week after the event.

Complications of subarachnoid haemorrhage

- Early communicating hydrocephalus is typical
- Low attenuation areas in a vascular distribution indicates ischaemia related to vasospasm, especially at days 4 to 10
- Late hydrocephalus (after discharge from hospital)
- Re-bleed

Meningitis

Suspected meningitis does not typically require CT before a lumbar puncture. A CT is usually normal in uncomplicated meningitis. Moreover, a normal study does not exclude the possibility of future brain herniation. A CT study is performed to exclude complications.

Meningitis complications

- Obstructive hydrocephalus
- Intraparenchymal abscess
- Subdural effusion or empyema
- Vasculitis with ischaemia/infarction
- Venous sinus thrombosis

Imaging signs in meningitis

General

- Often non-specific
- May be normal
- Signs of complications
- Subdural effusions (CSF density or intensity)

Non-enhanced CT

- Mild ventricular enlargement
- Effacement of basal cisterns
- High density subarachnoid space exudates.

Contrast Enhanced CT

- Enhancing exudates
- Prominent pial enhancement

Airspaces

- Sphenoid sinus – look for fluid level
- Frontal sinus/mastoids/middle ear – look for fracture or infection
- Pneumocephalus – look for sinus or vault fracture

Bones

- Look on bone windows and thin sections
- Look carefully over areas with soft tissue swelling

Brain Parenchyma

- Look for low density lesions
- Look for high density lesions
- Blood density and implications
- Look for signs of brain swelling

CSF spaces

- Look for blood
- Look for mass effect
- Look for hydrocephalus

Dura

- Look for subdural and extradural collections

Eyes

- Globe injuries
- Optic nerve injuries
- Fractures
- Extraconal

Face

- Fractures
- Foreign body

Survey (review areas)

- Scout
- Symmetry
- SAH
- Subtle
- Skull vault

Further reading

Barber PA, Demchuk AM, Zhang J, Buchan AM. Validity and reliability of a quantitative computed tomography score in predicting outcome of hyperacute stroke before thrombolytic therapy. ASPECTS Study Group. Alberta Stroke Programme Early CT Score. *Lancet* 2000;355:1670–1674.

Brown SC, Brew S, Madigan J. Investigating suspected subarachnoid haemorrhage in adults. *BMJ* 2011 May 6;342.

Lucas EM, Sánchez E, Gutiérrez A, Mandly AG, Ruiz E, Flórez AF, Izquierdo J, Arnáiz J, Piedra T, Valle N, Bañales I, Quintana F de. CT protocol for acute stroke: tips and tricks for general radiologists. *Radiographics* 2008 Oct;28(6):1673–87.

NICE guidelines for emergency head imaging. Available online at http://www.nice.org.uk.

Wardlaw JM, Mielke O. Early signs of brain infarction at CT: observer reliability and outcome after thrombolytic treatment – systematic review. *Radiology* 2005;235:444–453.

CHAPTER 9

Face

Simon Holmes[1], *Ravikiran Pawar*[2], *Jimmy Makdissi*[2] *and Otto Chan*[3]

[1]Barts Health NHS Trust, London, UK
[2]Barts Health NHS Trust, The London Hospital School of Medicine and Dentistry, London, UK
[3]The London Independent Hospital, London, UK

OVERVIEW

- Up to 70% of RTAs sustain facial injuries, mainly soft tissues. Head and cervical spine injuries must be ruled out before imaging the face
- Understand anatomy and classification of injuries
- Injuries occur mainly to the midface and mandible
- Always look for a second fracture in the mandible
- Plain radiographs are difficult to interpret and provide limited information. There should be a low threshold for use of CT and coned beam CT

The face is often injured in road traffic accidents, fights and assaults. Up to 70% of people who are in road traffic accidents sustain facial injuries, and most of these are soft tissue injuries. Associated injuries occur in up to half of patients with facial fractures, but, surprisingly, only 2% of these associated injuries occur to the cervical spine. The distribution of injuries to the face varies with patient population, but injuries usually occur to the midface or mandible.

Head and cervical spine injury should be excluded before patients are positioned for plain radiographs, in particular to avoid causing secondary neurological injury. Accurate radiological diagnosis is central to the management of maxillofacial trauma and other medical and surgical conditions that affect the facial bones. Although computed tomography (CT), and the more recently introduced cone beam CT (CBCT), is used increasingly in emergency assessment of such patients, plain radiographs play a central role in the initial management.

Plain radiographs are difficult to interpret, findings are subtle and there should be a low threshold for further imaging, in particular thin section MDCT with multiplanar reconstructions (MPRs) and 3D and CBCT. Using a systematic approach with a meticulous technique is essential, in particular studying the air-bone interfaces, cortical continuity, and symmetry helps the non-specialist to assess the facial bones.

ABC of Emergency Radiology, Third Edition. Edited by Otto Chan.
© 2013 John Wiley & Sons, Ltd. Published 2013 by John Wiley & Sons, Ltd.

Recommended radiological views

- Frontal sinuses – posteroanterior (PA) and lateral
- Orbits including detection of foreign bodies (FBs) – PA20 and occipitomental (OM)
- Midface – OM and OM30
- Nasal bone – none usually or a coned lateral
- Mandible – OPG, PA mandible and lateral oblique

Anatomy

The key to interpretation of imaging of maxillofacial injuries is to understand the basic anatomy and the radiological appearances of the face. The face can be divided into three areas (Figures 9.1 and 9.2):

- Midface (maxilla, zygoma, and nasal bones)
- Upper face (orbit and frontal sinuses)
- Lower face (mandible)

ABCs systematic assessment

- Adequacy: choose the correct view and ensure correct positioning and exposure
- Alignment: check Dolan's lines, McGrigor's lines, and Campbell's lines
- Bone: check all the bones in the midface and above and below the midface
- Cartilage and joints: check the zygomaticofrontal sutures and temporomandibular joints
- Sinuses: check for opacification and polyps, and check for the presence of an air-fluid level
- Soft tissues: look for soft tissue swelling and surgical/orbital emphysema. Check for FBs

Adequacy

The standard views are the occipitomental 0° (OM0) and occipitomental 30° (OM30) views. Lateral radiograph for facial injuries is rarely helpful and has been discarded as a routine view. It is important to obtain good quality radiographs in an emergency situation, although this is not always possible because patients can



Figure 9.1 Anatomical division of the face into upper, mid and lower regions.



Figure 9.2 Anatomy of the face. 1, frontal bone; 2, frontal sinus; 3, supra orbital rim; 4, orbit; 5, infra-orbital rim; 6, zygomatic frontal suture; 7, maxillary sinus; 8, nasal septum; 9, nasal cavity; 10, zygomatic bone; 11, maxilla; 12, postero-lateral wall of maxillary; 13, zygomatic arch; 14, coronoid process; 15, condylar process; 16, mandible.

be uncooperative, intoxicated, or unconscious. Additional views may be requested such as a posteroanterior (PA) views to look for injuries of the upper face or to look for radiopaque FBs (in particular glass, debris or metal) and submentovertical (SMV) to look for fractures of the zygomatic arch).

Thin-section MDCT provides exquisite detail of bony and soft tissue injuries and is able to add significant valuable information. MPR and three-dimensional (3D) reconstructions can be done in seconds using relatively low doses.

ABC assessment

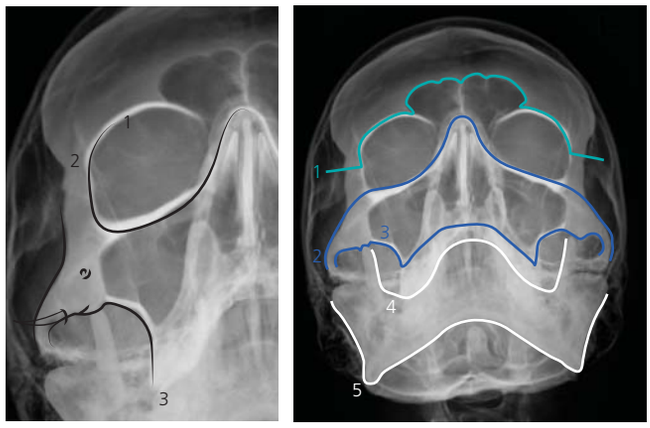
The remainder of the ABCs systematic assessment is dealt with under each individual view.

Occipitomental view

This view is simple to acquire and is usually obtained at 0° or 30°. It is able to demonstrate clearly most of the midface. Dolan described three lines that resemble an elephant's head and trunk.

Several other lines can be used to trace and look for step deformities, radiolucent lines, radio opaque areas and changes of contour. The left and the right sides of each image should be used to compare for symmetry (Figure 9.3).

- McGrigor's line 1 – Starts lateral to the right zygomaticofrontal suture. Check that the zygomaticofrontal suture is not wider than the opposite side, and then that the line goes up the superior orbital ridge, across the opposite side, and out through the contralateral zygomaticofrontal suture.
- McGrigor's line 2 – Starts at the superior and lateral aspect of the right zygomatic arch, runs medially to the infraorbital margin, over the contour of the nose, and across the other side.
- McGrigor's line 3 – Begins on the inferior and lateral surface of the zygomatic arch and moves medially. At the floor of the maxillary antrum, it goes across the alveolar process and repeats the movement across the other side.
- Campbell's line 4 – Runs along the medial aspect of the coronoid process inferomedially and across the superior surface of the body and ramus of the mandible. Finally, it crosses the midline over the superior surface of the symphysis menti and goes across the other side.
- Campbell's line 5 – Follows the inferior surface of the mandible from the lateral aspect of the right lateral condylar process to the angle of the mandible and along the inferior surface of the mandible, across the midline to the left condylar process.



(a) (b)

Figure 9.3 (a) Dolan's lines representing elephants head with its tusk and trunk; (b) McGrigor's (1–3) and Campbell's (4–5) lines.

When drawing these lines across the entire face, look for lucent or sclerotic areas of bones that cross or breach the cortex. These are likely to be fractures. Remember to check the zygomaticofrontal suture which should be of equal size. Widening of the sutures could well be suggestive of a fracture. The super imposition of different structures on plain film radiography makes it significantly more difficult to detect fractures of the midface.

Always ensure, that two views with two different angles are acquired and used to assess facial fractures. In the case of mid-face fractures these could be a combination of the OM, OM30 and SMV.

The panoramic radiograph – orthopantomogram (OPG)

This complex but very useful radiograph is able to demonstrate the full extent of the mandible, maxilla, arches and teeth. It is able to detect dental disease at the time of assessment of fractures. Some of these include teeth in the line of the fracture, retained roots and cystic areas that might weaken the mandible.

Check:

- Air–bone interface – Look for cortical discontinuity of the lower border of the mandible from the left to right condyle.
- Broken or missing teeth. Any missing teeth raise the possibility of aspiration by the patient.
- Condylar heads should lie centrally within the glenoid fossa with a smooth contour. Deviation of the condylar head from this position with a radiolucent line or increased radiopaque pattern (due to superimposition of fragments) could suggest an intra capsular condylar head/neck.
- Canal – Injuries with step deformities of the inferior alveolar canal often result in cortical disruption and might clinically present as paraesthesia.
- Dental occlusion – Spacing between the upper and lower teeth should be equal. Often a condylar neck fracture with shortening of the posterior face can be picked up in this way.
- Dento-alveolar injuries should be obtained.
- Diagnostic pitfalls of the OPG – Simulated fractures of the angle of the mandible (from air in the oropharynx) and symphysis (superimposition of the cervical spine).

Fractures of the mandible

These injuries are common and are the result of moderate to severe energy transfer to the lower face (Figure 9.4). The clinical symptoms for mandibular fractures can include a combination of but not limited to subjective alteration in bite, pain, swelling, paraesthesia or anaesthesia of inferior alveolar nerve, or inability to open the mouth following trauma. The clinical signs of a fractured mandible include deranged occlusion, bony pain, paraesthesia, fragments mobility, bleeding from the ear, and sublingual haematoma.

The mandible is a rigid ring that is similar to the pelvis, therefore if you see one fracture, always look for a second or a dislocation. The panoramic radiograph may not clearly show the midline fractures, so a PA mandible view is always performed as well.

Condylar neck and head fractures are difficult to identify unless more dedicated views are used (Table 9.1). A combination of an OPG and PA mandible is often sufficient; however, a reverse Towne's view may be necessary (Figures 9.5–9.7).

Middle third facial fractures

Central

- Nasal
- Nasoethnoid
- Maxilliary – LeFort I, II, and III

Lateral

- Zygomatic

The symptoms and signs of middle third fractures are epistaxis, diplopia, swelling, infraorbital nerve anaesthesia or paraesthesia, deranged occlusion, subconjunctival haematoma, facial asymmetry, and mobile or missing teeth.

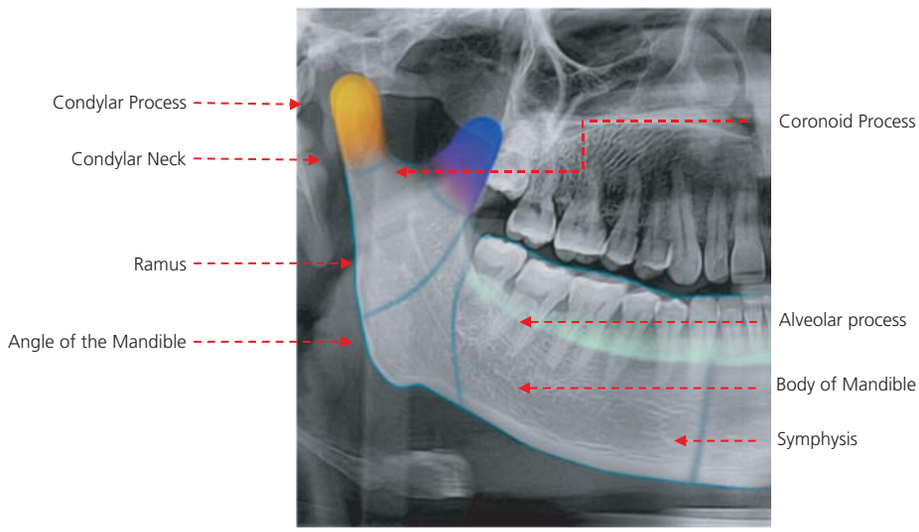


Figure 9.4 Anatomy of the mandible: 1, condylar process; 2, condylar neck; 3, coronoid process; 4, ramus; 5, alveolar process; 6, angle of the mandible; 7, body of mandible; 8, symphysis.

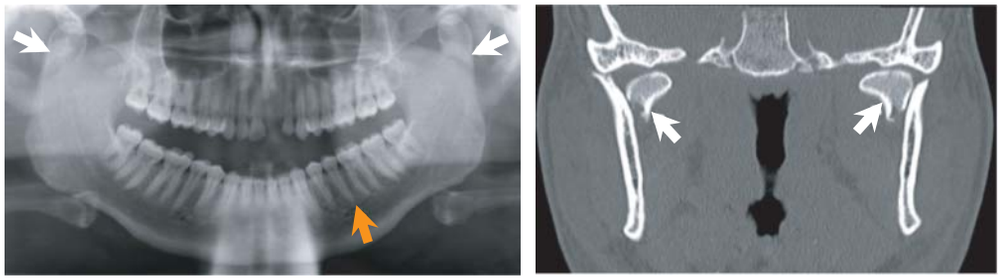


Figure 9.5 OPG and coronal CT shows bilateral condylar fractures (white arrows) with a dentoalveolar fracture (orange arrow).

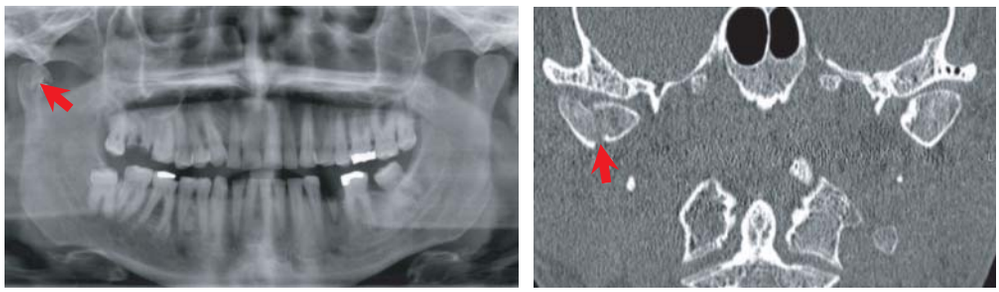
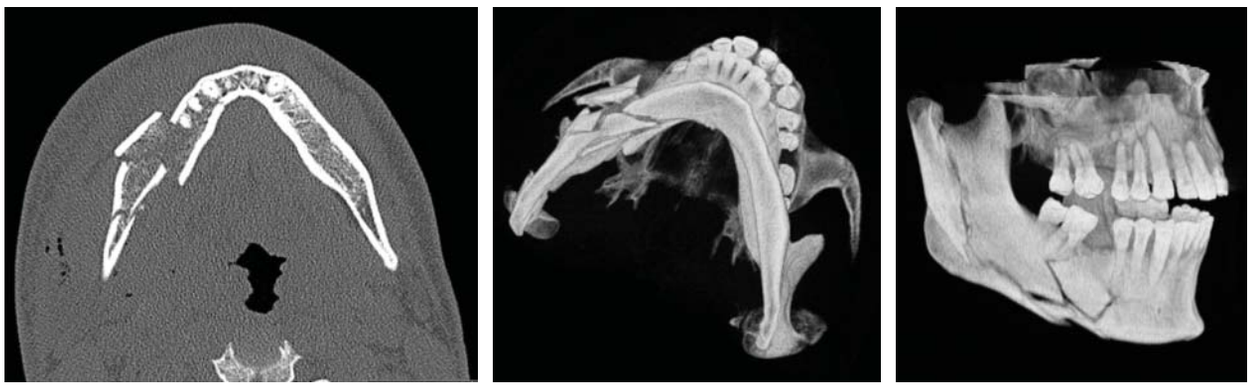


Figure 9.6 OPG and CT show a right intracapsular unilateral condylar fracture.



(a) (b) (c)

Figure 9.7 Axial CT (a) and CT 3D reconstruction (b, c) shows comminuted fracture of the right mandible.

Table 9.1 Fracture of the mandible – views.

Site	Cause	View
Angle	Unerupted third molar	OPG and PA
Body	Trauma	OPG and PA
Condyle	Anatomically thin	OPG, lat oblique, PA, Towne or CBCT
Symphysis	Trauma	OPG, PA or occlusal

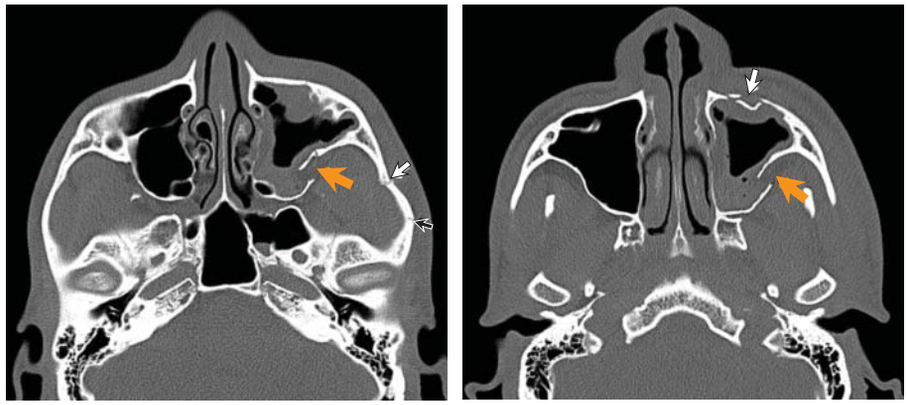
Nasal fractures are diagnosed clinically and usually do not need imaging. Maxillary fractures are classified using LeFort lines. In practice, the precise characterisation of these injuries is difficult and not of major importance in the emergency room. Mixed fracture configuration pattern is more common.

LeFort injuries

Rene LeFort was a French doctor who studied facial injuries in cadavers. He dropped heads from a height and then described patterns of facial injuries. All LeFort injuries require plain imaging and computed tomography to determine the extent, distribution and pattern of the injuries before further management is attempted

- LeFort I: a fracture above the alveolar process, which leads to the alveolar process being separated from the rest of the maxilla. Clinically, the upper teeth can be moved away from the nose.
- LeFort II: the fracture line extends above the nose. In theory, the upper teeth and nose can be moved en bloc away from the rest of the face.
- LeFort III: the face is separated from the rest of the head (cranio-facial dissociation).

Most of these injuries are not usually straightforward and not likely to be symmetrical either. Combination injuries are common and the final classification, however, is made on the basis of the highest or most severe injury.



(a) (b)

Figure 9.8 Axial CTs shows fractures of the lateral wall (orange arrow) and anterior wall (white arrow) of the left maxillary sinus and ZA (white and black arrow).

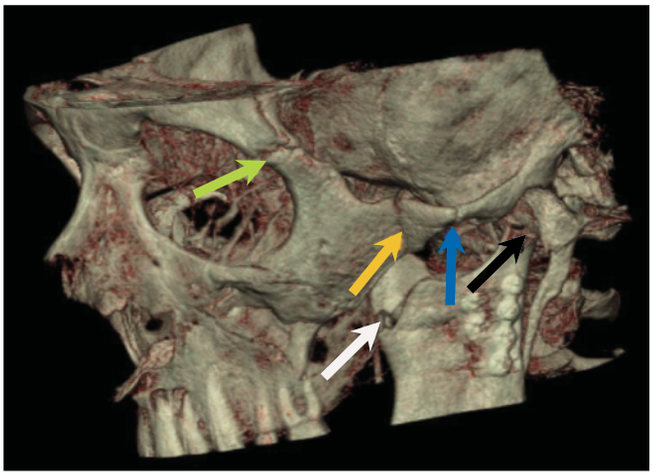


Figure 9.9 3D reconstruction of zygomatic complex fractures: ZF (green arrow), ZA (orange arrow), ZT (blue arrow), coronoid fracture (white arrow), condylar fracture (black arrow).

Zygomatic fractures

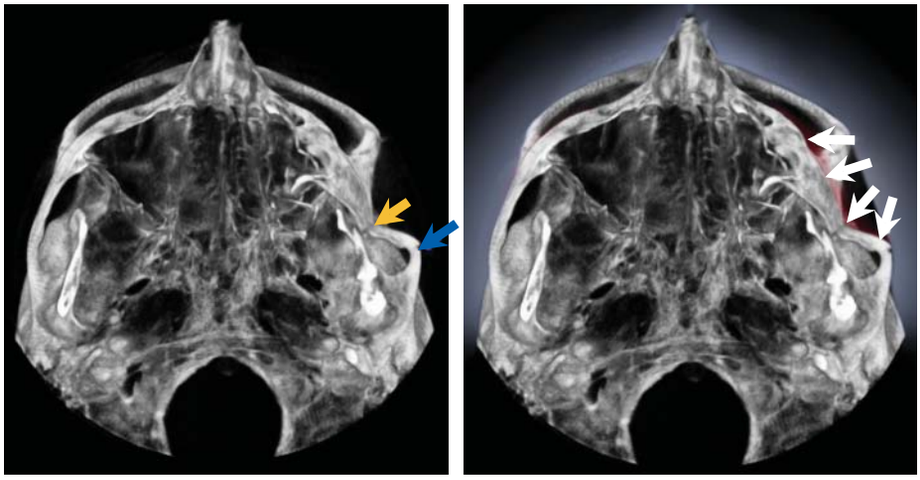
These are the most common facial fractures and usually result from a blow to the cheek and direct injury to the zygoma. They are labelled as tripod fractures although they involve the frontal process of the zygoma at the level of the zygomaticofrontal (ZF) suture, the zygomatic arch (ZA), the posterolateral wall of the maxillary sinus and the floor of the orbit/infraorbital margin. The OM0 and OM30 views are commonly used to assess these fractures. Look for soft tissue swelling and air-fluid levels. Check also for step deformities at the level of the infraorbital margin, posterolateral wall of the maxillary sinus and rotation of the zygomatic bones (look for asymmetry) (Figures 9.8–9.10).

Orbital injuries

These injuries are classified by the site of involvement.

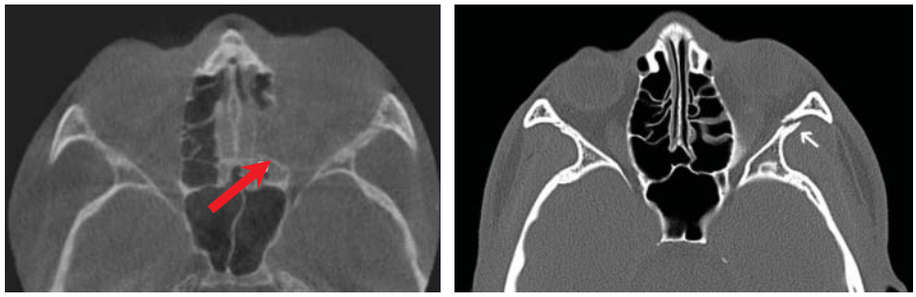
- Orbital rim
- Orbital floor
- Orbital floor
- Medial wall
- Lateral wall

The symptoms and signs of orbital injuries include ecchymosis, subconjunctival haemorrhage, diplopia, enophthalmos, and infraorbital anaesthesia or paraesthesia (Figure 9.11).



(a) (b)

Figure 9.10 CT 3D reconstruction showing a left ZA bowing fracture (orange arrow) and ZT fracture (blue arrow). Shaded area, outline of the left zygoma prior to fracture; white arrows, amount of displacement.



(a) (b)

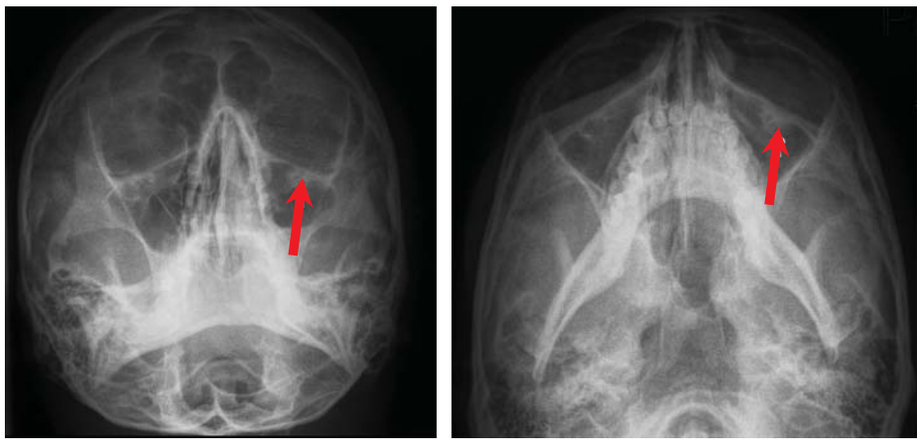
Figure 9.11 (a) Axial CBCT shows fracture of the medial wall of the orbit. (b) Axial CT shows fracture of the lateral wall of orbit.

Blowout fractures

These are injuries sustained by a direct blow to the eyeball, which then breaks either the floor and/or medial wall of the orbit, but not the orbital rim. Herniation of some contents may occur, particularly of orbital fat into the roof of the maxillary sinus in the case of orbital floor fracture or into the ethmoid air cells in the case of medial wall fracture. The extraocular muscles can become involved. The inferior rectus muscle can be trapped or herniate into the orbital floor fracture. The medial rectus muscle can be involved in medial wall fractures (Figures 9.12–9.14).

This may lead to enophthalmos, diplopia and numbness over the region of the inferior orbital margin.

Radiologically, the classic appearances are those of a teardrop on the roof of the maxillary sinus in the case of orbital floor fractures. Medial wall fractures are more difficult to see on plain film radiography. Plain radiography is the mainstay of imaging although CBCT should be performed in cases where plain radiographs fail to demonstrate a fracture in the presence of strong symptoms and signs of an orbital injury.



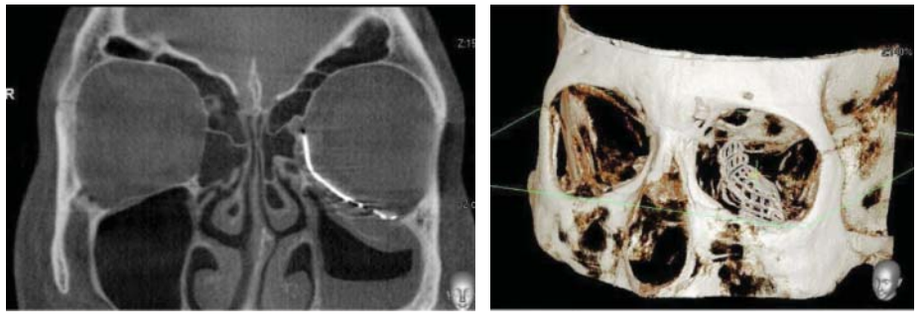
(a) (b)

Figure 9.12 OM0 (a) and OM30 (b) shows left blow ut fracture.



(a) (b)

Figure 9.13 Coronal (a) and sagittal (b) CT shows a very large blowout defect of the floor of the left orbit.



(a) (b)

Figure 9.14 Coronal CBCT (a) and 3D (b) of postoperative surgical repair of the floor of the orbit.

Upper third facial fractures

These are unusual injuries and include fractures of the frontal bone, extended nasoethmoidal fractures and supraorbital injuries.

Epistaxis, soft tissue swelling, deformity, cerebrospinal fluid rhinorrhoea, anaesthesia of infraorbital nerve and pain on upward gaze.

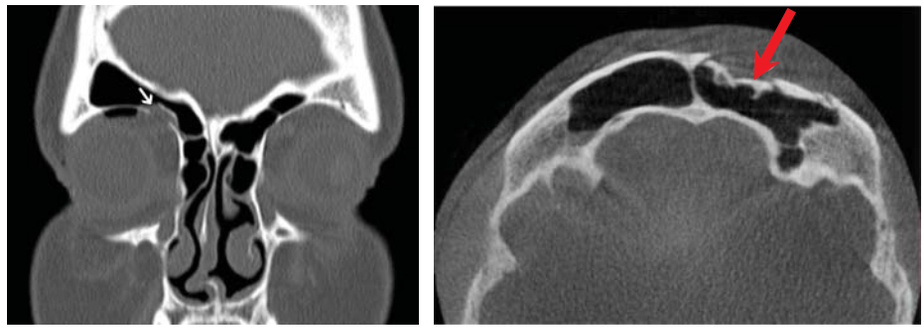
Accurate diagnosis is essential for upper facial third fractures. Precise information about fractures of the frontal sinus with respect to anterior and posterior walls is key to management. For this reason, CT (with MPR and 3D) are invariably required in these cases, particularly if any signs of retrobulbar haemorrhage are present clinically (proptosis, pain, ophthalmoplegia and diminishing visual acuity) (Figure 9.15).

Sinuses and soft tissues

Asymmetry of the face is an extremely helpful finding, particularly asymmetrical swelling of the soft tissues, air-fluid levels and/or mucosal thickening in the sinuses (Figures 9.16 and 9.17). Also, look for radio-opaque FBs, particularly glass and metal.

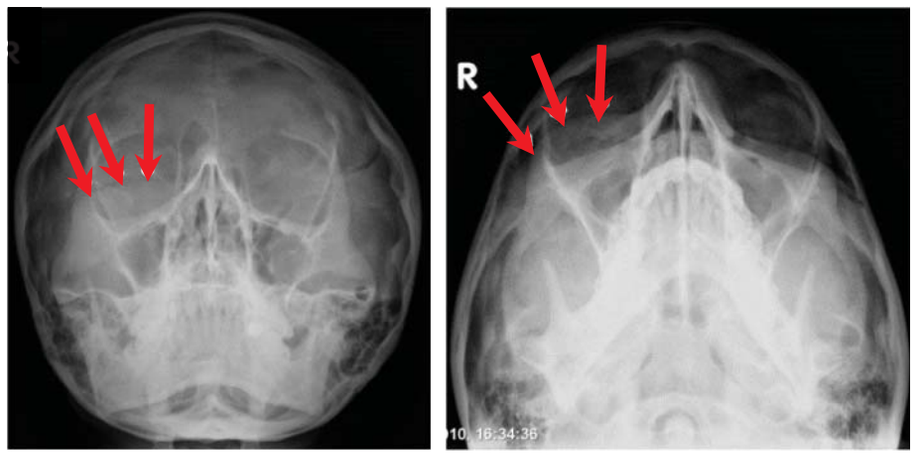
Indirect signs of orbital trauma

- Soft tissue swelling
- Surgical or orbital emphysema
- Opaque sinuses
- Air-fluid levels in the sinuses
- Teardrop sign



(a) (b)

Figure 9.15 (a) Coronal CT shows right supra orbital fracture. (b) Axial CBCT shows fracture of the left frontal sinus.



(a) (b)

Figure 9.16 OM0 (a) and OM30 (b) shows right infraorbital soft tissue swelling.



Figure 9.17 Axial CT shows intraconal (orange arrow) and extraconal air (white arrow).

ABCs systematic assessment

Adequacy

- Select correct views
- Request CT when necessary

Alignment

- Check Dolan's, McGrigor's, and Campbell's lines

Bones

- Check all bones in the midface and upper and lower third of the face.

Cartilage and Joints

- Check the ZF sutures and TMJs

Sinuses and Soft Tissues

- Check for local swelling of the soft tissue
- Surgical/orbital emphysema
- Air-fluid levels and opaque sinuses
- Teardrop injuries
- FBs such as glass and metal

Further reading

Holmes S. Reoperative orbital trauma: management of posttraumatic enophthalmos and aberrant eye position. *Oral Maxillofac Surg Clin North Am* 2011 Feb;23(1):17–29. Epub 2010 Dec 17.

Makdissi J. 3D imaging: the role of cone-beam computed tomography in dentistry: special reference to current guidelines *Faculty Dent J*, 2012;3(3):152–157.

Michael J. Gleeson (Ed.). Section editors: NS Jones, MJ Burton, R Clarke, G Browning, L Luxon, V Lund, J Hibbert, J Watkinson. *Scott-Brown's Otorhinolaryngology: Head and Neck Surgery*, 7th edn. Hodder Arnold Publishers, 2008.

Ramli R, Holmes S, Rahman RA. *Atlas Of Craniomaxillofacial Trauma*, 1st edn. Imperial College Press, 2011.

Shintaku WH, Venturin JS, Azevedo B, Noujeim M. Applications of cone-beam computed tomography in fractures of the maxillofacial complex. *Dent Traumatol* 2009 Aug;25(4):358–366.

CHAPTER 10

Cervical Spine

Leonard J. King

Southampton University Hospitals, Southampton, UK

OVERVIEW

- Most cervical spine injuries are relatively minor, but they can be potentially devastating, requiring prompt diagnosis and stabilisation
- Cervical spine radiographs are difficult to interpret and 20% of fractures may not be visible. Therefore, there should be a low threshold to proceed to CT
- CT is now the imaging modality of choice in major trauma
- MRI is indicated if there is suspicion of neurological, ligamentous or disc injury

Injuries to the cervical spine can occur either in isolation or in association with head injury or multisystem injury following major trauma. Most of these injuries are relatively minor, but they can be potentially devastating, requiring prompt diagnosis and stabilisation to minimise the risk and severity of associated neurological injury. The pattern, frequency and distribution of these injuries vary between different populations. In adults, the C1–2 and C5–6 levels are most typically affected. In children, injuries are less common and usually involve the upper cervical spine.

Up to 40% of cervical spine injuries are associated with neurological injury, with 5–10% reported as the result of missed injury and consequent lack of cervical stabilisation. About 0.1% of cervical spinal cord injuries do not present with a radiographic abnormality. These spinal cord injuries without radiographic abnormality (SCIWORA) most typically affect children and young adults but also occur in older patients, often with associated cervical spine degenerative disease.

Anatomy

The cervical spine (Figure 10.1) is comprised of seven bony segments, separated by intervertebral fibrocartilaginous discs and supporting ligaments. The third to seventh vertebrae are morphologically similar, each with a vertebral body and a posterior neural arch that is comprised of bilateral pedicles, facets and laminae with a single posterior spinous process. They form a protective bony spinal canal, around the spinal cord. Small transverse processes transmit the vertebral arteries via the foramina transversaria, usually from C2 to C6.

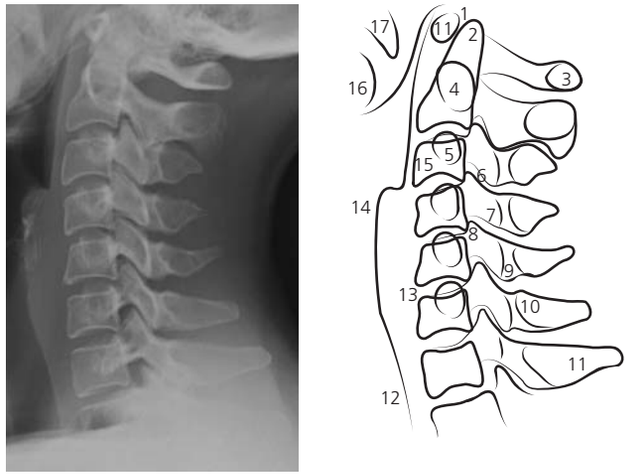


Figure 10.1 Anatomy of cervical spine with line drawing.

The ring-like C1 vertebra (atlas) has anterior and posterior arches but no vertebral body, articulating with C2 and the base of the skull via bilateral lateral masses and the anterior atlantodental joint. There is no C1–C2 intervertebral disc. The C2 vertebra (axis) is distinguished from the adjacent levels by a superior bony projection, the odontoid process or dens, which articulates with C1.

Stability of the cervical spine depends mainly on the integrity of soft tissue structures, in particular the spinal ligaments. The major longitudinal ligaments are the anterior and posterior longitudinal ligaments and the ligamentum flavum. The supraspinous and interspinous ligaments connect the spinous processes. Tough capsules support the facet joints. The apical ligament, alar ligaments and the tectorial membrane (continuation of the posterior longitudinal ligament) give support to the craniocervical junction, and the transverse ligament spans the interval between C1 lateral masses posterior to the dens supporting the C1–C2 articulation.

Imaging of the cervical spine

Patients who are fully conscious with no history of alcohol consumption or drug intoxication, no head injury, no distracting

ABC of Emergency Radiology, Third Edition. Edited by Otto Chan.
© 2013 John Wiley & Sons, Ltd. Published 2013 by John Wiley & Sons, Ltd.

injuries, no symptoms and no clinical signs do not require any imaging. A three-view plain film series (lateral, anteroposterior and open mouth odontoid radiographs) is often performed as the first line investigation for patients whose cervical spine cannot be cleared by clinical assessment alone. Unfortunately, plain radiographs are often suboptimal and even good quality radiographs can fail to demonstrate up to 20% of fractures, so there should be a low threshold to proceed to CT.

CT is a useful adjunct to plain films and is now the first line imaging modality for the spine in major trauma patients, where there is a high risk mechanism as part of whole body CT.

High risk parameters for cervical spine injury

- High velocity motor vehicle collision (>35 m.p.h.)
- Closed head injury
- Fall >10 ft
- Fractures (pelvic, multiple limbs)
- Spinal neurological symptoms
- Death at scene (motor vehicle collision)
- Neck pain/tenderness

Mechanisms of injury to the cervical spine

- Hyperflexion
- Hyperextension
- Rotation
- Axial compression
- Distraction
- Lateral bending/shearing
- Complex or combined vectors

MRI is also indicated where there is neurological injury or possible major ligamentous or intervertebral disc damage (Figure 10.2). Lateral flexion and extension radiographs are no longer recommended.

ABCs systematic assessment

- Adequacy
- Alignment
- Bone
- Cartilage and joints
- Soft tissues

Radiological projections and adequate anatomical coverage

- Lateral: base of skull to T1 superior endplate
- AP: C3 to T1 vertebrae and C2 spinous process
- Open mouth odontoid: C1 and C2 margins should be visible

Interpretation of lateral radiographs

Always review the lateral view as if the patient had turned to the right. This will orientate the lateral view in the same direction as the sagittal CT reconstructions and the sagittal MRI



Figure 10.2 Sagittal STIR MR image following a hyperflexion image demonstrating disruption of the C3/4 disc, ligamentous injury and cord contusion.

Adequacy (Figure 10.3)

The base of skull to the superior endplate of the T1 vertebral body should be demonstrated with clear cortical and trabecular detail. The outline of the pre-vertebral soft tissues and tip of the spinous processes should also be shown. The lower cervical spine should not be obscured by overlying anatomy (shoulders) or extrinsic structures such as jewellery or monitoring devices. If the C7–T1 junction cannot be seen, a swimmer's view should be performed, progressing to CT if still inadequate.

Alignment

The cervical spine normally forms a smooth lordotic curve, which may be flattened (Figure 10.4) or slightly reversed due to pain, muscle spasm, immobilisation or supine position. Pre-existing congenital anomalies or pathology such as degenerative change can also result in abnormal alignment. The anterior longitudinal line, posterior longitudinal line and spinolaminar line should all be traced looking for any abrupt alterations in alignment, which may infer ligamentous or disc injury and instability. The spinolaminar line may deviate slightly anteriorly between C1 and C3 on flexion and slightly posteriorly on extension.

The posterior margins of the facet joints should also form a smooth lordotic curve but this line can be difficult to assess due to rotation. The spinous processes form a tighter lordotic curve from C2 to C7 with no sudden widening of the interspinous distance although the curve may not be perfect due to anatomical variation.

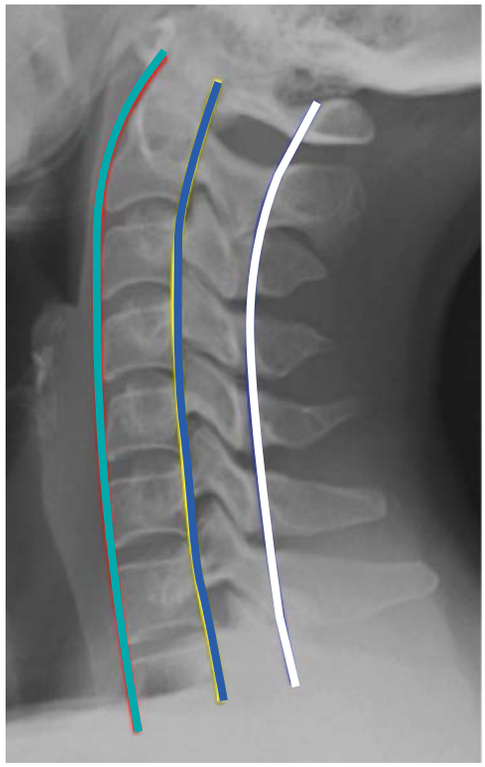


Figure 10.3 Lateral radiograph demonstrating the normal anterior longitudinal line (light blue), posterior longitudinal line (blue) and the spinolaminar line (white).



Figure 10.4 Lateral radiograph with patient immobilised on a spinal board demonstrating flattening of the normal lordosis.

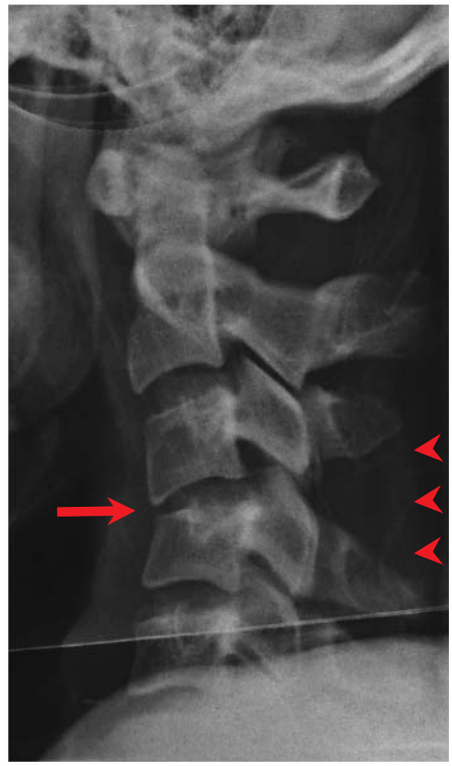


Figure 10.5 Hyperflexion injury with acute angulation at C3/4, facet joint subluxation and interspinous widening.

Hyperflexion injuries (Figure 10.5) result in a focal anterior angulation, which may be accompanied by abrupt widening of the interlaminar and interspinous distances, indicating injury to the posterior ligament complex and subluxation or dislocation of the facet joints.

Facet subluxation (Figure 10.6) is manifest by focal uncovering of the articular surfaces and anterior displacement of the more superior facet. Dislocation of a facet joint produces the 'naked facet sign' and when unilateral usually results in anterior displacement of the more superior vertebral body by less than one half of the vertebral body's width. The dislocated facet is displaced anteriorly, and the facet joints above the site of the injury may take on a 'bow tie' configuration as a result of associated rotation. Bilateral facet dislocation is characterised by anterior subluxation of the vertebral body by more than half of the vertebral body's width. The intervertebral disc space is usually narrowed, with little or no rotation.

Hyperextension injuries may be extremely subtle with widening of the anterior disc space and facet joints plus posterior displacement of the vertebrae above the injury.

Atlanto-occipital alignment (Figure 10.7) can be assessed by measuring the Powers ratio, which should lie within the range of 0.6–1.0. A ratio >1.0 indicates anterior subluxation/dislocation. The bony landmarks can however be difficult to visualise on plain radiographs and several alternative lines and measurements can be used (Figure 10.8 & 10.9).

Atlantoaxial alignment should be routinely evaluated on lateral films by measuring the atlantodental (predental) space, which

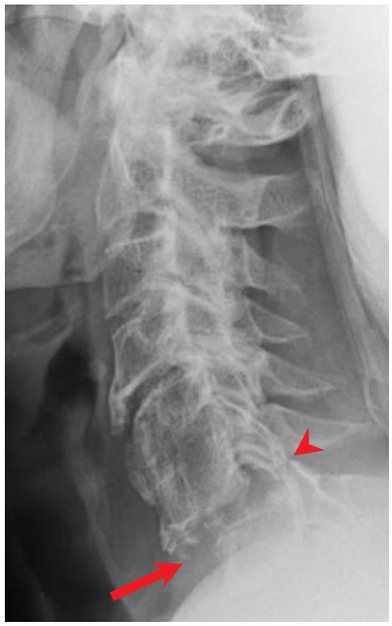


Figure 10.6 Bilateral facet joint dislocation with anterior subluxation of C6 on C7.

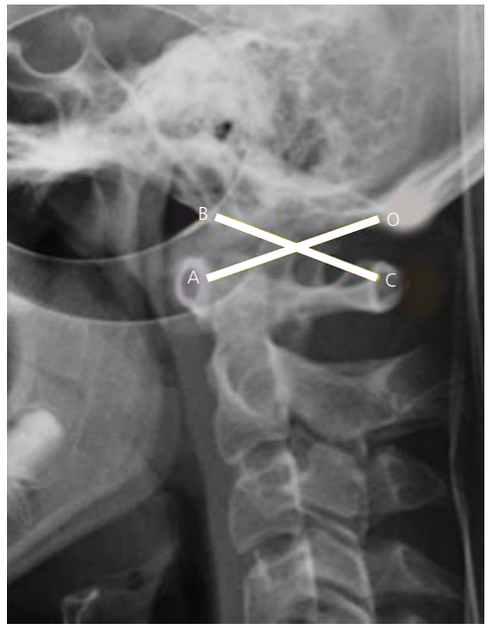


Figure 10.7 The Powers ratio (BC AO) for assessing craniocervical alignment: 0.6–1.0, normal; >1.0, anterior dislocation.

should be less than 3 mm in adults and 5 mm in children. Widening indicates anterior subluxation of C1 on C2 with associated transverse ligament injury.

Atlanto-occipital alignment

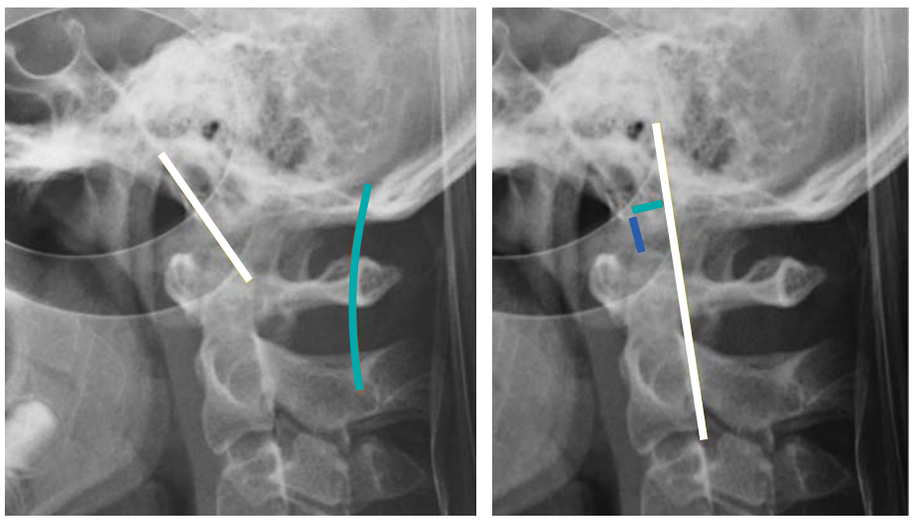
- Basiodental interval – distance from basion to tip of dens
- Posterior axial interval – perpendicular distance between the basion and posterior axial line (cranial extension of posterior longitudinal line)
- Line drawn along clivus intercepts tip of dens
- C1 spinolaminar line intercepts posterior margin of foramen magnum

Normal measurements

- Basiodental interval: ≤12 mm
- Posterior axial interval: <12 mm when basion anterior to posterior axial line; <4 mm when posterior to posterior axial line

Bone

The cortical outline and trabecular pattern of each vertebra should be examined looking for discontinuity, angulation, step off, bowing, or an abrupt alteration in density. No bony fragments should project over the spinal canal. Slight anterior wedging of the C3-C7 vertebral bodies by up to 3 mm can be a normal variant.



(a) (b)

Figure 10.8 (a). Line along clivus (white) intercepts odontoid. C1 spinolaminar line (light blue) intercepts opisthion. (b). Basion-dental line (dark blue) <12 mm, Line along posterior axis (white) within 12 mm of basion (light blue).

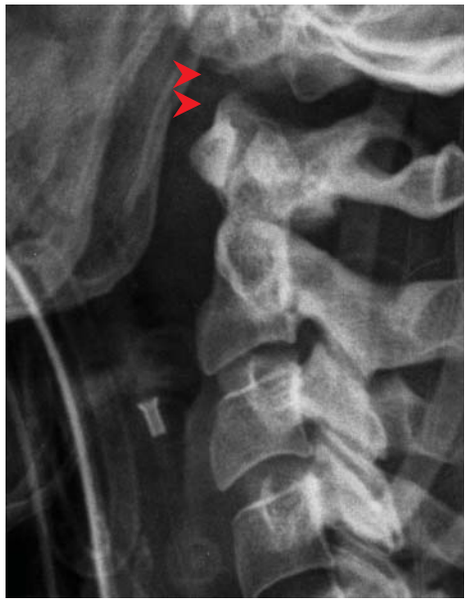


Figure 10.9 Lateral radiograph demonstrating disruption of the craniocervical junction.

Where there is loss of anterior vertebral body height by more than 3 mm a compression fracture should be suspected and may be associated with focal disruption of the anterior wall cortex or the anterosuperior rim. If the posterior wall of the vertebral body has also lost height it is considered a 'burst fracture' (Figure 10.10) and may be associated with retropulsion of a posterior wall fragment into the spinal canal, which can compress the spinal cord.

A large inferior 'teardrop' fragment with posterior displacement of the vertebral body indicates a hyperflexion teardrop fracture (Figure 10.11), which frequently occurs at the C5 level with associated posterior ligament injury and spinal canal compromise. By comparison a hyperextension teardrop fracture (Figure 10.12) typically affects the C2 vertebral body. It is distinguished by a small, triangular fragment at the anteroinferior rim of the vertebral body and may be associated with anterior disc space widening but usually no posterior displacement.

The odontoid peg should be examined for a cortical break, displacement or increased angulation. Up to 36° of posterior angulation relative to the C2 body can be seen with normal variation.

The C2 Harris ring (Figure 10.13) is a composite ovoid shaped ring projected over the body of C2, which may be incomplete inferiorly. Disruption of the ring or widening of the C2 vertebral body (the 'fat C2' sign) (Figure 10.14) suggests a C2 injury, typically a low dens fracture or an atypical 'hangman's fracture' involving the C2 body (Figure 10.15). The typical hangman's fracture is a traumatic disruption of the C2 pars interarticularis, which may be associated with anterior displacement or angulation of C2 on C3.

Posterior element fractures occur in isolation or in association with vertebral body, disc or ligamentous injury. The spinous processes may fracture at any level and when occurring at the C6-T1 levels, are also known as a 'clay shoveler's fracture' (Figure 10.16). Fractures of the transverse processes may breach the foramina transversarium and can be associated with a vertebral artery injury.



Figure 10.10 Sagittal CT reconstruction demonstrating a burst fracture of C7 with minor retropulsion of the posterior wall.



Figure 10.11 Flexion teardrop fracture of C6.



Figure 10.12 Extension teardrop fracture of C2.



Figure 10.13 Normal C2 Harris ring.

Cartilage and joints

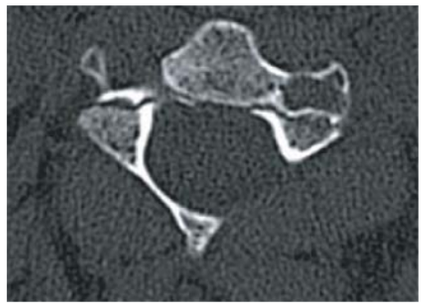
The intervertebral discs cannot be directly visualised unless calcified but may be involved in a variety of injury patterns. Injury can be inferred by widening, narrowing or asymmetry of the disc space or by angulation or translation between adjacent vertebrae. Degenerative narrowing is common in the adult population and may cause confusion but is often symmetric and associated with other features of degenerative change such as endplate sclerosis and osteophyte formation. The facet margins should be parallel, and incongruity should prompt scrutiny of the affected segment for other signs of injury, such as interspinous widening.



Figure 10.14 Disruption of the C2 ring and the 'fat C2' sign due to a complex C2 body fracture. A posterior arch fracture of C1 is also present.



(a)



(b)

Figure 10.15 (a) Lateral radiograph and (b) axial CT image demonstrating a hangman's fracture of C2.



Figure 10.16 Spinous process (clay shoveler's) fractures of the C6 and C7 spinous processes.

Soft tissues

Cervical spine injuries may cause anterior soft tissue swelling (Figure 10.17) due to haemorrhage and oedema. In the upper cervical spine from C2 to C4 the soft tissues should not exceed 7 mm or one third of a vertebral body width, and below C4 should not exceed 21 mm or one vertebral body width. Diffuse or localised prevertebral soft tissue swelling may be the only indicator of an injury, although the finding is not specific for injury and a normal prevertebral soft tissue shadow does not exclude an injury. The airway and pharynx should be checked for swallowed foreign bodies, teeth, and malpositioned life support devices. Foreign bodies may also be projected over the soft tissues.

Normal prevertebral soft tissue shadow (3–7–21 rule)

- <7 mm or one-third of width of vertebral body at C3 (C2 to C4)
- <21 mm or width of vertebral body at C7 (below C4)

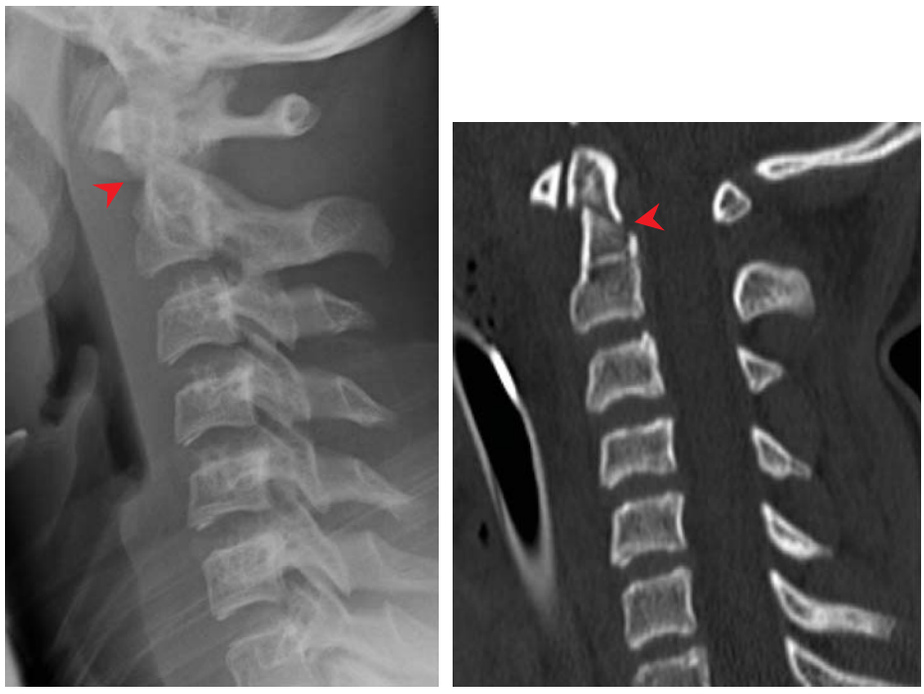
Causes of prevertebral soft tissue widening (other than cervical spine injury)

- Haemorrhage from face or skull base fracture
- Blood pooling in pharynx
- Prominent lymphoid tissue
- Endotracheal or orogastric tube
- Hypoaeration (child crying)
- Pus

Interpretation of anteroposterior radiographs

Adequacy

A true AP projection should be obtained which clearly demonstrates C3-T1. Overlying devices such as endotracheal tubes should not obscure vertebrae.



(a) (b)

Figure 10.17 Lateral radiograph (a) demonstrating upper cervical soft tissue swelling. Subsequent CT scan (b) demonstrates a type 2 odontoid peg fracture.



Figure 10.18 AP radiograph demonstrating abrupt rotation at C5/6 due to a unifacet dislocation.

Alignment

The vertebral body margins, articular pillars and spinous processes should be in line. If the neck is rotated, the spinous processes lose their vertical orientation with a gradual offset to the right or left. Abrupt alteration in alignment indicates injury, such as unilateral facet dislocation (Figure 10.18).

Bone

The vertebral bodies (Figure 10.19) should have a symmetrical rectangular shape. The facets should also be rectangular: height should be greater than width. An asymmetrically shortened facet with prominent joint spaces typically indicates an articular pillar fracture (Figure 10.20).

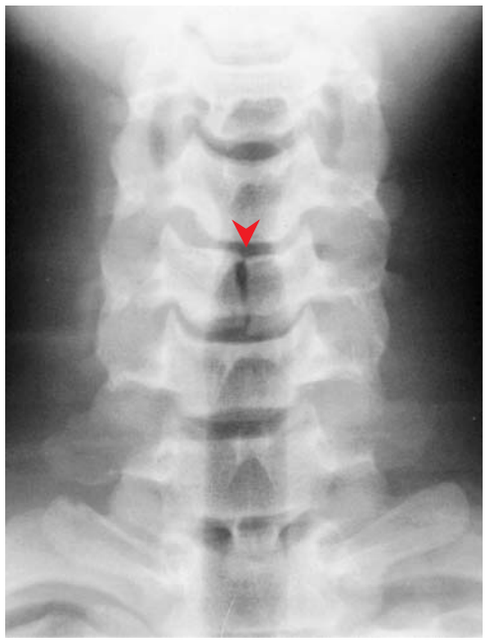


Figure 10.19 Sagittal split fracture of the C5 vertebral body.



Figure 10.20 AP radiograph demonstrating an isolated fracture of the right C7 articular pillar (arrow).

Cartilage and joints

Each intervertebral disc space should be symmetric with parallel vertebral endplates. The facet joints should be symmetric.

Soft tissues

Displacement or obscuration of the laryngotracheal air column may indicate a haematoma due to a spinal or soft tissue injury. Support tubes and lines should also be assessed and foreign bodies excluded.

Interpretation of open mouth odontoid radiographs

Adequacy

A true AP projection is required without rotation. The odontoid process should be visualised clearly (Figure 10.21) and not obscured by the occiput or overlying incisor teeth. The C1 and C2 lateral articulations should also be discernible.

Alignment

The lateral margins of C1 and C2 should line up with no more than 1–2 mm of overlap, and the lateral atlantodental intervals should be symmetric. Asymmetry is present with rotation (which may be positional or due to injury) or in association with C1 or C2 fractures (Figure 10.23). Widening of C1 with overlap of one or both of the articular facets relative to the lateral masses of C2 indicates a Jefferson burst fracture of the atlas (Figure 10.24) which commonly splits the ring into four pieces with bilateral anterior and posterior arch fractures.

The dens should also lie vertically with respect to the body of C2 and lateral angulation is indicative of an odontoid fracture.

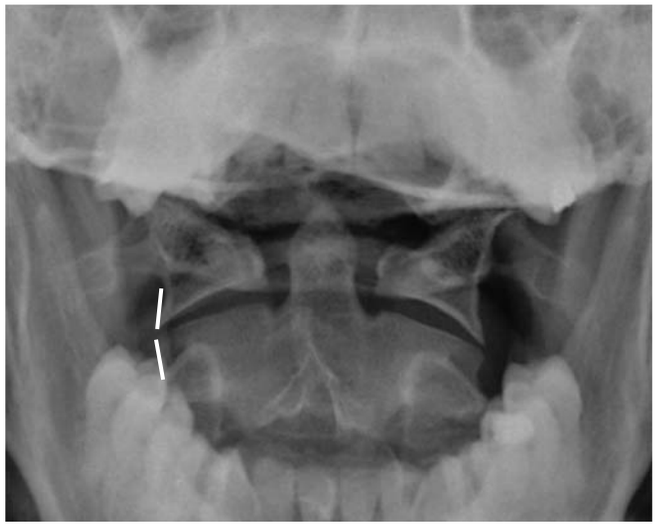


Figure 10.21 Open mouth AP odontoid radiograph demonstrating normal alignment (no overlap – white lines).

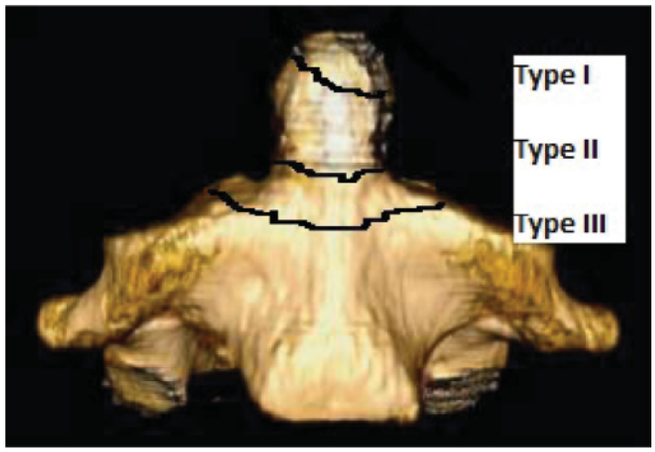


Figure 10.22 3D CT reformat illustrating Type I–III odontoid peg fractures.

Types of dens fractures (Figure 10.22)

- Type I: Tip of dens
- Type II: Base of dens
- Type III: Low dens fracture extending into C2 body

Bones

The bone margins should be traced looking for any cortical break or distortion of the normal contour. Small cortical notches are commonly seen at the base of the odontoid peg on each side and are a normal variant.

Cartilage and joints

The joint spaces between the inferior articular surface of C1 and the superior surface of C2 lateral should be parallel and symmetric.

Soft tissues

Soft tissue swelling is rarely apparent on this projection.

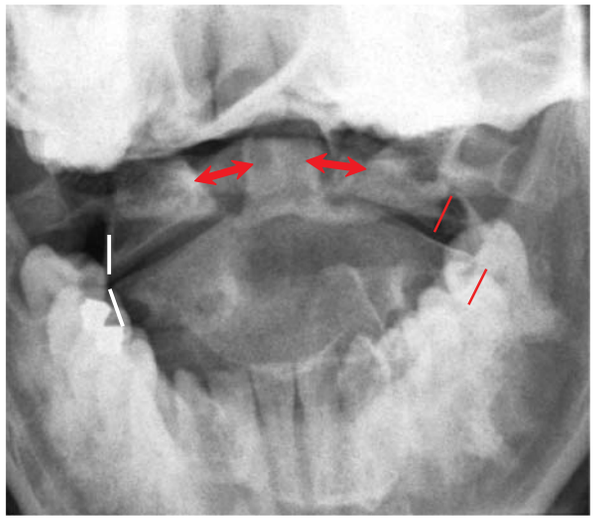
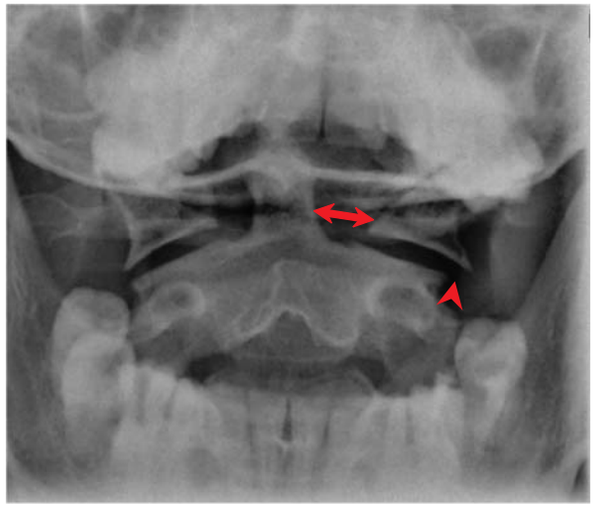


Figure 10.23 Asymmetry of the lateral atlantodental spaces with a C1 left lateral mass fracture.



(a)



(b)

Figure 10.24 Jefferson fracture of C1. (a) Open mouth odontoid radiograph demonstrating asymmetry of the lateral atlanto-odontoid spaces and overlap of the left C1 lateral mass. (b) Axial CT image confirms a three part fracture.



Figure 10.25 Congenital fusion of the C3 and C4 vertebrae (Klippel–Feil).

Pitfalls

All the cervical vertebrae from C1 to T1 may not be clearly demonstrated on plain radiographs, particularly the craniocervical and cervicothoracic junctions, both of which are prone to injury.

The presence of congenital variants (Figure 10.25), advanced degenerative changes or other spinal disorders such as ankylosing spondylitis (Figure 10.26) can make assessment of plain radiographs difficult. There should be a low threshold for progressing to CT in all these circumstances.

The upper cervical soft tissues may be artificially altered or widened by causes other than trauma.

Overlapping structures may mimic a fracture particularly at the C1 and C2 levels.

In children there are normal variants that can mimic injury such as pseudosubluxation where there is slight anterior translation of C2 on C3, or C3 on C4 in children up to eight years of age with normal alignment of the spinolaminar line.

ABCs systematic assessment

Adequacy

- Superior endplate of T1 is included on lateral view
- Open mouth odontoid view not rotated

Alignment

- Check the spinal lines (anterior longitudinal, posterior longitudinal line, spinolaminar line)
- Atlanto-occipital alignment
- Atlanto-dental space <3 mm (adults)

Bone

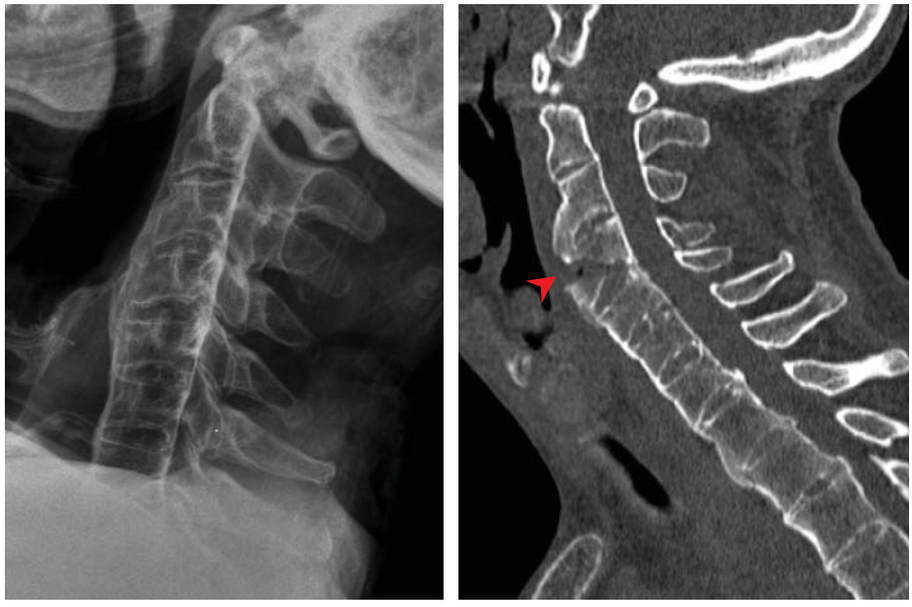
- Vertebral body height
- Bony contours
- Posterior neural arch

Cartilage and Joints

- Intervertebral disc space
- Facet joints
- Atlantodental joint and atlantooccipital joint

Soft Tissues

- Prevertebral soft tissues
- Exclude foreign bodies and teeth
- Check airway and life support devices



(a) (b)

Figure 10.26 Male patient with ankylosing spondylitis post trauma. (a) Lateral radiograph demonstrates cervical spine ankylosis but no clear fracture. (b) Sagittal reformat from a subsequent CT shows a C4 vertebral body fracture.

Injuries – a summary

- Atlanto-occipital dissociation – head and neck are separated
- Jefferson's fracture – burst fracture of C1 ring
- Odontoid fractures – types I – III
- Hangman's fracture – pars interarticularis fracture of C2
- Hyperflexion teardrop fracture – commonly C5
- Hyperextension teardrop fracture – commonly C2
- Unilateral facet dislocation – <50% subluxation of vertebral body. Abrupt rotation on AP film
- Bilateral facet dislocation – >50% anterior subluxation of vertebra body
- Clay shoveler's fracture – spinous process fracture C6 or C7

Further reading

Cassar-Pullicino VN, Imhof H (Eds). *Spinal Trauma – An Imaging Approach*. Thieme, 2006.

Hoffman JR, Mower WR, Wolfson AB et al. Validity of a set of clinical criteria to rule out injury to the cervical spine in patients with blunt trauma. *N Engl J Med* 2000;343:94–99.

Hogan GJ, Mirvis SE, Shanmuganathan K, Scalea TM. Exclusion of cervical spine injury in obtunded patients with blunt trauma: is MR imaging needed when multidetector row CT findings are normal? *Radiology* 2005;37:106–113.

Stiell IG, Wells GA, Vandemheen KL, et al. The Canadian C-spine rule for radiography in alert and stable trauma patients. *JAMA* 2001;286(15): 1841–1848.

CHAPTER 11

Thoracic and Lumbar Spine

Leonard J. King[1], *Andreas Koureas*[2] *and Otto Chan*[3]

[1]Southampton University Hospitals, Southampton, UK
[2]University of Athens, Athens, Greece
[3]The London Independent Hospital, London, UK

OVERVIEW

- The TS and LS are better protected than the CS
- Larger forces are necessary to cause serious injuries
- Spinal injuries are often associated with injuries elsewhere
- In major trauma, TS and LS CT is covered as part of the whole body CT protocol
- MRI is indicated if there is suspicion of neurological, ligamentous or disc injury

Injuries to the thoracic and lumbar spine (TS and LS) commonly occur as a result of high-energy trauma such as falls from a height or motor vehicle collisions with axial loading, hyperflexion, extension, distraction, rotation or shearing forces. Lower energy trauma such as simple falls can result in significant injury, particularly where there is a predisposing condition such as osteoporosis, ankylosing spondylitis or spinal metastases. Patients may present with specific signs or symptoms suggesting injury to the spine such as back pain or a cauda equina syndrome. Most significant injuries are encountered in victims of major trauma who may have other life-threatening injuries. Clinical examination of the thoracic and lumbar spine is part of the secondary survey and is deferred until life-threatening conditions have been stabilised. Clinical evaluation can be misleading, especially in patients with other distracting injuries and is of limited value in unconscious patients. In these patients, CT of the TS and LS is covered as part of the whole body CT protocol.

Spinal injuries may be either stable or unstable with risk of mechanical or neurological deterioration. Injuries should be assumed to be unstable with appropriate immobilization and log rolling, until fully assessed by an experienced clinician and appropriate imaging has been performed.

Anatomy (Figure 11.1)

There are normally 12 thoracic (Figure 11.2) and 5 lumbar vertebrae (Figure 11.3); however, variations are relatively common and it can be difficult on imaging to determine which are the T12/L1 or L5/S1 vertebrae. This is due partly to variation of the 12th ribs, but mainly to the presence of transitional vertebrae (Figure 11.4) at the lumbosacral junction with partial sacralisation of L5 or partial lumbarisation of S1. Six lumbar vertebrae may also occasionally be present. If images of the TS and LS are available then levels can be determined by counting down from T1; however, this may be further complicated by the presence of cervical ribs. The longest and most horizontal transverse processes are usually at L3.

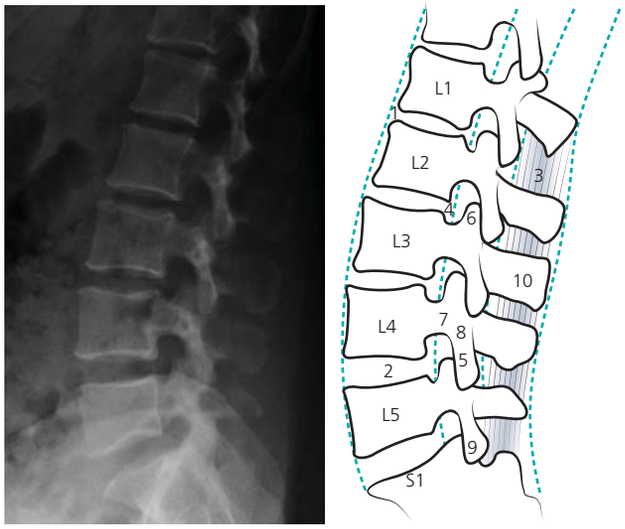
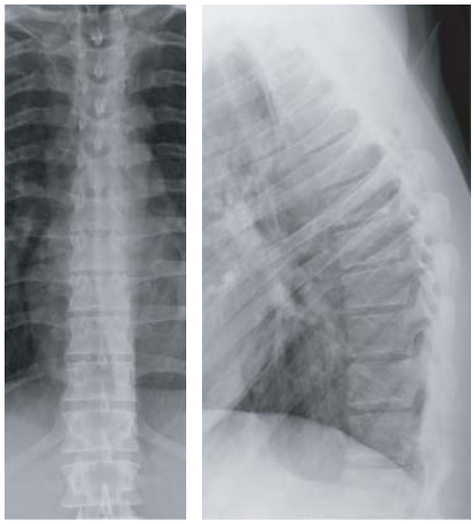


Figure 11.1 Anatomy of lumbar spine: lateral LS and drawing. 1, ALL; 2, IVDS; 3, interspinous ligament; 4, PLL; 5, inferior articular facet of L4; 6, superior articular facet of L3; 7, pedicle of L4; 8, pars interarticularis of L4; 9, ligamentum flavum; 10, spinous process of L3.

Each vertebrae comprises a body and spinous process, plus two paired pedicles, transverse processes, superior and inferior articular facets, pars interarticularis and laminae. In the TS, there are articular facets on the lateral aspect of the vertebral bodies for articulation with the ribs. The lumbar vertebral bodies are larger and have a more horizontal spinous process.

Numerous strong ligaments support the spine, including the anterior and posterior longitudinal ligaments, the ligamentum flavum, and the interspinous and the supraspinous ligaments. The thoracic column is also stabilised by the upper ribs which form the

ABC of Emergency Radiology, Third Edition. Edited by Otto Chan.
© 2013 John Wiley & Sons, Ltd. Published 2013 by John Wiley & Sons, Ltd.



(a) (b)

Figure 11.2 (a) Normal AP and (b) lateral views of the thoracic spine.



(a) (b)

Figure 11.3 (a) Normal AP and (b) lateral views of the lumbar spine.

thoracic cage. The lower ribs and the LS have strong surrounding muscles which augment the intrinsic stability provided by the discs, ligaments and facet joints.

The transition between the relatively immobile TS and the more flexible LS renders the thoracolumbar junction relatively vulnerable to injury, and around 60% of all injuries occur between T11 and L2. Upper and mid TS injuries are relatively uncommon in adults. By contrast, children have a relatively more mobile spine and injuries

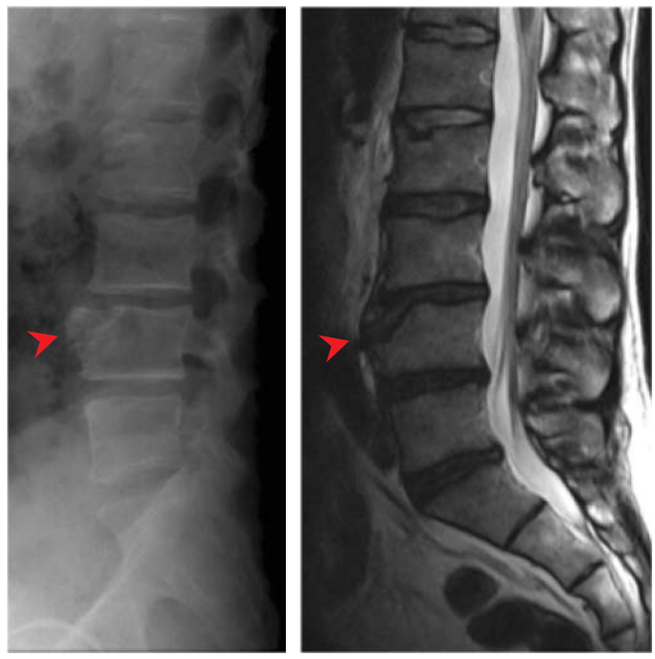


Figure 11.4 AP view of the lumbar spine demonstrating a transitional lumbosacral vertebra with articulation on the left side (Bertolotti's syndrome if patient is symptomatic).

are most common at T4/5 and L2. The injuries are often multiple and contiguous.

Congenital vertebral anomalies such as hemivertebrae and butterfly vertebrae, or limbus vertebrae (Figure 11.5) due to non-fusion of the ring apophyses, can be confusing and may be mistaken for acute fractures.

The spinal cord terminates at the conus medullaris, which usually lies between T11 and L2. Below this level, neurological injuries are lower motor neurone due to nerve root injury, whereas more



(a) (b)

Figure 11.5 (a) Lateral radiograph and (b) sagittal T2 weighted MR image demonstrating an L4 limbus vertebra.



Figure 11.6 Lateral radiograph demonstrating minor anterior wedge compression fractures of L1 and L2.

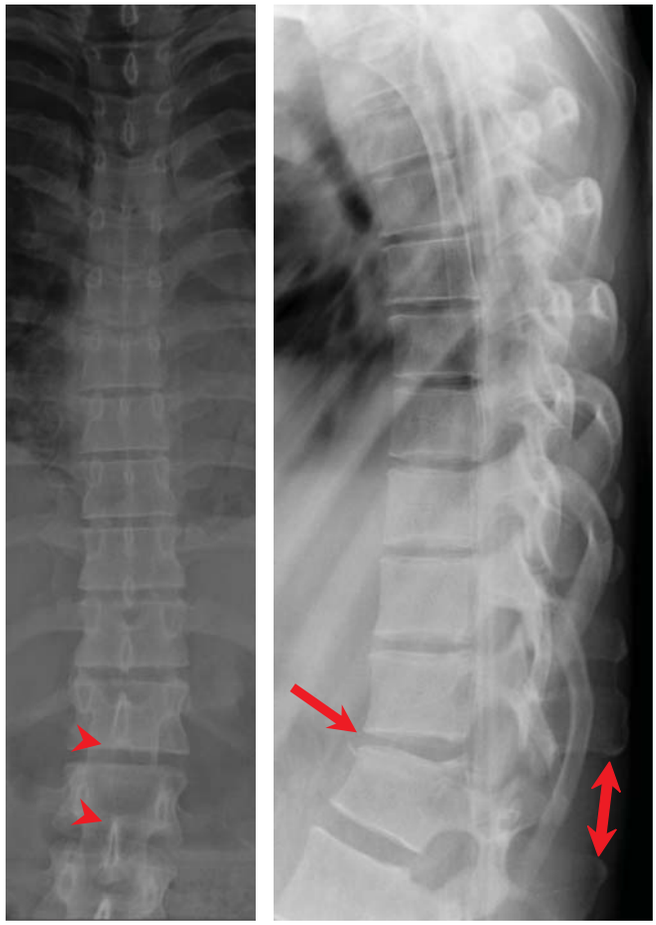
proximal spinal cord injuries are upper motor neurone resulting in hyperreflexia, spinal shock and spasticity.

Mechanism of injury

There are several definable force vectors, which can result in spinal trauma, producing predictable patterns of injury (Box 11.1). Injuries are frequently the result of hyperflexion with forced bending around a fulcrum centered on the posterior third of the vertebral body. This produces anterior vertebral compression fractures (Figure 11.6) and when severe is associated with posterior element distraction (Figure 11.7). Axial loading for example due to a fall from a height produces compressive forces which result in burst fractures of the vertebral body (Figure 11.8). Hyperextension, rotation and shearing forces also produce defined patterns of injury although in many cases injuries are due to a combination of forces such as hyperflexion and axial loading, or flexion and rotation.

Box 11.1 **Mechanisms of thoracic and lumbar spine injury**

- Hyperflexion – usually at thoracolumbar junction (T11–L3) with a wedge fracture
- Hyperextension – tears the anterior longitudinal ligament and widens the disc space
- Axial compression – discs and vertebral bodies explode (burst injuries)
- Distraction – rare but may cause ligament damage without bony injury
- Shearing – slip in any direction, causing disruption of ligaments
- Rotation – leads to facet joint and combination injuries
- Complex or combined vectors



(a) (b)

Figure 11.7 AP (a) and lateral (b) radiographs of a hyperflexion injury at T12/L1 with interspinous widening, perched facets and disc disruption.

In motor vehicle collisions, seat belts act as a fulcrum around which the spine can move. Three-point fixation belts with a lap belt and sash combination may result in upper or mid TS injuries due to flexion and rotation. Lap belts however are associated



Figure 11.8 Axial CT image demonstrating a burst fracture of L4 with retropulsed bony fragments.



(a) (b)

Figure 11.9 (a) AP radiograph and (b) sagittal CT reformat image of an L2 Chance fracture in a child.



(a) (b)

Figure 11.11 (a) CT sagittal reformat and (b) short TI inversion recovery (STIR) MR image of a thoracic spine translation injury with spinal cord transection in a patient with ankylosing spondylitis.

with flexion distraction injuries where the spine is flexed around an anterior fulcrum (the lap belt) producing anterior as well as posterior distraction with little or no anterior compression. The classic 'Chance fracture' type of flexion distraction injury occurs at the thoracolumbar junction or the mid LS, horizontally splitting the posterior elements including the spinous process as well as the posterior portion of the vertebral body (Figure 11.9). There are several variants however which can disrupt the interspinous ligaments or the intervertebral disc.

Underlying bone disease such as osteoporosis, metastases (Figure 11.10), myeloma, Paget's disease or ankylosing spondylitis (Figure 11.11), predispose to spinal fractures and should be suspected if an injury appears out of proportion to the mechanism and degree of trauma (Box 11.2). Expansion, destruction, osteopenia, lucencies or sclerosis of a vertebrae, should also raise the suspicion of underlying pathology.



Figure 11.10 Sagittal T2 MR image of an L2 pathological fracture through a vertebral body metastasis.

Box 11.2 **Conditions predisposing to spinal injury**

- Degenerative disease
- Malignancy (e.g. metastases or myeloma)
- Osteoporosis / osteomalacia
- Infection
- Paget's disease
- Haemangioma
- Ankylosing spondylitis
- Developmental or congenital anomalies

Imaging of the thoracic and lumbar spine

In general, two orthogonal views are taken as the first line of investigation (Box 11.3)

Box 11.3

- Thoracic spine – anteroposterior and lateral views (Figure 11.2)
- Lumbar spine – anteroposterior and lateral views (Figure 11.3)
- Additional views of LS – coned LS view or oblique LS (suspected pars defect)

CT is a useful adjunct to plain films and is now the first line imaging modality for the whole spine in major trauma patients, where there is a high-risk mechanism as part of the whole body CT protocol.

MRI is also indicated where there is neurological injury or possible major ligamentous or intervertebral disc damage. This allows assessment of any cord injury and demonstrates ongoing neurological compression by disc, bone fragments, subluxation or epidural haematoma. It is also useful to assess ligamentous or disc disruption and can demonstrate radiographically occult vertebral body fractures.

ABCs systematic assessment

The thoracic and lumbar spine should be assessed in a systematic fashion using the ABCs technique.

- **A**dequacy
- **A**lignment
- **B**one
- **C**artilage and joint
- **S**oft tissue

Interpretation of lateral radiographs

> Always review the lateral view as if the patient had turned to the right. This will orientate the lateral view in the same direction as the sagittal CT reconstructions and the sagittal MRI

Adequacy

The whole of the TS and LS and the TL junction should be demonstrated. The upper TS can be difficult to demonstrate on lateral radiographs due to the overlying shoulders. Artefactual lines from clothing, sheets, drips, and ECG wires are common and should not obscure the spinal anatomy.

Alignment

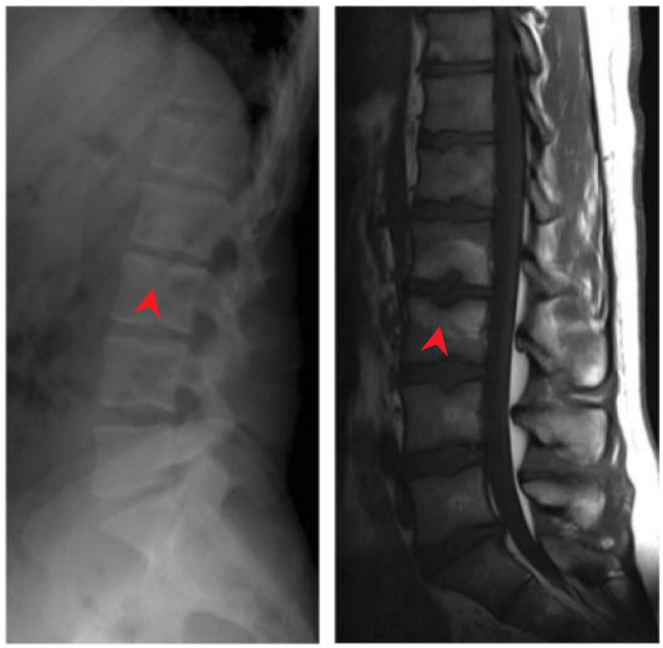
On lateral radiographs, the TS should have a gentle midthoracic kyphosis and the LS a slightly more pronounced lordosis. The anterior and posterior longitudinal lines (ALL and PLL), the spinolaminar line (SLL) and the facet joints should form smooth curves with no abrupt steps.

Bones

The bony outlines of each vertebra should be sharply defined with no loss of continuity of the cortex other than the posterosuperior cortical margin which is difficult to define. The superior and inferior endplates should be minimally concave and the anterior cortex should be flat or minimally concave. Schmorl's nodes (Figure 11.12) are small areas of disc herniation though the vertebral endplates causing scalloping of the cortex, which are developmental or degenerate and may be associated with Scheuermann's disease. They are commonly seen in the TL spine and should not be confused with acute trauma. No bony fragments should be projected over the spinal canal. The vertebral bodies should increase slightly in height extending caudally from T1 to L5. The thoracic vertebrae often demonstrate slight anterior wedging as a normal variant particularly at T11-L1 which can be mistaken for a compression fracture.

Cartilage

The intervertebral disc spaces should be relatively uniform increasing slightly in height extending caudally down to the L4-L5 level. The L5/S1 disc is usually slightly narrower than the L4/L5 disc. The lumbar discs are usually slightly wider anteriorly than posteriorly. Diffuse widening or posterior widening of an intervertebral disc space suggests a flexion distraction injury with disc disruption. Anterior widening can indicate a hyperextension injury. Disc narrowing is usually degenerative but can be the result of an acute disc injury or herniation.



(a) (b)

Figure 11.12 (a) Lateral radiograph and (b) sagittal T1 weighted MRI image demonstrating multiple Schmorl's nodes with prominent marrow reaction at L2/3.

Soft tissues

The soft tissue outlines are of limited value on the lateral view but a large prevertebral haematoma may occasionally be seen in the thoracic region. Widening of the facet joints or interspinous distances indicates ligamentous injury. Foreign bodies such as bullets or glass fragments may also be demonstrated.

Interpretation of anteroposterior radiographs

Adequacy

The whole of the TS and LS and the thoracolumbar junction should be demonstrated without rotation. The bony structures and the paraspinal soft tissues should be visualised without overlying artefact.

Alignment

The lateral margins of the vertebral bodies, the facet joints and the spinous processes should be vertically aligned with no sudden lateral deviation or angulation (Figure 11.13). The pedicles should form two slightly diverging columns with gradual widening of the interpedicular distance from T1 to L5. Abrupt widening can be a feature of burst fractures (Figure 11.14).

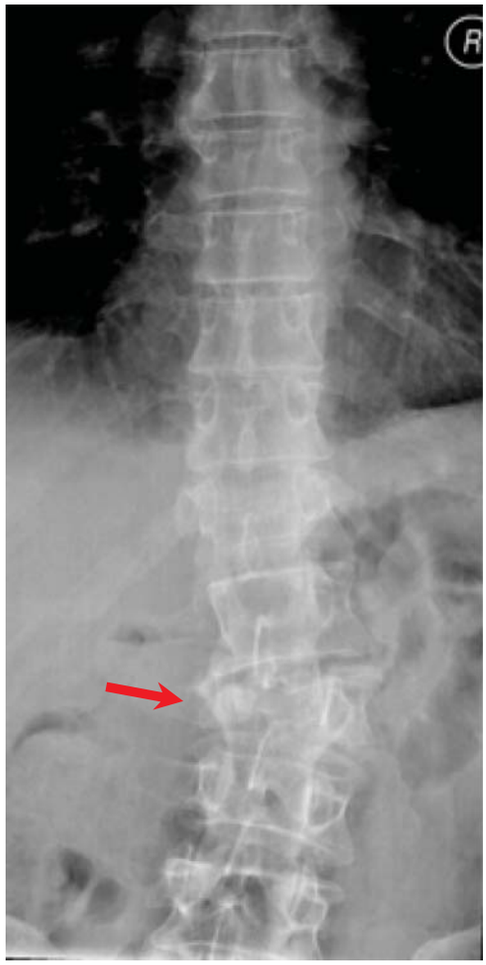


Figure 11.13 AP radiograph demonstrating loss of mid lumbar coronal alignment due to an L2 fracture.

Bones

As on the lateral view the cortical outlines should be smooth and sharp with minimally concave endplates. The height of the vertebral bodies should be similar. Loss of height is indicative of a wedge or burst fracture. The pedicles should be oval, distinct and symmetrical.

The spinous processes should lie in the midline, between the pedicles. Widening of the interspinous spaces indicates disruption of the supraspinous and interspinous ligaments.

Cartilage

The disc spaces should be symmetric and parallel, increasing slightly in height from T1 to L4. The L5/S1 disc space is poorly visualised on the anteroposterior (AP) view.

Soft tissues

The soft tissue contours and fat planes should be smooth and regular. In the TS, the left paraspinal line is usually wider and easier to see than the right paraspinal line, but focal or diffuse widening of the paraspinal lines indicates a posterior mediastinal haematoma (Figure 11.15) due to a spinal or mediastinal injury. Airway deviation and apical pleural capping may also be demonstrated.

In the LS, loss, asymmetry or blurring of the psoas shadow may indicate a retroperitoneal haematoma or collection.

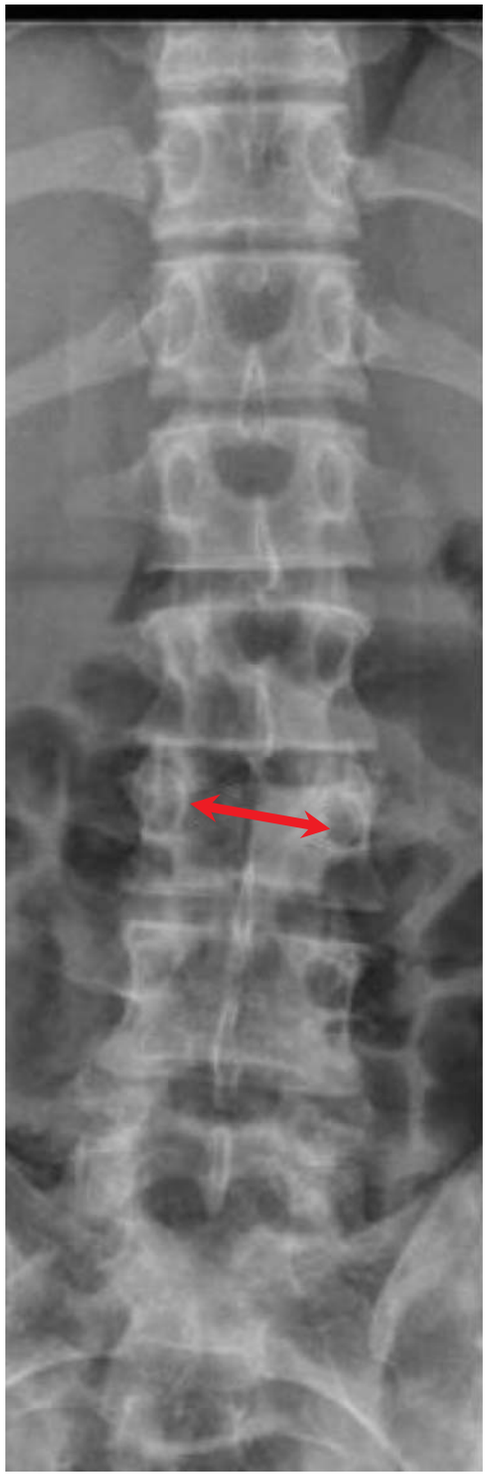


Figure 11.14 AP radiograph demonstrating widening of the interpedicular distance due to an L3 burst fracture.

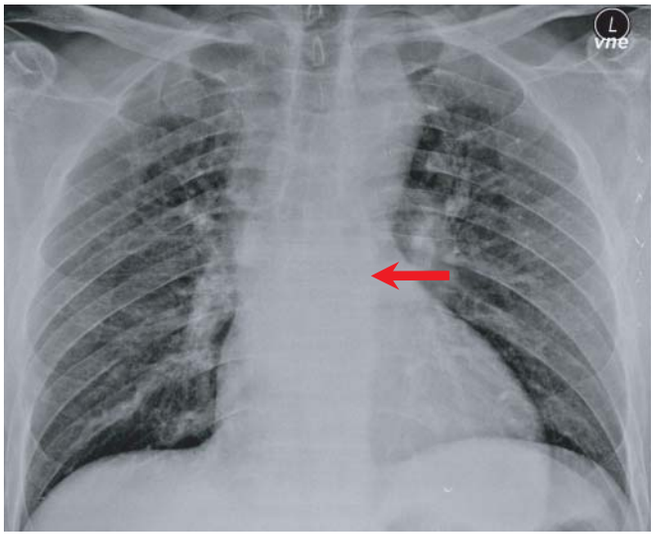


Figure 11.15 Chest radiograph demonstrating widening of the left paraspinal line due to a mid thoracic fracture.

Classification of injuries

Injuries are usually classified according to the pattern of damage or the mechanism by which the injury occurred (Box 11.4). Classification of injuries can help to determine their stability and the likely requirement for surgical stabilization. Numerous classification systems have been described for injuries to the thoracic and lumbar spine. The more complex systems classify injuries in detail but can be difficult to use in practice and are prone to lack of inter observer agreement. Simple classification systems such as the three column model described by Denis (Figure 11.16) are therefore commonly referred to although this system does not necessarily accurately predict which patients will require surgery.

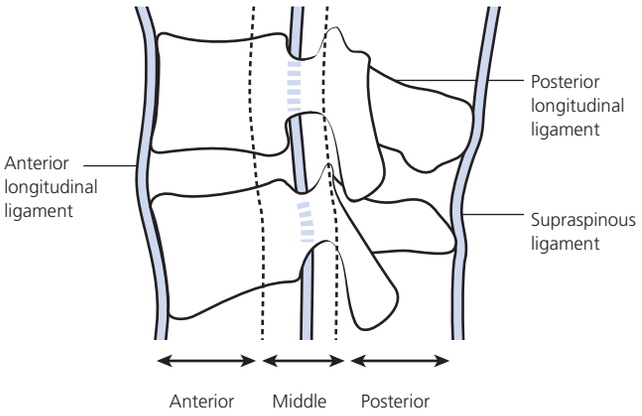


Figure 11.16 Denis's three column model of spinal stability divides the spine into three columns – anterior, middle and posterior. Disruption of two columns indicates that an injury is unstable. Definite disruption of the middle column indicates that an injury is unstable. Assume instability until it is proved otherwise.

Box 11.4 **Injuries – a summary**

- Wedge fracture – an isolated anterior body compression fracture
- Hyperflexion injuries – compress the anterior column with distraction of the middle column and posterior columns. Usually unstable
- Burst fracture – common and usually unstable with a body fracture, widening of the pedicles and disruption of the posterior bony ring
- Chance fracture – flexion distraction injury with a horizontal body fracture, extending into the pedicles and posterior elements
- Translation injury – alignment disrupted by shear forces

ABCs systematic assessment

Alignment

- Normal kyphosis and lordosis on lateral view
- Check 3 lines (ALL, PLL and SLL) on lateral view
- Check lateral margins of vertebral body on AP view

Bones

- Check each vertebra for fractures
- Check height of each vertebra body on both AP and lat views
- Assess the anterior, middle, and posterior columns

Cartilage

- Check disc spaces
- Exclude focal and diffuse narrowing of disc spaces
- Exclude focal and diffuse widening of disc spaces

Soft Tissues

- Check the paraspinal lines
- Check for symmetrical psoas shadows
- Check interspinous distance – exclude widening

Further reading

Cassar-Pullicino VN, Imhof H (Eds). *Spinal Trauma – An Imaging Approach*. Thieme, 2006.

Mirvis S, Shanmuganathan K (Eds). *Imaging in Trauma and Critical Care*, 2nd Edn). Saunders, 2003.

Wintermark M, Mouhsine E, Theumann N, Mordasini P. Thoracolumbar spine fractures in patients who have sustained severe trauma: depiction with multi-detector CT. *Radiology* 2003; 227:681–689.

CHAPTER 12

Chest

Arjun Nair[1] *and Ioannis Vlahos*[2]

[1]St George's Hospital, London, UK
[2]St George's, University of London, London, UK

OVERVIEW

- Plain radiographs remain the mainstay of imaging
- It is important to understand the basic technical concepts underpinning CXRs and thoracic CT to appreciate their benefits and limitations
- A systematic approach is crucial to evaluating the imaging appearances of various traumatic and non-traumatic conditions of the chest

The chest radiograph (CXR) remains the initial method of assessing the thorax in most patients presenting to the emergency department. At the same time, limitations of the CXR may mean that further imaging with other modalities, usually computed tomography (CT) is needed. This chapter provides a basis for understanding the normal appearances of the thorax on imaging, a structured evaluation approach, and descriptions of the common traumatic and non-traumatic conditions relevant to the emergency department.

Imaging techniques

Chest radiograph (CXR)

The posteroanterior (PA) view is the best CXR technique, taken with the patient in an erect position, facing the film, and with the X-ray tube behind the patient. The lungs are clearly viewed due to the full inspiration and the projection of scapulae outside the lungs (Figure 12.1).

However, the anteroposterior (AP) view is the most commonly performed view in the emergency department, as patients often cannot be positioned erect or require a portable film (Figure 12.2).

Both views have advantages and limitations (Table 12.1) (Figure 12.3).

The lateral view is not normally performed in the emergency setting but can be useful in evaluating suspected sternal fractures or manubriosternal dislocation.

Computed tomography (CT)

CT scans can provide more cross-sectional detail of the thorax compared to standard CXR (Box 12.1). This is especially because

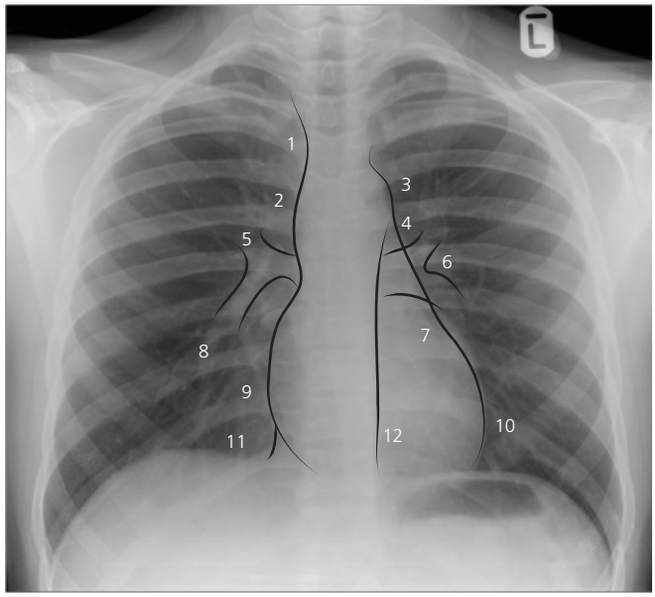


Figure 12.1 Normal PA CXR, with some of the mediastinal and hilar structures outlined. Note the position of the scapulae, which do not overlap the lungs. 1, right brachiocephalic vein; 2, superior vena cava; 3, aortic arch; 4, main pulmonary artery; 5, right upper lobe pulmonary artery; 6, left pulmonary artery; 7, Left atrial appendage; 8, right lower lobe pulmonary artery; 9, right atrium; 10, left ventricle; 11, inferior vena cava; 12, descending thoracic aorta.

CT scans do not suffer from the superimposition of structures (e.g. the mediastinal structures over one another and over the vertebrae; or the ribs, clavicle and scapula over the upper lungs).

Box 12.1 **Uses of CT**

- To further characterise abnormalities detected on CXR
- To exclude pathology when clinical suspicion is high, but the CXR is normal (e.g. vascular injury, acute aortic syndromes and pulmonary embolism)
- In major trauma

The patient is placed on a table that is moved along its axis through a rotating gantry with an X-ray source and detectors positioned at

ABC of Emergency Radiology, Third Edition. Edited by Otto Chan.
© 2013 John Wiley & Sons, Ltd. Published 2013 by John Wiley & Sons, Ltd.

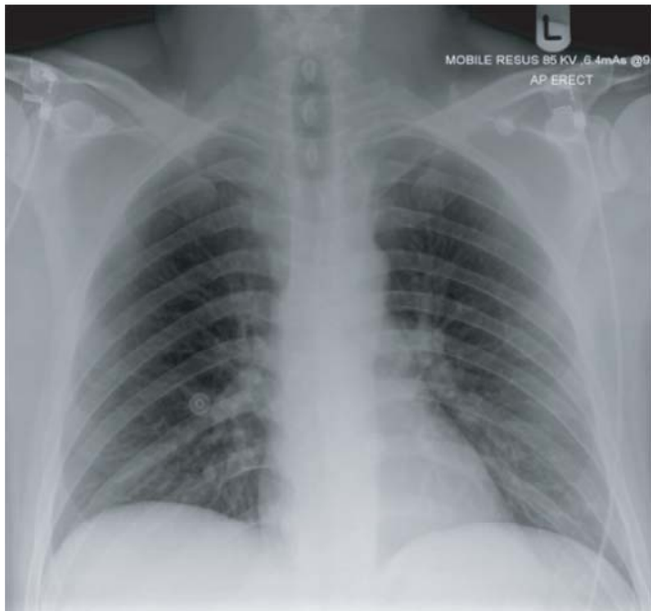
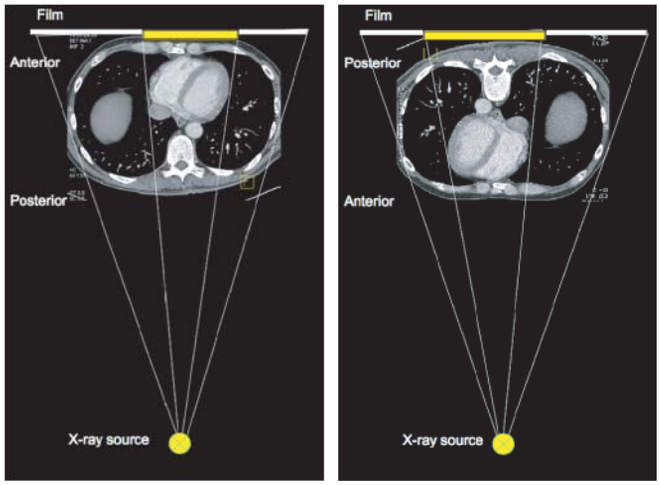


Figure 12.2 Normal AP CXR. The scapulae partially overlap the lungs.



(a) (b)

Figure 12.3 Differences in magnification of the cardiac contour on PA and AP projections, illustrated using an axial CT. The cardiac contour is represented by the yellow region on the film. (a) On the PA image, the heart is closest to the film, and so the magnification is kept to a minimum, compared to (b) the AP image.

Table 12.1 Advantages and limitations of PA and AP CXRs.

Posteroanterior (PA)	Anteroposterior (AP)
Excellent visualisation of lungs and mediastinum	Reasonable for lungs, poor for mediastinum
Poor for evaluating the skeleton	Good for evaluating the skeleton
Cannot be performed supine or portable	Can be erect or supine, and portable if necessary
Patient can be well-centred	Patient may be rotated
Can ensure better inspiration	May have a poor inspiration

opposite ends. Images reconstructed from the signals transmitted by the detectors provide detail regarding location (anatomy) as well as the density.

Scans are often performed with intravenous iodinated contrast, unless there are contraindications such as severe asthma, allergy or renal impairment. The timing of scanning with respect to contrast injection can be optimised to visualise the structures of most interest, such as the aorta during a CT aortogram.

Modern multidetector CT (MDCT) scanners allow quick scanning in a single breath-hold, with little distortion, and also allow synchronisation of scanning with the cardiac cycle (cardiac gating), as long as there is no limiting arrhythmia or tachycardia. This can provide good visualisation of the heart if required. MDCT scanners can provide 2D reconstructions in multiple planes, and 3D reconstructions to highlight specific structures.

On axial (transverse) CT images, the body is viewed from a 'bottom looking up' perspective, such that the patient's right will be located on the left of the image, and vice versa. The images can be viewed to show different structures, such as the lung, soft tissue or skeleton (greyscale windows) and in different planes (multiplanar reconstructions – MPR) or in 3D.

Ultrasound (US)

US assessment of the thorax is usually helpful in confirming or excluding pleural fluid, and in guiding thoracocentesis (Figure 12.4). Thoracic US is usually performed with the patient sitting upright if possible.

CXR anatomy

The lungs above the diaphragm are conventionally divided into upper, mid and lower 'zones' to facilitate description, but these

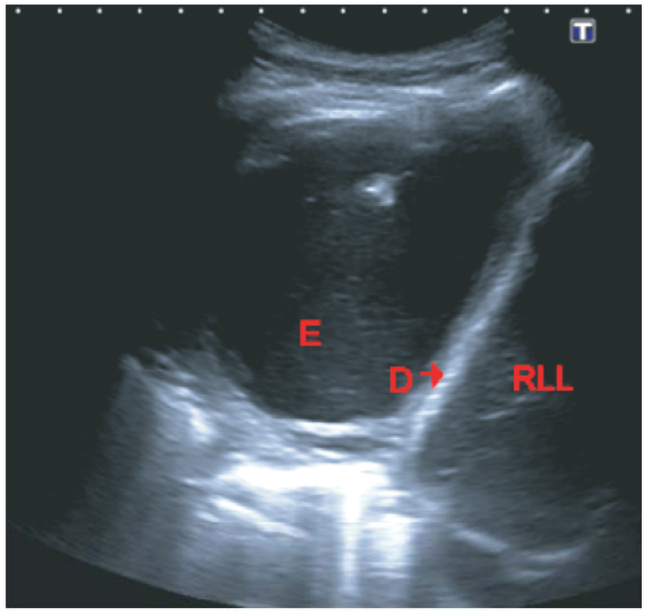


Figure 12.4 Ultrasound demonstrating a loculated right empyema (E), above the right hemidiaphragm (D). RLL, right lobe of liver.

do not bear any correlation to normal anatomical landmarks. Each of these zones occupies arbitrarily one-third of the height of the lungs.

Only the horizontal fissure (which divides the right upper lobe from the middle lobe) is usually seen on a normal PA CXR.

A significant volume of lung parenchyma lies posterior to the heart and below the level of the diaphragm. The diaphragm is attached onto the 12th rib inferiorly. The posterior ribs lie horizontally and arise from the spine. The anterior ribs tend to slope inferiorly and anteriorly, and they fade medially (due to the orientation of the anterior aspects of the ribs as they join the sternum).

The right side of the mediastinum (superior to inferior) consists of the right brachiocephalic vein, superior vena cava and right atrium. The left mediastinal border (superior to inferior) comprises the left subclavian artery, aortic arch, main pulmonary artery, left atrial appendage and left ventricle.

The hila are usually smooth and taper laterally. The right hilum is usually lower than the left, but may be at the same level in about 3% of cases. The right hilum should never be higher than the left (Figure 12.1).

ABCs structured assessment

An ABCs system of assessment can be applied to CXRs and adapted to thoracic CT scans. An ABC method specifically for reviewing the lungs may also be used. Once such approaches have been completed, however, one should always ask if the specific clinical question has been satisfactorily answered.

CXR
- Adequacy, **a**irways, **a**ll lines
- Breathing
- Circulation
- Diaphragm
- Edges
- Skeleton, **s**oft tissues

CT
- Adequacy, **a**irways, **a**ll lines
- Breathing
- Circulation, **c**entral structures
- Diaphragm
- Edges
- Skeleton, **s**oft tissues

Lungs
- Apical zone
- Basal zone
- Central (middle) zone
- Density
- Extra signs

Adequacy

Check:

- Demographic details
- Side markers
- Type of film
- Coverage: entire lung should be covered, from apices to costophrenic angles
- Inspiration: at least five anterior ribs should be seen above the midpoint of the hemidiaphragms
- Rotation: medial ends of the clavicles should be equidistant from the spinous process of the vertebra at that level. Some degree of rotation may be acceptable, as long as the film is still interpretable
- Exposure: on a correctly exposed film, the lower thoracic vertebrae (T8/T9 disc) and the left lower lobe pulmonary vessels should be visible through the cardiac silhouette

Airways

The trachea should be central above the manubrium but deviates slightly to the right below this. The right mainstem bronchus should have a more vertical alignment than the left main bronchus. Check the position of the endotracheal tube, and exclude foreign bodies while assessing the airways.

Any deviation towards a particular side that is not accounted for by rotation suggests either:

- Ipsilateral volume loss: collapse (Figure 12.5), scarring, fibrosis, or surgery; or
- Contralateral mass effect: tension pneumothorax, haemothorax, or large effusion.

All lines

Endotracheal tube

The tip of the endotracheal tube should be at the level of the aortic arch or at least 3.5–5.5 cm above the carina, if the neck

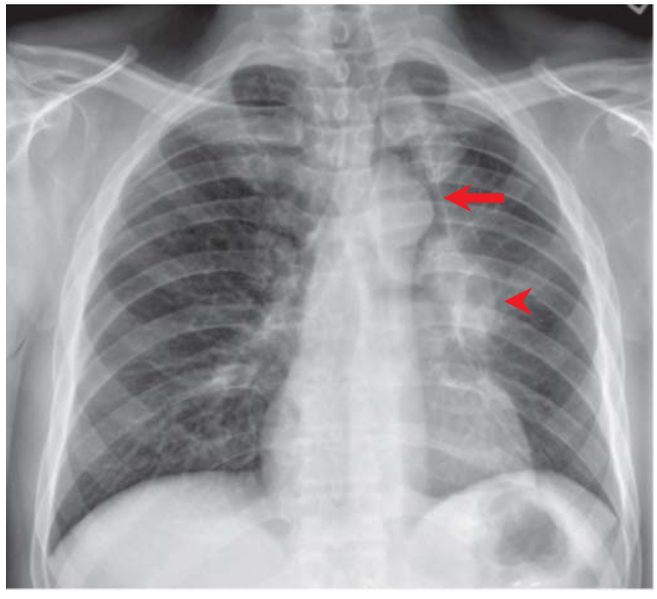


Figure 12.5 Left upper lobe collapse with tracheal deviation to the left. The left upper lobe collapses anteriorly, resulting in a decreased size of the left lung, with a veil-like opacity. A lucency is noted adjacent to the aortic knuckle (arrow), due to the compensatory expansion of the apical segment of the left lower lobe between the collapsed left upper lobe and the aortic arch. This is known as the 'Luftsichel' sign. The collapse is due to a left hilar mass (arrowhead).

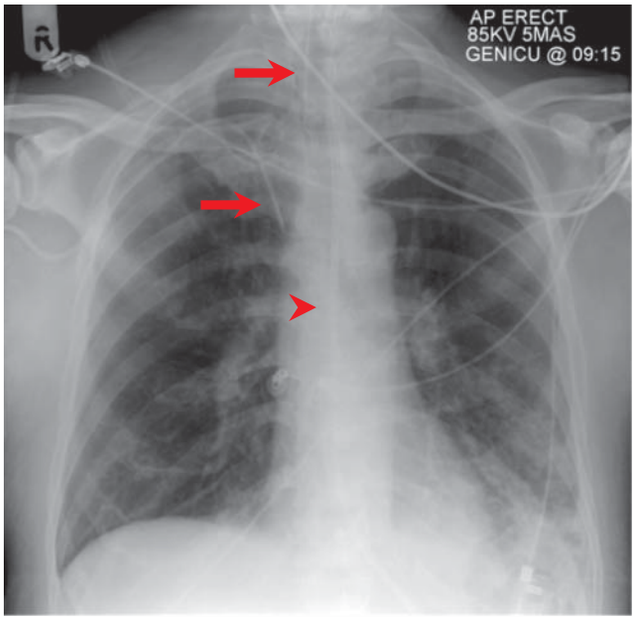


Figure 12.6 Intubated patient on general intensive care unit. Satisfactory position of the endotracheal tube (arrow), right subclavian vein central venous catheter (block arrow), and nasogastric tube passing below the diaphragm (arrowhead).

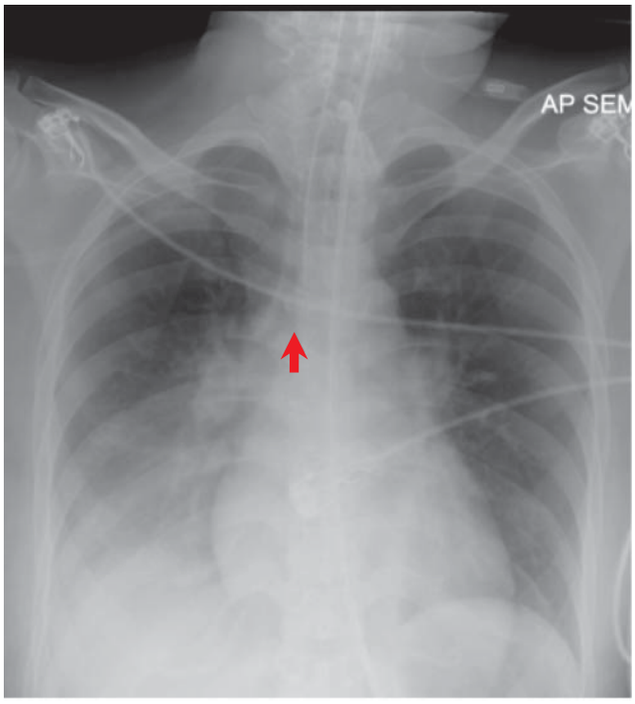


Figure 12.7 Suboptimal endotracheal tube position, approximately 1.5cm proximal to the carina (arrow). Note the right lower lobe consolidation- this had developed secondary to collapse of the right lower lobe due to previous positioning of the endotracheal tube in the right lower lobe bronchus.

is in extension (Figures 12.6 and 12.7). Having the tip of the endotracheal tube at least 3.5 cm above the carina ensures that the tube does not extend past the carina if the neck is flexed, and so is less likely to obstruct a main bronchus.

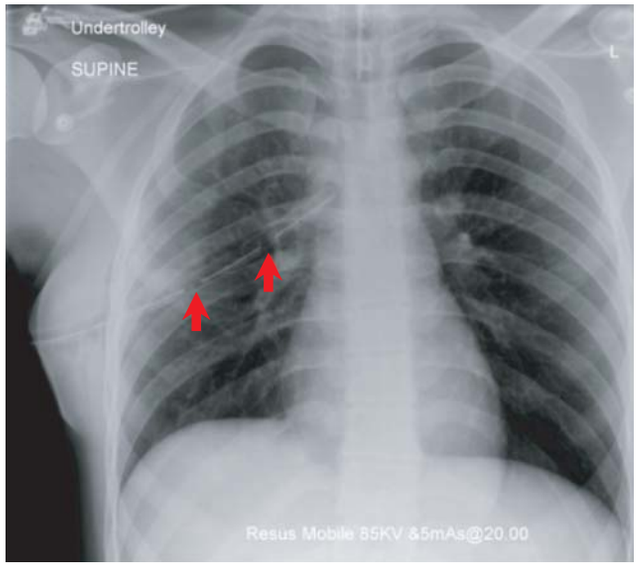
Venous catheters

An intravenous central venous catheter (CVC) should not be kinked and should follow the expected smooth curve of the vein into which it has been placed (Figure 12.6). The ideal position for the tip of a CVC is at the junction of the superior vena cava and right atrium. The CVC may occasionally be malpositioned in another vein, such as the azygos vein.

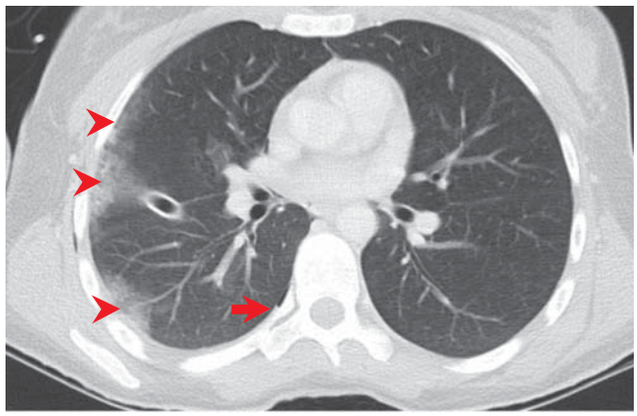
Chest drains

Chest drains have a radio-opaque line within their wall. A break in this radio-opaque line indicates the site of the last hole in the tube, and it is essential to ensure that this hole lies within the thoracic cavity (Figure 12.8).

If there is still significant air leak and surgical emphysema despite adequate intrathoracic depth of the drain, its tip may be situated in the lung parenchyma itself (Figure 12.9).

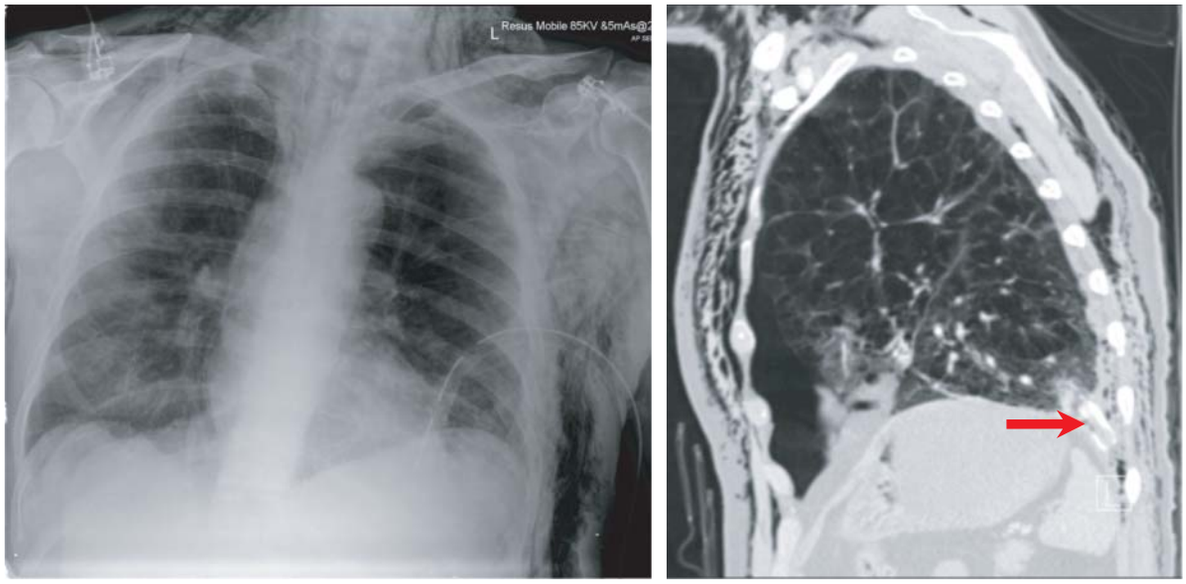


(a)



(b)

Figure 12.8 (a) Good position of right intercostal drain, with the holes (arrows) well within the thoracic cavity. (b) CT more accurately demonstrates the position of the right-sided intercostals drain, with its tip in the right oblique fissure. A small right haemopneumothorax (arrow) and multiple pulmonary contusions (arrowheads) are present.



(a) (b)

Figure 12.9 (a) Suboptimal left intercostal drain. Although the drain is situated within the thoracic cavity, there is a large amount of surgical emphysema, suspicious for an intrapulmonary location of the drain tip. (b) Sagittal CT demonstrates the tip of the drain in the posterior left lower lobe (arrow).

Nasogastric tube

If a nasogastric tube has been placed, ensure that its tip passes below the diaphragm into the stomach, and has not been inadvertently passed into an airway.

Breathing

Systematically assess the lungs and pleural spaces, looking for any parenchymal or pleural abnormalities (see later).

Circulation (mediastinum, hila and pulmonary vasculature)

Check:

- Cardiac silhouette size (remember: this will appear larger on an AP film). If enlarged, it could indicate cardiomegaly or a pericardial effusion
- Mediastinal position: one-third to the right, two-thirds to the left of the midline
- Mediastinal contour: clearly defined margins, especially aortic contour
- Widening of mediastinum: mediastinal widening, especially if > 8 cm may indicate mediastinal haematoma and traumatic aortic injury which should be excluded with computed tomography, in the trauma setting. In the absence of trauma, it usually indicates a mass or lymphadenopathy (Figure 12.10)
- Hila: evaluate size, shape, and position. Enlargement of one hilum usually indicates a mass or lymphadenopathy. Enlargement of both hila is either the result of lymphadenopathy or is vascular in nature (Figure 12.10)

Diaphragm

Hemidiaphragms should have a sharp outline throughout their course. Loss of this outline indicates a pathological process in the lower lobe, or possible diaphragmatic rupture in the context

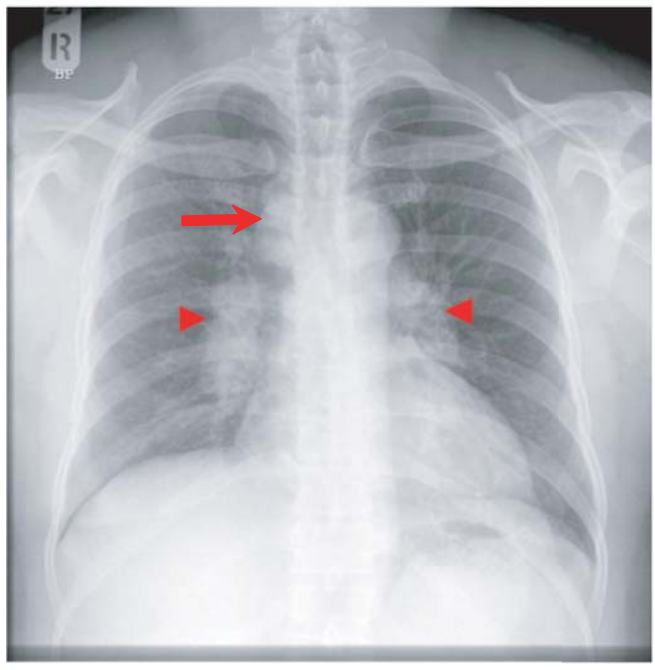
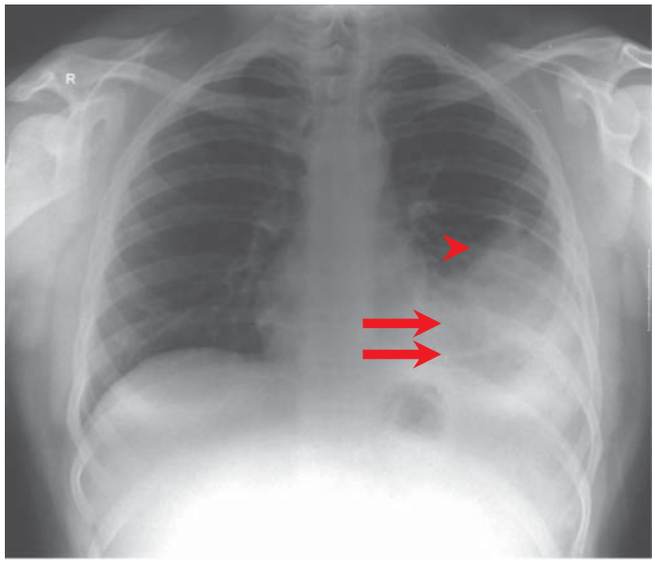


Figure 12.10 Widened mediastinum due to right paratracheal lymphadenopathy (arrow), with coexistent bilateral hilar lymphadenopathy (arrowheads) in a young patient with sarcoidosis.



(a)



(b)

Figure 12.11 (a) Obscuration of the left hemidiaphragm in a patient stabbed in the left chest. Increased abnormal lucencies are seen in the left lower zone (arrows) in association with some consolidation (arrowhead). (b) Sagittal CT demonstrates a rupture of the left hemidiaphragm with the contracted edges of the hemidiaphragm visible (arrows). There has been herniation of the transverse colon and stomach. The herniated transverse colon has caused the lucencies on the chest radiograph.

of penetrating trauma (Figure 12.11). The right hemidiaphragm normally lies 1.5–2.5 cm above the left hemidiaphragm. The area below the diaphragms should be assessed for free intraperitoneal air or abnormal areas of calcification.

Edges (pleura)

The costophrenic angles normally form an acute angle. Obliteration of this angle is seen in the presence of pleural fluid or thickening. Pleura are not normally seen on a chest radiograph, except at the fissures. Visualisation of the pleura indicates the presence of air in the pleural cavity (pneumothorax) (Figure 12.12).

Skeleton

Bones should be assessed for fractures or focal lesions such as metastatic deposits. In addition, the vertebrae can be assessed through the cardiac silhouette on a correctly exposed film. Bilateral paravertebral stripes are present: the left paravertebral stripe should measure <1cm and the right paravertebral stripe should be <3 mm. These may become displaced by paravertebral haematomas secondary to the vertebral fractures. Assess the ribs for fractures, and flail segments in particular.

Soft tissues

Soft tissues should be examined with regard to the presence of air (surgical emphysema) and foreign bodies. Check that the breasts are bilaterally present with symmetrical contours to exclude chest wall discrepancy as a cause for lung density differences.

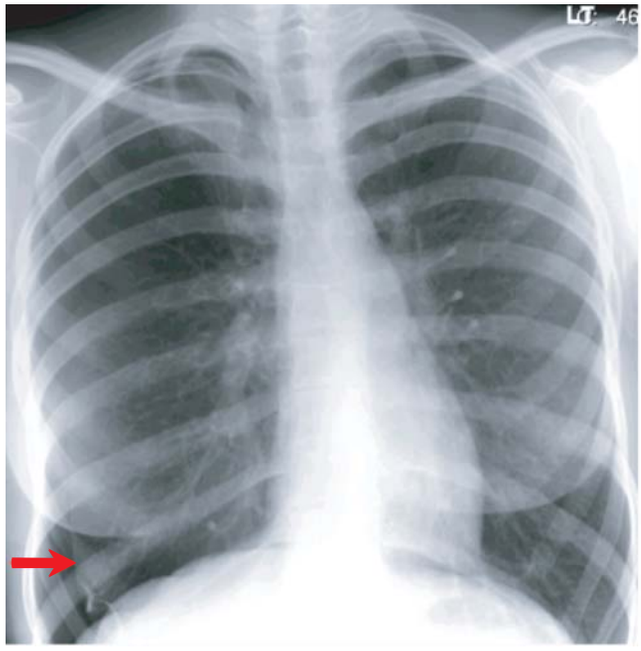


Figure 12.12 Right-sided pneumothorax with visible visceral pleural line (arrow) and no markings lateral to this.

In addition to assessing the above criteria, the ABCs assessment of CT scans may involve a few additional points.

Adequacy
Check that the scan covers the entire area of interest, and has been performed in the correct phase, with the correct reconstructions available. Note if there is a large amount of respiratory motion that may impair interpretation.

Airways
Look for any abnormal contour of the tracheobronchial tree, or any abnormal extraluminal air, that could suggest tracheobronchial disruption.

All lines
Chest drains
The tips of chest drains are more easily localised on CT as compared to CXR. Check if the tip is located within an intraparenchymal rather than intrapleural location (Figures 12.8b and 12.9b).

Circulation
Assess:

- The thoracic aorta: its contour and main branches
- Cardiac chambers: thrombus or ventricular aneurysms may be visible (Figure 12.13)
- The pulmonary arteries: especially if pulmonary embolism is suspected (Figure 12.13)
- Relevant vessels in the setting of penetrating injuries

Central structures
Pneumomediastinum can be more readily detected on CT, especially if small. This in turn can suggest oesophageal injury. A markedly distended and fluid-filled oesophagus can also identify a patient who is at potential risk of aspiration.

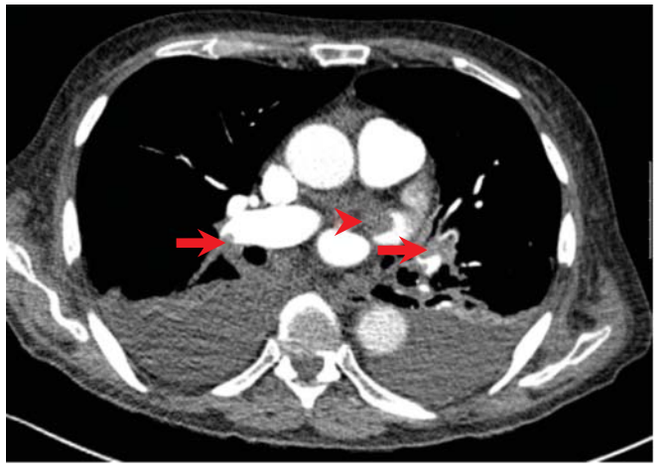
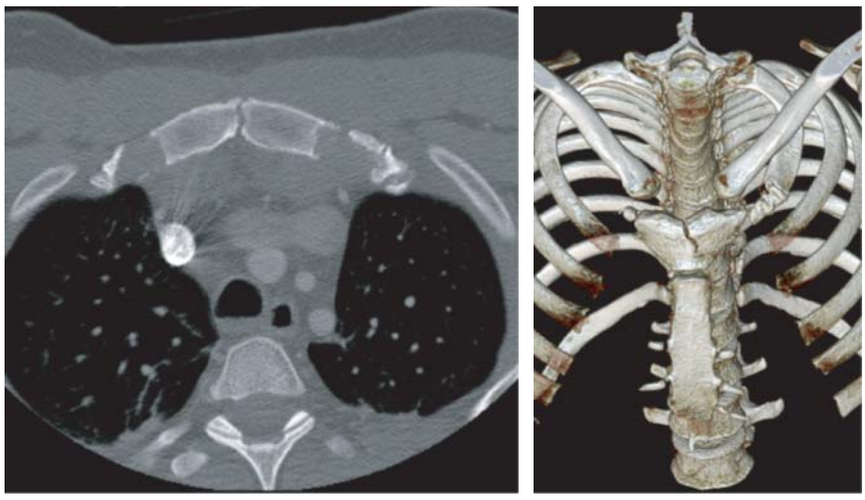


Figure 12.13 Filling defects in the pulmonary arteries bilaterally (arrows), consistent with bilateral pulmonary emboli, as well as thrombus in the left atrium (arrowhead). Bilateral pleural effusions are present.

Diaphragm
On CT, in addition to the loss of contour and change in position, the diaphragm itself can be evaluated for rupture or herniation (Figure 12.11b). Coronal or sagittal reconstructions can aid in this regard. Also, if the CT has been limited to the thorax and not included the abdomen, look at the available views of the upper abdomen to identify any overt abnormality, such as a subphrenic haematoma or free intraperitoneal air.

Skeleton
Assess the bones not as readily visible on a frontal CXR, such as the scapula, sternum and the anterior and extreme lateral aspects of the ribs (Figure 12.14).

ABCs approach to lung review
The following is only one of many methods to evaluate the lungs. This method employs a density-based approach to assess each zone.



(a) (b)

Figure 12.14 (a) Axial CT demonstrating manubrial fracture following a motor vehicle collision. (b) 3D oblique reconstruction from the same CT scan can demonstrate the fracture and its relationship to the sternoclavicular joints more clearly.

1 First divide the lungs into Apical, Basal and Central zones.
2 Next, assess a particular zone only for asymmetry of Density, while mentally ignoring ('masking') the other two zones.
3 If there is an asymmetry, decide which side is abnormal.
4 A more hyperlucent lung may still be normal, but be the result of mastectomy, atrophy of pectoral muscles, or rotation. In such cases it should still be possible to see pulmonary vessels extending to the periphery.
5 Abnormally hyperlucent lung may be due to pneumothorax, air-trapping, e.g. due to bronchial obstruction, or bullae.
6 Increased lung density may be due to collapse, air-space shadowing, linear opacities, nodules or masses (Table 12.2).
7 Look for Extra signs e.g. mediastinal deviation that support the likely diagnosis. Bear in mind that both sides could be abnormal.

Common traumatic conditions in the emergency department

Blunt chest trauma

The thorax is the third most commonly injured region in blunt trauma, after the head and extremities, most often as a result of motor vehicle accidents. CXR helps exclude life-threatening emergencies, but CT has an integral role to play, particularly in the exclusion of vascular and co-existent injuries.

Table 12.2 Types and causes of increased lung density on chest radiograph.

Type of abnormality		Examples
Airspace shadowing	Due to:	
	Water	Pulmonary oedema
	Pus	Infection
	Blood	Trauma, vasculitis
	Eosinophils	Pulmonary eosinophilia
	Tumour	Adenocarcinoma, lymphoma
Collapse	Passive: due to compression	Pleural effusion
	Obstructive	Tumour
	Cicatrical: contraction	Fibrotic lung disease
Lines	Septal lines	Pulmonary odema, lymphangitis carcinomatosis, interstitial lung disease
	Reticulation	Fibrotic lung disease
	Rings with tram-lines	Bronchiectasis
	Rings with no tram-lines	Cystic lung disease
	Tubular	AV malformations, mucus plugging ('finger-in-glove')
Nodule (defined as a rounded opacity ≤3 cm diameter)	≤3 mm: miliary nodule	Miliary TB, metastases
	3 mm–3 cm	Primary tumour, metastases
Mass (defined as opacity>3 cm diameter)		Tumour, abscess, haematoma

Pneumothorax

Pneumothoraces may occur due to the rupture of alveoli, resulting from either a sudden rise in intrathoracic pressure, a crushing force, or sudden deceleration. There may be associated rib fractures.

Features on erect CXR include:

- Visible visceral pleural line (Figure 12.12)
- Absence of vessels lateral to the visceral pleural line
- Shift to the contralateral side, together with cardiovascular compromise, suggesting tension
- Beware contours or lines not paralleling the chest wall, with vessels or increased density seen peripherally; these likely reflect skin folds and will be absent on repeat films

However, in the setting of significant trauma and suspected spinal injury, patients often have to be kept immobilised and supine. In such cases, a pneumothorax can be harder to diagnose, although the following signs may help:

- Increased transradiancy of the affected hemithorax
- Increased sharpness of the adjacent hemidiaphragm, mediastinum or cardiac border
- A deep anterior costophrenic sulcus

CT is invaluable in these situations (Figure 12.15).

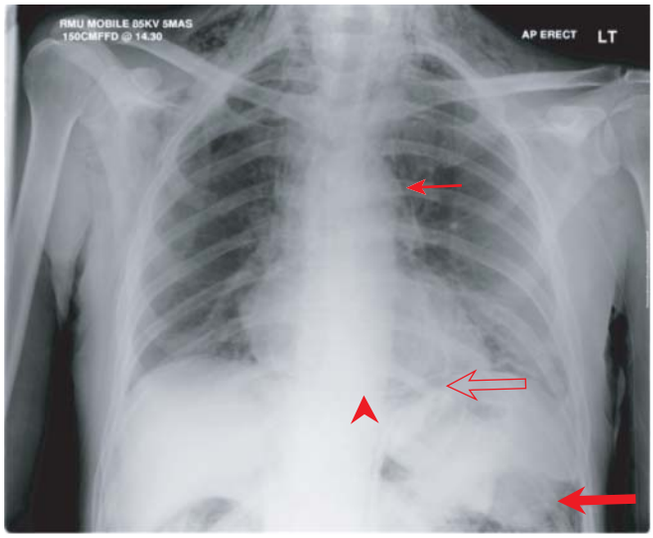
Pneumomediastinum

Pneumomediastinum in blunt trauma may be the result of alveolar rupture from compressive force, coexistent pneumoperitoneum, or less commonly from tracheobronchial disruption or oeseophageal rupture. Features on CXR include:

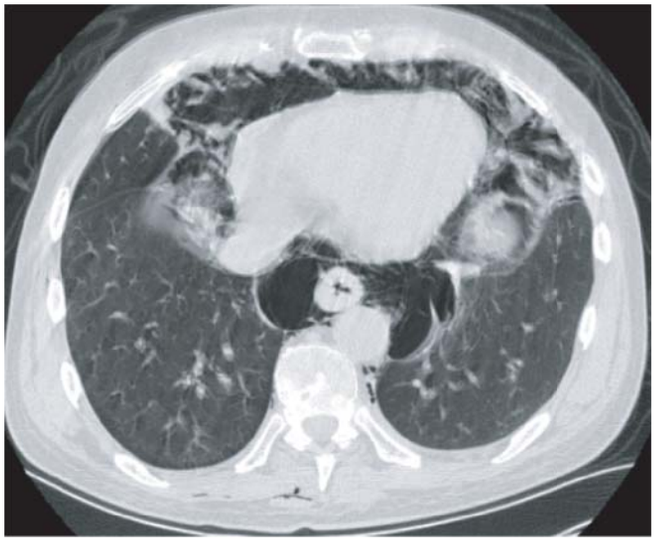
- Air outlining the mediastinal vessels or the cardiac border
- Air dissecting the mediastinal pleura, sometimes outlining the thymus
- Air along the superior aspects of the diaphragm, tracking between the diaphragm and heart (the 'continuous diaphragm sign') (Figure 12.16)



Figure 12.15 Left pneumothorax from multiple stab wounds. CT shows the stab wound tract (arrow), as well as other associated injuries such as pulmonary contusions in the left lower lobe (arrowheads), and a right pleural effusion. The pneumothorax and contusions were not visible on the patient's supine anteroposterior radiograph.



(a)



(b)

Figure 12.16 (a) Pneumomediastinum and pneumoperitoneum. Lucency adjacent to the aortic arch is seen (arrow), and there is a continuous diaphragm sign (arrowhead). In addition, there is air below the left hemidiaphragm which outlines the spleen (transparent block arrow) as well as highlights the bowel wall of the splenic flexure inferiorly (solid block arrow). (b) Axial CT more clearly demonstrates the pneumomediastinum surrounding the oesophagus and within the pericardial fat.

CT is invaluable in confirming the above pathologies, suggesting the cause of pneumomediastinum (intra-or extrathoracic) (Figure 12.16b), ensuring correct chest drain placement, and identifying co-existent injuries such as haemopneumothorax and rib fractures.

Pulmonary contusions and lacerations

Contusions are the most common form of lung injury in blunt trauma, manifesting as non-segmental patchy air-space shadowing on CXR. CT is more sensitive in detecting contusions as they are usually seen immediately and may occur at the site of impact or in contrecoup locations (Figure 12.10b).

Pulmonary lacerations are less common, and heal more slowly as compared to contusions. They result in cavities that may be air-filled or blood-filled at CT.

Traumatic aortic injury

Injury to the aorta most commonly occurs at the aortic attachments, most frequently at the ligamentum arteriosum due to a rapid deceleration force. Mediastinal or periaortic haematoma consequently develop. Such injuries are usually fatal.

Aortic injury may be suggested by the following signs on CXR (Figure 12.17):

Direct signs of mediastinal haematoma:

- Mediastinal widening >8 cm at the level of the aortic arch
- Deviation of the nasogastric tube and trachea to the right
- Depression of the left main bronchus
- Left apical pleural shadowing

Indirect signs (indicating significant force):

- First to third rib fractures
- Scapular, vertebral or sternal fracture
- Left haemothorax or pneumothorax
- Pulmonary contusion

The CXR is thought to be quite sensitive, but poorly specific for aortic injury. Overall, aortic injury cannot reliably be excluded by a normal CXR. In contrast, imaging with CT angiography can have a sensitivity and negative predictive value of 100%. CT angiography can characterise intimal tears, pseudoaneurysms, and periaortic haematoma, as well as illustrate other coexistent injuries, and help in planning therapeutic strategies (Figure 12.18).

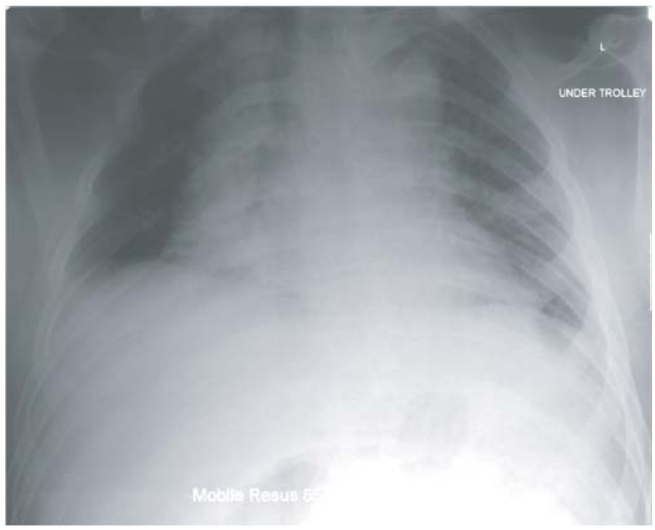
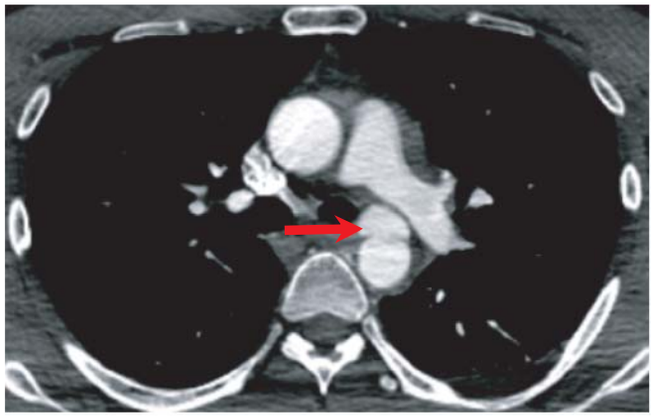


Figure 12.17 Motorcyclist involved in a collision, with markedly widened mediastinum, and tracheal deviation to the right even allowing for film rotation.



(a)



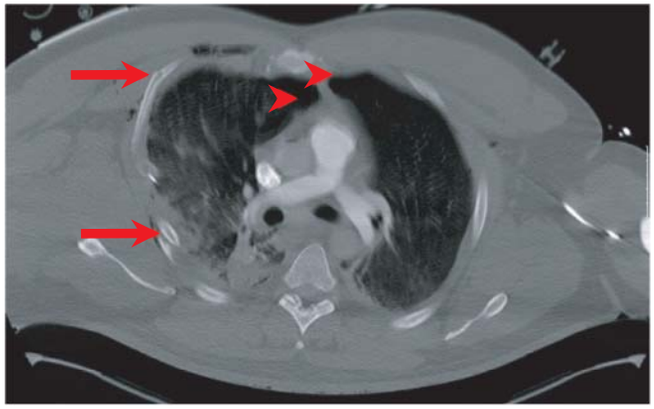
(b)

Figure 12.18 (a) Motor vehicle collision with traumatic aortic injury. Axial CT aortogram demonstrates a pseudoaneurysm arising from the anterior aspect of the distal aortic arch (arrow). (b) 3D reconstruction of the aorta can be performed to demonstrate the position of the pseudoaneurysm (arrow) relative to the great vessels.

Skeletal injuries

In the setting of significant blunt chest trauma, CXR can detect multiple or bilateral rib fractures which could suggest high energy impact.

Furthermore, a flail segment can be revealed on both CXR and CT (Figure 12.19). A flail segment occurs when at least three contiguous ribs have each been fractured in at least two locations, leading to paradoxical chest wall motion on spontaneous ventilation.



(a)



(b)

Figure 12.19 (a) Patient who had a flail segment clinically as a result of being trapped under a train. Axial CT demonstrates fractures of the right 3rd and 4th ribs at this level (arrows), as well as bilateral pneumothoraces (arrowheads). (b) 3D reconstruction of the right thoracic cage, with the spine and left rib cage removed to obtain a clearer view, demonstrates a flail segment of the right fourth to sixth ribs.

Scapular fractures are more easily identified on CT, and should prompt suspicion of other injuries, such as spinal injuries.

Penetrating Injury

The pulmonary, pleural and vascular injuries that can occur in blunt chest trauma can also occur in penetrating trauma. It is useful to place markers at the entry and exit (if present) sites on CXR, to more closely assess these regions. Any vessels close to the trajectory of penetration should be carefully assessed on CT.

Pneumothorax may also develop belatedly in such patients, and so it is sometimes useful to repeat the CXR 3–6 hours after injury.

Ten to thirty percent of patients with penetrating chest injury may have abdominal involvement.

Common non-traumatic conditions in the emergency department

Airspace shadowing

This is characterised by an increase in lung density. The causes of airspace shadows are outlined in Table 12.2.

Airspace shadowing encompasses a range of CXR descriptions, such as:

- Nodular opacities
- Ground-glass opacity:
  - on CXR- a homogeneous veil-like opacity which obscures the underlying vessels
  - on CT- a homogeneous opacity which does not obscure the underlying vessels
- Consolidation: increased opacity with air bronchograms (Figure 12.20)

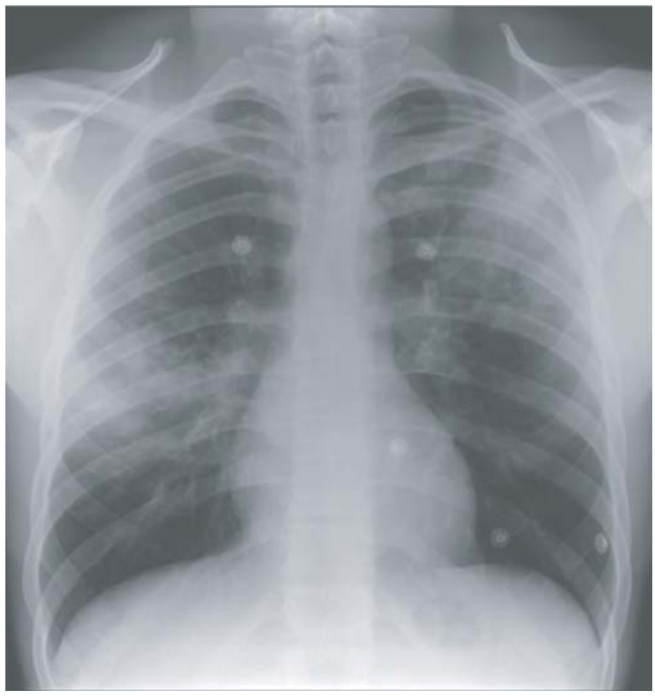


Figure 12.20 Multifocal consolidation in a patient with community-acquired pneumonia.

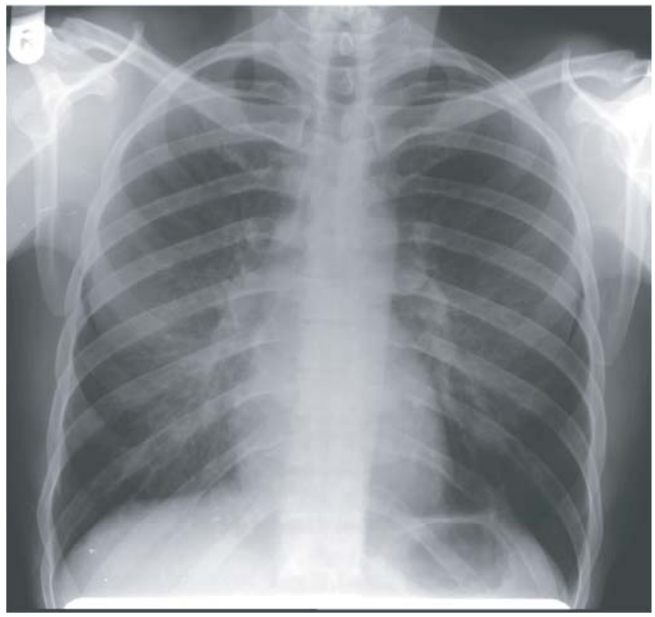


Figure 12.21 HIV patient with severe shortness of breath. There are bilateral ill-defined ground-glass opacities in a perihilar distribution, with fine reticulation seen.

Infection in the immunocompromised host may have specific features. For example, Pneumocystis pneumonia may manifest as perihilar or sometimes diffuse ill-defined ground-glass opacities on CXR (Figure 12.21). On CT, this can appear as ground-glass opacities with or without interlobular septal thickening.

Pulmonary oedema

This may be the result of cardiogenic (e.g. myocardial infarction) or non-cardiogenic (e.g. inhalation of noxious gases, raised intracranial pressure) insults.

CXR appearances include:

- Cardiac enlargement (if cardiogenic)
- Basal vasoconstriction
- Upper lobe blood diversion
- Loss of clarity of pulmonary vessels (perivascular haziness)
- Thickening of bronchi (peribronchial cuffing)
- Septal lines: thin linear opacities caused by interstitial fluid that are either located centrally, radiating from the hila, or peripherally, perpendicular to pleural surface
- Associated pleural effusions or airspace shadowing

CT is not normally necessary in the assessment of pulmonary oedema.

Pulmonary embolism

The CXR signs of pulmonary embolism (PE), such as wedge-shaped consolidation and oligaemia, are neither specific nor sensitive. CT pulmonary angiography (CTPA) has become the most widely accepted method of detecting pulmonary embolism. However, it is

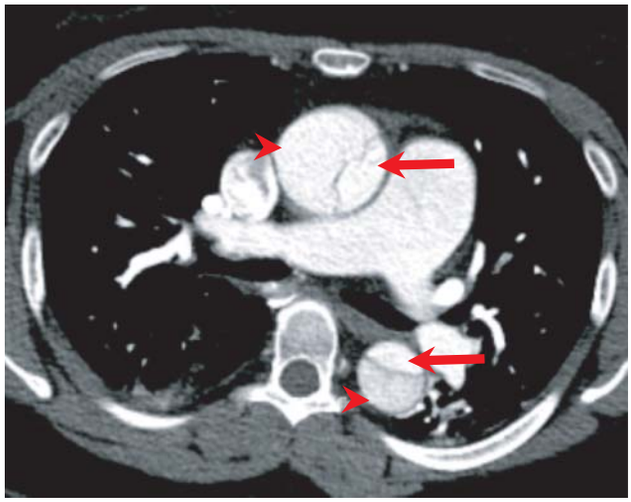


Figure 12.22 Type A aortic dissection. Axial CT image demonstrates the true (arrows) and false (arrowheads) lumens. In the aortic arch, the false lumen lies close the aortic root, lying anterolateral and to the right of the true lumen, while in the descending thoracic aorta it lies posterior or posterolateral, and to the left, as the dissection usually has a spiral configuration.

important to determine the clinical pre-test probability of PE, and interpret the CTPA result in conjunction with this probability.

Signs of a PE on CTPA are:

- Intraluminal filling defect (Figure 12.15)
- In complete occlusion, the artery may be enlarged in comparison with adjacent patent vessels
- Parenchymal changes, e.g. haemorrhage, atelectasis
- Features of right ventricular strain if present, e.g. bowing of the interventricular septum to the left

If CTPA is unavailable or contraindicated, ventilation–perfusion scintigraphy (V/Q scan) is an alternative consideration, and Doppler ultrasound of the lower limbs can exclude coexistent DVT.

Acute aortic syndromes

These encompass the acute non-traumatic presentation of aortic dissection, intramural haematoma and penetrating aortic ulcers. A normal CXR cannot exclude these pathologies in patients with appropriate presentation symptoms or signs. This is because even significant dissection of the aorta may result in no distortion of the mediastinal planes but is readily apparent on CT aortography (Figure 12.22).

Acknowledgements

Dr Ali Naraghi and Dr Otto Chan, authors of the chest section of the second edition of *ABC of Emergency Radiology*.

Further reading

Berger FH, van Lienden KP, Smithuis R, Nicolaou S, van Delden OM. Acute aortic syndrome and blunt traumatic aortic injury: pictorial review of MDCT imaging. *Eur J Radiol.* 2010;74(1):24–39.

Hansell DM, Lynch DA, McAdams H, Page, Bankier AA. *Imaging of Diseases of the Chest*, 5th edn. Chapter 2: The normal chest, and Chapter 17: Chest trauma. Elsevier, 2010.

Kaewlai R, Avery LL, Asrani AV, Novelline RA. Multidetector CT of blunt thoracic trauma. *Radiographics* 2008;28(6):1555–1570.

LeBlang, Suzanne D; Dolich, *Matthew O. Imaging of blunt penetrating thoracic trauma. J Thor Imag* 2000;15(2):128–135.

Schnyder P, *Wintermark M. Radiology of Blunt Trauma of the Chest*. Springer, 2000.

CHAPTER 13

Abdomen

Katie Planche and Niall Power

Royal Free London NHS Foundation Trust, London, UK

OVERVIEW

- The patient with acute abdominal pain requires rapid assessment to exclude life threatening pathology (e.g. ruptured aortic aneurysm)
- The AXR is quick and easy to obtain, but is difficult to interpret and provides limited information
- CT (rarely US) is required in patients with acute abdominal pain

The patient presenting with abdominal pain may be suffering from a wide variety of conditions ranging from common, benign self-limited pathologies such as gastroenteritis to life-threatening emergencies such as a ruptured aortic aneurysm. It is vital to be able to differentiate these conditions using the most appropriate imaging modality (Box 13.1). These include the plain abdominal radiograph (AXR), ultrasound (US) and computed tomography (CT). Magnetic resonance imaging (MRI) does not currently have a role in the initial management of abdominal emergencies. There are only a few common causes of acute abdominal pain and these will be highlighted in this chapter. AXRs are difficult to interpret and often non-diagnostic and therefore in these patients, CT (or sometimes US) should be performed initially.

Box 13.1 **Indications for AXR**

- Suspected bowel obstruction
- Suspected perforation
- Renal colic
- Foreign body ingestion

Anatomy

Normal appearances of the AXR vary (Figures 13.1 and 13.2), but Tables 13.1 and 13.2 show some useful general points to remember when assessing the radiographs.

The solid organs are outlined by fat planes and can therefore be identified on the AXR. The bowel normally contains a variable amount of gas and the different segments of bowel can usually be differentiated by their site and morphology. Any gas seen outside the bowel is abnormal and is highly suggestive of perforation. The AXR is difficult to interpret and gives limited information and further investigations such as US or CT are often needed. In patients with severe abdominal pain, CT (or sometimes US) is advised as the first line of investigation.

Table 13.1 Positions of organs.

Organ	Position	Appearance on radiograph
Liver	RUQ	Subhepatic edge visible
Spleen	LUQ	Rarely seen below twelfth rib
Kidneys	Flanks	Outlined by fat and psoas (L1–4), left kidney higher.
Pancreas	Central	Not visible and retroperitoneal
Bladder	Pelvis	May be visible if full

Table 13.2 Position of bowel.

Organ	Position	Appearance on radiograph
Stomach	Upper	Lies transverse across upper left and central abdomen
Small bowel	Central	<3 cm and contains air
Large Bowel	Peripheral	Contains air and faeces

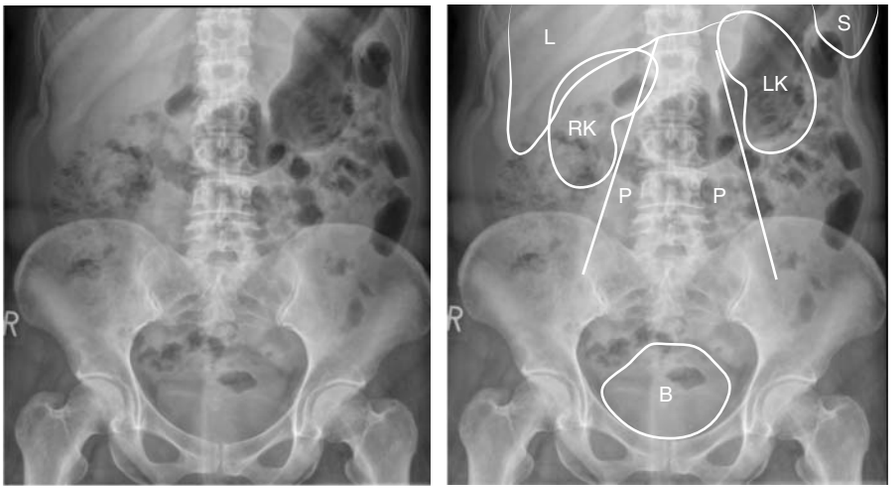
ABCs systematic assessment

- **A**dequacy – must include the pubic symphysis
- **A**ir – exclude free intraperitoneal and retroperitoneal air
- **B**owel – check gas pattern, size, and distribution. Exclude small bowel (SB) and large bowel (LB) obstruction
- **C**alcifications – check renal tract, vascular and other structures
- **D**ensities – look for tablets and foreign bodies
- **E**dges – check hernial orifices and lung bases
- **F**at planes – check psoas, properitoneal and perivesical fat planes
- **S**olid organs – look for liver, spleen and kidneys
- **S**keleton – look at the bones for fractures

Adequacy

The standard AXR (Figure 13.1) is an anteroposterior view taken with the patient supine, not rotated and should include the pubic symphysis and show the hernial orifices and the properitoneal fat

ABC of Emergency Radiology, Third Edition. Edited by Otto Chan.
© 2013 John Wiley & Sons, Ltd. Published 2013 by John Wiley & Sons, Ltd.



(a) (b)

Figure 13.1 (a),(b) Anteroposterior abdominal radiograph illustrating the position of the organs: L, liver; S, spleen; RK, right kidney; LK, left kidney; P, psoas; B, bladder.

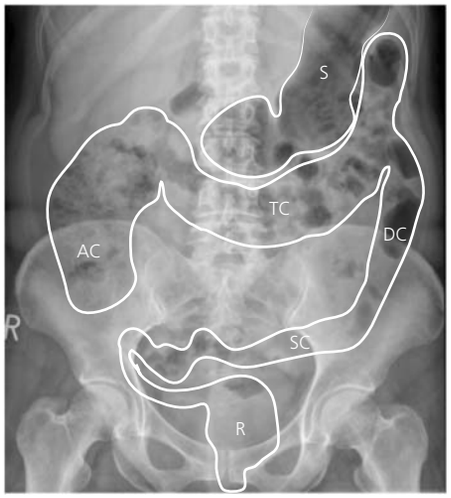


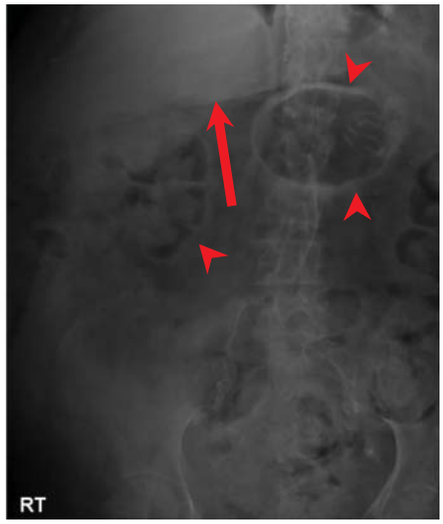
Figure 13.2 Abdominal radiograph showing the position of the bowel. S, stomach; AC, ascending colon; TC, transverse colon; DC, descending colon; SC, sigmoid colon; R, rectum.

planes. These fat planes are thin layers of fat between the parietal peritoneum and the lateral wall muscles. An additional view of the upper abdomen may be necessary in tall patients.

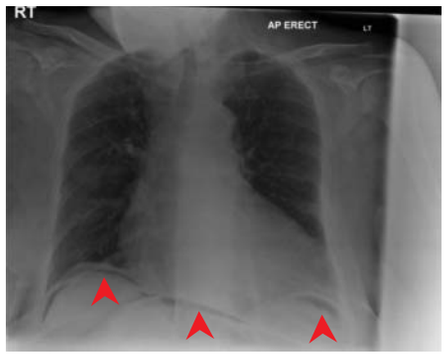
If a perforation is suspected an erect CXR should be performed (Figure 13.3). Small amounts of free air can be seen under the hemidiaphragm on the CXR, if enough time (at least 10 minutes) is allowed for the free air to rise. However, if perforation is suspected, a CT scan is indicated, as it is more sensitive at detecting free air and the underlying cause. The erect CXR may sometimes show chest pathology simulating an acute abdomen, such as pneumonia or aortic dissection.

Air

Free intraperitoneal air rises to the front of the abdomen on a supine AXR (Figure 13.3). This free air can be very subtle and hard to detect, so an erect chest radiograph is mandatory if perforation is suspected. Look for extraluminal air (Figure 13.4) – any gas outside the bowel wall is abnormal.



(a)



(b)

Figure 13.3 Abdominal radiograph and erect chest radiograph showing free gas (arrows) in a patient with perforated diverticulitis.

Bowel

When the patient is supine, bowel gas rises to the parts of the gastrointestinal tract that are most anterior, in particular the stomach, transverse colon and sigmoid colon. The stomach is located above

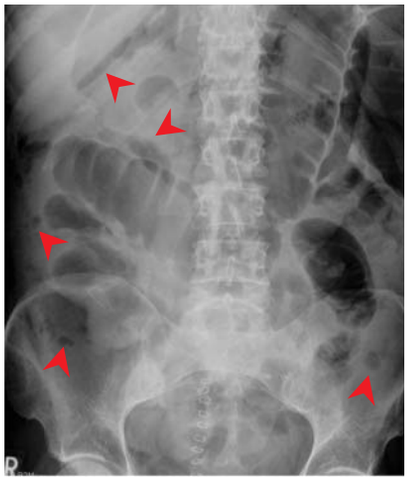


Figure 13.4 Abdominal radiograph showing free gas (arrows) in a patient with a postoperative perforation.

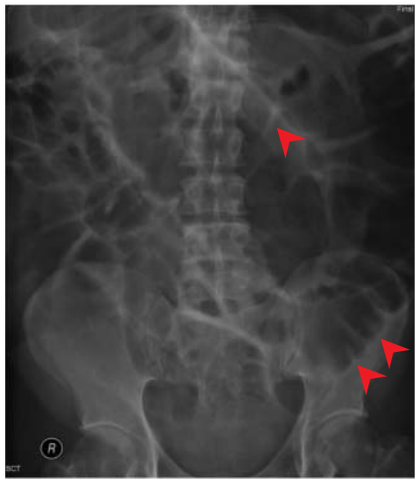


Figure 13.6 Abdominal radiograph showing large bowel obstruction in a patient with sigmoid cancer. Note the haustra (arrowhead) extend part of the way across the bowel.

the transverse colon. The SB can be differentiated from the LB by the following features:

- Position: the SB lies in the central abdomen; the LB lies peripherally.
- Size: the SB should measure no more than 3 cm in diameter and is smaller than the LB. The large bowel has no definite measurement, but if the caecum dilates to more than 9 cm diameter in the presence of a suspected bowel obstruction, it infers impending perforation. In the presence of colitis, any part of the LB that measures more than 5.5 cm in diameter indicates a megacolon, but normal colon can easily be larger than this.
- Pattern: the SB has characteristic thin folds (Figure 13.5) (valvulae conniventes), which are close together and run across the whole bowel. The LB has thicker folds (Figure 13.6) (haustra) that do not run across the whole dilated LB. The distal ileum and sigmoid colon are relatively featureless and contain no folds.
- Content: the SB contains fluid and air, whereas the colon contains faeces, which have a characteristic mottled or solid appearance.

Calcification

Normal calcifications:

- Costal cartilage (Figure 13.7) can sometimes be seen in the upper abdomen as an incidental finding
- Phleboliths (Figure 13.7) are small calcified veins in the pelvis. They can be confused with ureteric stones
- Coarse, nodular calcification in mesenteric lymph nodes is an incidental finding lying between the left L2 transverse process and the lower right sacroiliac joint
- Vascular calcification is often seen in the aorta

Abnormal calcifications:

- Around 45% of renal (Figure 13.8) and ureteric calculi are visible on an AXR



Figure 13.5 Abdominal radiograph in a patient with small bowel obstruction. Note the valvulae conniventes (VC) extend all the way across the bowel. A calcified fibroid (F) is noted in the pelvis.

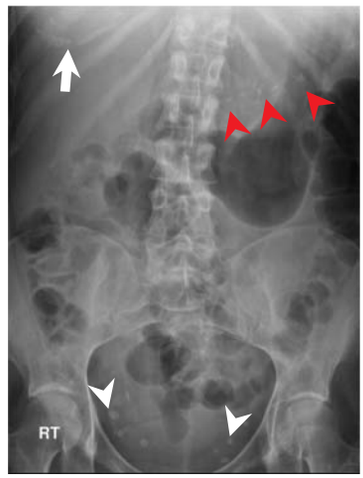


Figure 13.7 Abdominal radiograph showing pancreatic calcification (red arrowhead), phleboliths (white arrowhead) and costal cartilage calcification (white arrow).

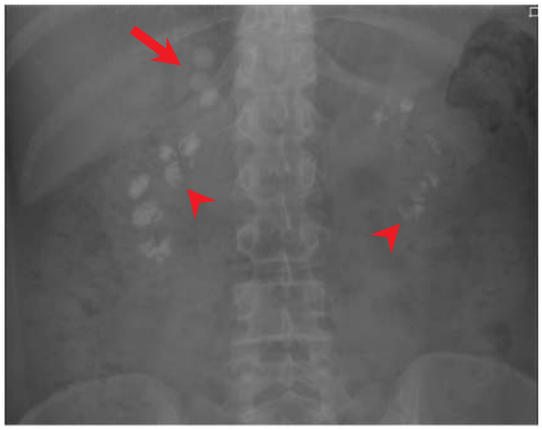


Figure 13.8 Abdominal radiograph showing calcified gallstones (red arrow) and renal calcification (arrowhead).



Figure 13.9 AP magnified view of the pelvis showing a Dermoid with teeth.

- Abnormal vascular curvilinear calcification may outline aneurysms or thrombosed veins
- Only 10–15% of gallstones (Figure 13.8) are radio-opaque. Rarely, the gallbladder wall can calcify (porcelain gallbladder)
- Punctate fine stippled nodular calcification in the pancreas indicates chronic pancreatitis (Figure 13.7)
- Calcification in the spleen is usually caused by previous trauma or granulomatous or parasitic infections
- Appendicoliths and faecoliths may occasionally be seen
- Tuberculosis and schistosomiasis infections can cause calcification of the bladder wall
- Teeth can sometimes be seen in benign teratomas of the ovary (dermoid cysts) (Figure 13.9), and rarely, ovarian tumours can calcify.
- Calcification of the seminal vesicles is often seen in patients with diabetes or renal failure.
- Uterus: it is common for fibroids to calcify as large masses in the lower pelvis (Figures 13.5 and 13.10).

Densities

These include foreign bodies (Figure 13.11 and 13.13), tablets and tampons. Foreign bodies of any type can be ingested or inserted via any orifice. Common sites of obstruction for foreign bodies are the distal oesophagus, pylorus of the stomach and terminal ileum. Tablets often contain calcium. Tampons can be seen as air-filled tubular structures in the lower pelvis (Figure 13.13).

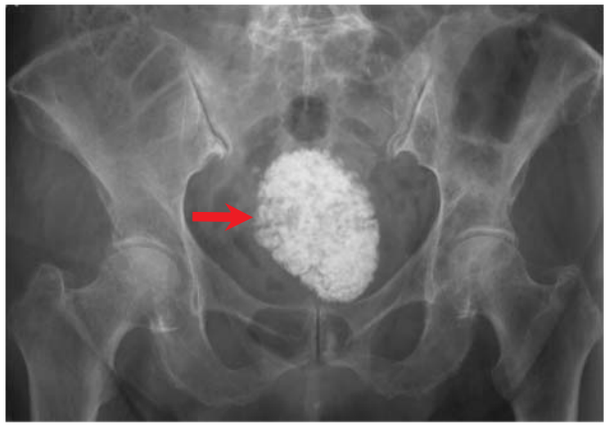


Figure 13.10 Abdominal radiograph showing a calcified fibroid (arrow).

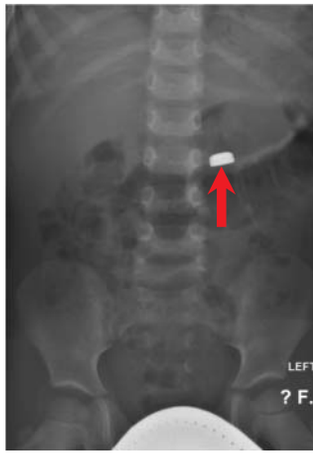


Figure 13.11 Abdominal radiograph in a 4 year old showing a button battery (arrow) in the stomach.

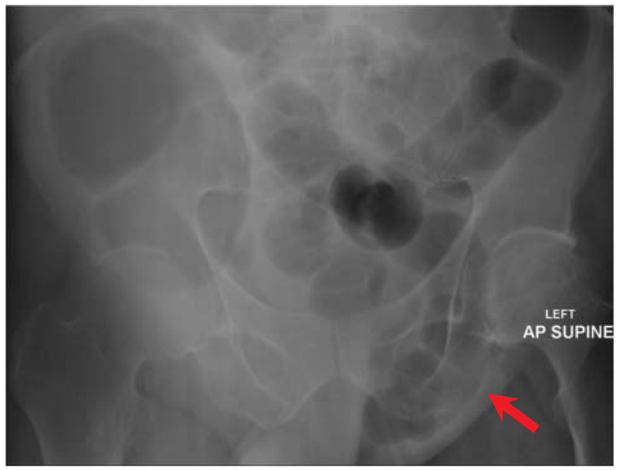
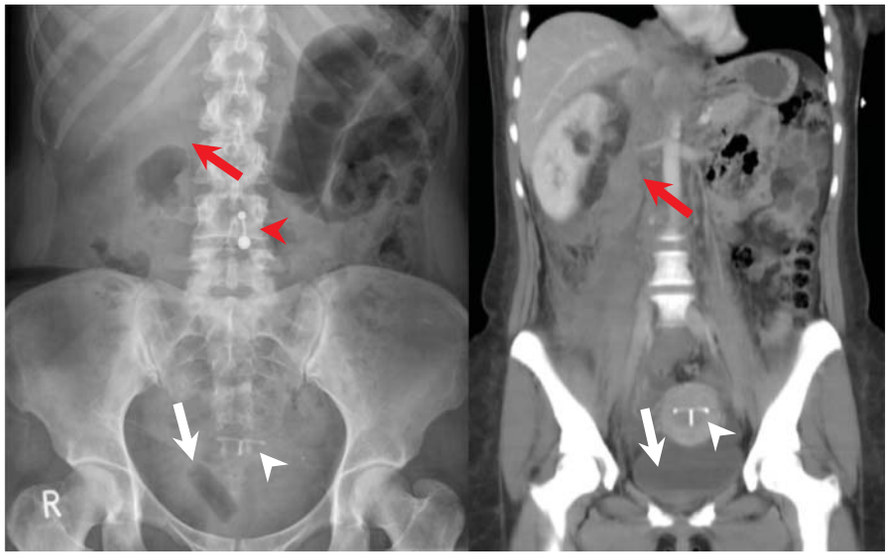


Figure 13.12 Abdominal radiograph showing large bowel obstruction secondary to incarcerated left inguinal hernia (arrow).



(a) (b)

Figure 13.13 (a) Abdominal radiograph and (b) coronal CT image showing displaced right kidney (red arrow) following haemorrhage from a renal mass. Also note piercing (Red arrowhead), intrauterine contraceptive device (IUCD, white arrowhead) and tampon (white arrow).

Edges

In particular, look at the hernial orifices (Figure 13.12) for bowel in the hernia (this is a common cause of SB obstruction). Central lines are sometimes inserted via the groin. Pathology may be seen in the lung bases, such as pneumonia and pleural effusions.

Fat planes

Identification of normal fat planes is important because absence, distortion or displacement (Figure 13.13) can indicate pathology. Visible fat planes include:

- Psoas – loss of the psoas fat plane may indicate a retroperitoneal mass or collection or haemorrhage
- Perirenal fat plane – outlines kidneys
- Perivesical fat plane – outlines bladder and is often displaced in the presence of pelvic fractures
- Properitoneal fat planes – outlines the lateral margin of the ascending and descending colon

Skeleton

The visualised skeleton, in particular the lower ribs, spine, pelvis and hips should be assessed for fractures and bony metastases (Figure 13.14) .



Figure 13.14 Abdominal radiograph showing extensive sclerotic bony metastases in a patient with prostate cancer.

Important plain film findings

Small bowel dilatation

The most common causes of dilated SB loops are mechanical obstruction and paralytic ileus and rarely infarction.

Mechanical obstruction of the small bowel may be caused by:

- Adhesions (75%) due to previous surgery (Figure 13.15)
- Obstructed hernia – commonest cause in the absence of previous surgery
- Inflammation
- SB volvulus
- Intussusception

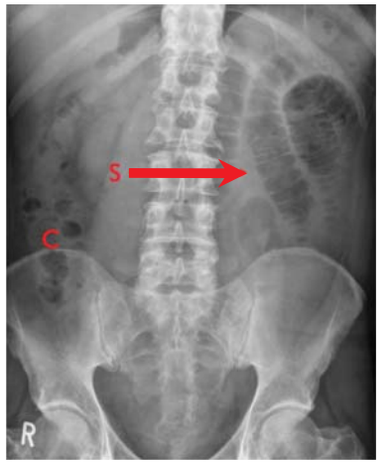
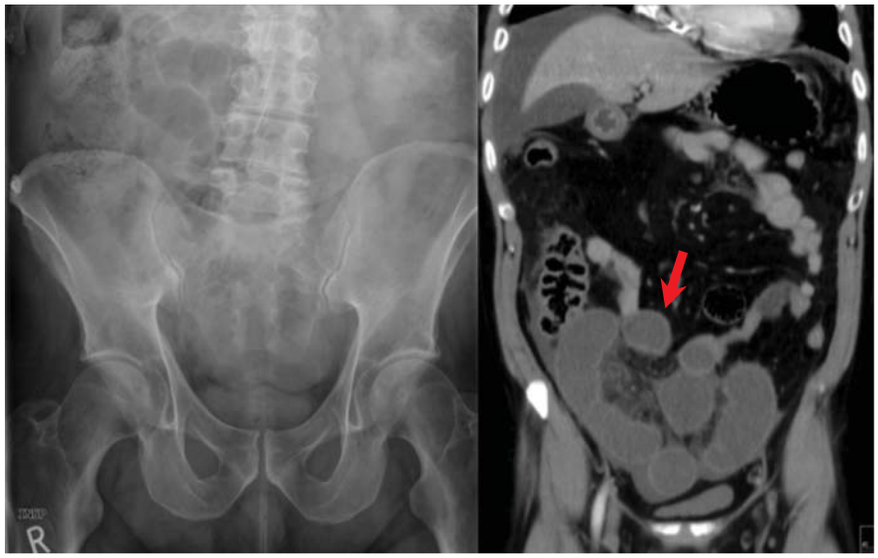


Figure 13.15 Abdominal radiograph showing small bowel obstruction (S) secondary to adhesions. Note the colon (C) is collapsed.



(a) (b)

Figure 13.16 (a) Abdominal radiograph and (b) coronal CT scan showing small bowel obstruction (red arrow), which cannot be seen on the abdominal radiograph.

- Malignancy
- Gallstone ileus – may be seen in elderly patients (Figure 13.26)

The cardinal features of SB obstruction are dilated loops of SB (usually >3 cm in diameter) containing variable amounts of air and fluid with collapse of the LB. SB obstruction can be difficult to differentiate from paralytic ileus. In the latter, the LB is also often dilated, and bowel sounds are absent. CT should be performed in all patients with suspected SB obstruction (Figure 13.16).

Large bowel dilatation

LB can be dilated due to paralytic ileus, colonic pseudo-obstruction (Figure 13.17) or mechanical obstruction. Pseudo-obstruction is a form of ileus and is characterised by dilatation of the LB without an obstructing lesion. This is often seen in elderly patients who are clinically relatively well and comparison with previous radiographs is useful.



Figure 13.17 Abdominal radiograph showing colonic pseudo-obstruction. The radiograph was unchanged over 2 years.

Commonest causes of mechanical large bowel obstruction

- Malignancy (Figure 13.6)
- Diverticular disease
- Volvulus
- Adhesions

Volvulus is the twisting of a bowel loop, and it affects loops with redundant long mesentery. The most common sites are the sigmoid colon and rarely, the caecum and transverse colon.

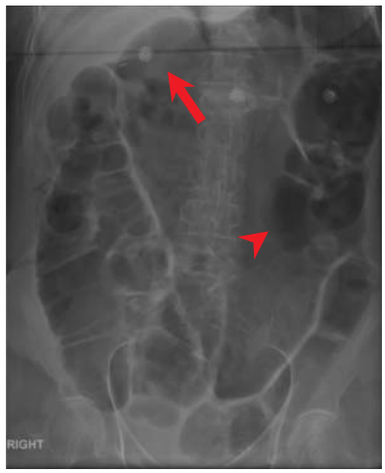
In sigmoid volvulus (Figure 13.18), the redundant loop of sigmoid classically rotates towards the right upper quadrant to give an inverted U appearance devoid of haustra (coffee bean sign) and a characteristic central stripe with the apex above T10 and the liver (liver overlap sign) and descending colon (bowel overlap sign) can be seen through the dilated loop of LB.

Caecal volvulus usually rotates to the left upper quadrant with associated SB obstruction.

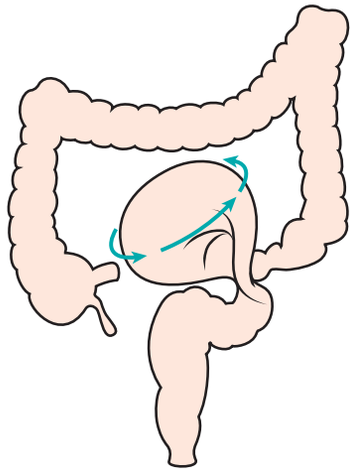
Extraluminal air (Figure 13.4 and 13.19)

Air outside the lumen of the bowel has an array of causes of varying clinical significance. These include:

- Free intraperitoneal air (pneumoperitoneum) – In the absence of recent surgery, it implies a perforation, usually of a peptic ulcer or diverticulitis. Free air can be difficult to see on a supine radiograph and if clinically suspected, an erect CXR or CT should always be obtained.
- Air may be seen on the supine AXR in the hepatorenal recess (Morrison's pouch), subhepatic space, under the diaphragm (unicopula sign or visualisation of the falciform ligament), central abdomen (football sign), or between bowel loops. Rigler's sign is the visualisation of both sides of the bowel wall caused by the presence of air on both sides (normally bowel or fat abuts the outside of the wall).



(a)



(b)

Figure 13.18 (a) Abdominal radiograph (showing liver edge – 'liver overlap' sign and decending colon – 'bowel overlap' sign) and (b) diagram showing a sigmoid volvulus and illustrating how the sigmoid twists on its mesentery.

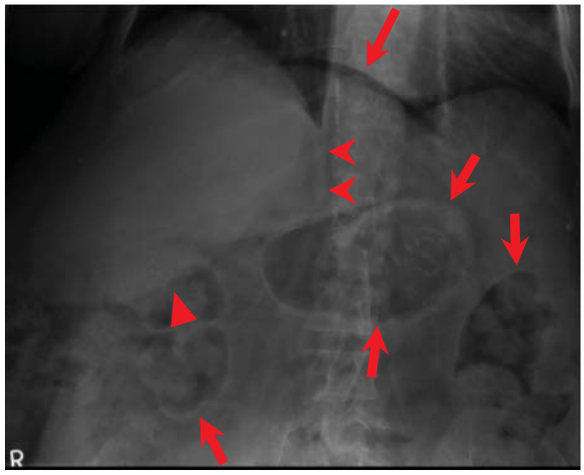


Figure 13.19 Abdominal radiograph showing multiple sites of free air. Rigler's sign (small arrow), Unicupola sign (large arrow), subhepatic air (large arrowhead) and the falciform ligament (small arrowhead).

Signs of free intraperitoneal air on supine AXRs (Figure 13.19)

- Rigler's sign (small arrow) – both sides of the bowel wall can be seen
- Unicopula sign (large arrow) – air in the central leaf of the diaphragm
- Subhepatic air (large arrowhead) – free air under the inferior margin of the liver
- Falciform ligament (small arrowhead) – air outlines the falciform ligament over the liver

Air in the bowel wall – pneumatosis intestinalis

Linear streaks of intramural air are important as they may indicate infarction of the bowel wall, which may be a sequelae of severe inflammation or ischaemia (Figure 13.20). In elderly patients air in the bowel wall, usually colon (Figure 13.21), may be secondary to benign causes such as longstanding obstruction or chronic lung disease (pneumatosis coli).

Other causes – Gas in the portal venous system should be differentiated from air in the biliary system (aerobilia) by its peripheral location in the liver. This is a sinister sign in the adult patient that indicates transmural bowel infarction with tracking of air into the mesenteric veins.

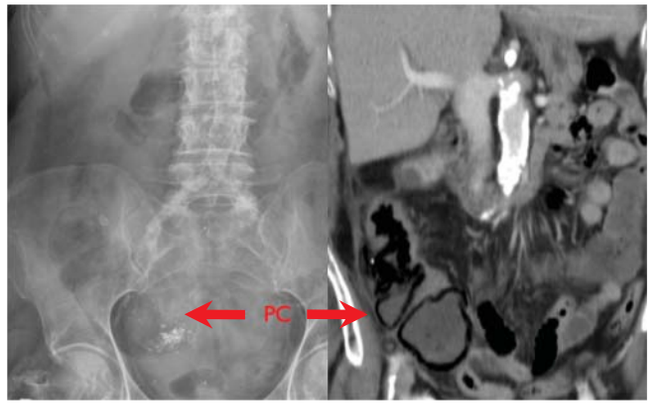


Figure 13.20 Abdominal radiograph and coronal CT showing gas in the bowel wall – pneumatosis coli (arrow) in a patient with acute ischaemia of the ascending colon.

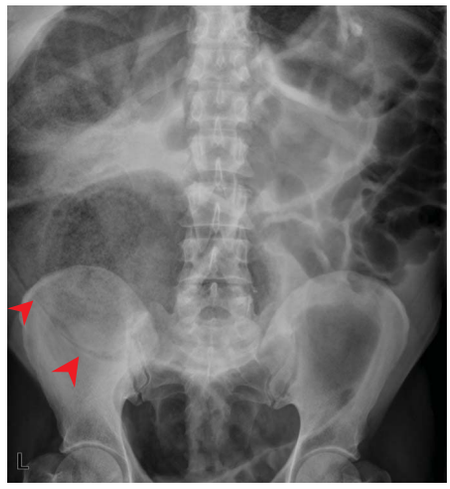


Figure 13.21 Abdominal radiograph showing gas in the bowel wall (red arrowheads) – *Pneumatosis coli*.

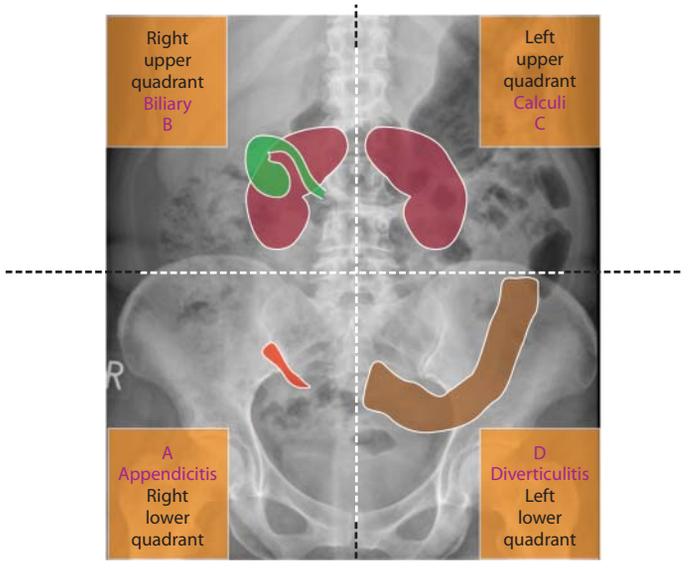


Figure 13.22 Abdominal radiograph showing the most common sites of pain and causes of the acute abdomen.

Aerobilia and air in the gallbladder can be iatrogenic, caused by endoscopic procedures (ERCP), percutaneous transhepatic cholangiograms (PTC), biliary stents or erosion of a gallstone through the gallbladder wall into the SB. This may cause SB obstruction (gallstone ileus), usually in elderly patients (Figure 13.26).

Air may also be seen in an abscess, where it may have a mottled appearance or produce an abnormal air-fluid level. An abscess may have mass effect and displace adjacent structures. CT or US are the investigations of choice if an abscess is clinically suspected (Figure 13.23).

Common abdominal emergencies

Sites of pain (Figure 13.22)

- RUQ – Biliary – gallstones/cholecystitis
- RLQ – Appendicitis
- LLQ – Diverticulitis
- Central – SBO, pancreatitis, peptic ulcer, aneurysm

Box 13.2 gives the common causes of abdominal pain and Box 13.3 indicates which type of investigation to use.

Box 13.2 **Common causes of acute abdominal pain**

A – Appendicitis/aneurysm/acute pancreatitis
B – Bowel obstruction/perforation
C – Cholecystitis/calculi
D – Diverticulitis
E – Ectopic pregnancy

Appendicitis (Figure 13.23)

This is the commonest abdominal surgical emergency. Peak incidence is in late teenage years, but also common in children and adults. The AXR will usually be normal, unless there is associated small bowel obstruction or if an appendicolith is present (30% but often not visible on AXR). For children or young women, the investigation of choice is US. Adult patients should have a CT to exclude other causes and also to confirm the diagnosis. CT has a high negative predictive value for acute appendicitis, therefore this algorithm avoids unnecessary surgery.

Box 13.3 **Investigating acute abdominal pain**

If you suspect . . .	– request
Appendicitis	– US in children/young women, otherwise CT
Aneurysm	– CT
Acute pancreatitis	– US to exclude gallstones, CT after 48 hours if not settling
Bowel obstruction	– AXR then CT
Bowel perforation	– AXR + CXR then CT
Cholecystitis	– US
Calculi	– CT KUB
Diverticulitis	– CT
Ectopic pregnancy	– US

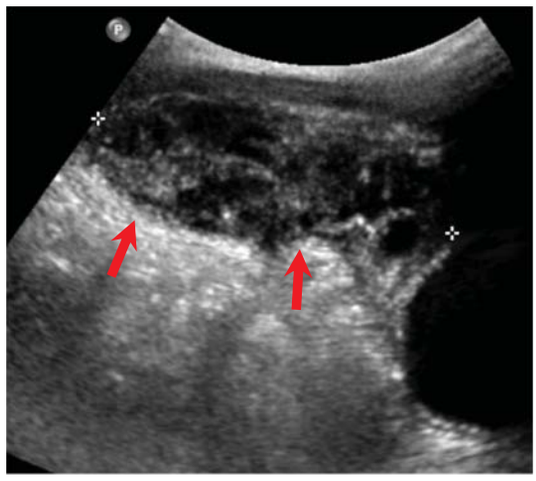
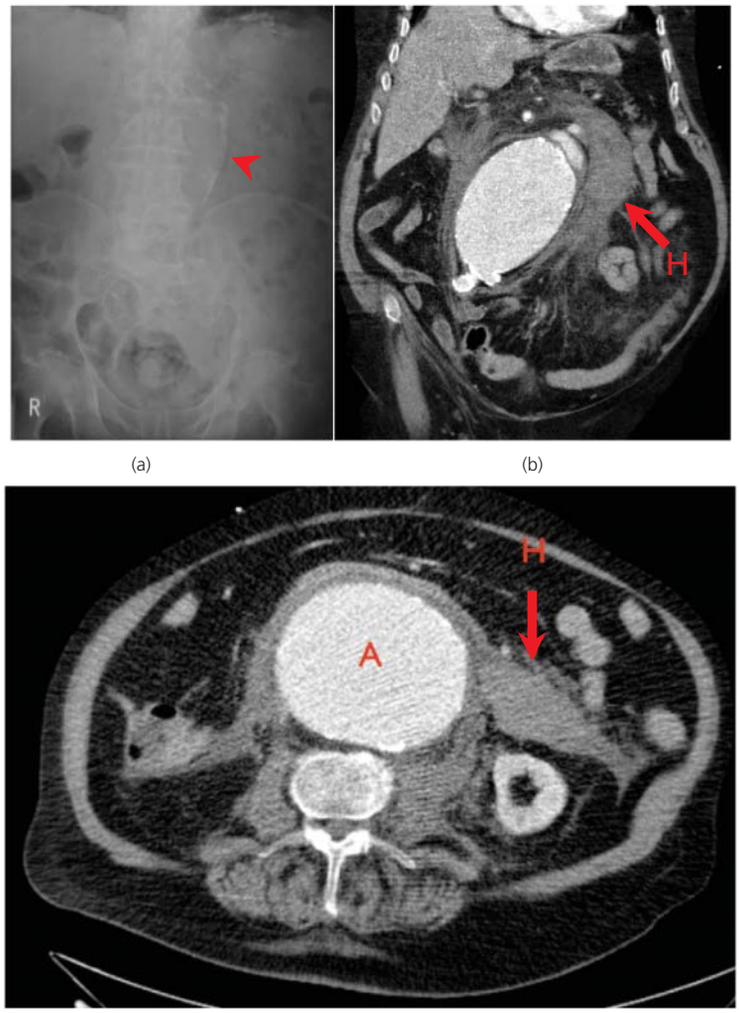


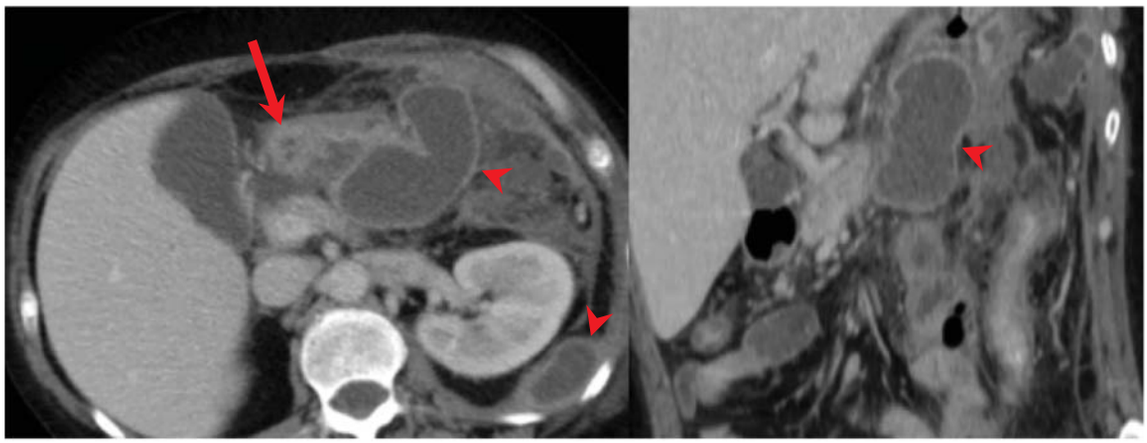
Figure 13.23 Ultrasound showing appendix abscess in an 8 year old boy.



(a) (b)

(c)

Figure 13.24 (a) Abdominal radiograph showing calcification (red arrowhead) in the wall of a large abdominal aneurysm with corresponding (b) coronal and (c) axial CT scans showing large aneurysm (A) which has ruptured showing haemorrhage (H).



(a) (b)

Figure 13.25 (a) Axial and (b) coronal CT showing severe pancreatitis with inflammation of the pancreas (red arrow) and extensive peripancreatic collections (red arrowheads) within the abdomen.



Figure 13.26 Axial and coronal CT showing small bowel obstruction (S) secondary to an obstructing gallstone (G) in a patient with gallstone ileus.

Abdominal aortic aneurysm (Figure 13.24)

An aneurysm may be suggested on the plain film by vertical curvilinear calcification, whilst a leak or rupture will present with signs of a retroperitoneal haematoma, with displacement or loss of the psoas fat plane or planes, displacement of the kidney and displaced bowel loops. Leak or rupture on CT is confirmed by extra luminal extravasation of contrast and the presence of a retroperitoneal haematoma.

Acute pancreatitis (Figure 13.25)

If the clinical diagnosis is confirmed with an elevated amylase, no imaging is required, although ultrasound may be performed to look for gallstones. CT is useful after 48hours in patients who are not improving to look for complications such as pancreatic necrosis, abscess, pseudoaneurysms, and collections.

Bowel obstruction and perforation (Figure 13.26, 13.27)

A normal AXR does not exclude either diagnosis and if clinical concern persists CT is indicated. If the AXR is abnormal, then CT is indicated.

In mechanical obstruction a transition zone from dilated proximal bowel to collapsed distal bowel should be sought (Figure 13.26). CT in perforation can confirm the diagnosis and the cause, usually peptic ulcer disease or diverticulitis (Figure 13.3, 13.4, 13.19).

Cholecystitis (Figure 13.28)

There is no role for an AXR if this is suspected. Ultrasound typically shows a thick walled gallbladder with pericholecystic fluid and gallstones. Right upper quadrant tenderness on scanning over the gallbladder is known as an ultrasound positive Murphy's sign. Ultrasound is more sensitive than CT for gallstones.

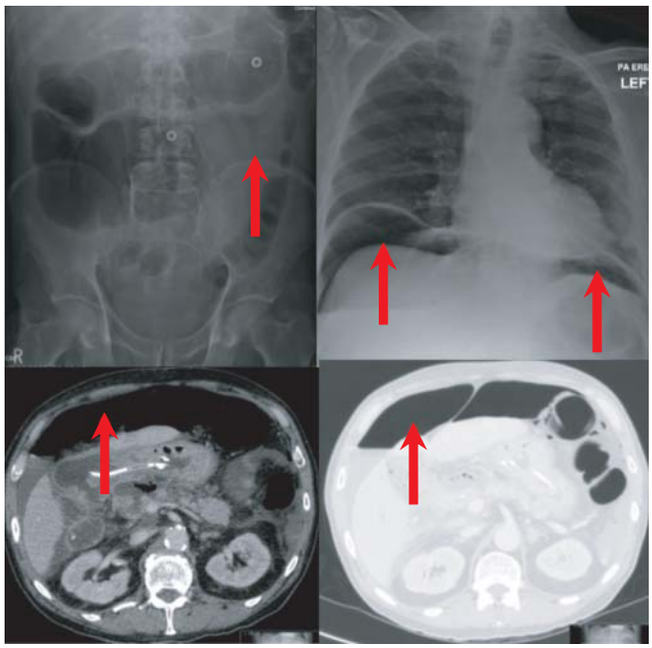


Figure 13.27 Abdominal radiograph, erect chest radiograph and CT (soft tissue and lung windows) showing free gas in a patient with perforation – an anastamotic breakdown following surgery.

Renal tract calculi (Figure 13.29)

Ultrasound and limited IVU have been superseded by low dose CT KUB. CT KUB can show calculi more accurately, as well as secondary signs of obstruction such as hydronephrosis, hydroureter and perinephric fat stranding, a urinary leak or an abscess and other pathologies such as a leaking abdominal aneurysm. Therefore unlike a limited IVU, CT KUB is quick, very sensitive and specific and can diagnose other causes of abdominal pain.



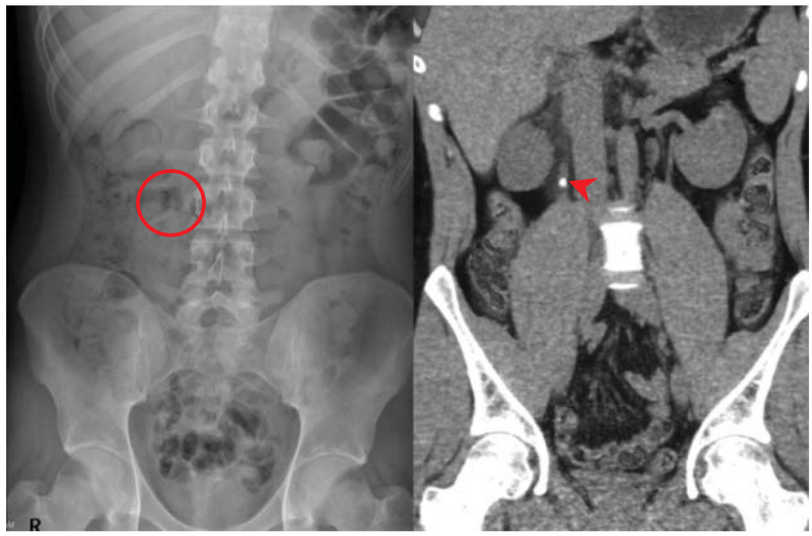
Figure 13.28 Ultrasound scan showing thick-walled abnormal gallbladder (G) containing calculi in a patient with acute cholecystitis.

Diverticulitis (Figure 13.30)

This is a common cause of an acute abdomen in elderly patients with pain classically localised to the left lower quadrant. CT is highly sensitive and specific and can show the typical findings of inflammation around a diverticulum, usually in the sigmoid colon, and can show complications such as perforation and abscess formation.

Ectopic pregnancy (Figure 13.31)

Pregnancy should be excluded in all women of childbearing age with an acute abdomen. An ectopic pregnancy is a surgical emergency due to the risk of tubal rupture and associated haemorrhage. Transvaginal US is the investigation of choice.



(a) (b)

Figure 13.29 (a) Abdominal radiograph and (b) coronal CT showing renal calculus in right proximal ureter (circled). Note that this is difficult to see on the abdominal radiograph.

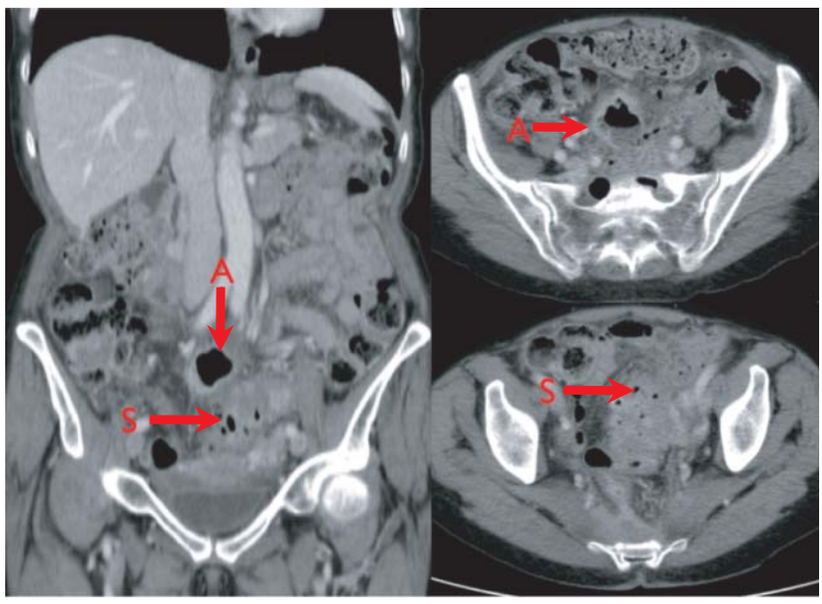


Figure 13.30 Coronal and axial CT scans in a patient with perforated diverticulitis showing an abscess (A) containing gas and fluid. Extensive inflammatory change is seen around the sigmoid colon (S).

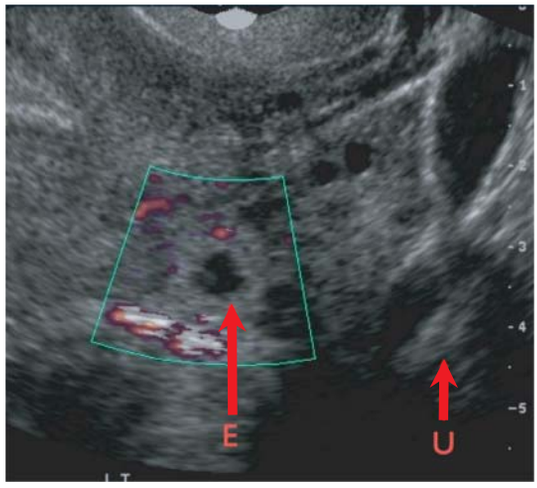


Figure 13.31 Transvaginal ultrasound showing ectopic pregnancy (E), separate to the uterus (U).

ABCs systematic assessment

Air

- Exclude free intraperitoneal or abnormally sited air

Bowel gas

- Check size, distribution, and pattern

Calsification

- Check for normal and abnormal calcification

Densities

- Check for inserted or ingested foreign bodies

Edges

- Check the hernial orifices
- Check the lung bases and pleural spaces

Fat planes

- Check presence and symmetry of psoas shadows
- Check presence of perivesical fat plane
- Check that properitoneal fat planes are present

Soft tissues

- Check for enlarged or absent organs. Confirm with US

Skeleton

- In trauma, check that there are no obvious fractures
- If malignancy is suspected, exclude bony metastases

Further reading

http://www.learningradiology.com/toc/tocorgansystems/tocgi.htm
Stoker J, van Randen A, Laméris W, Boermeester MA. Imaging patients with acute abdominal pain. *Radiology* October 2009;253:31–46.
The Radiology Assistant – Abdomen. http://www.radiologyassistant.nl/en/
LearningRadiology.com

CHAPTER 14

Computed Tomography in Emergency Radiology

Anmol Malhotra and Jeremy Rabouhans

Royal Free London NHS Foundation Trust, London, UK

OVERVIEW

- Introduction of how a CT scanner works
- The dramatic increase in the use of CT
- MDCT provides rapid and accurate diagnosis
- Ionising radiation, doses and the ALARA principle
- Dangers of ionising radiation in children and pregnant women

There have been huge technological advances in the past decade, not least in diagnostic radiology, with the advent of multidetector CT (MDCT), US, MRI, digital radiography and picture archiving and communication systems (PACS). The role of the radiologist in trauma and emergency medicine has also dramatically changed, not least with almost an exponential increase in the use of CT. In 2007, there were over 60 million CT scans performed in the USA and it is estimated that over 100 million scans will be performed this year in the USA alone.

The new generation of MDCT scanners have over 256 detectors, rotation times of less than 0.3 s, 0.4 mm resolution and they can do whole body scans in less than 10 s and acquiring isotropic voxels. The continuingly evolving software packages process the continuously changing cross sections as the table (gantry) moves through the X-ray circle producing multiplanar reconstructions to allow viewing in any plane with similar resolution and 3D images at the touch of a button (almost real time).

The images are 'windowed' in order to be able to demonstrate the information based on the ability of the body structures to block (attenuate) the X-ray beam.

Typical windows are shown in Table 14.1.

As the number of applications for CT expand with these newer generation MDCT scanners, so the radiologist's role becomes central in the management of patients, not least in ER. Radiologists are involved not only in interpretation, but also in developing and implementing new protocols that take advantage of the new advances in CT technology. The increase in use has led to an increase in exposure to ionising radiation and although CT only represents about 20% of the general workload in radiology, it is responsible for over 90% of the radiation. Recent advances in dose reduction mean that whole body CT scans can now be done with a dose of under 5 mSv (Figure 14.1a,b). Despite this, it is essential that everyone adopts the ALARA (as low as reasonably achievable) principle when using CT and restricts the use in children and pregnant women. This chapter will concentrate on the general principles of CT and the role of CT in the acute abdomen.

Table 14.1 Typical window levels and widths.

	Window level	Window width
Abdomen	60	360
Liver	100	200
Lungs	600	1600
Bone	800	2000
Supratentorial	40	80
Infratentorial	35	150
Acute haemorrhage	100	200
Mediastium	35	350
Colon	0	2000
Cardiac	90	750

Definition of the acute abdomen

A clinical syndrome of sudden onset of severe abdominal pain requiring emergency medical or surgical treatment.

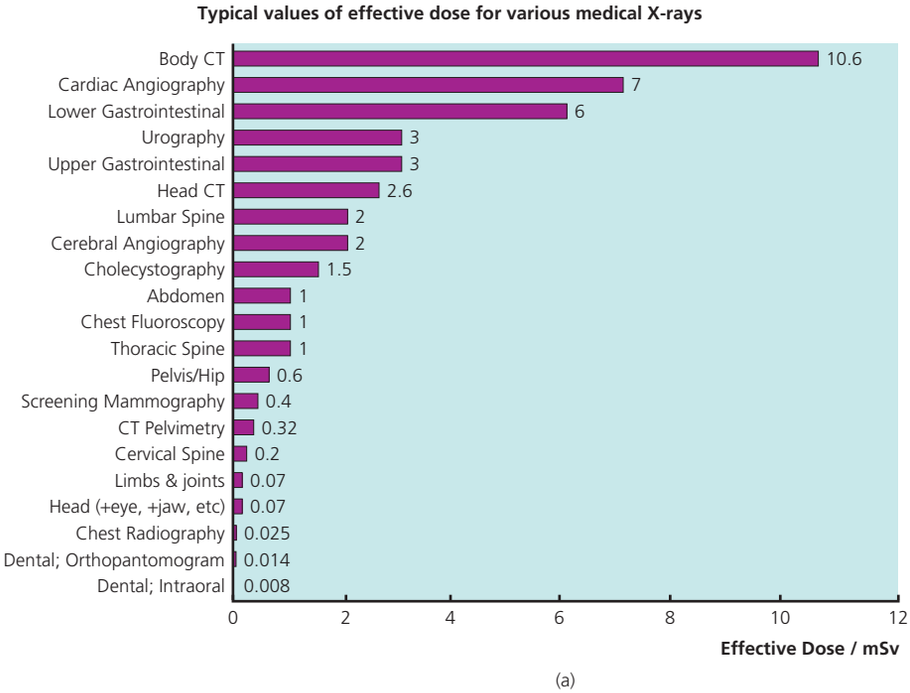
Imaging of the acute abdomen has been revolutionised by multidetector computed tomography (MDCT) and every emergency department should now have access to one. Previously a supine AXR and an erect CXR were the first line of investigations, but the AXR is now almost obsolete. Kellow et al. (2008) stated 'when imaging is needed, the emergency physician should be encouraged to immediately request more definitive imaging modalities' (e.g. MDCT and ultrasound (US)).

There has been a dramatic increase in the use of MDCT in the past decade, in particular in the ER.

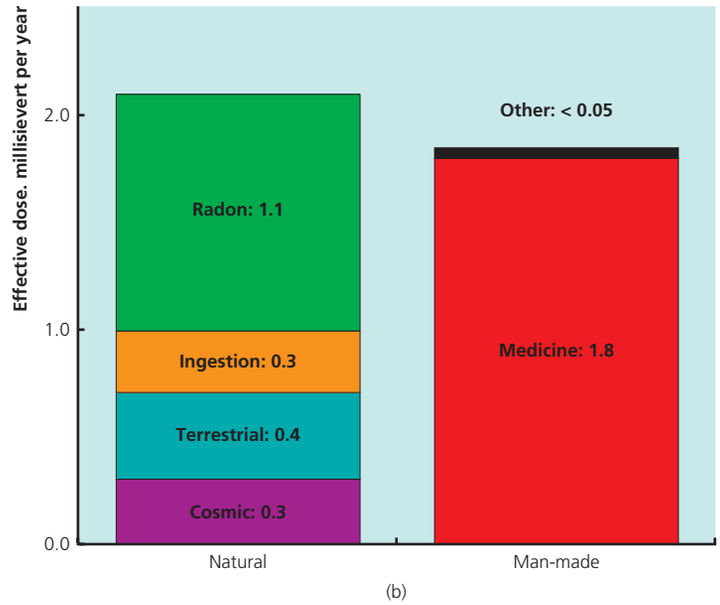
Indications for acute abdominal CT

MDCT is accurate and cost effective for the evaluation of acute abdominal pain, and provides an earlier diagnosis. When surgical intervention may be required, CT provides additional information to facilitate and limit it to the minimum necessary, reducing patient hospital stay and peri-operative morbidity.

ABC of Emergency Radiology, Third Edition. Edited by Otto Chan.
© 2013 John Wiley & Sons, Ltd. Published 2013 by John Wiley & Sons, Ltd.



(a)



(b)

Figure 14.1 (a) Graph illustrating the rapid increase in the number of CT scans per year in the USA. (b) Note the average number of CT scans per person per year is now more than 1 in 5.

US and CT complement each other as US has greater accuracy than CT for some conditions and involves no ionising radiation dose. This is the major limiting factor with CT, particularly with multiple phases or repeated examinations. The average dose of an adult abdominal and pelvic MDCT is 8.4 mSv; *equivalent to 3.4 years of UK background radiation or 400 chest radiographs*. Young patients are more sensitive to radiation-induced carcinogenesis, so the dose from CT should be considered when requesting imaging. Magnetic resonance imaging (MRI) also has no radiation dose but does not have an important role in the initial management of the acute abdomen. Your radiologist will advise on the most appropriate investigation given the relevant clinical information.

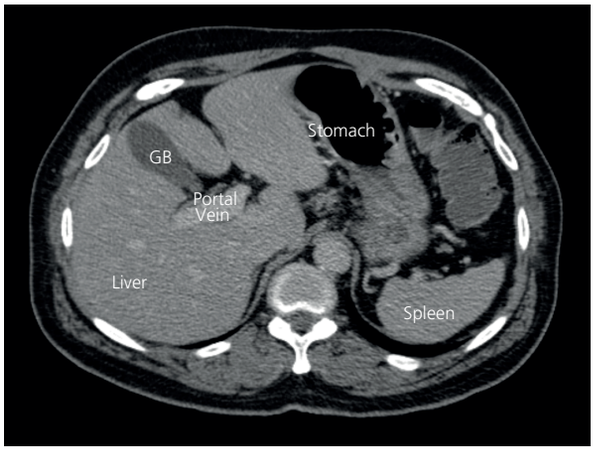
This chapter will present a systematic approach to the findings on MDCT of the most common causes of acute abdominal conditions.

Relevant abdominal anatomy

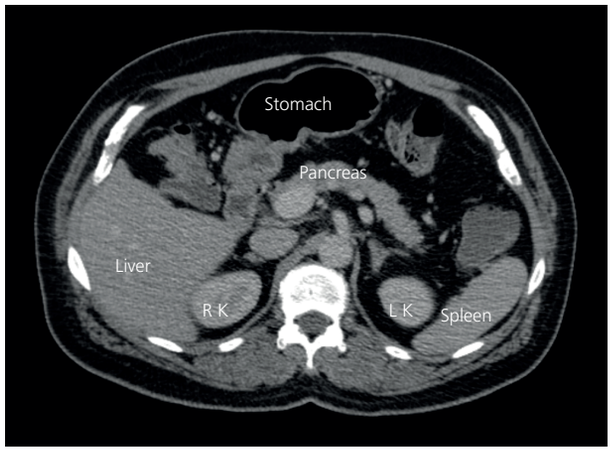
Normal positions of the upper abdominal organs are shown in Figures 14.2 and 14.3.

Causes of acute abdominal pain by quadrant

Causes of acute abdominal pain are shown in Figure 14.4 .



(a)



(b)

Figure 14.2 (a) Level of the hepatic hilum; (b) level of the pancreas (© Commonwealth of Australia 2012, as represented by the Australian Radiation Protection and Nuclear Safety Agency (ARPANSA)).

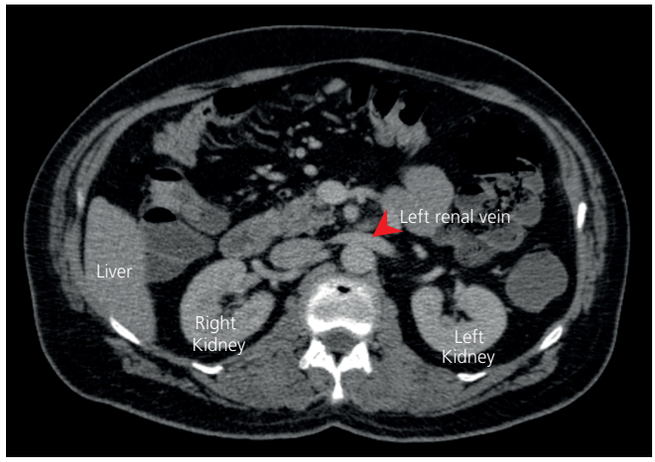


Figure 14.3 Level of the renal hilum (Informationskreis KernEnergie, Berlin).

Abdominal CT protocols

The MDCT examination will vary according to the clinical question.

Most patients with suspected acute abdominal inflammation or infection require only a single phase intravenous iodinated contrast-enhanced CT (CECT) from the diaphragm to the pubic symphysis. The portal venous phase (60–70 s delay after injection) provides optimal organ enhancement and is considered the standard protocol.

Certain indications will require non-enhanced (NECT), arterial phase imaging (30–40 s delay), or delayed imaging after several minutes, either alone or with a portal venous phase, and these will be discussed.

A CT KUB (kidneys, ureters and bladder) is a non-enhanced examination that is extremely sensitive and specific for the presence of urolithiasis (renal tract stones). The radiation dose of a CT KUB approaches that of a plain AXR, but it provides far more information. Although some extra-renal diagnoses can be made with NECT, a CT KUB should only be requested when the diagnosis of ureteric colic is suspected.

In most acute abdominal settings, there is no requirement or time to give oral contrast (drinking takes up to one hour). However, oral contrast is sometimes administered (either as water or diluted water-soluble iodinated contrast), in specific clinical scenarios.

If NECT is performed because of renal impairment or allergy, the images can be difficult to interpret; particularly in slender patients without intra-abdominal fat, as the organs and bowel are poorly

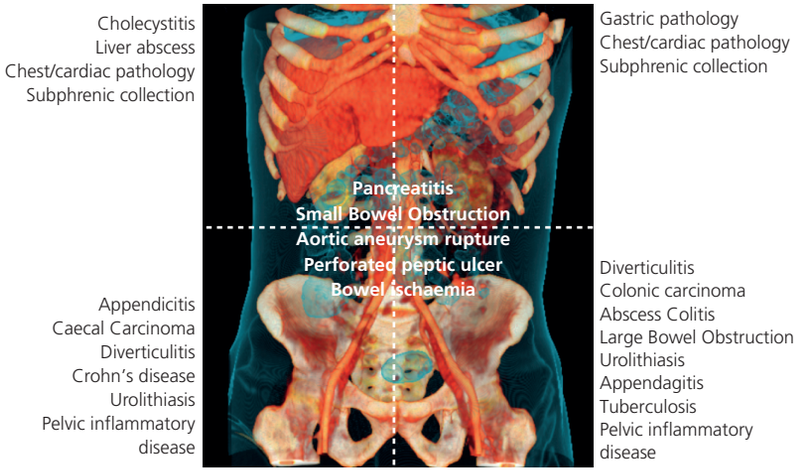


Figure 14.4 Causes of acute abdominal pain by quadrant.

defined. In such cases we recommend the use of oral positive contrast or consider using US instead.

Interpretation of abdominal CT

A systematic review is required because of the number of structures and pathologies that may be encountered.

An ABC approach is recommended (Table 14.2).

CT features of conditions causing acute abdominal pain

Signs of inflammation (non-specific)

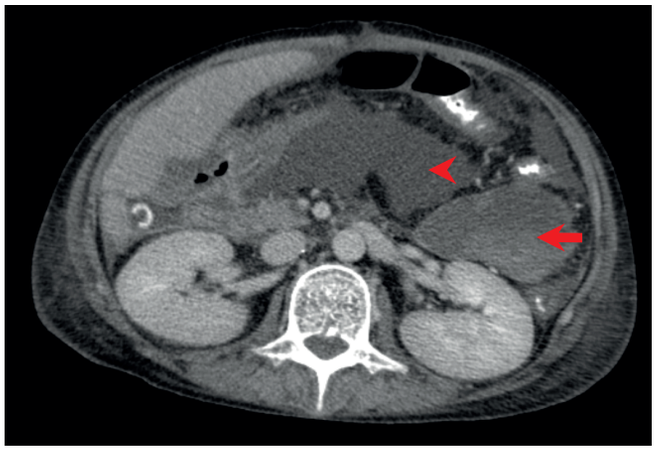
- Normal fat looks 'clean' – dark grey/black on abdominal CT window
- 'Dirty' oedematous and inflamed fat is misty/streaky and lighter grey – a clue to local pathology
- Low density tissue oedema
- Mural thickening
- Inflammatory soft tissue density, enhancing mass (phlegmon, an abscess in the making)
- Free or localised fluid (Table 14.3; Figure 14.5)
- Poor or increased contrast enhancement
- Localised dilated loops of bowel (ileus)

Table 14.2 ABCs approach to abdominal CT – $A^3B^3C^2DEFGHS^2$.

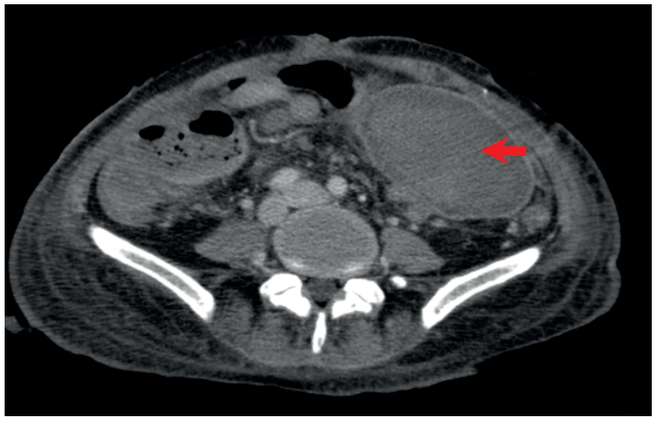
A – All the organs	Each organ must be examined in turn
A – Air	Search for extra-luminal air (on lung CT window)
A – Appendicitis	If the appendix is not seen, it is normal or not present
B – Bowel	Trace bowel lumen carefully Bowel dilatation, wall thickening and masses
B – Bleeding	Haematoma (previous haemorrhage) Contrast extravasation (on-going haemorrhage)
B – Bases of lungs	Lung or pleural pathology can cause abdominal pain
C – Calcification	Urological tract (obstructing calculus) Vascular (aneurysm and ischaemia)
C – Circulation	Vessel opacification and calibre
D – Dirty fat	Examine the organ-fat interface carefully, especially around appendix, colon, gallbladder and pancreas
E – Enhancement	Increased vascularity and enhancement with inflammation Decreased perfusion and enhancement with tissue oedema, ischaemia or necrosis
F – Fluid	Free fluid and collections Location may point to the site of pathology Infected or not? Take care to distinguish collections from bowel
G – Gynaecological	Pelvic inflammatory disease, ovarian torsion and ectopic pregnancy
H – Hernias	Examine hernial orifices and abdominal wall
S – Skeleton	Examine skeleton (on bone CT window, and in sagittal/coronal planes)
S – Summary	Check PACS for previous imaging and reports; often helpful information is available

Table 14.3 Fluid collections – CT characteristics.

Simple	Homogeneous fluid of lower density than soft tissue No wall No surrounding fat stranding
Infected	Usually homogeneous or mixed low to medium density fluid Thin enhancing wall Surrounding fat stranding
Abscess	Heterogeneous variable density fluid Less dense centrally, sometimes with gas locules Thick irregular, enhancing wall Marked surrounding fat stranding Fistula tracts
Haematoma	Initially higher density than soft tissues on NECT Over time, less dense from the periphery inwards May have enhancing wall in absence of infection Variable fat stranding depending on amount of blood, age and presence of infection
Faeculant	Heterogeneous solid material with mixed fat, fluid or soft tissue density with tiny specks of gas Usually with associated signs of infection



(a)



(b)

Figure 14.5 (a) Central fluid collection (arrowhead) and (b) adjacent haematoma with evidence of layering (arrow).

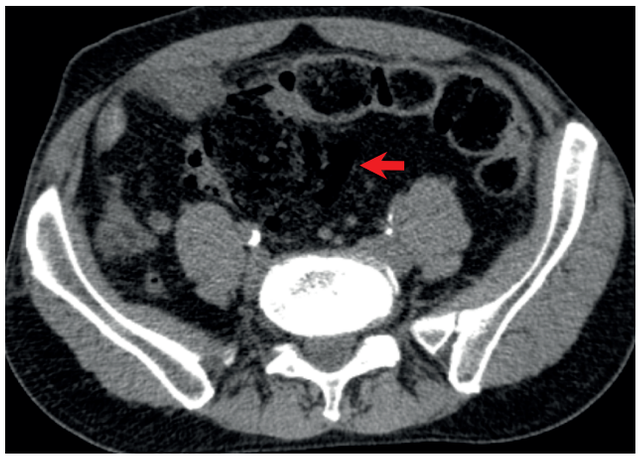
Signs of gastrointestinal tract perforation

Free intraperitoneal or retroperitoneal gas implies perforation (most commonly from a peptic ulcer). Pneumoperitoneum can also be caused by diverticulitis and can be present after a recent laparotomy. MDCT has a very high sensitivity and specificity for even small amounts (<2 ml) of free gas (Figures 14.6 and 14.7).

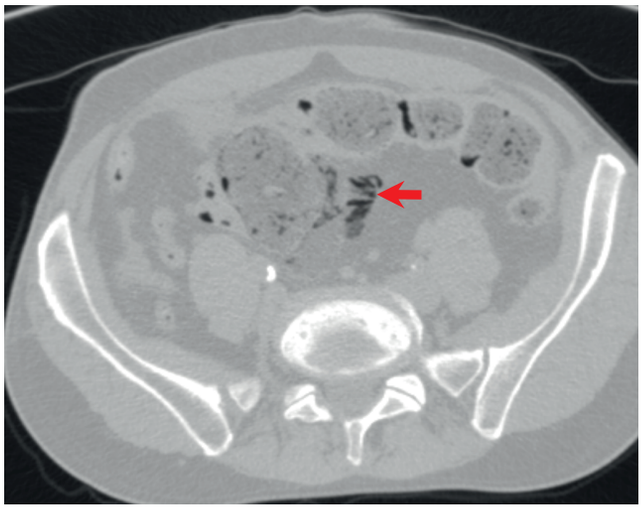
Extraluminal gas may also form in a walled off collection anywhere in the abdominal cavity, forming a gas-fluid level (as in the diverticular abscess described later) or as small bubbles of gas trapped in solid material or sited in anti-dependent locations when the patient is supine for the CT examination (as in the example of necrotising pancreatitis seen later).

Tips

- Carefully look under the anterior abdominal wall and around the liver for tiny locules of gas that may be the only sign of a perforation.
- Lung windows should always be used to search for free gas.



(a)



(b)

Figure 14.6 Pneumoperitoneum (arrow). On soft tissue windows (a) this localised sigmoid colon perforation may be missed, whereas on lung windows (b) it is clearly seen to be extraluminal.



Figure 14.7 Retroperitoneal gas from a perforated duodenal ulcer surrounds the right kidney and left renal vein.

Acute appendicitis

Role of CT

Ultrasound is the investigation of choice but CECT has a role if US is non-diagnostic or inconclusive; if the history is atypical (in 25–33%), or if complications or other pathologies are suspected such as caecal carcinoma in elderly patients. CT has increased the positive laparotomy rate, and reduced the surgical misdiagnosis rate to 5–10%.

CT features

The normal appendix appears as a tubular serpiginous structure arising from the caecal pole. It is thin walled, <6 mm in diameter, and fluid or gas filled. Box 14.1 shows the signs of acute appendicitis.

Box 14.1 **Signs of acute appendicitis**

- Circumferential symmetric mural thickening
- Appendiceal enlargement
- Dilatation >7 mm with fluid
- Homogenous enhancement
- Peri-appendiceal fat haziness and stranding, or fluid (Figure 14.8)
- Calcified appendicolith (Figure 14.9)
- Mild caecal or terminal ileal thickening
- Right iliac fossa lymph node enlargement

Complications

- Perforation
- Appendiceal mass (phlegmon)
- Abscess formation

Consider the differential diagnosis

It is important to consider diagnoses for which the correct surgical approach is not appendicectomy or those which are managed conservatively.

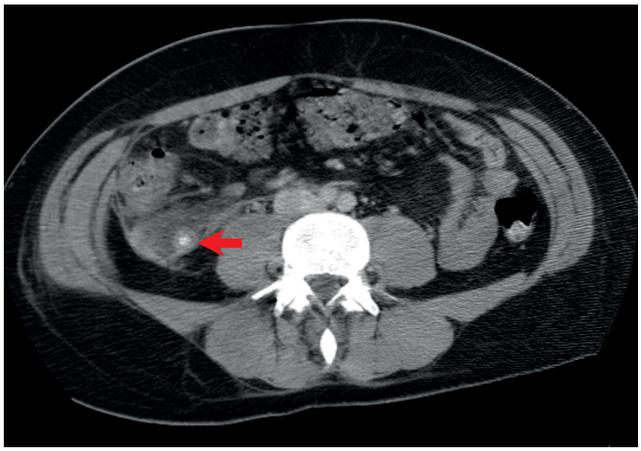


Figure 14.8 Enlarged enhancing appendix (arrow) with appendicolith and peri-appendiceal fat stranding in acute appendicitis.

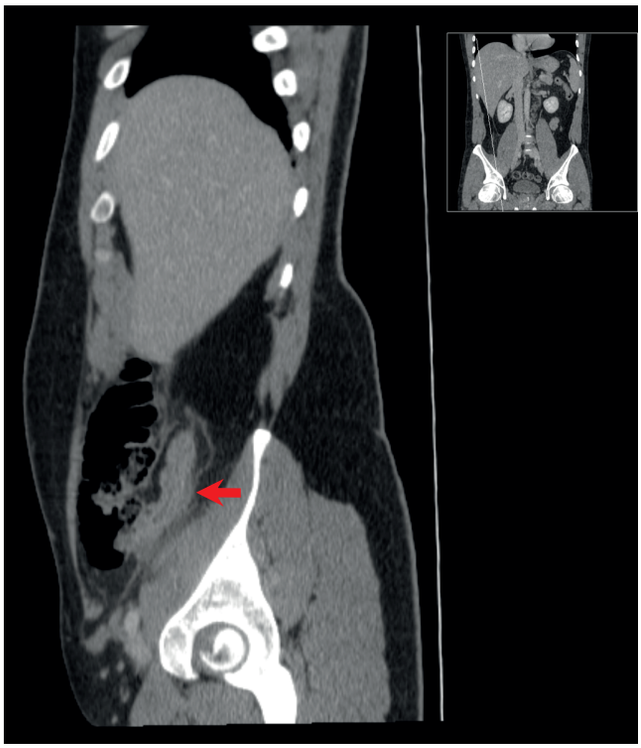


Figure 14.9 Thickened enhancing appendix containing a calcified appendicolith (arrowhead). Sagittal reconstruction shows the retrocaecal location of the appendix (arrow).

- Mesenteric adenitis; enlarged mesenteric nodes
- Caecal carcinoma or right-sided diverticulitis
- Crohn's terminal ileitis/abscess

Tips

- Coronal or sagittal reformats can aid identification of the appendix
- Important features which increase the difficulty of appendicectomy: a retrocaecal location, presence of perforation with fragments or appendiceal mass

Diverticulitis

Role of CT

Left lower quadrant pain in a patient over the age of 40 years should be investigated with CECT. The most likely diagnosis of colonic diverticulitis can be confirmed, complications discovered, and other pathology such as unsuspected colon carcinoma can be diagnosed.

CT features

Uncomplicated diverticulosis is frequently an incidental finding; the prevalence increases with patient age and involves the sigmoid colon in 95%. It manifests as a diffuse symmetrical colonic mural thickening (>4mm), and multiple saccular out-pouchings. The peri-colonic fat should have normal density.

Diverticulitis occurs in 10–25% of patients with diverticulosis, resulting from local perforation of a diverticulum into the peri-colonic fat. The perforation is usually contained, and free pneumoperitoneum is uncommon. Box 14.2 shows the signs of diverticulitis.

Box 14.2 **Signs of diverticulitis**

- Presence of diverticulosis – suspect other pathology if this is absent elsewhere
- Peri-colonic fat inflammation and increased vascularity in the mesocolon
- Symmetrical mural thickening (usually <1 cm) over a long segment
- Phlegmon formation
- Free fluid

Complications

- Abscess formation (Figures 14.10–14.12)
- Large or small bowel obstruction
- Intraperitoneal perforation
- Fistula formation with adjacent organs
- Portal vein gas, liver abscess
- Diverticular haemorrhage

Consider the differential diagnosis

- The most important diagnosis to exclude is colonic carcinoma (eccentric wall thickening >1 cm over a short segment, enlarged lymph nodes, liver metastases)
- Ischaemic or infective colitis
- Appendagitis (inflammation of epiploic fat)

Tips

- Look for other causes of acute abdomen with coexisting diverticulosis; fat inflammation is the clue
- Initial treatment is conservative, with percutaneous drainage of collections or bowel resection for severe complications

Pancreatitis

Role of CT

If the clinical diagnosis of acute pancreatitis is obvious, then there is no need for CT within the first 48 hours. Non-improving patients

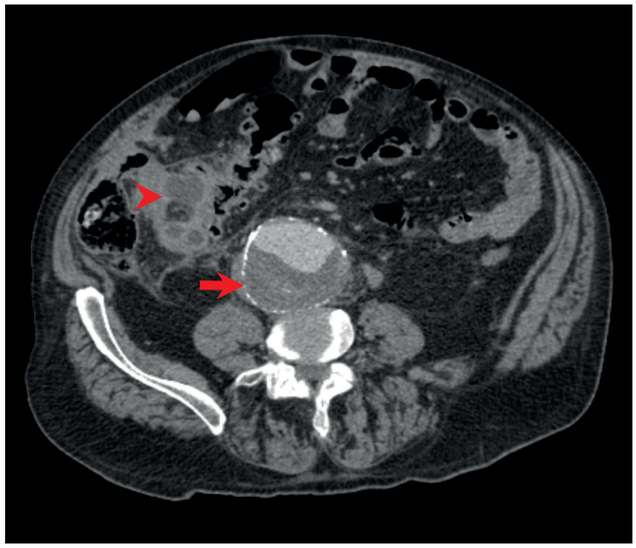


Figure 14.10 Localised diverticular perforation with peri-colic abscess (arrowhead) and incidental non-ruptured aortic aneurysm (arrow).

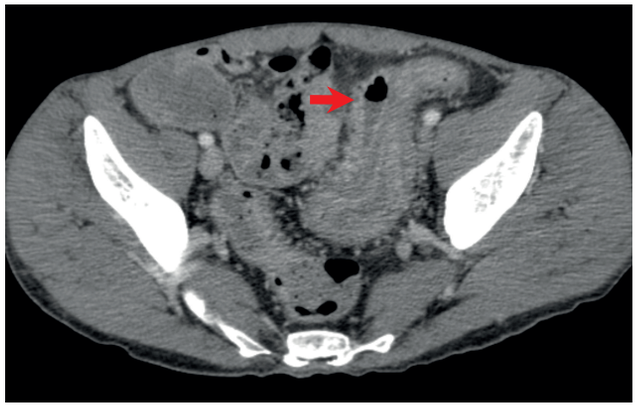


Figure 14.11 Intramural diverticular abscess in the sigmoid colon.

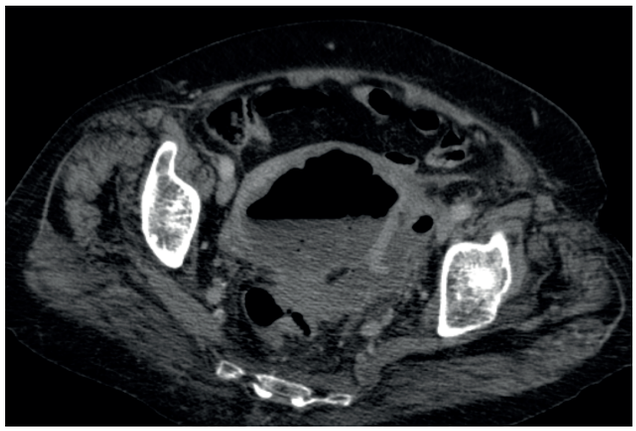


Figure 14.12 Large sigmoid diverticular abscess with gas-fluid level.

benefit from CT to stage the disease severity and prognosis, identify complications and to guide intervention.

If the diagnosis is not clear clinically, early CT can exclude other causes such as perforated peptic ulcer, but normal pancreatic appearances do not exclude pancreatitis. In this situation, a single portal venous abdominal CT is sufficient.

However, in severe pancreatitis, unenhanced, arterial and portal venous phases are required for assessment of haemorrhage, necrosis and pseudoaneurysm formation.

CT features

The normal pancreas is a slender retroperitoneal organ with a smooth or slightly lobulated contour. The pancreatic duct can normally be seen as a thin fluid-filled tube, 2–3 mm in diameter. Box 14.3 shows the signs of mild and severe pancreatitis (Figures 14.13–14.16).

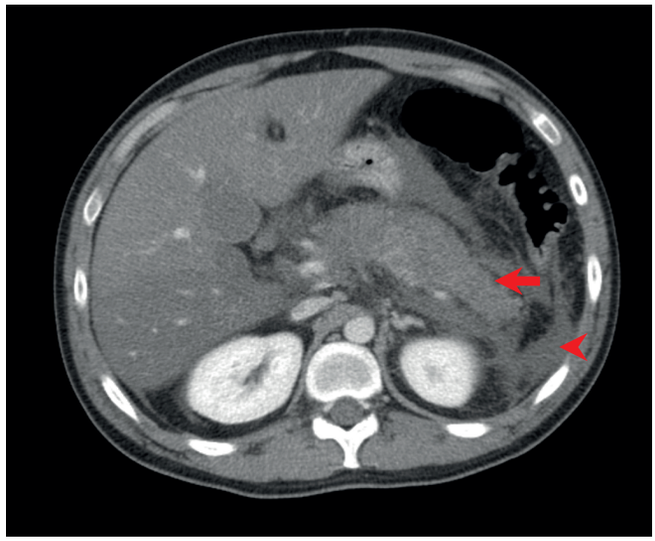


Figure 14.13 In mild pancreatitis the pancreas is swollen, with an indistinct outline (arrow) and with inflammation of the surrounding fat (arrowhead).

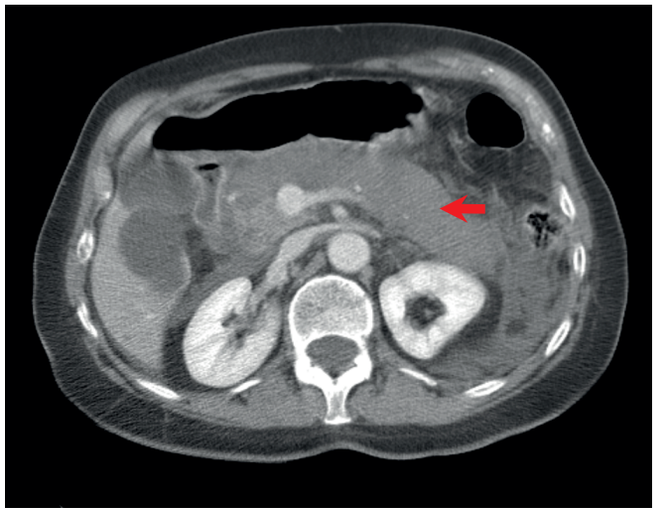
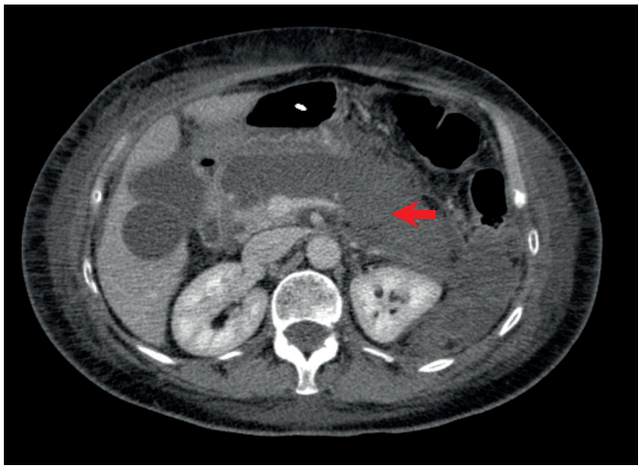
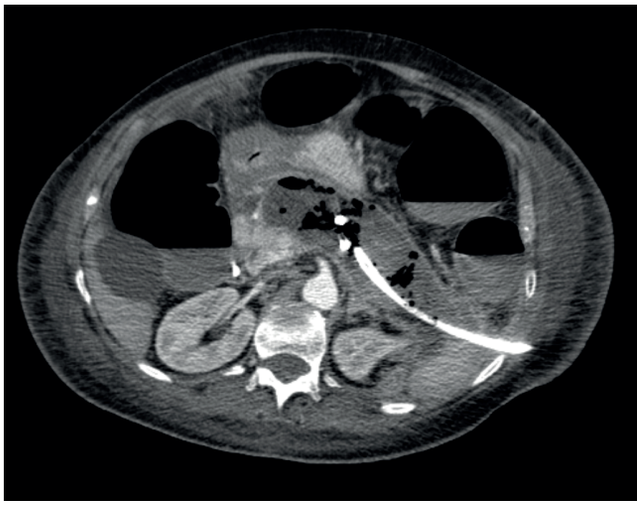


Figure 14.14 In severe pancreatitis there is globally poor pancreatic enhancement (arrow) when compared to the liver parenchyma.



(a)



(b)

Figure 14.15 Necrotising pancreatitis . Same patient as Figure 14. (a) One week later the pancreas is necrotic (arrowhead). It no longer enhances and has the same density as fluid in a liver cyst (b) One month later, after insertion of a percutaneous drain the pancreas is replaced by necrotic debris containing gas locules and an enhancing abscess wall. The splenic vein is also thrombosed.

Complications

- **Abscess** – an infected collection of fluid without necrosis, usually >3 weeks after initial attack
- **Infected pancreatic necrosis** – partially or totally liquefied tissue with high mortality rate
- **Pseudoaneurysms** – usually splenic, gastroduodenal or pancreaticoduodenal arteries. **Life threatening haemorrhage** can occur, and therefore it is imperative to detect these so they can be treated by embolisation. Portal venous imaging alone may miss pseudoaneurysms, hence the need for an arterial phase
- **Pseudocyst** – localised peri-pancreatic fluid collection with a thick fibrous wall, occurring 4–6 weeks after an acute attack

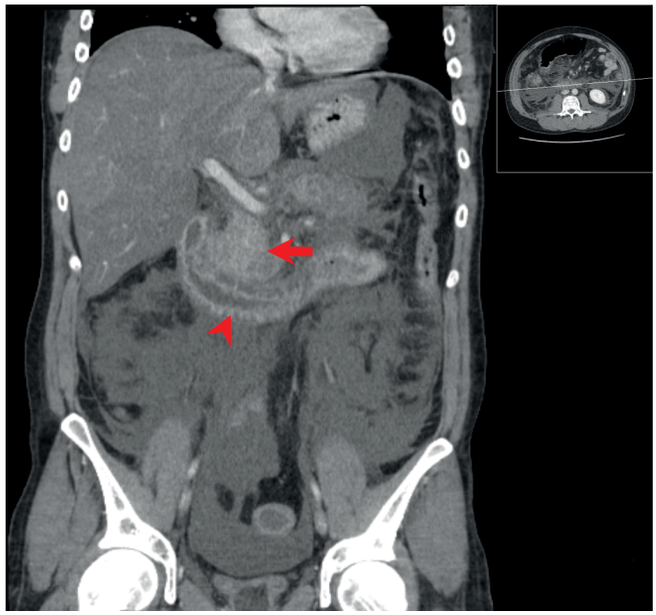


Figure 14.16 Retroperitoneal fat stranding in acute pancreatitis. Coronal section through the retroperitoneum shows inflamed pancreatic head (arrow), with hyperenhancement of the adjacent duodenum (arrowhead), and widespread inflammation across the fascial planes of the retroperitoneum (arrowhead) with pelvic ascites.

Box 14.3 **Signs of pancreatitis**

Signs of mild pancreatitis

- Normal pancreas (28%)
- Oedematous swollen/enlarged gland
- Peri-pancreatic fat stranding and thickened fascial planes
- Usually homogenous enhancement
- Cause may be identified – gallstones (US more accurate)
- Parenchymal calcification – previous or chronic pancreatitis

Signs of severe pancreatitis

- Enlarged gland
- Haemorrhage: high density on NECT
- Necrosis: poorly enhancing parenchyma
- Obliterated peri-pancreatic fat
- Inflammation of fat penetrates across fascial and peritoneal boundaries
- Peri-pancreatic collections and free fluid
- Splenic vein thrombosis

Cholecystitis

Role of CT

US is the investigation of choice as the detection of gallstones is more sensitive. CT has a limited role, for example in suspected gallbladder perforation.

CT features

The gall bladder is dilated, with an oedematous thickened wall (>3 mm), although this is non-specific, and there is surrounding fat surrounding or fluid (Figure 14.17).

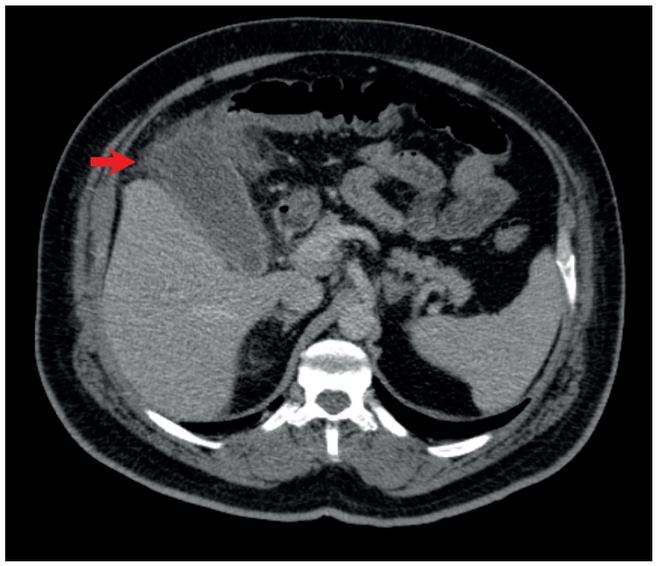


Figure 14.17 Acute cholecystitis. Oedematous inflamed gall bladder wall with non-calcified gall stone.

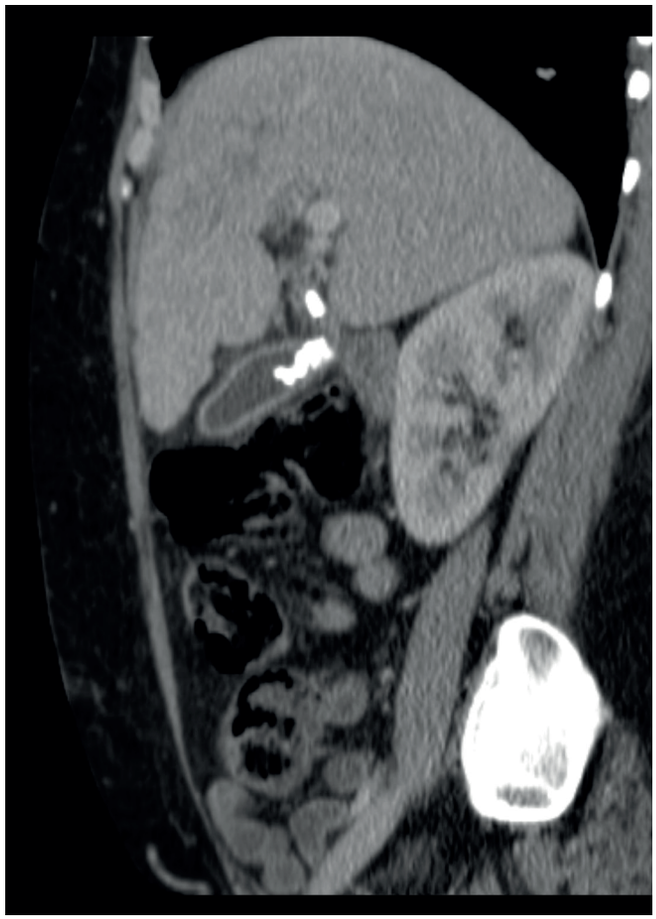


Figure 14.18 Sagittal section with a chronically inflamed thickened enhancing gall bladder wall with calcified stones in the gall bladder and cystic duct.

Calcified gallstones may be seen on CT, but often stones appear isodense to bile, and sometimes contain gas (Figure 14.18).

Tips

- Check carefully for biliary dilatation, as an obstructing stone in the common bile duct (CBD) warrants urgent ERCP.
- Coronal reformats can help show the length of the CBD.
- Gall bladder perforation may produce a liver abscess, but carcinoma can present similarly.

Colitis/enteritis

Role of CT

Infection is the commonest cause of enterocolitis and usually does not require imaging. CT is helpful in acute exacerbations or the initial presentation of inflammatory bowel disease (IBD).

CT features

The gut responds to insult with non-specific mural thickening and surrounding fat stranding. Mucosal and serosal enhancement with intervening oedematous submucosa gives a target sign appearance. This may be focal (single or multiple 'skip' lesions) or diffuse, and involve small and/or large bowel (Table 14.4; Figures 14.19 and 14.20).

Table 14.4 Distinguishing CT features of bowel pathology.

All conditions	Gut wall thickening Fat stranding
Crohn's disease	Terminal ileum (or anywhere along GI tract) Focal/skip lesions Acute/active disease: stratified wall enhancement (target sign) Chronic/inactive disease: homogenous wall enhancement Mesenteric fat proliferation and hypervascularity Lymph node enlargement Abscess or fistulae
Ulcerative colitis	Extends proximally from rectum Diffuse symmetrical thickening Target sign Lack of haustra, toxic megacolon (inflamed dilated colon) Ascites unusual
Pseudomembranous colitis (*C. difficile* infection)	Predisposing antibiotic or chemotherapy use Rectum/sigmoid/pan-colitis Irregular thickening with marked oedema Limited fat stranding Ascites
Ischaemia	Predisposing hypotension, vasculitis, obstruction, or embolus Arterial/venous origin Circumferential thickening ≫ fat stranding High density haemorrhage Poor enhancement or target sign Gas in bowel wall (pneumatosis) or portal vein

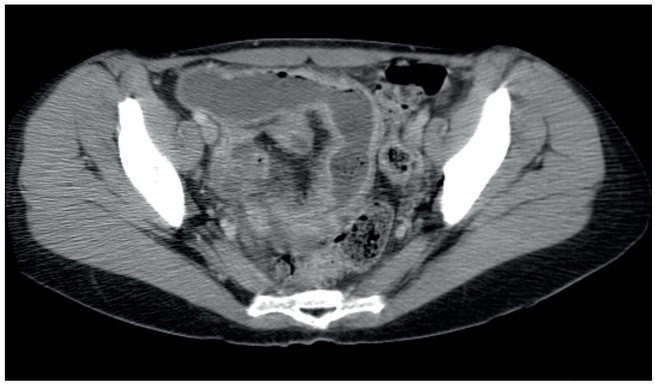


Figure 14.19 Terminal ileitis in Crohn's disease. A long segment of ileum is dilated, with a thickened enhancing wall and surrounding mesenteric fat inflammation.

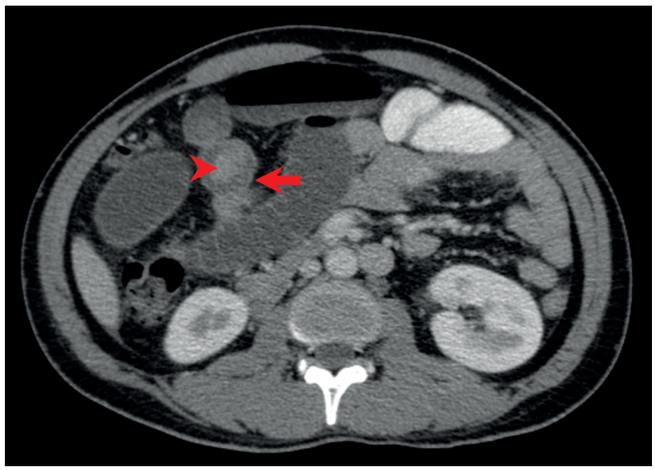


Figure 14.20 Target sign in Crohn's disease. The bowel wall is thickened with three layers visible – inner mucosal (arrow) and outer serosal (arrowhead) enhancement with intervening low density oedema of the submucosa. Proximal small bowel is dilated.

Tips

- If fat stranding is much greater than bowel wall thickening – consider external pathology: epiploic appendagitis or omental infarction (both treated conservatively).
- If bowel wall thickening is much greater than fat stranding – infection or ischaemia are more likely (Figures 14.21 and 14.22).

Tuberculosis (TB)

TB is an important differential diagnosis for inflammation within the abdomen. The findings can be non-specific but in the right clinical context there are important signs on CT which can aid in its diagnosis.

The most common finding in the abdomen is lymph node enlargement, predominantly involving the lesser omental, mesenteric, and upper para-aortic lymph nodes although any group can be involved. They can demonstrate a variety of patterns of enhancement but the most characteristic is central low density (Table 14.5; Figure 14.23).

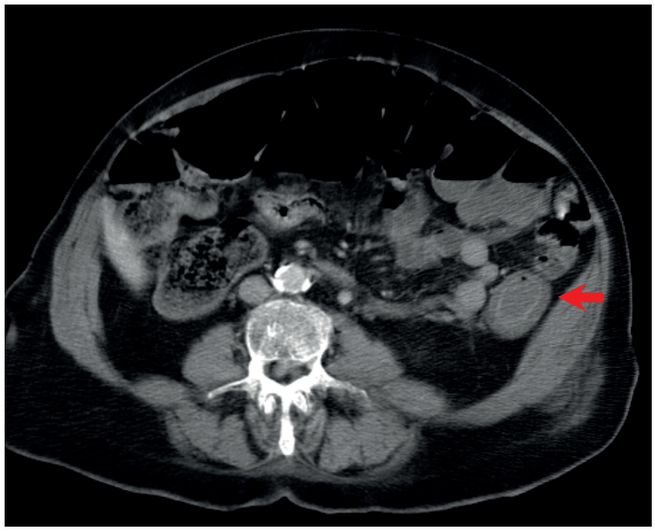


Figure 14.21 Target sign in infective colitis with little fat stranding.



Figure 14.22 Diffuse marked oedema of the colon in pseudomembranous colitis.

Small bowel and large bowel obstruction (SBO/LBO)

Role of CT

MDCT can often localise the level and cause of obstruction, differentiate between high and low grades of SBO, and assess the presence of complications. In patients with paralytic ileus, pseudo-obstruction can be seen (dilated large bowel with no obstructing cause).

CT features

A mechanical blockage of the bowel causes dilatation of proximal loops. The key to diagnosis is the identification of a transition point from dilated to collapsed bowel. This is often best visualised by starting at the rectum and working backwards. Signs of small bowel obstruction are shown in Box 14.4 and Figures 14.24 and 14.25.

Table 14.5 Signs of abdominal tuberculosis.

Gastrointestinal tract	
Bowel	Bowel wall thickening (usually terminal ileum/caecum) Often adjacent mesenteric lymphadenopathy
Lymph Nodes	Enlarged enhancing lymph nodes Often with central low attenuation
Peritoneum	Often present with extensive disease Wet type: viscous ascites (free or loculated) Fibrotic fixed type: omental masses, adherent loops of bowel/mesentery, and loculated ascites Dry type: caseous nodules, fibrous peritoneal reaction, and dense adhesions
Liver and Spleen	Miliary TB: tiny low density foci scattered in liver/spleen Macronodular form is rare: diffuse liver and splenic enlargement with multiple low attenuating lesions or a large tumour like mass
Genitourinary tract	
Renal	Parenchymal calcifications Hydronephrosis: focal or generalised
Adrenal	Unilateral or bilateral adrenal mass with areas of low attenuation centrally
Ureters	Wall thickening and peri-ureteral inflammatory changes
Bladder	Shrunken thick walled bladder
Spine	
Lumbar Spine	Affects the anterior part of the vertebral body adjacent to superior and inferior end plates Involves disc space leading to collapse of intervertebral disc space Paravertebral abscess Psoas abscess

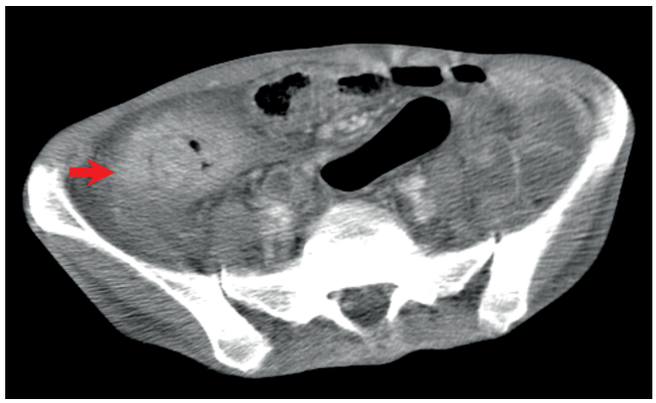
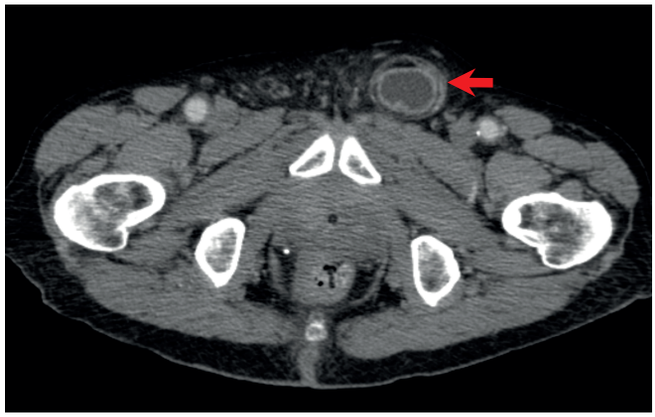
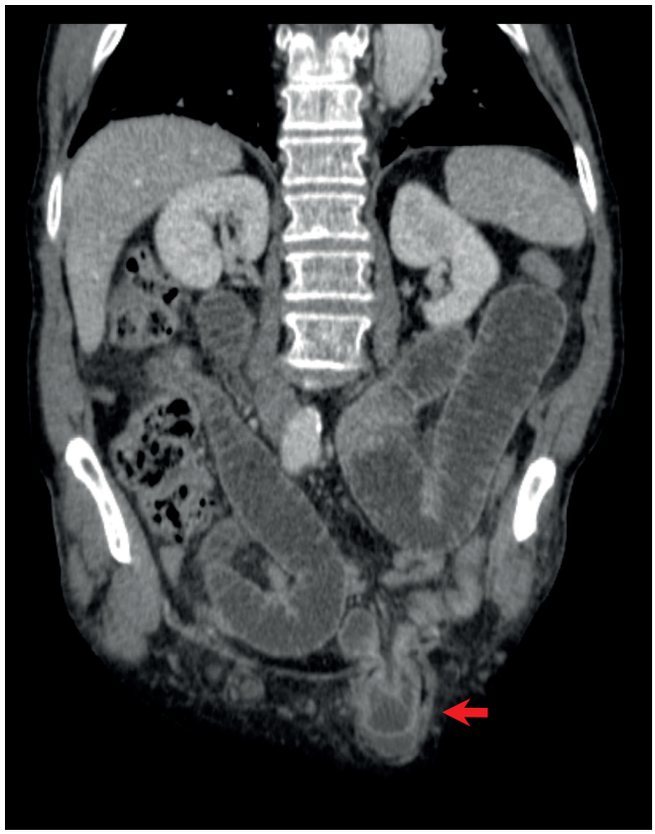


Figure 14.23 Large inflammatory ileo-caecal mass and ascites in tuberculosis.



(a)



(b)

Figure 14.24 Small bowel obstruction from an incarcerated left inguinal hernia (a) axial and (b) coronal.

Box 14.4 **Signs of small bowel obstruction**

- Loops of small bowel >2.5 cm on MDCT; gas or fluid filled
- Transition point with distal collapsed small bowel loops
- Solid small bowel faeces proximal to obstruction
- Large bowel usually collapsed

Box 14.5 **Signs of large bowel obstruction**

- Dilated loops of large bowel; gas, fluid, or stool filled
- Distal colon collapsed to the obstruction
- If transverse colon is >5.5 cm and or the caecum is >9 cm there is a significant chance of perforation
- Look for underlying cause and complications



Figure 14.25 The presence of solid faeces in the small bowel usually occurs just proximal to the obstruction point.

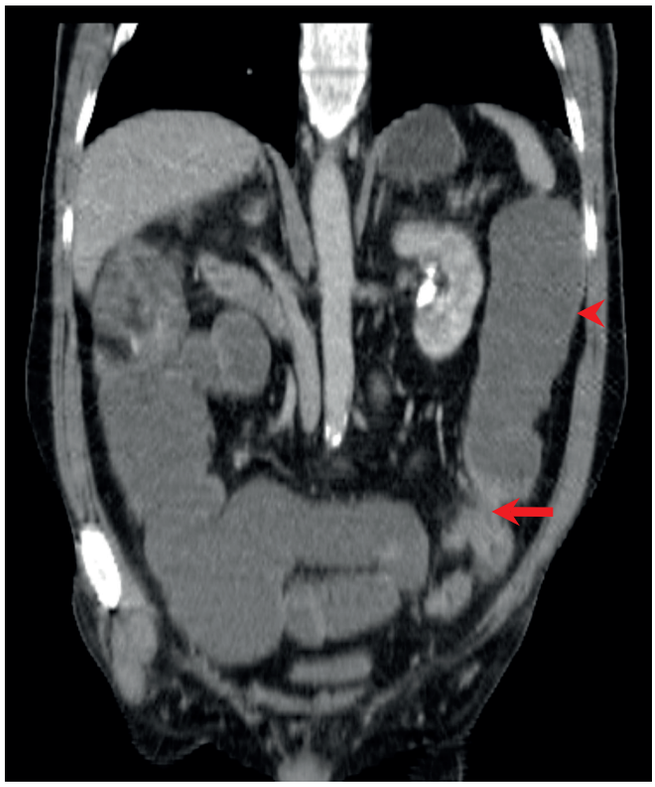
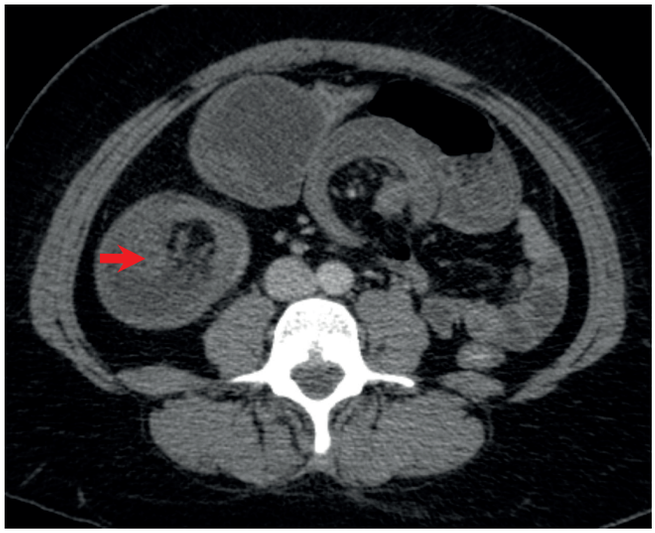


Figure 14.26 Coronal view of an obstructing cancer of the descending colon (arrow), with fluid filled dilated colon proximally (arrowhead).

Signs of large bowel obstruction are shown in Box 14.5 and Figure 14.26.

Consider the underlying cause

Table 14.6 gives the causes of bowel obstruction.



(a)

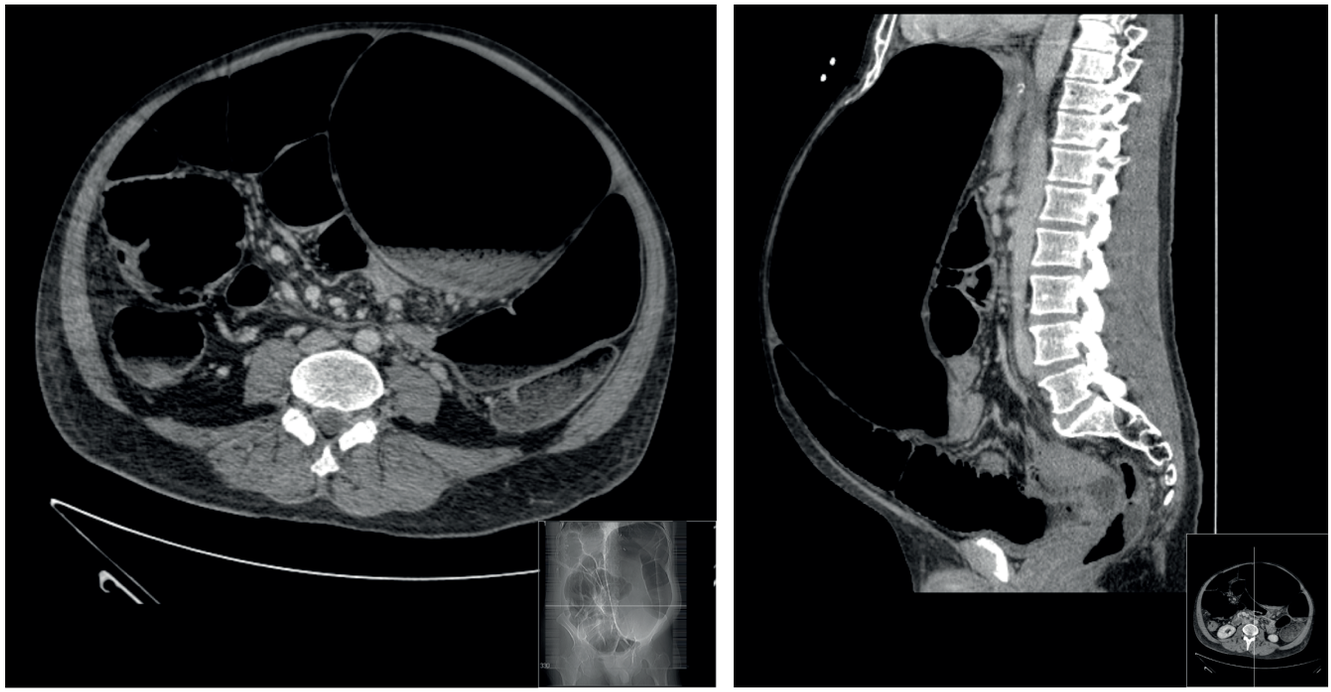


(b)

Figure 14.27 A large ileo-colic intussusception. The fat of the small bowel mesentery is seen within the lumen of the colon as the ileum (the *intussusceptum)* (arrow) invaginates into the caecum (the *intussuscipiens*) (a) axial (b) coronal.

Table 14.6 Causes of bowel obstruction.

Small bowel	Commonest (80%): adhesions, hernias, and neoplasia (including non-gut tumours) Less common causes include volvulus, intussusceptions (Figure 14.27) and gallstone ileus Appendix abscess
Large bowel	Commonest: colorectal carcinoma Other causes: faecal impaction, volvulus
Either	Inflammation: Crohn's disease and diverticulitis



(a) (b)

Figure 14.28 Hugely distended loops of colon in sigmoid volvulus. (a) Axial view shows the typical radiographic 'coffee bean' sign in the scout image. (b) Sagittal view shows the extent of distension to the diaphragm.

- Colonic carcinoma appears as an enhancing mural mass that may cause obstruction. Search for secondary features of malignancy; lymphadenopathy and metastases (liver/lung/bone).
- Volvulus is a twisting of part of the gut on its mesenteric axis, resulting in a closed loop obstruction and can occur with stomach, small bowel, caecum and sigmoid colon. Colonic volvulus has characteristic AXR appearances.
- Sigmoid volvulus is commonest (50–75% of all colonic volvulus) presenting with a very large dilated loop arising from the left lower quadrant, and dilated proximal colon and small bowel (Figure 14.28). It is more commonly seen in institutionalised patients.
- Caecal volvulus presents with a dilated caecum in an ectopic location usually in the left upper quadrant. It is associated with markedly distended small bowel loops and a collapsed distal colon.

Complications of bowel obstruction

- Ischaemia (poor enhancement, and adjacent free fluid)
- Infarction/necrosis (no enhancement of bowel wall, intramural gas)
- Gas in the mesenteric and/or portal veins (usually a pre-morbid sign; Figure 14.29)
- Perforation (pneumoperitoneum, pneumoretroperitoneum from colon)

Tips

- SBO with a transition point but no visible cause is usually secondary to adhesions
- Gas in intrahepatic portal veins is distributed more peripherally than the common finding of gas in the biliary tree (aerobilia)

Urolithiasis (renal tract calcification)

The formation of renal tract calculi is multifactorial in origin and heterogeneous in demographics. It commonly manifests as acute colicky flank pain radiating to the groin. Urolithiasis is divided into upper tract (calyceal, renal pelvis and pelvi-ureteric junction), ureteric and lower tract (bladder, urethral, prostatic, preputial).

Role of CT

CT can assess the presence, number, location, and complications of calculi, and exclude other causes of abdominal pain, especially in the absence of any obstructing calculi.

CT features

When assessing for urolithiasis, a non-enhanced examination is required (CT KUB) (Figure 14.30), as contrast may obscure the stone. Calculi are usually homogenous with calcium density on CT (check using bony windows) and most stones can be identified using NECT with the exception of indinavir (protease

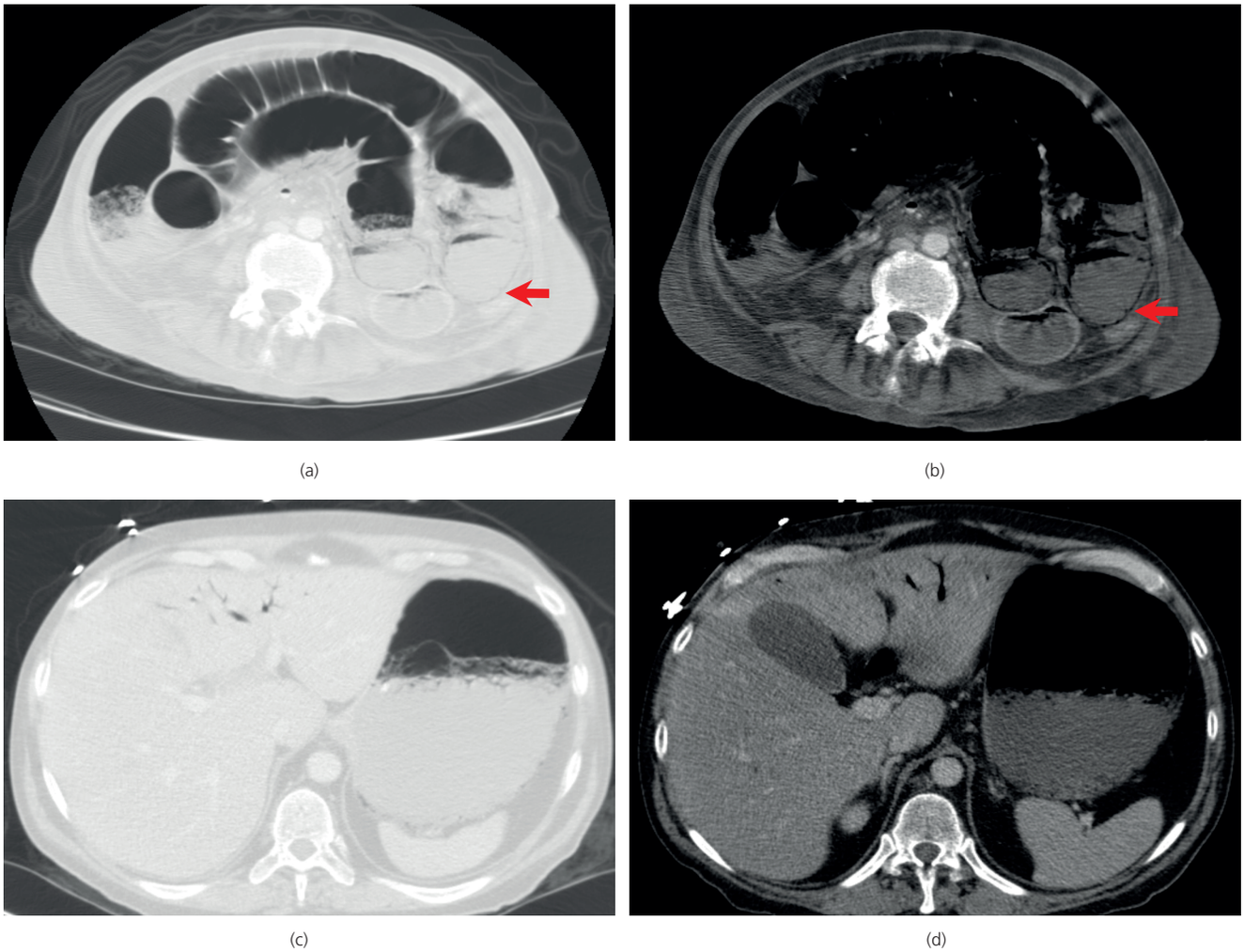


Figure 14.29 Dilated loops of bowel with intramural and mesenteric venous gas in small bowel infarction on (a) lung and (b) soft tissue windows. Branching gas pattern in the intra hepatic portal vein on (c) lung and (d) soft tissue windows.

inhibitor used in HIV) stones which have low density. 93% of ureteric calculi <6 mm will pass spontaneously (Box 14.6).

Box 14.6 **Secondary signs of obstructing renal tract calculus**

- Perinephric/periureteric fat stranding
- Dilated pelvicalyceal system (hydronephrosis)
- Dilated ureter above calculus (hydroureter)
- Ureteric rim sign – ureteric oedema around an impacted calculus
- Pseudoureterocele: ureterovesical oedema around a calculus
- If there is the possibility of a low density stone (indinavir) then the excretory phase of a MDCT urogram may localise the site of obstruction and stone

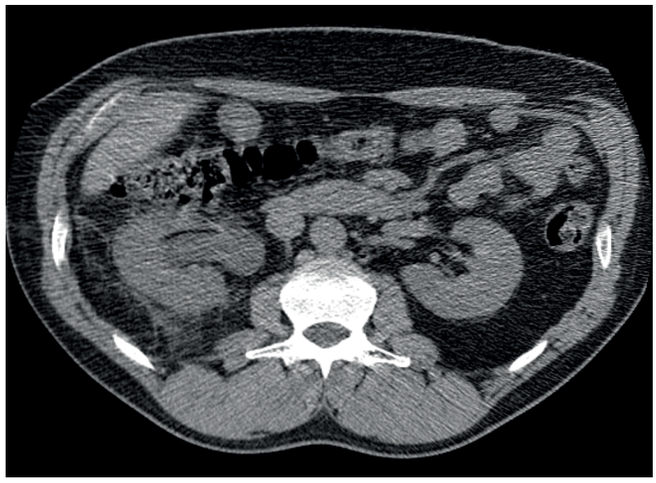
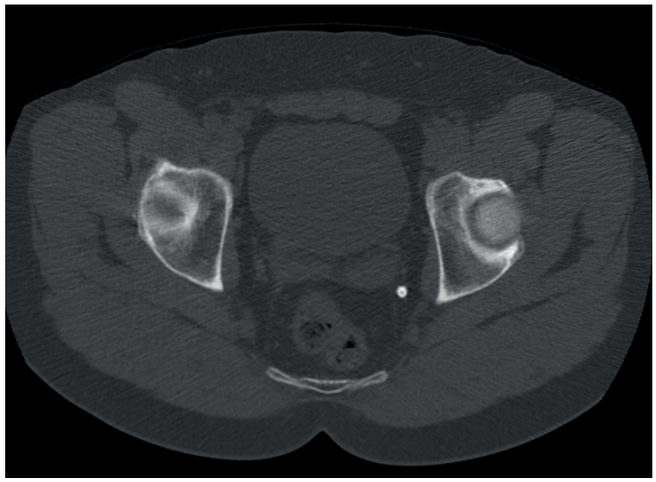


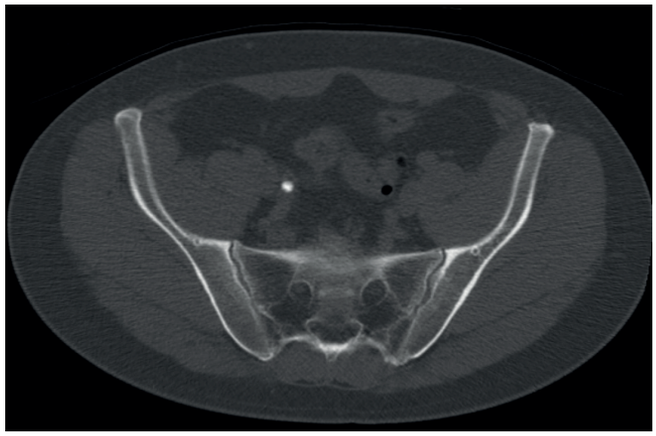
Figure 14.30 CT KUB showing right hydonephrosis and peri-renal fat stranding from a distal ureteric calculus (not shown).

Tips

Distinguishing between venous phleboliths and distal ureteric stones can be difficult; phleboliths usually are ring shaped rather than solid and lie lateral to the ureters (Figure 14.31).



(a)



(b)

Figure 14.31 (a) Phlebolith with ring like calcification, usually low in the pelvis. (b) Right ureteric calculus with solid calcification.

Abdominal aortic aneurysm (AAA) rupture

Role of CT

This is a life-threatening emergency that should be excluded in patients over 75 years with acute severe abdominal or back pain. The rupture rate with AAA diameter <4.9 cm is 1% per year, but 25% per year if diameter >6.0 cm. Patients that survive to hospital usually have a contained retroperitoneal rupture, and are usually stable enough for emergency CT (Figure 14.32). An aneurysm or rupture can be confirmed with NECT (Table 14.7), but an arterial phase is paramount in determining management: either open or endovascular repair.

Table 14.7 Signs of abdominal aortic aneurysm.

Aneurysm	Aortic diameter >3 cm Non-enhancing thrombus Calcified wall
Impending rupture	Extravasation of contrast into thrombus or wall Interruption of circumferential intimal calcification
Contained rupture	Bulging or indistinct aortic margin
Frank rupture	Large retroperitoneal haematoma Extraluminal contrast

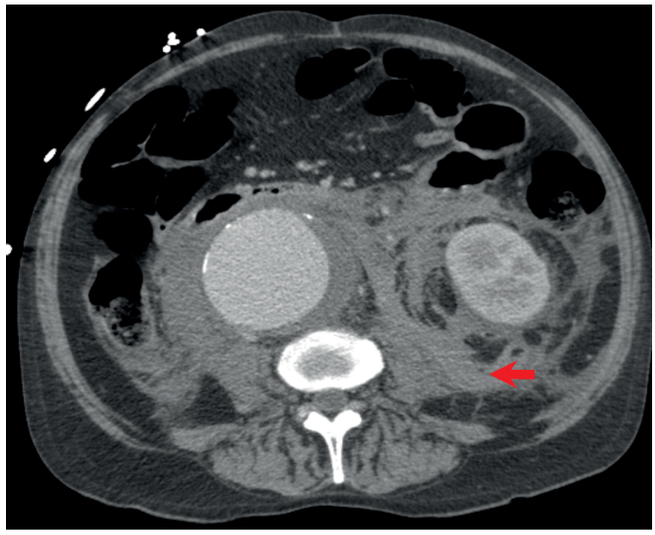


Figure 14.32 Large abdominal aortic aneurysm rupture with extensive retroperitoneal haemorrhage (arrow), but no extravasation of contrast.

Tips

AAA are often tortuous; measurements should be made perpendicular to the longitudinal axis, which may not be in the axial plane.

Gastrointestinal haemorrhage

Role of CT

If endoscopic measures are unsuccessful in identifying the source of upper or lower gastrointestinal tract bleeding, CT may localise the site prior to embolisation or surgery. A triple phase protocol is required (NECT, arterial and portal venous). Oral contrast should not be used as it will obscure luminal contrast extravasation.

CT features

NECT demonstrates high density sentinel clot in the vicinity of the bleeding point, and confirms that any high density blush present on CECT truly represents intravenous contrast. If bleeding is not on-going at the time of imaging, this may be the only sign (Figure 14.33).

On-going haemorrhage is typified by a small jet of contrast in the arterial phase, (as dense as blood in the aorta) which dissipates and becomes less dense in the venous phase, however only the venous blush may be seen (Figure 14.34).

Tips

- Advanced workstation techniques such as comparing the three phases together slice by slice, MIP (maximal intensity projection)

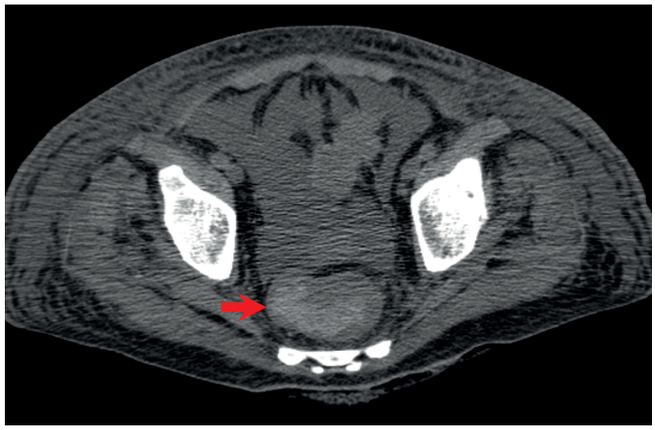


Figure 14.33 Sentinel high density clot. On this unenhanced image there is high density blood within the rectum; the 'sentinel clot'. Blood may travel a long way proximally or distally in the bowel lumen.

slabs and multi-planar reformats aid localisation of the bleeding source.

- Intraluminal blood may pass proximally or distally away from the site of bleeding

Other causes of acute abdominal pain

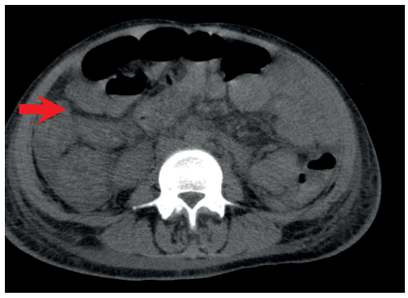
There are many causes of acute abdominal pain, and it is beyond the remit of this chapter to describe them all. Those that require urgent intervention have been discussed, but others which require only conservative treatment include:

- Mesenteric adenitis (Figure 14.35)
- Epiploic appendagitis (Figure 14.36)
- Omental infarction (Figure 14.37)
- Rectus sheath haematoma (Figure 14.38)

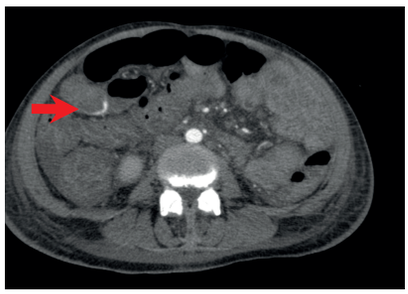
In women, consider gynaecological causes such as:

- Pelvic inflammatory disease and tubo-ovarian abscess (Figure 14.39)
- Torsion or rupture of ovarian cyst
- Ectopic pregnancy

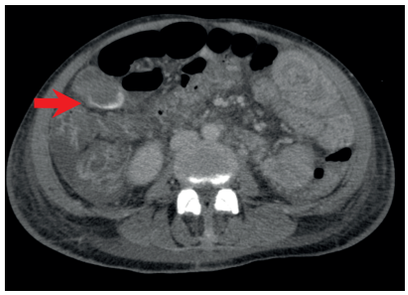
Ultrasound is usually the best imaging modality to start with when assessing gynaecological disorders.



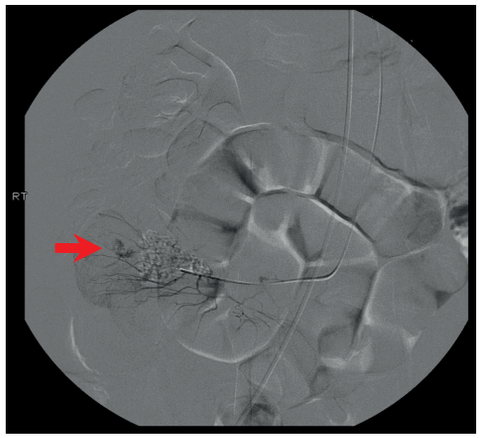
(a)



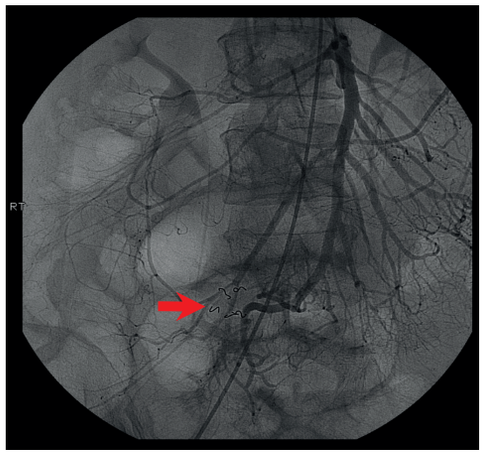
(b)



(c)



(d)



(e)

Figure 14.34 Small bowel haemorrhage. Pre (a), arterial (b) and venous (c) phase CT showing arterial extravasation of contrast in the ileum, which dissipates. Selective mesenteric angiogram (d) locates the bleeding vessel and (e) a superior mesenteric arteriogram post embolisation with coils shows cessation of haemorrhage.

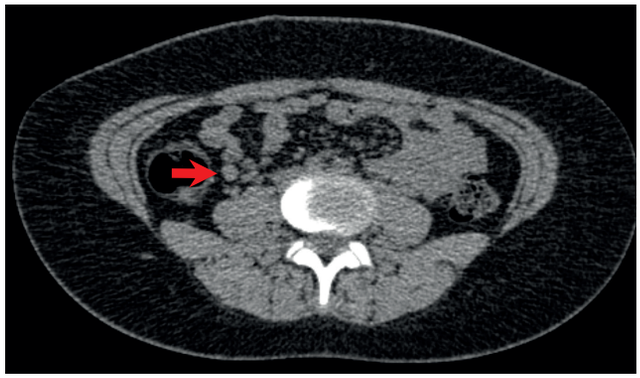


Figure 14.35 Enlarged right iliac fossa lymph nodes in mesenteric adenitis.

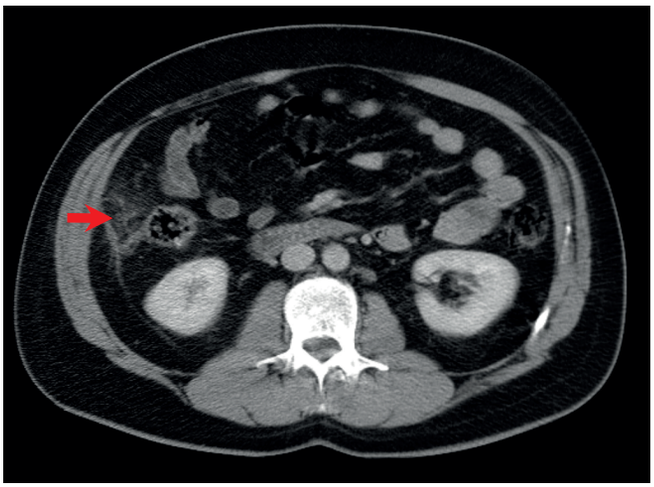


Figure 14.36 Peri-colic inflammation in epiploic appendagitis.

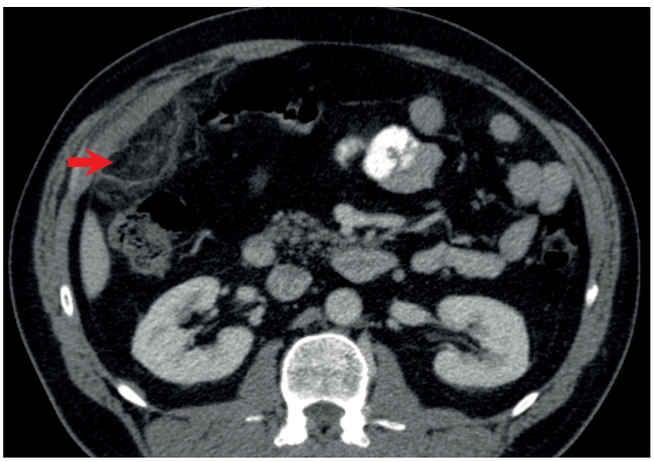


Figure 14.37 Omental infarction.

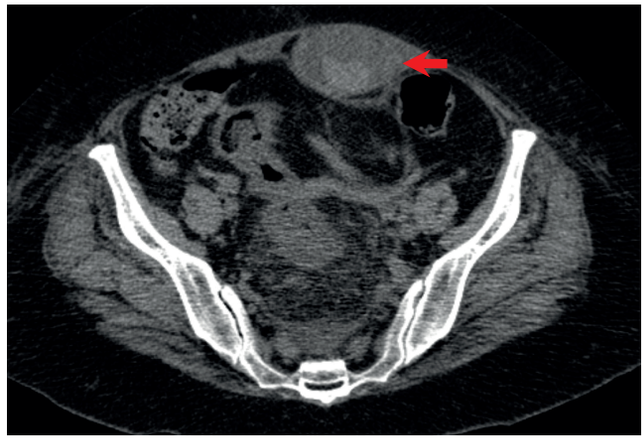


Figure 14.38 Enlargement of the left rectus abdominal muscle with high density haematoma (arrow).

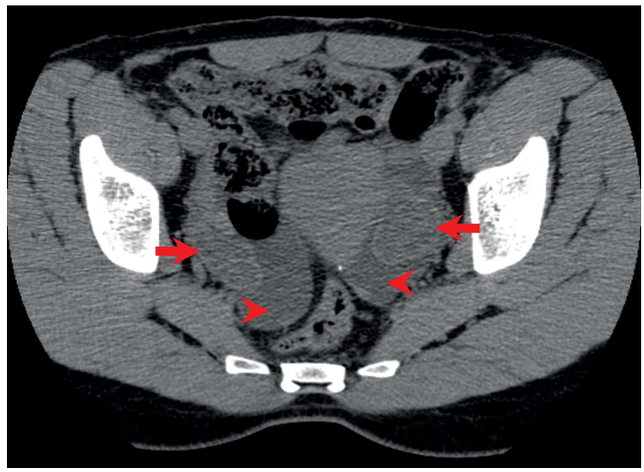


Figure 14.39 Severe pelvic inflammatory disease with bilateral dilated fallopian tubes (pyosalpinx) (arrows) and tubo-ovarian abscesses (arrowheads).

Further Readings

Federle M, Jeffrey RB, Woodward PJ, Borhani A. *Diagnostic Imaging: Abdomen*, 2nd edn. Amirsys 2010. ISBN 978-1-1931884-71-6.

Kellow ZS, MacInnes M, Kurzencwyg D, et al. The role of abdominal radiography in the evaluation of the non-trauma emergency patient. *Radiology* 2008;248(3):887–893.

Lameris W, van Randen A, van Es H, van Heesewijk JP, van Ramshorst B, Bouma WH, et al. Imaging strategies for detection of urgent conditions in patients with acute abdominal pain: diagnostic accuracy study. *BMJ* 2009;26:338. doi: 10.1136/bmj.b2431.

Marincek B, Dondelinger RF (Eds). *Emergency Radiology – Imaging and Intervention*, Springer, 2007. ISBN 978-3-540-26227–5.

Stoker J, van Randen A, Laméris W, Boermeester MA. Imaging patients with acute abdominal pain. *Radiology* 2009;253(1):31–46.

The Royal College of Radiologists. iRefer Guidelines: Making the best use of clinical radiology – Version 7.0.1. Available online at www.irefer.org.uk

CHAPTER 15

Emergency Ultrasound

Tim Fotheringham[1], *Otto Chan*[2] *and Ian Renfrew*[1]

[1]Barts Health NHS Trust, The Royal London Hospital, London, UK
[2]The London Independent Hospital, London, UK

OVERVIEW

- The only imaging modality that is portable and real-time
- Can be used for diagnosis and treatment/intervention
- Quick, easy and safe – no radiation, so therefore safe for children and pregnancy
- MUST BE ADEQUATELY TRAINED BOTH FOR DIAGNOSIS AND INTERVENTION
  - NB Clinicians must therefore be aware of their limitations

Ultrasound (US) is the only imaging modality that is portable and real-time (Figure 15.1). US is now readily available to all clinicians and used widely in all clinical settings. The absence of ionising radiation makes it safe for all patient groups, in particular in children and pregnancy. US offers a quick and easy evaluation to diagnosis and to assist interventions.

Due to its portability, US is the only imaging modality that can be used at the emergency scene and – in addition to plain films – can be used in the emergency room (ER) without needing to move the patient.

US can be used in virtually any clinical setting, BUT operators need to be suitably trained and in particular need to understand their limitations and the limitations of US.

Short, focused training is sufficient for a novice to do a focused assessment with sonography for trauma (FAST), further directed training is necessary to detect aortic abdominal aneurysms (AAA), but specialist training is necessary for its general use in the abdomen, chest and in particular for intervention.

All patient groups presenting to ER can benefit from ultrasound, from the diagnosis of a deep vein thrombosis (DVT) to checking viability of a foetus, to aiding intervention in major trauma (insertion of arterial lines, central lines or chest drains).

Knowledge of the basic principles of US, artefacts and 'knobology' (where the buttons are and what they do!) is invaluable, but beyond the scope of this chapter (Box 15.1).

Box 15.1 **Essential knobs**

- Selection of probes
- Selection of setting (abdomen, vascular, soft tissues . . .)
- Depth
- Focal zone
- Freeze/cine review
- Imaging – print or video

Probes

- Low frequency – abdomen, pelvis and chest
- Medium/high frequency – children, vascular, MSK, neck and scrotum

ABCs systematic assessment – emergency uses

- A – appendicitis, AAA, ascites
- B – bladder
- C – calculi (gallbladder and kidneys), cardiac assessment (asystole), cysts
- D – DVT
- E – effusions/fluid (pleural, pericardial, peritoneal collections),
- F – FAST, foreign body (FB), foetus
- G – gallbladder
- S – soft tissues, skeleton

Appendicits

The classical appearances of appendicitis (Figure 15.2) are a blind ending, dilated thick-walled structure/viscus with an appendicolith. Ancillary features may suggest the diagnosis – aperistaltic small bowel loops, localised fluid and a positive provocation test (pain on direct palpation with the probe). Unfortunately, the normal appendix is rarely visualised in adults and even in children and therefore US cannot reliably exclude the diagnosis.

ABC of Emergency Radiology, Third Edition. Edited by Otto Chan.
© 2013 John Wiley & Sons, Ltd. Published 2013 by John Wiley & Sons, Ltd.



Figure 15.1 Ultrasound machine and probes.

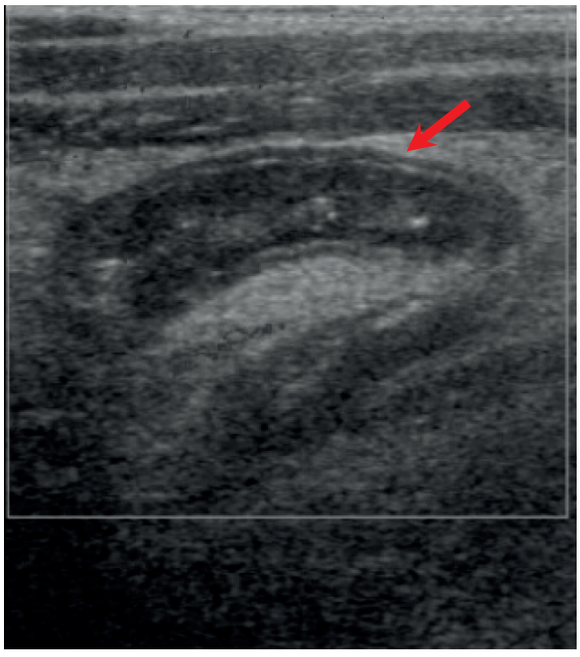
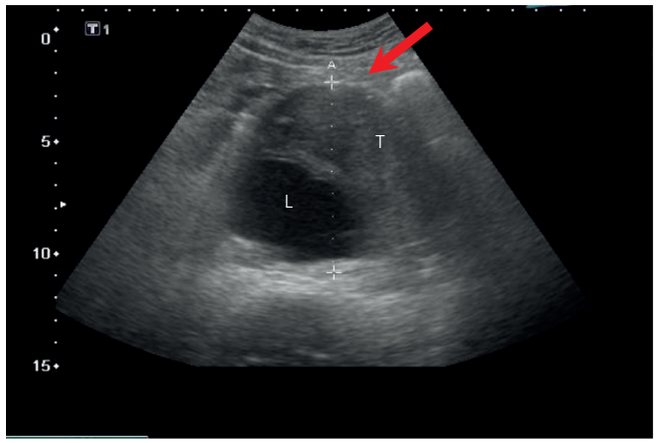
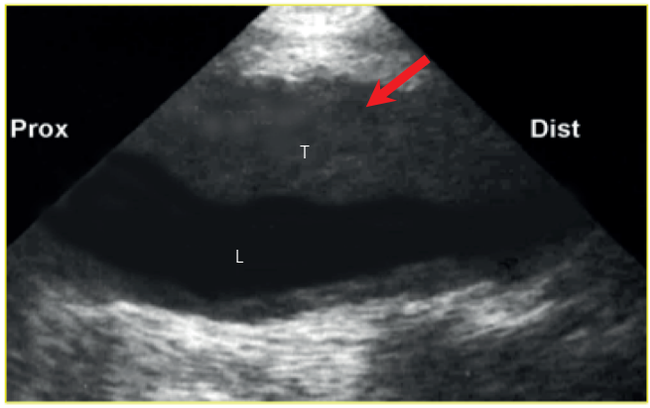


Figure 15.2 Appendicitis. Dilated blind-ending non-compressible thick-walled structure.



(a)



(b)

Figure 15.3 (a) TS and (b) LS ultrasound of abdominal aortic aneurysm. L, lumen; T, thrombus.

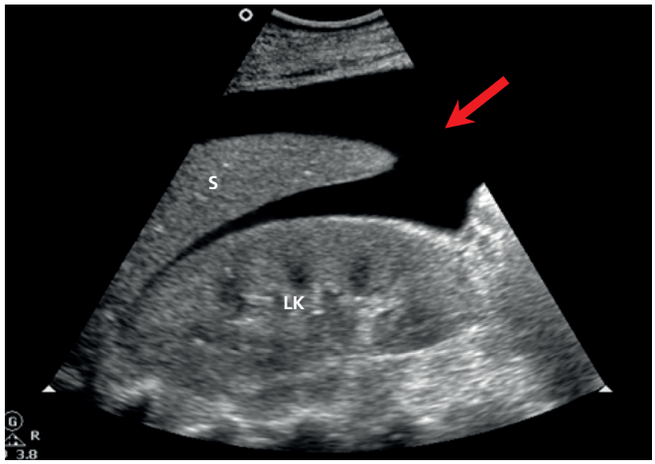


Figure 15.4 Left upper quadrant: ascites with normal spleen (S) and left kidney (LK).

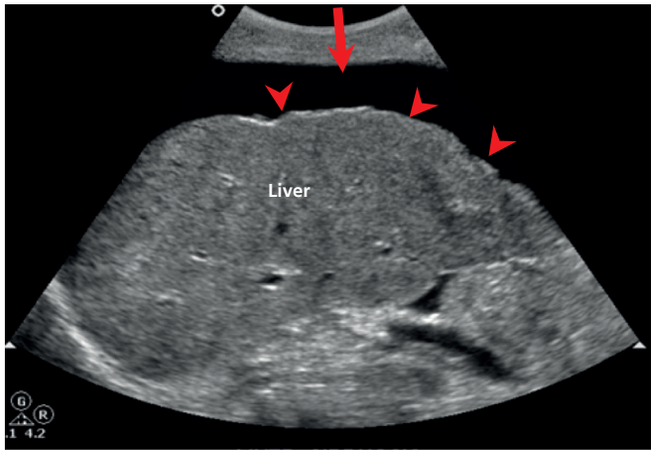


Figure 15.5 Right upper quadrant: ascites with a nodular cirrhotic liver (arrowheads).

Abdominal aortic aneurysm

US reliably detects AAA (Figure 15.3), but cannot be reliably used to exclude a leak. Therefore in the correct clinical setting, CT should be performed if the patient is haemodynamically stable.

Ascites

US can detect even small volumes of intraperitoneal fluid, but is poor at determining the nature of the fluid (blood, pus, fluid) (Figures 15.4 and 15.5).

Bladder

In anuric patients, it can be used to confirm bladder outflow obstruction or renal failure.

Calculi

The presence of a mobile echogenic intraluminal structure with posterior acoustic shadowing is pathognomonic of a gallstone (Figure 15.6).

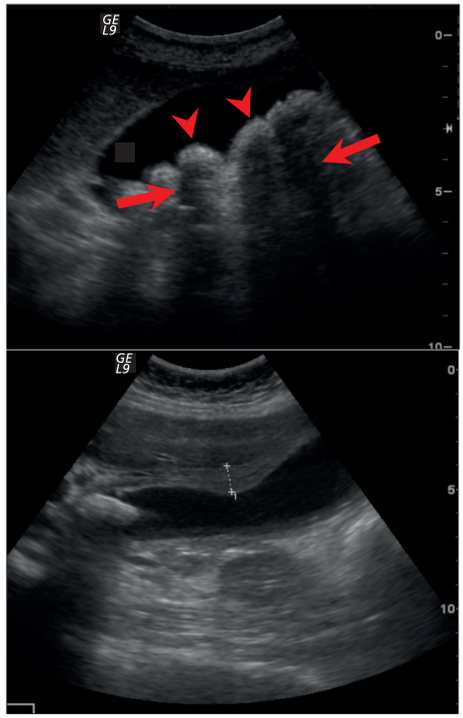


Figure 15.6 Gallstones: echogenic well-defined lesions (arrowheads) with posterior acoustic shadowing (arrows).

Renal calculi and hydronephrosis

The renal calculi can be parenchymal or pelvicalyceal or ureteric; the latter two lead to renal colic and may cause obstruction and therefore a hydronephrosis (Figure 15.7).

Cardiac assessment

In a cardiac arrest situation, US is invaluable to confirm cardiac motion or asystole or a large pericardial effusion.

Cysts – ovarian

Low abdominal pain can be caused by physiological or pathological ovarian cysts (Figure 15.8). Pathological cysts can bleed, undergo torsion or obstruct.

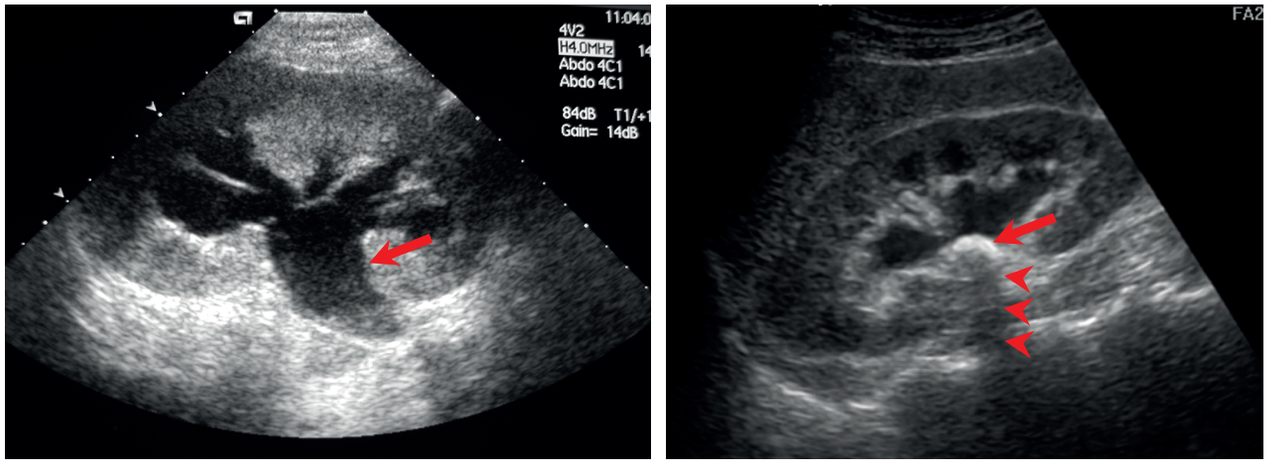
Deep vein thrombosis

All veins should be anechoeic, fully compressible, and show variance with respiration and calf compression that can be seen and detected with Doppler. Clots can be seen as echogenic intraluminal material, which may be obstructive or non-obstructive and not compressible, typically causing distention of the vein (Figure 15.9).

Effusions

Pleural and peritoneal – reliable identification of the diaphragm is essential to determine whether its pleural or inraperitoneal. A pleural effusion or ascites is usually seen as anechoeic fluid, with posterior acoustic enhancement but occasionally may contain echogenic debris (Figures 15.10 and 15.11).

Pericardial (Figure 15.12) – fluid is restricted between the heart and pericardium. A trace of fluid can be a normal finding.



(a) (b)

Figure 15.7 (a) Hydronephrosis: dilated PC system with normal kidney. (b) Renal calculus: PUJ calculus (arrow) with posterior acoustic shadowing (arrowheads) causing proximal dilated PC system.

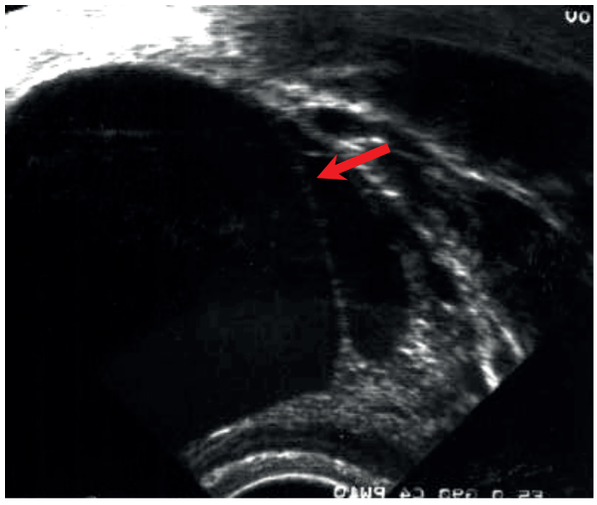


Figure 15.8 Ovarian cyst: a well-defined, thin-walled echofree mass with posterior acoustic enhancement.

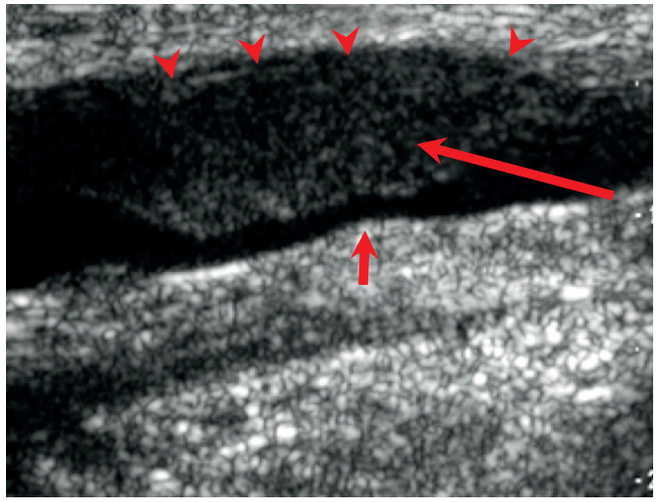
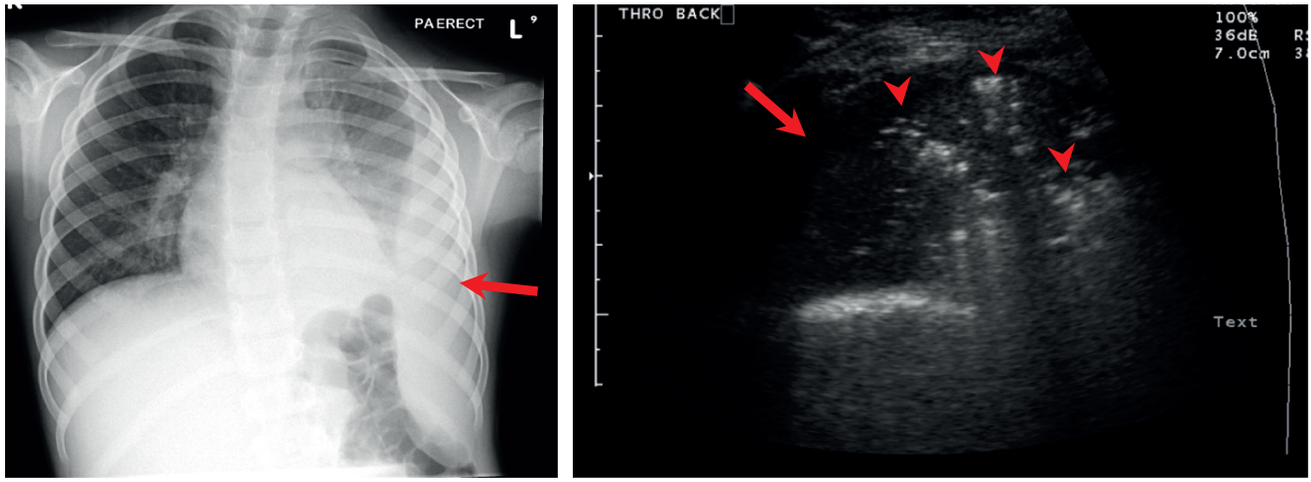


Figure 15.9 DVT: non-compressible echogenic material (red arrow) almost occluding lumen (yellow arrow).



(a) (b)

Figure 15.10 (a) Left pleural empyema on CXR (child). (b) US confirms fluid with echogenic material (arrowheads) consistent with pus.

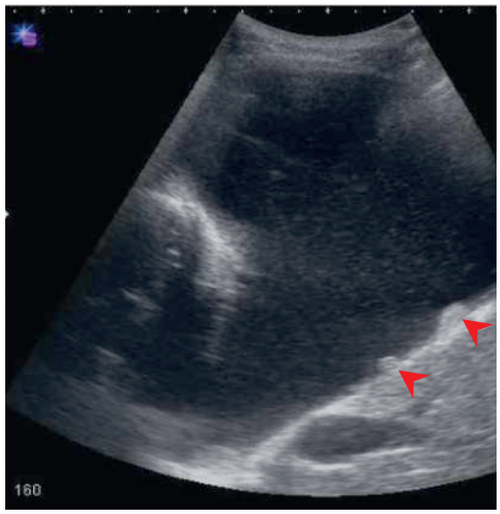


Figure 15.11 Malignant effusion: pleural fluid with pleural metastases (arrowheads).

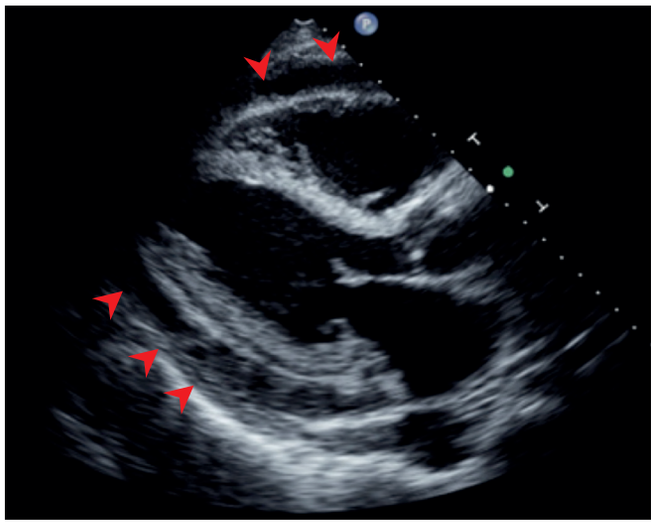


Figure 15.12 Pericardial effusion (arrowheads).

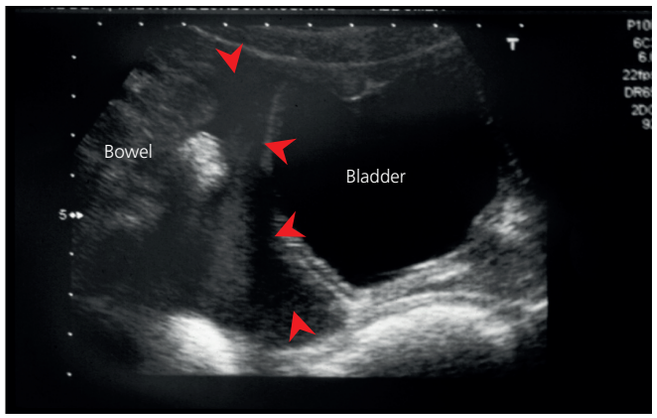


Figure 15.13 FAST: free fluid (arrowheads) in the lower pelvis between bladder and bowel.

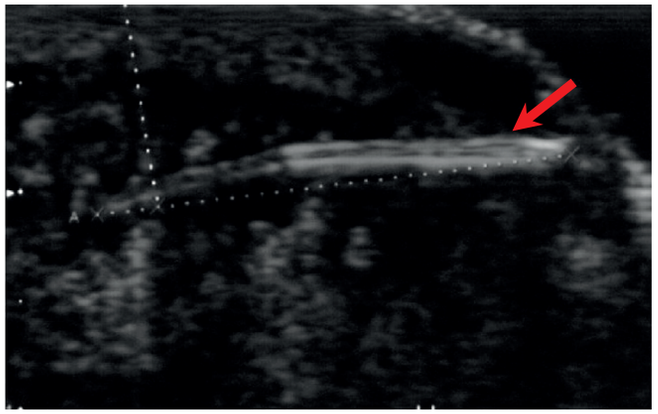


Figure 15.14 Foreign body: irregular linear echogenic structure with no posterior acoustic shadowing consistent with wood splinter FB

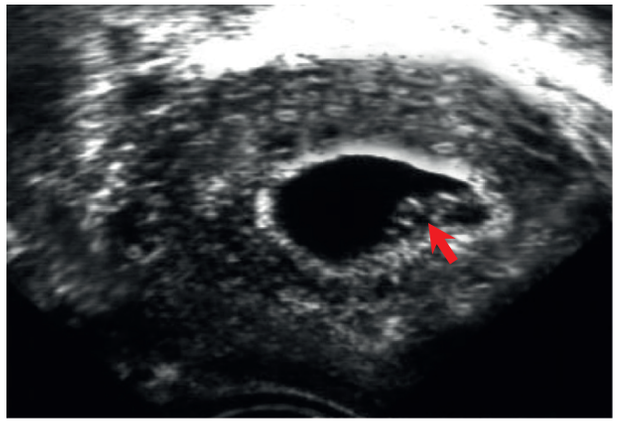


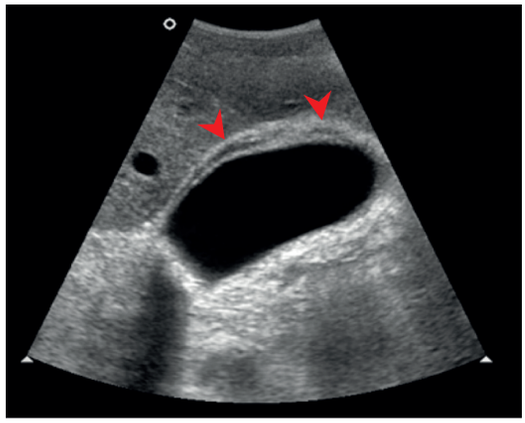
Figure 15.15 Intra-uterine cystic structure with a foetus (arrow) and a visible foetal heart seen on real-time US (gestation 6 weeks).



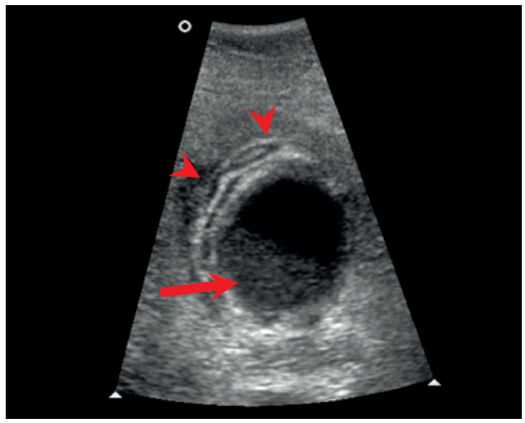
Figure 15.16 Intra-uterine foetus (gestation 12 wks).

FAST

Limited training has been shown to be sufficient for accurate detection of intraperitoneal fluid implying haemorrhage in trauma (Figure 15.13). FAST is now being used in pre-hospital assessment (at scene, ambulance or helicopter) of trauma patients.



(a)



(b)

Figure 15.17 (a) LS and (b) TS of acalculous cholecystitis: thick-walled structure with echopoor rim (arrowheads) and echogenic material (arrow) with no gallstones.

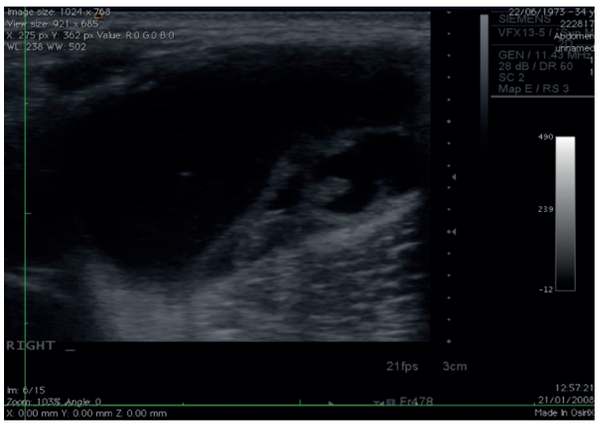
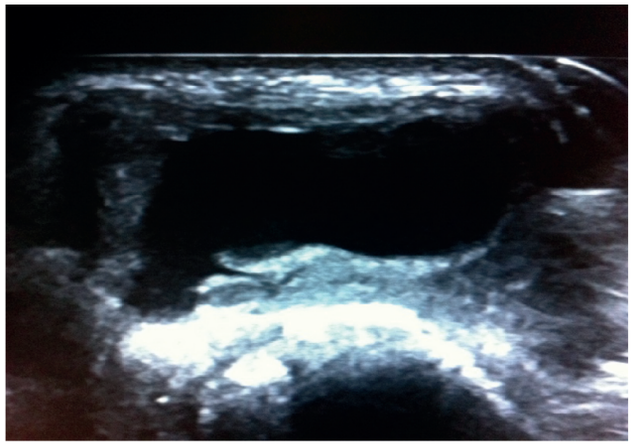


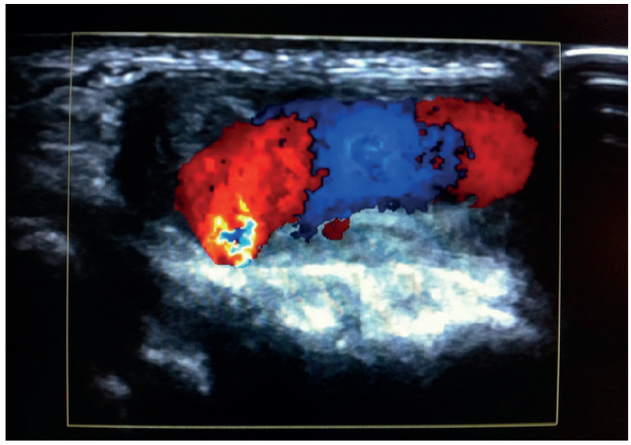
Figure 15.18 Soft tissue abscess: irregular thick-walled mass with echogenic material.

Foreign body

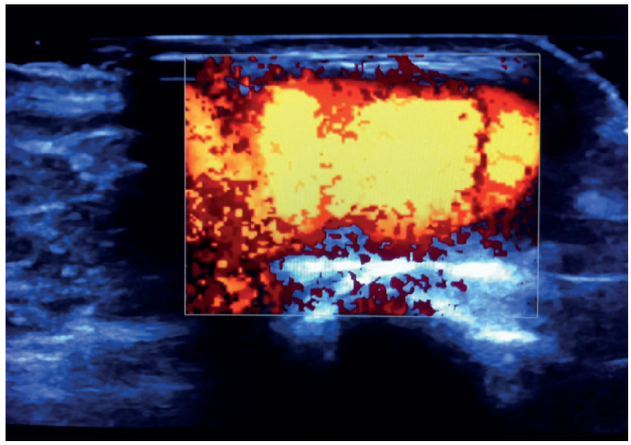
Most FBs can be seen as echogenic material with posterior acoustic shadowing (Figure 15.14). However, if the wound is open or there is gas within the wound, US may be of limited value.



(a)



(b)



(c)

Figure 15.19 Pseudoaneurysm: US of hand following dog bite, with a well-defined thin-walled structure: (a) with a huge amount of colour; (b) power Doppler; (c) signal seen and swirling flow seen on real-time US.

Foetus – viability and ectopic pregnancy

The normal foetus can be seen from about 4 weeks and the foetal heart at 6 weeks. Confirmation of an intrauterine pregnancy is possible with a transabdominal approach with a full bladder (Figures 15.15 and 15.16).

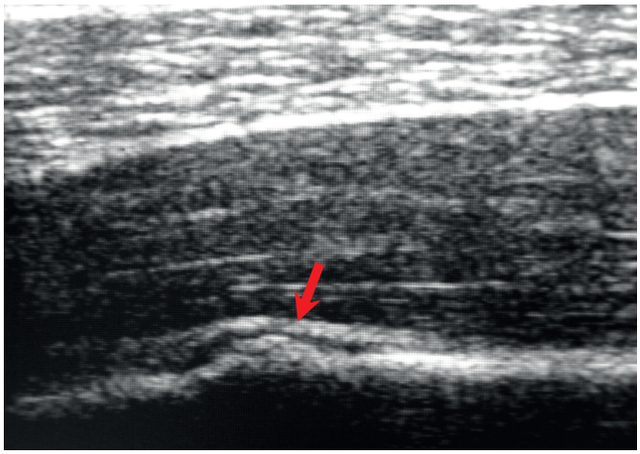


Figure 15.20 Normal CXR with a rib fracture seen on US.

With a positive pregnancy test and an absent intrauterine pregnancy, an ectopic pregnancy should be excluded with a transvaginal US.

Gallbladder – biliary colic, acute cholecystitis and empyema

US can be used to differentiate between biliary colic, cholecystitis and an empyema.

The features depend on seeing a thickened wall (3mms or more) and pericholecystic fluid (acute cholecystitis; Figure 15.17) and debris within the GB (empyema) and a positive provocation test (tenderness directly over the GB).

Soft tissues

Induration, oedema and collections (including haematomas) can be differentiated (Figure 15.18).

In addition, US is widely used in MSK to assess joints, muscles, tendons and ligaments, but not in the emergency room.

Pseudoaneurysm (Figure 15.19) post dog bite seen in the right hand with a well-defined, echofree thick-walled mass with swirling flow seen real-time and confirmed with colour Doppler.

Skeleton

US can show fractures and callus of superficial bones with normal XRs, in particular ribs (Figure 15.20). In children, it may show a periosteal reaction or a fracture not visible on an XR.

Clinical scenarios

Abdominal Pain

- Ascites
- Appendicitis
- Abscess
- Bladder outflow obstruction
- Calculi – gallbladder and kidneys
- Cysts and pregnancy

Breathlessness or Chest Pain

- Pleural effusion
- Pericardial effusion
- Paralysis of diaphragm
- DVTs

Cardiac Arrest

- Cardiac motion – systole or asystole
- Size of IVC – hypovolaemia
- Pneumothorax
- Pleural effusion
- Pericardial effusion
- AAA

Interventions

- Arterial access
- Ascites,
- Abscess
- Bladder outflow obstruction
- Balloon puncture in foleys catheter
- Chest drains for pleural and pericardial collections *
- Central venous access **

*British Thoracic Society recommends.
**NICE guidelines.

Further reading

Brooks A, Connolly J, Chan O. *Ultrasound in Emergency Care*. Blackwell Scientific 2004. ISBN 0-7279-1731-5.

http://guidance.nice.org.uk/TA49

http://www.brit-thoracic.org.uk/clinical-information/pleural-disease/pleural-disease-guidelines-2010.aspx

CHAPTER 16

Emergency Paediatric Radiology

R. J. Paul Smith[1], *Rosy Jalan*[1] *and Marina J. Easty*[2]

[1]Barts Health NHS Trust, The Royal London Hospital, London, UK
[2]Great Ormond Street Hospital, London, UK

OVERVIEW

- The common types of paediatric emergency differ with the age of the presenting child
- Paediatric fractures exhibit different types and patterns to adults
- Ultrasound is often the first line investigation of paediatric abdominal emergencies
- Be vigilant for possible non-accidental injury
- Minimise radiation exposure wherever possible

Children make up about one-third of all patients who attend emergency departments (Box 16.1). Skeletal injuries in infants (<1 year), children (>1 year), adolescents and adults all differ greatly.

Box 16.1 **Definitions used in paediatric medicine**

- Premature infant: ≤37 weeks' gestation
- Neonate: birth to 28 days old
- Infant: 1 month–1 year old
- Toddler: 1–3 years old
- Child: ≥3 years old

Children are more agile, more flexible and lighter than adults. When they fall, the forces generated are smaller. Boys sustain more injuries than girls, and most injuries occur at home or playing sport at school (Box 16.2).

Box 16.2 **Emergency paediatrics**

- Children often present at accident and emergency departments
- Boys present more commonly than girls
- Seasonal variations in the type of injury occur
- Children have different problems to adults

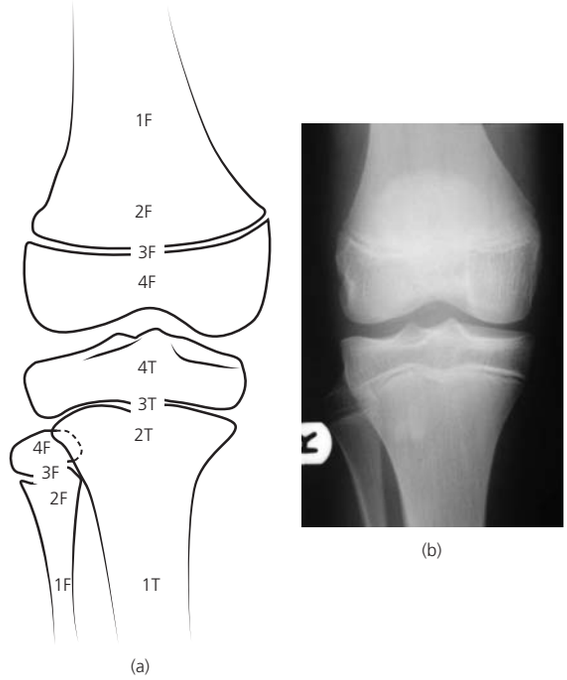


Figure 16.1 Anteroposterior view of the right knee in a child.

Fractures in infants are rare. Toddlers tend to sustain skull and tibial fractures, whereas distal forearm, ankle and foot injuries are often seen in schoolchildren.

Minimising radiation exposure is an important principle in medical imaging. Children have an increased sensitivity to the risk posed from X-ray radiography. As such, any request for radiographs should give a clear indication and ask a relevant question.

This chapter gives an overview of common paediatric fractures and other radiological emergencies (Figure 16.1). It outlines a systematic approach of how to interpret the relevant radiographs. Common fractures in the paediatric population will be discussed, followed by a list of common abdominal and other childhood emergencies.

Fractures

Fractures in children are different to those in adults because of anatomical, biomechanical, and physiological differences.

ABC of Emergency Radiology, Third Edition. Edited by Otto Chan.
© 2013 John Wiley & Sons, Ltd. Published 2013 by John Wiley & Sons, Ltd.

In addition, a range of fractures is caused in children, because paediatric bones are softer and more pliable than adult bones.

Anatomy

At birth, many bones or the ends of bones are not visible. In time, ossification centres appear (sometimes several); they enlarge and coalesce, eventually fusing to the adjacent bone. The time interval between these changes varies from bone to bone. Predictable timescales vary slightly between boys and girls, and between different ethnic origins (Figure 16.2).

The physis (growth plate) is avascular after infancy. Damage to this area is shown radiographically by changes in its width or changes in adjacent bone. Damage to the epiphyseal vessels leads to death of the physeal chondrocytes and growth arrest.

The periosteum in the paediatric population is thick and strong. The attachment of the periosteum to the shaft of the bone is loose in children, and so periosteal reactions and subperiosteal collections are common.

Biomechanical differences

Paediatric bones are more porous than adult bones, and they can bend more without breaking. The weak point lies at the physis, and so physeal fractures are common before bony fusion. The thick, strong periosteum resists displacement of the fracture (unless it is torn).



2

Figure 16.2 Radiographs of the wrist in children at 18 months (top left), 3 years (top right), 6 years (bottom left), and 12 years (bottom right).

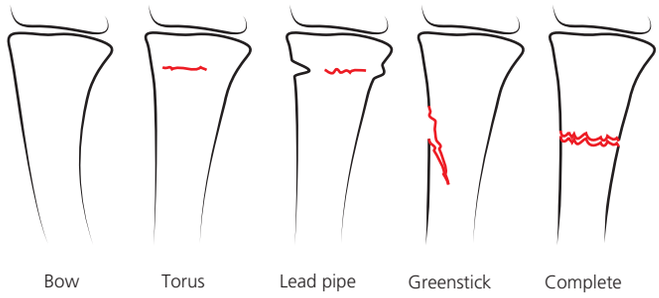


Figure 16.3 Types of fracture.

Physiological differences

Fractures heal faster in children than in adults, and remodelling is quicker because children have rapid bone turnover. Normal alignment occurs in the plane of motion of the adjacent joint. Fracture healing results in longitudinal overgrowth, therefore in long bone diaphyseal fractures, overlap (up to 2 cm of bone) is accepted. The fracture should be described like an adult fracture – for example, transverse, oblique, comminuted, or compound. After the age of 12 years, fractures are treated more like those in the adult population due to slower remodelling.

Types of fracture

Types of fracture are shown in Figure 16.3.

Complete diaphyseal fractures – The fracture site should be examined for an underlying bony abnormality, such as a bone cyst or generalised demineralisation. For infants and the non-ambulant, a careful history should be taken to exclude non-accidental injury.

Torus or buckle fractures – Failure on the compression side of a bending bone causes a torus or buckle fracture – an outward buckling of the cortex margin (torus is a latin term for bulge or swelling). Torus fractures usually occur near the metaphysis, where the cortex is thinnest. They often occur at the distal radius due to a fall on an outstretched hand (Figure 16.4).

Greenstick fracture – When a bone is bent beyond its limits, a greenstick fracture is produced. It is caused by the bone bending on the compression side, with complete failure on the tension side of the bone. The fracture may later hinge open because of muscle pull (Figure 16.5).

Bowing injuries – caused by acute plastic deformation of the bone secondary to longitudinal stress. An increase in longitudinal compression leads to bowing, buckle fractures, lead pipe fractures (Figure 16.6), greenstick fractures, and complete fractures.

Physeal fractures

Salter–Harris classification

The standard classification for physeal injuries is that of Salter and Harris (Box 16.3; Figure 16.7). This classification divides the

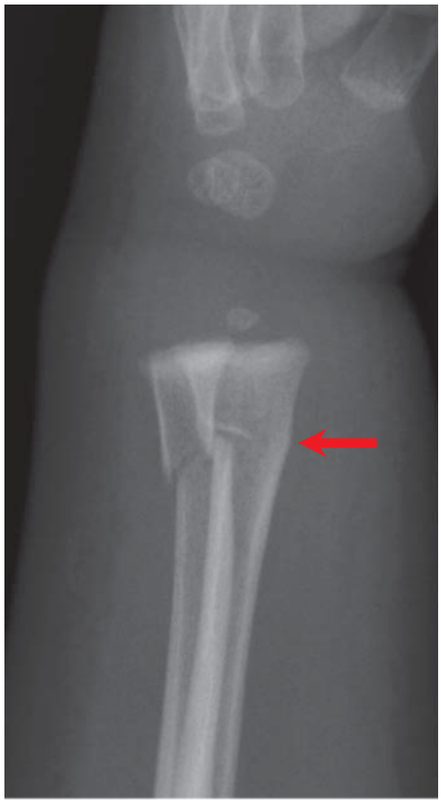


Figure 16.4 Lead pipe fracture of the distal radius (arrow) and complete fracture of the distal ulna.

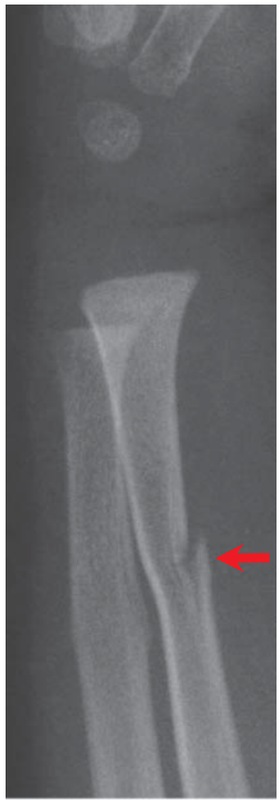


Figure 16.5 Greenstick fracture of the mid radius (arrow).

common types (I–IV) according to the course of the fracture through the physis and the adjacent epiphyseal and metaphyseal bone. Type V injuries are rare, may be occult radiographically, and are caused by compression of the physeal cartilage (Box 16.4).

Box 16.3 **Salter–Harris classification**

- Type I – **S**lipped or **s**eparated
- Type II – **A**bove
- Type II – **L**ower
- Type IV – **T**hrough
- Type V – **E**venly **r**ammed

Box 16.4 **Common sites of physeal injuries**

Type I (incidence 6% of Salter–Harris fractures)

- Common locations – proximal humerus, distal humerus, proximal femur, distal tibia, and distal fibula

Type II (incidence 75% of Salter–Harris fractures)

- Common locations – distal radius, distal tibia, distal fibula, distal femur, distal ulna, and phalanges

Type III (incidence 8% of Salter–Harris fractures)

- Common locations – distal tibia, proximal tibia, and distal femur

Type IV (incidence 10% of Salter–Harris fractures)

- Common locations – distal humerus, and distal tibia

Type V (incidence 1% of Salter–Harris fractures)

- Common locations – ankle and knee

Type I

These are caused by a shearing stress through the physis (Figure 16.8). Most apophyseal injuries and slipped upper femoral epiphyses are type I fractures. Neonates may sustain these fractures at the proximal humerus. In the prepubertal child, a supination-inversion injury of the ankle may result in a type I fracture through the distal fibula. Invariably, this fracture will be reduced at the time of presentation and radiographical assessment. Type I fractures have a good prognosis.

Type II

These are the most common physeal fractures (75% of physeal fractures). The avulsion or shearing force fractures the physis and extends into the metaphysis (Figure 16.9). Radiographs show a triangular metaphyseal fracture known as the Thurston–Holland fragment. Between one-third and one-half of all type II injuries involve the distal radius. Reduction of the fracture is usually uncomplicated, and these injuries have a good prognosis.



Figure 16.6 Torus fracture of the distal radius (arrow).

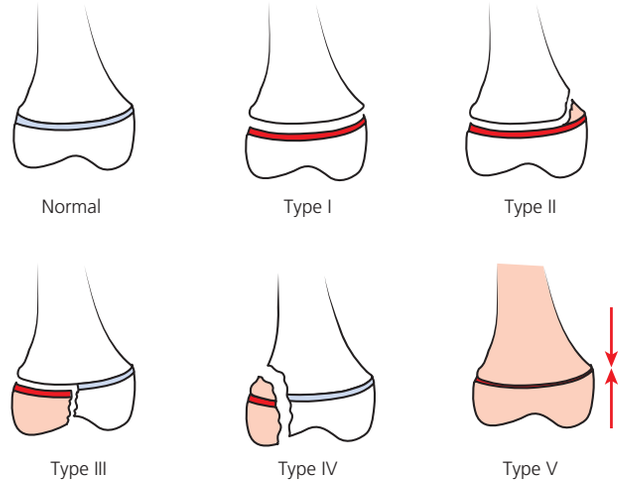


Figure 16.7 Salter–Harris classification for physical injuries.

Type III

Type III injuries are partly intra-articular, with splitting of the epiphysis and a transverse fracture through the physis (Figure 16.10). As they involve all layers of the physis, they cause growth arrest. Type III injuries occur in adolescents about the time of closure of the physis and they often require operative reduction to prevent displacement.

Type IV

These injuries cross the epiphysis, physis and metaphysis. They are caused by a longitudinally orientated splitting force, and they usually arise in the distal humerus or distal tibia. These injuries generally require open reduction to oppose the fracture fragments. Consequent angulation and leg length abnormalities may occur.



Figure 16.8 Salter–Harris type I fracture of the distal phalanx of the ring finger. Compare this with the normal epiphysis of the neighbouring digit.



Figure 16.9 Salter–Harris type II fracture of the distal tibial metaphysis (arrow). There is also a transverse fracture of distal fibula.

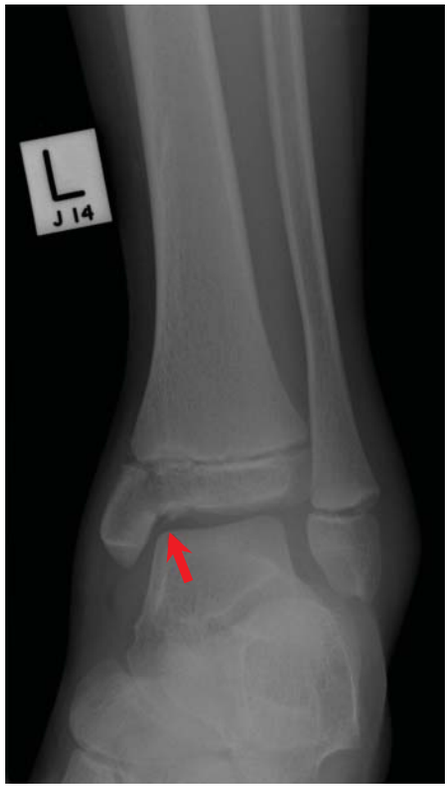


Figure 16.10 Salter–Harris type III fracture of distal tibial epiphyses (arrow).

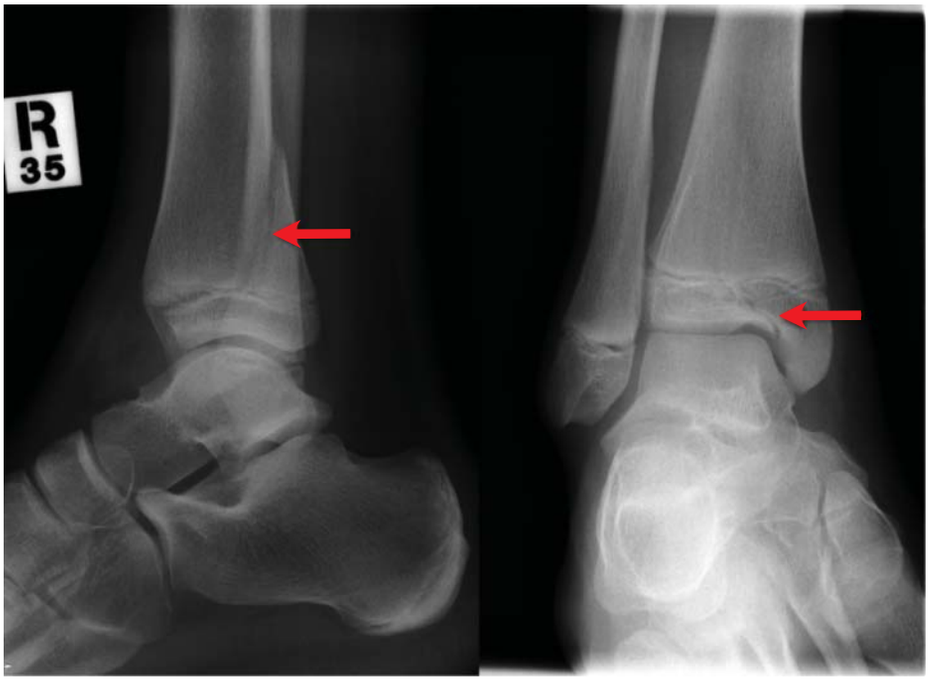


Figure 16.11 Salter–Harris type IV fracture (arrows) through the distal tibial metaphysis (lateral view) and epiphysis (AP view).



Figure 16.12 The calcaneal apophysis is often fragmented as part of normal variation and should not be mistaken for a fracture.

Type V

Type V injuries are often diagnosed in retrospect, when growth arrest occurs after the injury. They are caused by a substantial loading or compressive force that damages the vascular supply and germinal cells of the growth plate (Figure 16.11). Most isolated type V injuries occur in the ankle or knee.

Common pitfalls

Apophyses may be irregular and fragmented as part of natural variation, leading to a mistaken diagnosis of a fracture (Figure 16.12).

Elbow injuries

Injuries of the three bones around the elbow are the most common fractures seen in infancy and childhood. There are six secondary ossification centres around the elbow (CRITOL, or CRITOE).

Fracture types include supracondylar fractures, epicondyle fractures and fractures and dislocations of the radial head. The frequency of the fracture types vary with the age of the child and some have specific radiographic signs (Box 16.5).

Box 16.5 **Average age of appearance of ossification centres (CRITOL)***

- **C**apitellum – 12 months
- **R**adial head – 3–6 years
- **I**nternal epicondyle – 4–7 years
- **T**rochlear – 7–10 years
- **O**lecranon – 6–10 years
- **L**ateral or external epicondyle – 11–14 years

*Appear earlier in girls

Evaluation of the elbow radiograph, and description of the paediatric ossification centres is dealt with in detail in Chapter 4 'Elbow' and will not be reiterated here.

Forearm fractures

These include Monteggia fractures and Galeazzi fractures. A Monteggia fracture is a fracture of the proximal to the middle third of the shaft of the ulna with a dislocated radial head. Care must be taken when assessing apparent isolated ulna fractures, so that a radial head dislocation is excluded. Galeazzi fractures are rare in children. The radius is fractured and dislocation of the distal radio-ulnar joint is present.

Monteggia and Galeazzi's fractures are described in chapter 3 'Wrist'

Painful hips

Perthes disease (Legg-Calve-Perthes disease) occurs commonly in Caucasian boys, with a male: female sex ratio of 4:1. Bilateral disease is present in up to 13% of patients who present with Perthes disease. The age of presentation ranges from 3–12 years, with children typically presenting at 5–8 years. Girls present at a younger age. Children with Perthes disease invariably have delayed bone age. They have pain in the hip, groin, thigh, or knee, and they have limited internal rotation.

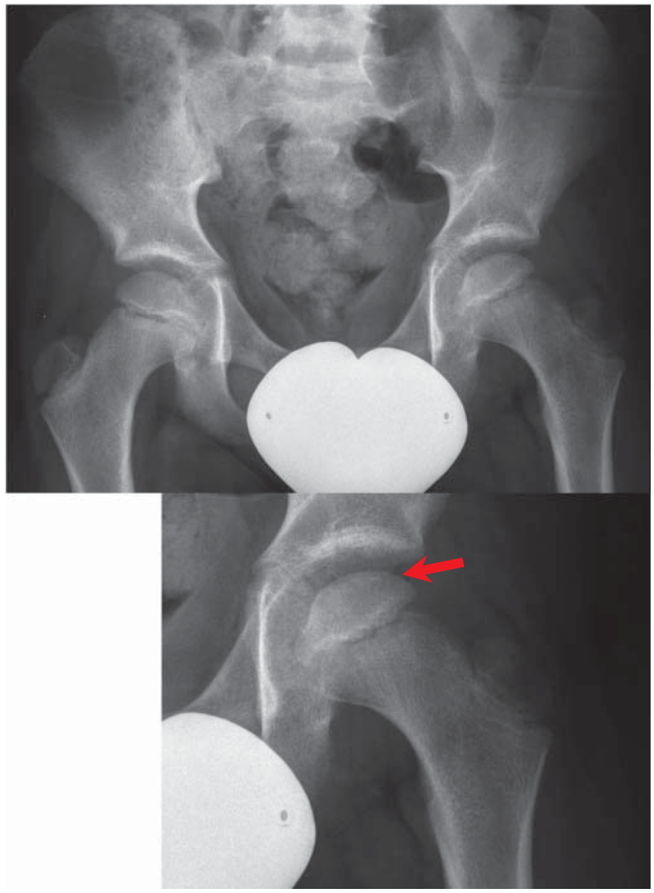


Figure 16.13 Early Perthes disease of the left femoral head – note the subchondral lucency of the epiphysis(arrow)

Perthes disease is idiopathic avascular necrosis of the femoral capital epiphysis. The disease sometimes occurs after trauma or an effusion. The cause of Perthes disease, however, is not known.

The typical radiological findings depend on the stage of the disease. Early findings may show a small femoral capital epiphysis with a subchondral lucency (Figure 16.13). Magnetic resonance imaging and scintigraphy of the hip may pick up early changes better than plain radiography. Marrow oedema may be seen on a magnetic resonance image and absent radionuclide uptake in the affected epiphysis in the bone scan (Figure 16.14). Findings on plain radiography that occur later are fragmentation, flattening, and sclerosis of the femoral capital epiphysis (Figure 16.15). Coxa magna may also develop during the reparative stage. Treatment may be minimal or simply rest. The aim is to prevent the hip subluxing, prevent pain, and minimise degenerative disease.

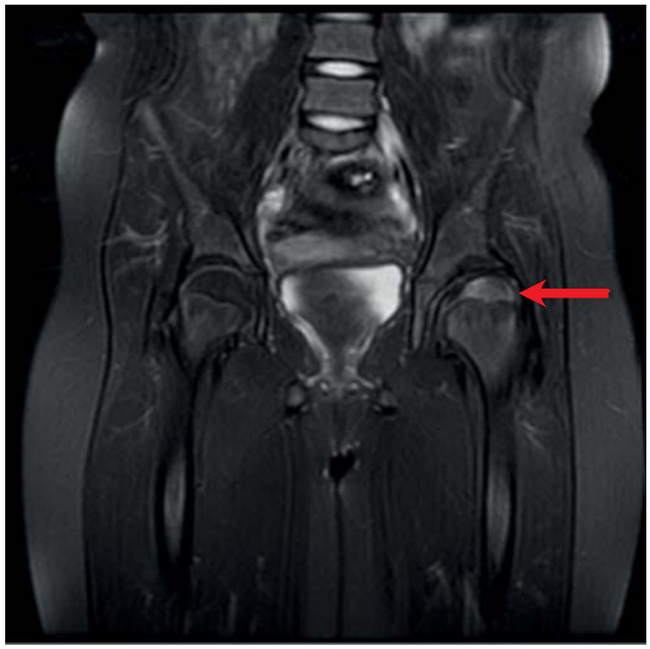


Figure 16.14 Coronal magnetic resonance T2 weighted fat suppressed reconstruction of the hips – note the increase in signal in the left femoral epiphysis (arrow) indicating marrow oedema consistent with early Perthes disease.

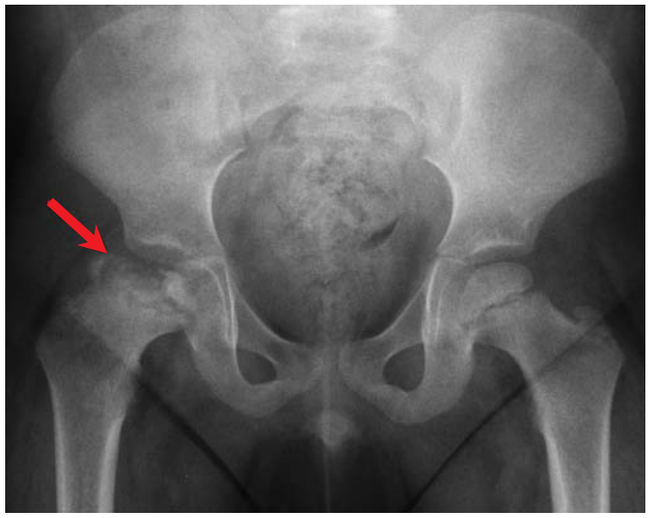


Figure 16.15 Late changes of Perthes disease of the right femur- note the flattening, fragmentation and sclerosis of the capital epiphysis (arrow).

Slipped upper femoral epiphysis

The male:female ratio is 2.5:1. The age of presentation is 12–15 years in boys and 10–13 years in girls. There may be familial cases of slipped upper femoral epiphysis (SUFE).

Children with SUFE are usually overweight or tall for their age and have some delay in skeletal maturation. Half of affected patients give a history of serious trauma. The most common presentation is hip pain and limp, but 25% of patients complain of knee pain. Bilateral slip occurs in 20–32% of patients, and more commonly in girls.

Slipped upper femoral epiphysis is a Salter–Harris type I injury. The initial imaging is an anteroposterior pelvic radiograph and a frog's leg lateral view of both hips (Figure 16.16).

The imaging findings may be subtle on the anteroposterior projection. The slip is initially posterior and therefore the frog's leg lateral view is essential, as only 75% of patients have a significant medial component to the slip.

The frontal view shows osteopenia of the affected femur. The physis may be wide. The metaphyseal margin of the physis is usually blurred. A line drawn tangential to the lateral femoral neck should bisect the femoral capital epiphysis, so that about one sixth of the diameter of the femoral capital epiphysis is lateral to this line. The epiphyseal height is reduced because of the posterior slip. In chronic slip, callus formation may be seen.

Treatment is to fix the hip to prevent further slip. The hip is pinned in situ, because realignment may lead to avascular necrosis.

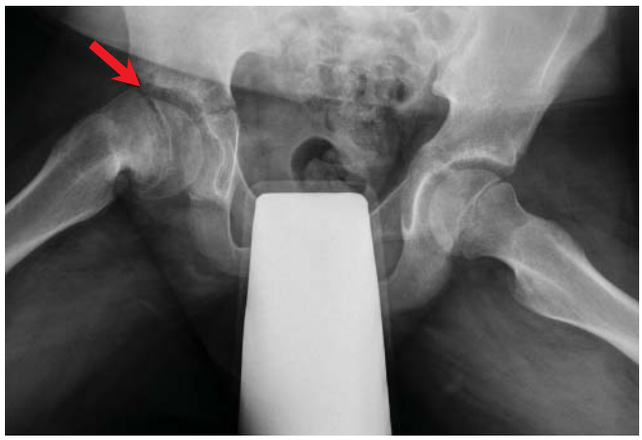


Figure 16.16 Frog's leg lateral view of the hips shows slip of the right femoral epiphysis inferomedially (arrow) and blurring of the metaphyseal margin.

Septic arthritis

Fever, pain, a raised white cell count, and raised levels of acute phase proteins may increase suspicion of septic arthritis. An ultrasound scan of the hip follows the pelvic radiograph (Figure 16.17). The findings on the plain film may be subtle and include osteopenia

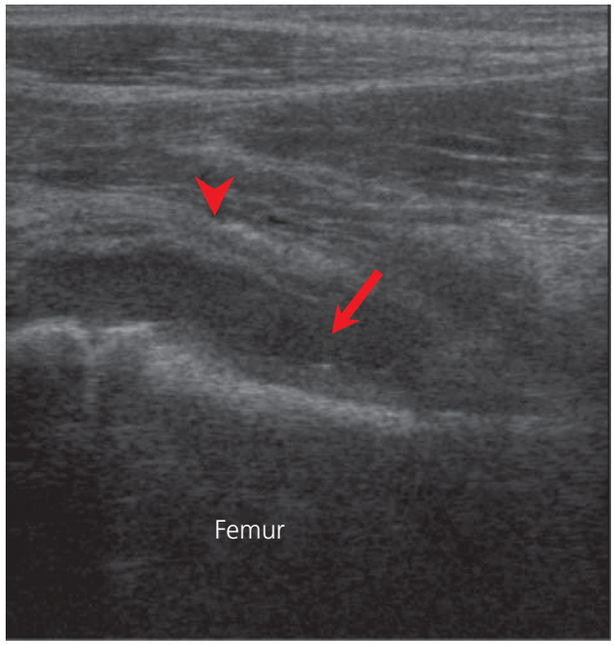


Figure 16.17 An ultrasound image of septic arthritis in a 9-year-old girl taken in the sagittal plane along the long axis of the femur (superior to the right). The thickened joint capsule (arrowhead) is bowed by a joint effusion (arrow).

of the femur and bowing of the gluteus fat pad. The femoral head may be displaced laterally, with widening of the medial joint space caused by accumulated fluid. The hip joint is then imaged in the sagittal plane by ultrasonography, with comparison views of the unaffected side (Figure 16.18). Pus in the joint will cause bowing of the capsule, and debris may be seen in the fluid. Treatment is surgical washout of the affected joint.



Figure 16.18 A follow-up gadolinium-enhanced magnetic resonance scan 2 weeks later for the same child as in Figure 16.17 demonstrates avid enhancement of the thickened joint capsule on this T1 fat suppressed coronal image. Note patchy enhancement of the underlying bone. The child developed osteomyelitis of the femoral head.

Avulsion fractures around the hips

Avulsion fractures around the pelvic bones are common in children. Common sites are the anterior superior iliac spine (ASIS), the anterior inferior iliac spine (AIIS), and the ischial tuberosity. Plain films, and careful clinical examination, will usually identify these injuries (Figures 16.19 and 16.20).



Figure 16.19 Right anterior inferior iliac spine avulsion injury (arrow).



Figure 16.20 Left anterior superior iliac spine avulsion injury (arrow).

Toddler's fracture

This is a non-displaced oblique or spiral fracture of the midshaft of the tibia often sustained as toddler's begin to walk (Figure 16.21). Presentation may be with failure to bear weight on the leg or failure to continue to walk.

Non-accidental injury

Skeletal presentations of non-accidental injury tend to occur in children who cannot talk, hence 50% occur before the age of one year and 80% before the age of two years. In 50% of proven cases of non-accidental injury, the skeletal survey is normal.



Figure 16.21 Minimally displaced spiral fracture of the midshaft of the right femur (arrow) – a toddler's fracture.

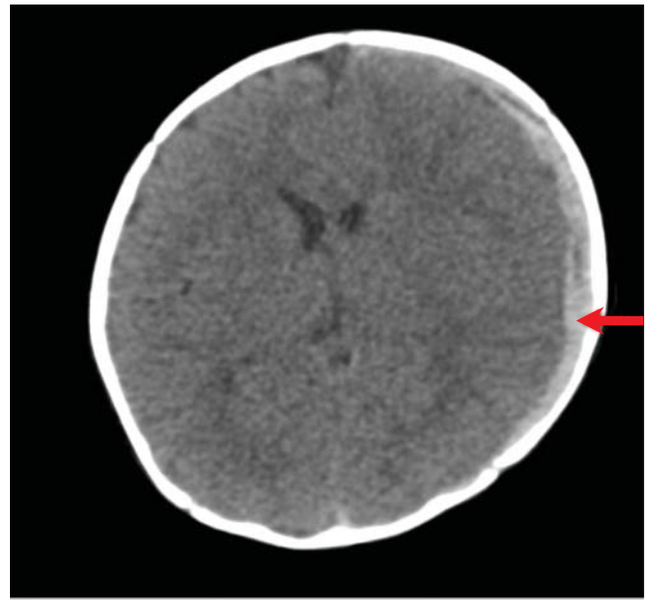


Figure 16.22 CT axial reconstruction of the head in an 11-year-old child demonstrating an acute subdural haematoma (arrow).

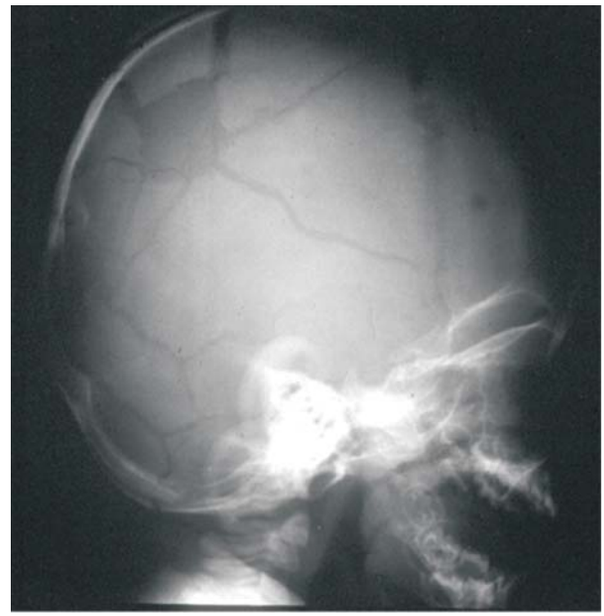


Figure 16.23 Complex skull fracture in non-accidental injury.

Injuries with a delayed presentation, an unlikely explanation, a changing history, an unusual mechanism, or multiple fractures of differing ages should raise the suspicion of non-accidental injury. The importance of taking an accurate history in these cases cannot be overstated. The height of the fall, mechanism of the fall, the leading part involved and the surface onto which the child fell all need to be ascertained, as does the exact timing of the injury. Remember that a fall from a bed onto a carpeted floor usually will not lead to a fracture in a child with normal bones. Retinal haemorrhages caused by shaking are an important sign in non-accidental injury, as are marks on the skin, such as bruises and burns.

Many battered children present with skull fractures and underlying subdural haematomas. An unexplained skull fracture, particularly one that crosses sutures, or a diastased fracture are suggestive of non-accidental injury. A computed tomography scan of the brain will show intracerebral injuries (Figure 16.22 and 16.23).

The classic fractures in non-accidental injury are metaphyseal corner fractures, caused by violent shaking or twisting of the baby; however, less than 50% of babies present with these fractures. They may present with other injuries, such as spiral or oblique fractures of the long bones, soft tissue injuries, or abdominal injuries (pancreatic and duodenal injuries). In babies younger than one year, an isolated long bone fracture should be considered suggestive of non-accidental injury, and a skeletal survey may be warranted (Box 16.6; Figure 16.24).

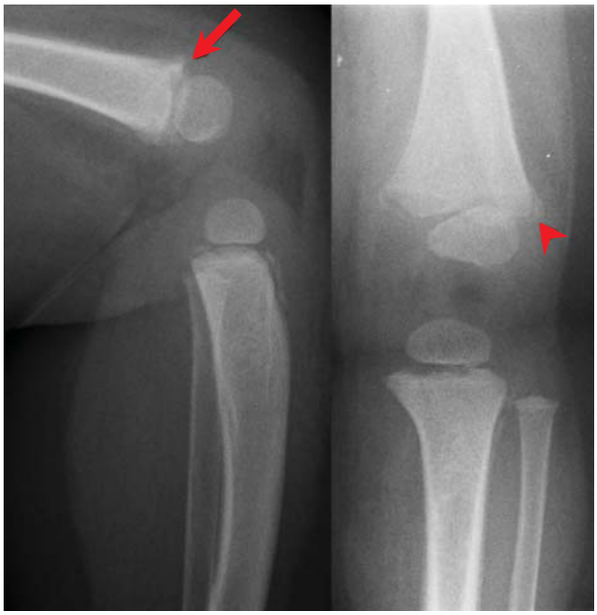


Figure 16.24 Left image shows a metaphyseal corner fractures of the distal femur (arrow) and proximal tibia. Right image demonstrates a bucket handle fracture of the distal femur (arrowhead).

Box 16.6 **Skeletal survey for non-accidental injury**

- Skull radiograph – anteroposterior and lateral views, and Townes if an occipital fracture is suspected
- Lateral view of the whole spine
- Chest radiograph – repeat in 10 days
- Oblique views of the ribs
- Anteroposterior view of abdomen and pelvis
- Frontal views of arms and hands
- Frontal views of legs and feet
- Computed tomography scan of the brain

Note that lateral views of fractured bones are also advised

Rib, clavicular, spine, pelvis, and scapular fractures may all be seen in non-accidental injury. Rib fractures, particularly posterior fractures, are highly suggestive of non-accidental injury, although lateral and anterior fractures are also common in non-accidental injury (Figure 16.25). They result from squeezing the child. Anterior fractures occur by squeezing and shaking the child and are caused by costochondral separation. The fractures are seen best when callus forms, so a repeat chest radiograph is advised 10 days after presentation. Anterior rib fractures may be associated with intra-abdominal injury.

Chest emergencies

Airway obstruction

Inhaled foreign body

An expiratory radiograph is advised to reveal air trapping. The chest radiograph may show an area of consolidation, collapse, or air trapping, with a transradiant lung. The foreign body may be visible.

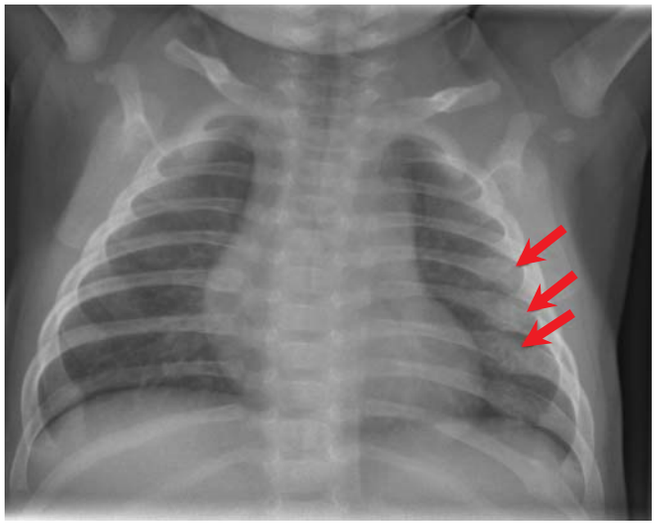


Figure 16.25 Chest radiograph demonstrating multiple, healing, left posterior rib fractures (arrows).

The most common cause of partial upper airway obstruction in young children is acute laryngotracheobronchitis or croup. With a peak incidence in 1 year olds, this is often a clinical diagnosis, but upper airway radiographs may occasionally show subglottic narrowing (not routinely performed).

Other chest emergencies

Asthma – No radiological abnormality is seen, except a degree of air trapping with large volume lungs. It is important to exclude a pneumothorax.

Pneumonia – May present as a focal area of consolidation (air-space shadowing).

Viral lung infections – may cause oedema of the bronchial walls, demonstrated on the chest radiograph as wall thickening radiating from the hila (Figure 16.26).

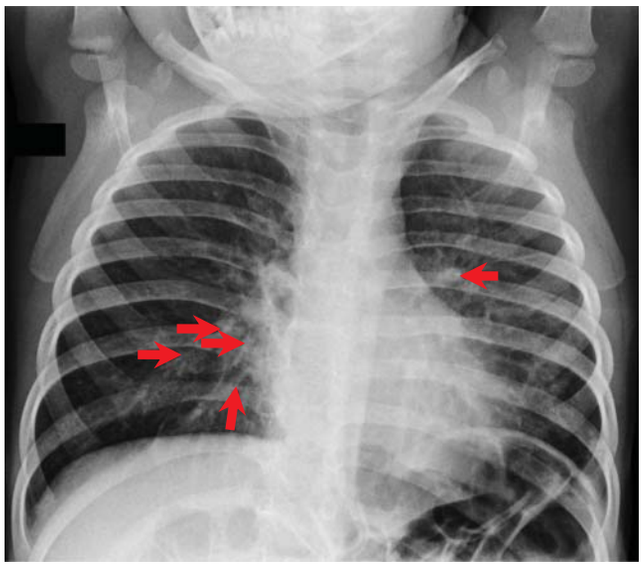


Figure 16.26 Chest radiograph demonstrating bilateral bronchial wall thickening (arrows) consistent with a viral chest infection.

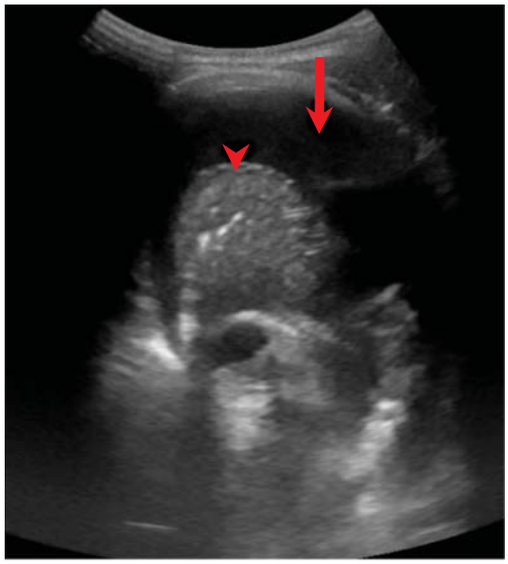


Figure 16.27 This ultrasound scan taken in an axial plane between the ribs demonstrates a large pleural effusion (arrow), dark on the image, and underlying collapsed lung (arrowhead) bright on the image.

Pleural empyema – An ultrasound scan will show the pleural effusion and the presence of loculations (Figure 16.27). Drainage guided by ultrasonography is advocated.

Pneumothorax – May be difficult to diagnose if the chest radiograph has been taken supine.

Cardiac abnormalities – Chest radiograph may show cardiac enlargement, a right sided aortic arch, elevation of the cardiac apex, or selective chamber enlargement, but it is often unhelpful. Referral to specialists for echocardiography is advised for further management.

Oesophageal atresia and tracheo-oesophageal atresia – These children often present with respiratory symptoms for example choking on feeds. The chest radiograph may show atelectasis or airspace disease should aspiration have occurred.

> If the patient has a history of an inhaled foreign body, the chest film may be normal and a bronchoscopy may be required

Acute abdominal emergencies

Clinical examination and ultrasonography are the initial investigations for children with acute abdominal emergencies (Figures 16.28 and 16.29). Unlike adults, computed tomography should be reserved for specific conditions in children and only requested by the paediatric specialists. A list of possible conditions is given in Box 16.7 without detailed description of the radiological abnormalities. Plain abdominal radiographs may be helpful in neonates but are less useful in older children.

Some of the more common abdominal emergencies are detailed below:

Hypertrophic pyloric stenosis – Presents with non bilious vomiting typically at 4–6 weeks. It can be diagnosed with ultrasound if the pylorus cannot be palpated.



Figure 16.28 High obstruction due to a malrotation. Distended bowel loops are evident in the upper abdomen with no gas below the level of obstruction.

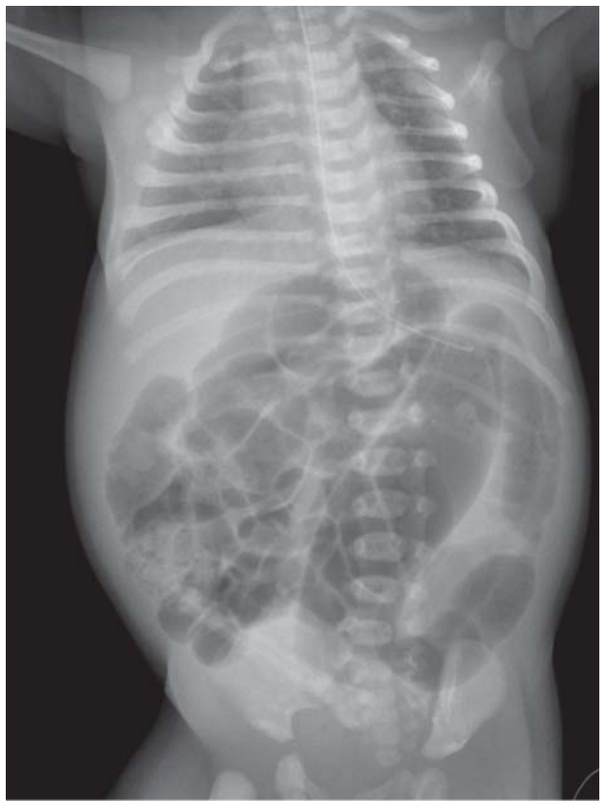


Figure 16.29 Low obstruction. Note the multiple distended bowel loops throughout the abdomen.

Box 16.7 **Acute abdominal emergencies**

Obstruction in the neonate
High obstruction

- Malrotation and volvulus
- Duodenal atresia, duodenal web, duodenal stenosis, and annular pancreas all give a ''double bubble'' appearance
- Jejunal atresia
- Duodenal duplication cyst causing obstruction

Low obstruction

- Hirschsprung's disease
- Meconium ileus. May be diagnosed in utero. Note meconium peritonitis with calcification
- Meconium plug syndrome (left sided microcolon)
- Ileal atresia
- Ano-rectal malformation
- Anal stenosis
- Milk curd obstruction
- Obstructed hernia

Obstruction in infants and older children

- Intussusception, diagnosed with ultrasonography
- Appendicitis
- Adhesion obstruction
- Hernia
- Constipation
- Do not forget malrotation at all ages

Abdominal masses

- Duplication cysts
- Ovarian cysts
- Mesenteric cysts
- Tumours

Intussusception – Occurring in infants and young children often presenting with intermittent colicky pain, obstructive symptoms or 'redcurrent jelly' stools, one segment of bowel telescopes into another. It may be accurately diagnosed with ultrasound.

Appendicitis – The most common abdominal emergency in children, most do not require imaging. Ultrasound may help diagnose or exclude the condition in atypical presentations.

Renal tract emergencies

If renal abnormalities are suspected, request an ultrasound scan.

Urinary tract infection

Ultrasound imaging routinely in acute UTI is not recommended unless the child is seriously ill, has poor urine flow or abdominal mass, raised creatinine, septicaemia, fails to respond to antibiotics within 48hrs or has infection with non-ecoli organisms.

Outpatient ultrasound and fluoroscopy will aim to detect renal obstruction, ureteric reflux or renal parenchymal scarring.

Other renal abnormalities

- Renal stones
- Haematuria, trauma, infection, renal vein thrombosis, glomerulonephritis, and nephrotic syndrome

Renal masses

- Hydronephrosis
- Complicated duplex kidney
- Multicystic dysplastic kidney
- Renal tumour – usually a Wilms' tumour in children younger than 10 years with mesoblastic nephroma diagnosed at birth
- Autosomal recessive polycystic kidney disease

Simple ovarian cysts – These occur in pubertal girls when the follicle does not involute. Most are asymptomatic, but when complivated by haemorrhage, rupture or tortion the patient may present with lower abdominal pain. US is useful in the evaluation and differentiating the condition from other abdominal patholgy.

Further reading

Borden S. Roentgen recognition of acute plastic bowing of the forearm in children. *AJR* 1975;125:524–30.

NICE clinical guideline 54 Urinary tract infection in children: diagnosis, treatment and long-term management

Rang M. *Children's Fractures*. Philadelphia: JP Lippincott, 1983

Salter RB, Harris WB. Injuries involving the epiphyseal plate. *J Bone Joint Surg Am* 1963;45:587–622.

CHAPTER 17

Major Trauma

Dominic Barron[1], *Sujit Vaidya*[2] *and Otto Chan*[3]

[1]Leeds Teaching Hospitals, Leeds, UK
[2]Barts Health NHS Trust, The Royal London Hospital, London, UK
[3]The London Independent Hospital, London, UK

OVERVIEW

- Trauma is common and a leading cause of morbidity and mortality
- Time is a critical factor in determining patient outcome
- MDCT is the single greatest recent advance in trauma care
- Advanced trauma life support (ATLS) principles for initial management – primary survey
- Primary CT survey versus primary clinical survey

Trauma has been and remains one of the leading causes of death, in particular in the 1- to 44-year-old age group. Despite this, trauma has been neglected and remained a subject unworthy of study, research and funding. There are an estimated 3.8 million deaths worldwide and 10 million people permanently disabled every year.

In 1966, a landmark white paper, 'Accidental death and disability, the neglected disease of modern society', highlighted the problems in the management of trauma, leading to guidelines to establish regionalised trauma care. The standard of trauma care and clinical outcomes varies hugely, not only between developed and third world countries, but also within developed countries. Severely injured patients in the UK have a 20% higher mortality than in the USA. It is estimated that 3000 of the 16,000 annual trauma deaths are preventable. Despite two highly critical reports of trauma care – 'Retrospective study of 1000 deaths from injury in England and Wales (1988)' and 'The management of patients with major injuries (1988)' – and the implementation of ATLS, there has been a 'Lack of change in trauma care in England and Wales since 1994 (2002)' and 'The National confidential enquiry of patient outcome and death (2007)' reported recently that 60% of trauma victims had substandard care in the UK. Specific recommendations were made to address these recognised deficiencies, firstly by organisation of trauma care into regional systems and secondly by a multidisciplinary approach.

There have been huge technological advances in radiology in the past decade, not least the advent of PACS (Picture Archiving and Communications systems) and multidetector computed tomography (MDCT). This has revolutionised the role of radiology and of the radiologist, requiring a 24/7 round-the-clock service in specialist trauma centres. It is widely accepted that MDCT is the single greatest recent advance in trauma care. A complete review of present practice is necessary in order to benefit from MDCT, not least the fundamental principle of ATLS that *definitive diagnosis is not necessary for the initial management of a traumatised patient*.

Nevertheless, ATLS remains the standard method of care for the initial management of severely injured patients. The principle is simple – treat the greatest threat to life first. Loss of airway will kill before inability to breathe, and inability to breathe will kill before bleeding and loss of circulation. Although a definitive diagnosis is not necessary for initial patient care, with the advent of MDCT, it is now recognised that a definitive diagnosis where possible is preferable and often guides the overall patient care. The most important principle to remember is *do no harm* to the patient during examination, investigation and treatment.

The notion that *Time is Golden* makes good common sense and two factors have been shown to correlate with improved patient outcome, namely *time from initial admission to CT* and *time from admission to definitive care*. Clinical examination of the obtunded traumatised patient has been shown to be unreliable at best and misleading at worst, therefore *don't examine patients to death* and taking unnecessary X rays or even taking X rays at all may delay definitive care, so *don't X-ray patients to death*.

The management of severely injured patients is divided into the primary and secondary survey. This chapter deals with the imaging during the primary survey.

Primary survey – ATLS

The main goal of the pre-hospital phase of ATLS is to deliver a patient rapidly and safely to hospital (Box 17.1). Patients are transferred to the resuscitation room and the aim of the primary survey in ATLS is to do a rapid evaluation of the patient, resuscitate and stabilise the patient with a view to proceeding to definitive treatment. This process is called the ABCDE of trauma (Box 17.2). Adjuncts to the primary survey include relevant imaging during resuscitation and re-evaluation.

ABC of Emergency Radiology, Third Edition. Edited by Otto Chan.
© 2013 John Wiley & Sons, Ltd. Published 2013 by John Wiley & Sons, Ltd.

Box 17.1 **Primary clinical survey – ATLS**

- Airways and cervical spine control
- Breathing and ventilation
- Circulation and haemorrhage control
- Disability and neurological status
- Exposure and environment

Box 17.2 **ABCDE of trauma**

- Airway and cervical spine control
- Breathing and ventilation
- Circulation and haemorrhage control
- Disability and neurological status
- Exposure and environment

ATLS works on a step-by-step approach carried out by a single operator (vertical approach) with minimal assistance, treating the greatest threat to life first. Nowadays it is a concept or a common language and in practice, most of the steps of the ABCDE are carried out simultaneously by a trauma team (horizontal approach). Anaesthetists will usually deal with the airway and intravenous access, while the surgeon evaluates the chest, abdomen, and pelvis for potential life-threatening injuries.

Imaging is requested as part of the primary survey while the patient is assessed, life-threatening injuries are dealt with, and resuscitation procedures instituted. Imaging should not be performed if it interferes with the rest of the primary survey or definitive care, and only investigations that may have a direct effect on the patient's initial problems should be carried out.

Traditionally, imaging performed as part of the primary survey includes the supine chest and pelvis radiographs (Figures 17.1 and 17.2) and limited ultrasonography (FAST – focused assessment with sonography for trauma). The advent of MDCT scanners now means that in major trauma centres, CT can be incorporated into the primary survey, even in relatively unstable patients (Box 17.3).

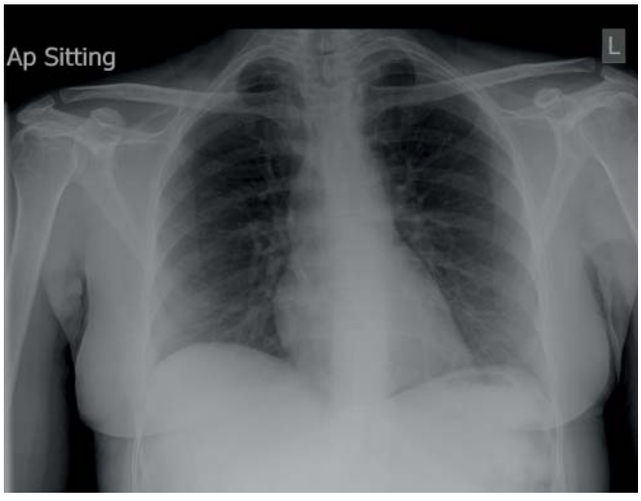


Figure 17.1 Normal anteroposterior (AP) chest.



Figure 17.2 Normal pelvis.

The main problem is delay of transfer from the emergency room to the CT room.

Box 17.3 **Primary CT survey – ATLS with MDCT**

- Airways and cervical spine control
- Breathing and ventilation
- CT, contrast and circulation
- Definitive diagnosis and treatment
- Evaluation

Airway and cervical spine control

The airway should be assessed for patency. Foreign bodies and vomit should be removed and facial, mandibular, tracheal and laryngeal injuries should be excluded clinically.

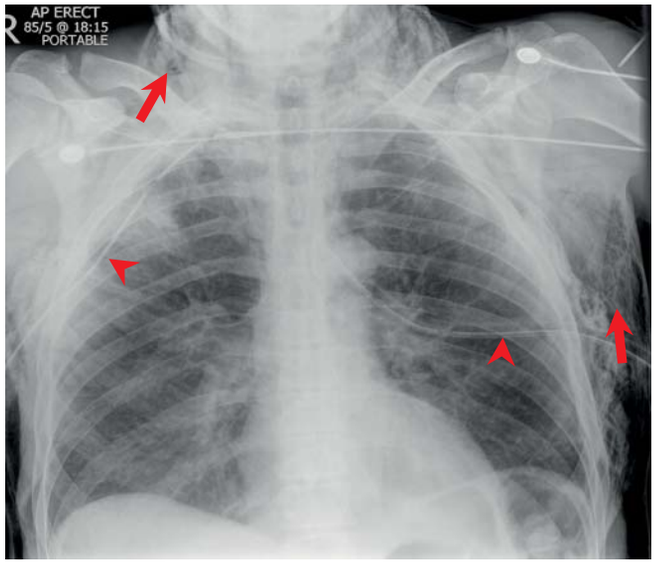
If the patient is conscious and talking, there is usually no need for airway intervention. If the patient is unconscious and breathing spontaneously, an oropharyngeal airway may suffice as a temporary measure. Any patient who has a head injury and a score on the Glasgow coma scale of 8 or less should be intubated. However, intubation may be required for optimal control of airways in patients with higher scores.

If the patient has been intubated, a chest radiograph should be taken to check the position of the endotracheal tube. The tip of the tube should not lie below the level of the aortic arch in a supine chest radiograph and a minimum of 3.5 cm (and preferably 5 cm) above the carina.

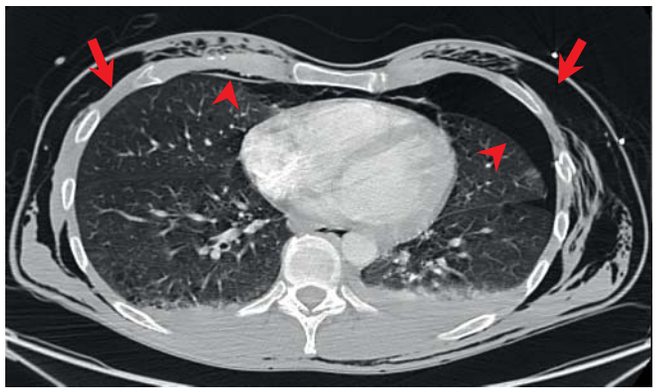
Care should be taken to avoid worsening a potential cervical spine injury while establishing and safeguarding an airway. If the airway has been secured, the neck should be immobilised with a cervical collar, sandbag and tape. Should the collar need to be removed, an experienced member of the trauma team should carry out in-line manual immobilisation of the head and neck.

Breathing and ventilation

A patent airway does not guarantee adequate ventilation. The lungs, chest wall and diaphragm must be assessed for potential injuries



(a)



(b)

Figure 17.3 (a) AP chest radiograph with bilateral chest drains. Extensive surgical emphysema. (b) CT chest in the same patient clearly demonstrating the left pneumothorax as well as the extensive surgical emphysema.

that could compromise ventilation acutely. These life-threatening injuries include tension pneumothorax, tension haemothorax, flail chest and open pneumothorax. It can be difficult to exclude these injuries in a patient with multiple trauma. A chest radiograph must be taken as soon as possible (Figure 17.3a,b). If the patient is subsequently intubated or ventilated, a second radiograph should be taken to confirm that the endotracheal tube is in a satisfactory position and that life-threatening injuries have not been made worse. Ventilation can cause a simple pneumothorax to become a tension pneumothorax.

Circulation and haemorrhage control

The patient's haemodynamic state must be assessed quickly and accurately because bleeding is a major cause of preventable death. Clinical evaluation is essential, in particular the level of consciousness, skin colour and pulse. Any external source of bleeding should be identified and dealt with immediately using manual pressure. When the examination or history suggests internal injury a limited

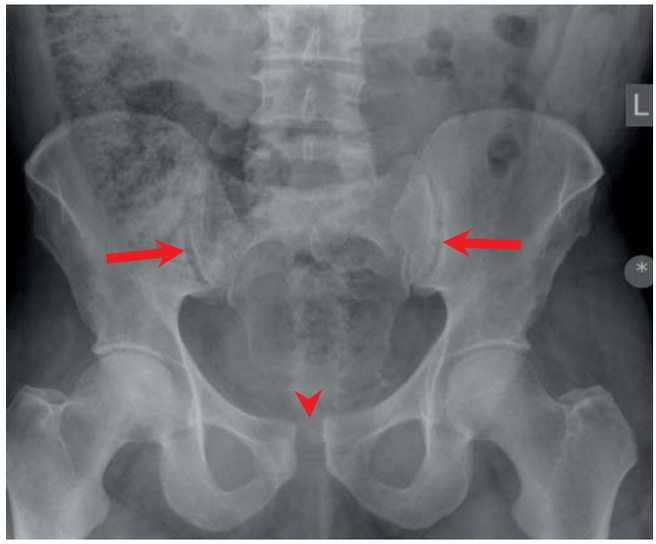


Figure 17.4 Pubic symphyseal diastasis with bilateral widened SIJs, consistent with an AP compression injury.

ultrasonography (FAST) should be done to exclude hidden blood loss (Box 17.4).

Box 17.4 **Main causes of hidden blood loss**

- Chest, abdomen, and retroperitoneal injuries
- Pelvic fractures
- Multiple long bone fractures

FAST can be performed by a physician, surgeon, radiologist or paramedic and has been shown to be valuable in the assessment of blunt trauma patients in the emergency room, especially in unstable patients with multiple injuries. FAST performed in the pre-hospital setting is extremely useful, as this can then give the receiving unit advanced warning of potential injuries and help to triage patients.

Ultrasonography should be performed in five areas. These areas are the five Ps – perihepatic, peripluric, and pelvis in the abdomen, and pericardial (to exclude a pericardial tamponade) and pleural (to detect fluid or a pneumothorax) in the chest or consolidated lung.

The presence of a pelvic fracture (Figure 17.4) or free fluid on ultrasonography mandates a specialist opinion. In appropriate centres, CT is the investigation of choice in these patients as not only will this identify all bleeding sources, but it can differentiate between arterial bleeding and venous bleeding.

This is important as embolisation is now well recognised as a definitive treatment option for defined arterial bleeding. This particularly applies to the spleen, liver, kidneys and pelvis (Figures 17.5–17.7).

Disability (neurological examination)

The patient's neurological state is assessed with the Glasgow coma scale (Box 17.5). It is easy and quick to use and is a determinant of patient outcome and possible further management.



Figure 17.5 Sagittal CT chest reformat showing sternal fracture (arrow) and retrosternal haematoma (asterisk).



Figure 17.6 Coronal CT abdominal reformat showing active arterial bleed (arrow).

All patients with a head injury or who are unconscious or ventilated should have CT of the head, especially if they have lost consciousness, have amnesia or have severe headaches. Up to 18% of patients with mild head injuries have abnormalities on CT, and 5% of these patients may require surgery.

If the patient has a head, scan it – missing a serious head injury may have catastrophic consequences



Figure 17.7 Coronal CT abdominal reformat showing active left gluteal bleed.

Box 17.5 **Glasgow coma scale score**

Eye opening (graded 1–4)

- Spontaneous – 4
- To speech – 3
- To pain – 2
- None – 1

Best motor response (graded 1–6)

- Obeys command – 6
- Localises pain – 5
- Normal flexion – 4
- Abnormal flexion – 3
- Extension (decerebrate) – 2
- None – 1

Verbal response (graded 1–5)

- Orientated – 5
- Confused conversation – 4
- Inappropriate words – 3
- Incomprehensible sounds – 2
- None – 1

- Maximum score 15, minimum score 3
- Mild injury 14–15
- Moderate injury 9–13
- Severe injury 3–8
- Coma <8

CT should be done as soon as possible because morbidity and mortality rises substantially if surgery is delayed. The intracranial findings of CT may include no abnormality, extradural haematoma, subdural haematoma, contusions and intracerebral haematomas,



Figure 17.8 CT head demonstrating right subdural haemorrhage.



Figure 17.9 CT head demonstrating intraventricular haemorrhage.

subarachnoid blood, diffuse axonal injury and combination injuries (Figures 17.8 and 17.9).

The National Institute of Clinical Excellence (NICE) introduced UK guidelines for management of head injury in 2003 that support the ATLS guidelines. They emphasise that CT must be done within an hour of the patient arriving at the hospital.

Exposure and environment

The patient should be fully exposed (by cutting off all clothes) to allow a full examination. It is, however, critical to keep the patient warm with blankets and a heated emergency room. Large volumes of fluids may be infused, and these intravenous fluids should be warmed.

Adjuncts to primary survey and resuscitation

As a minimum, patients should have electrocardiography, their blood pressure monitored, pulse oximetry, a nasogastric tube and a urinary catheter. Blood gases should also be monitored. If a fracture at the base of the skull is suspected, the nasogastric tube can be inserted after CT of the head or an orogastric tube placed.

Interpreting primary survey images

All imaging must be supervised and done without fuss or undue delay and with meticulous technique. Attention to detail is essential. In particular, the film must be labelled (including the patient's name and a side marker) (Boxes 17.6 and 17.7).

Box 17.6 **ABCDEs interpretation of the supine chest radiograph (Figure 17.1)**

Airways

- Check trachea is clear and central
- Is airway patent?
- Check position of endotracheal tube
- Are there any teeth or foreign bodies?
- Check all lines and tubes

Breathing

- Exclude tension pneumothorax and haemothorax
- Check there is no radiological flail segment
- Exclude rib fractures
- Check lungs are clear

Circulation

- Check heart size and mediastinal contours are normal
- Make sure that the aortic arch is clearly seen
- Check the hila and vascular markings are normal

Diaphragm

- Check that diaphragms appear normal (size, shape, and position)
- Can both diaphragms be clearly seen?
- Check under each diaphragm

Edges

- Check the pleura and costophrenic recesses
- Exclude a subtle pneumothorax or effusion

Soft Tissues and Skeleton

- Look for surgical emphysema
- Check clavicles and shoulders and exclude rib fractures
- Look at the paraspinal lines and check the spine

The supine chest radiograph should be taken as soon as possible after the patient has been exposed and centred correctly. Attention must be paid to stop patients being rotated and to keep them in the middle of the trolley.

Box 17.7 **ABCs interpretation of pelvic radiographs (Figure 17.2)**

Alignment

- Check the pubic symphysis is symmetrical and not widened
- Carefully check that the sacroiliac joints are intact

Bones

- Check that all three pelvic rings are intact
- Use a bright light to check iliac crests and hips
- Look at the lumbar spine and hip joints separately

Cartilage

- Check the distance of the pubic symphysis
- Again check the sacroiliac joints
- Check both hips

Soft Tissues

- Check the soft tissue planes are symmetrical
- Look for obturator internus
- Carefully delineate the perivesical fat plane
- Make sure the gluteus medius and psoas fat planes are intact

A polytrauma CT should be dealt with in exactly the same way as all other trauma management. Therefore the initial readout should be the primary survey looking for major life-threatening injuries (see later). A secondary survey by a radiologist should then follow, which involves a detailed assessment of all the imaging.

All major trauma patients ideally should have a whole body CT
Don't X-ray patients to death!

Primary CT survey – ATLS and MDCT

The problem with the standard ATLS approach is that there are delays built into this step-wise approach, plain radiographs provide only limited information into the state of the patient and injuries sustained and in addition, almost all major trauma patients need further imaging with CT.

The need to save time and avoid unnecessary transfers to major trauma patients is critical and the most time-efficient method is to transfer patients from pre-hospital care directly to the CT scanner, performing the initial part of the primary survey (Airways and Breathing) on the CT scanner table and then doing a CT whole-body scan on a MDCT and then continuing with the primary survey (re-evaluation of A and B and then continuing with C).

The patient avoids transfer from the resuscitation room to the CT scanner room and back again to the resuscitation room, each transfer usually taking at least 45 minutes. Furthermore, the relatively 'stable patient' can potentially be made 'unstable' by the transfer, in addition to the other dangers involved in transferring patients, such as tubes, drains and lines being moved and spinal injuries made worse.

Only in exceptional circumstances, where the patient is deemed extremely unstable and when the pre-hospital FAST scan shows free fluid in the abdomen or a pericardial collection in a penetrating injury, does the patient go directly to theatre for an emergency laparotomy or thoracotomy.

Dedicated resuscitation rooms are now available, where the patient can be resuscitated, have plain radiographs or MDCT, angiography and interventional procedures (such as embolisation) and the room is also an operating suite. Clearly these all in one rooms are expensive, need planning and will only be available in major trauma centres, but the advantages are clear, not least in saving time and transfers and, in effect, optimising treatment, improving outcome and avoiding preventable deaths.

ABCs of CT interpretation

Primary Survey

This should be done immediately as per ATLS protocol with the aim being to identify major life-threatening injuries.

A – Airway

- Check for airway obstruction
- Check for ET tube placement
- Look for obstructing foreign bodies

B – Breathing

- Exclude tension pneumothorax and haemothorax
- Check for pulmonary contusion
- Check for pulmaonary lacerations
- Assess chest drain placement

C – Circulation

- Asses for active bleeding in the Thorax / Abdomen / Pelvis and Soft Tissues

D – Disability

- Assess for major intra-cranial bleed / oedema
- Look for major spinal Injury

Secondary Survey

This should be done by a radiologist and involves a detailed review of everything. Ideally this is proforma driven to ensure nothing is missed.

Further reading

ACS. *ATLS Student Course Manual*, 8th edn. Chicago: American College of Surgeons, 2008. ISBN 978-1-880696-31-6.

Mirvis SE, Shanmuganathan K. *Imaging in Trauma and Critical Care*, 2nd edn. Philadelphia: Saunders, Elsevier, 2003. ISBN 7216-9340-7.

Mirvis SE, Shanmuganathan K, Miller LA, Sliker CW. *Emergency Radiology: Case Review Series*. Mosby, Elsevier, 2009.

The Royal College of Radiologists. *Standards of Practice and Guidance for Trauma Radiology in Severely Injured Patients*. London: the Royal College of Radiologists, 2011. ISBN 987-4-905034-51-2.

Index

AAA *see* abdominal aortic aneurysms
ABCDE of trauma 171–2, 175
ABCs systematic assessment 8–10
  abdomen 123–7, 134, 138
  ankles and feet 59–62, 70
  cervical spine 94–9, 102
  chest 113–18
  elbows 23–6, 28
  emergency ultrasound 152–8
  face 85–7, 92
  hands and wrists 11–14, 21
  head 71–7
  knees 50–1, 58
  major trauma 176
  pelvis and hips 38–41, 44–5, 48
  shoulders 30–2, 37
abdomen 123–34
  ABCs systematic assessment 123–7, 134, 138
  anatomy 123, 136–7
  common abdominal emergencies 130–4
  emergency ultrasound 154–5
  important plain film findings 127–30
  paediatric patients 168–9
  see also acute abdominal pain
abdominal aortic aneurysms (AAA) 131–2, 149, 152–4
abdominal X ray (AXR) 1, 10, 123–33, 135
abscesses
  emergency radiology 138, 140–2, 145, 150–1
  emergency ultrasound 157
acetabular fractures 46–7
ACJ *see* acromioclavicular joint
ACL *see* anterior cruciate ligament
acromioclavicular joint (ACJ) 30–1, 34–6
acute abdominal pain 130–4, 135–51
  ABCs systematic assessment 138
  abdominal aortic aneurysms 131–2, 149, 152–4
  abdominal CT protocols 137–8
  anatomy 136–7
  appendicitis 130–1, 139–40
  causes by quadrant 136–7
  choleocystitis 132–3, 142–3
  colitis/enteritis 143–4
  CT features of conditions 138–9
  definition of acute abdomen 135
  diverticulitis 133, 140–1
  ectopic pregnancy 132, 134, 150, 156–8
  emergency ultrasound 154–5, 158
  gastrointestinal haemorrhage 149–50
  indications for CT 135–6
  paediatric patients 169–70
  pancreatitis 132, 140–2
  tuberculosis 144–5
  urolithiasis 147–9
acute cholecystitis 157–8
acute pancreatitis 131–2
acute parenchymal haemorrhage 74
adequacy 9
  abdomen 123–4
  ankles and feet 59–60
  cervical spine 94–5, 99–100, 102
  chest 113, 117
  elbows 23
  face 85–6, 92
  hands and wrists 12
  head 73
  knees 50
  pelvis and hips 39, 44–5, 48
  shoulders 30–1
  thoracic and lumbar spine 108
advanced trauma life support (ATLS) 8, 171–6
aerobilia 129–30
AHL *see* anterior humeral line
AIIS *see* anterior inferior iliac spine
airspace 9
  chest 118, 121
  head 73, 75–6, 83
airways
  chest 113, 117
  major trauma 172–3, 175–6
  paediatric patients 168
alignment 9
  ankles and feet 60–1, 70
  cervical spine 94–6, 100–2
  elbows 23–4, 28
  face 92
  hands and wrists 12–13, 21
  knees 50
  major trauma 176
  pelvis and hips 39–40, 44–5, 48
  shoulders 31, 37
  thoracic and lumbar spine 108–10
aneurysmal rupture 82
ankles
  ABCs systematic assessment 59–62, 70
  anatomy 59
  injuries 62–6
ankylosing spondylitis 102, 107
anterior cruciate ligament (ACL) 49, 56–7
anterior dislocations 32–3
anterior humeral line (AHL) 24–5
anterior inferior iliac spine (AIIS) 165–6
anterior superior iliac spine (ASIS) 165–7
anteroposterior (AP) views 2–3
  abdomen 123–4
  ankles and feet 59–61, 63, 65–6, 69
  cervical spine 99–100
  chest 111–12
  elbows 23–6, 29
  hands and wrists 11–12, 15, 19–21
  knees 50, 55–8
  pelvis and hips 39, 44–5
  shoulders 30–1, 33–4
  thoracic and lumbar spine 105–7, 108–10
anteroposterior compression (APC) 42, 43, 46
aortic aneurysms 131–2, 149, 152–4
aortic injury 119–20
AP *see* anteroposterior
APC *see* anteroposterior compression
appendicitis 130–1, 139–40, 152–3
appendicoliths 140, 152
arthritis 165–6
ascites 154
ASIS *see* anterior superior iliac spine
asthma 168
atlantoaxial alignment 95–6
atlanto-occipital alignment 95–6
ATLS *see* advanced trauma life support
avascular necrosis (AVN) 64
avulsion fractures 5–6
  ankles and feet 62, 64
  hands and wrists 14–15, 17
  knees 57–8
  paediatric patients 161, 165–7
axial skeleton 9
axial views
  abdomen 131, 133, 147
  cervical spine 98, 101
  chest 112, 117, 120, 122
  face 88–90, 92
  knees 55
  shoulders 30–1, 33–5
  thoracic and lumbar spine 106
AXR *see* abdominal X ray

Barkart fractures 33
Barton's fracture 18

beam hardening 71–2
Bennett's fracture 15–16
biliary colic 158
bladder injuries 43–4
bladder obstructions 154
bleeding *see* haemorrhage
blood gases 175
blowout fractures 90–1
blunt trauma 77–8, 118, 120
Böhler's angle 67
bone disease 107
Boutonniere deformity 14
bowels 124–9, 132, 143–7, 150
bowing injuries 160
bow-put fractures 6
Boxer's fracture 15
brain injuries 73–6, 77–8
brain parenchyma 9, 71–2, 74, 80–3
brain stem injury 77
breathing 115, 172–3, 175–6
breathlessness 158
bronchogenic carcinomas 7
buckle fractures 160
burst fractures 97, 106, 109
butterfly vertebrae 105

caecal volvulus 128, 147
calcaneal apophysis 164
calcaneus 61, 63, 65–6, 68–9
calcifications
  abdomen 125–6, 131–2, 134, 140, 143, 147–9
  emergency radiology 140, 143, 147–9
  emergency ultrasound 154
  shoulder 32
Campbell's line 86
capitellar fractures 27–8
capsular avulsions 14–15
carcinomas 7, 147
cardiac abnormalities 168
cardiac arrest 154, 158
carpal bone injuries 18–19
carpometacarpal joint dislocations 15–17
cartilage 9
  ankles and feet 62, 70
  cervical spine 98–9, 100–2
  elbows 25, 28
  face 92
  hands and wrists 13, 21
  knees 51
  major trauma 176
  pelvis and hips 40, 44–5, 48
  shoulders 32, 37
  thoracic and lumbar spine 108–10
CBCT *see* cone beam computed tomography
CBD *see* common bile duct
CDH *see* congenital dislocation of the hip
CECT *see* contrast-enhanced computed tomography
cerebrospinal fluid (CSF) 9, 72, 75–6, 83
cervical spine 93–103
  ABCs systematic assessment 94–9, 102
  anatomy 93
  imaging considerations 93–4
  interpretation of AP views 99–100
  interpretation of lateral views 94–9
  interpretation of open mouth odontoid views 100–2
  major trauma 172
  pitfalls 102
Chance fractures 107
Chauffeur fracture 18–19
chest 111–22
  ABCs systematic assessment 113–18
  anatomy 112–13
  approach to lung review 117–18
  common non-traumatic conditions 121–2
  common traumatic conditions 118–21
  emergency ultrasound 158
  imaging techniques 111–12
chest drains 114–15, 117
chest pain 158
chest X ray (CXR) 7–8, 9–10, 111–13, 117–21
  emergency ultrasound 158
  major trauma 173, 175
  paediatric patients 168
  thoracic and lumbar spine 110
children *see* paediatric patients
choleocystitis 132–3, 142–3
chronic stress fractures 54–5
circulation
  chest 115, 117
  major trauma 173, 175–6
clavicular fractures 35
clay shoveler's fracture 97, 99
Coach's finger 14
colitis 143–4
Colles' fracture 17–18
colonic carcinoma 147
common bile duct (CBD) 143
community-acquired pneumonia 121
complete diaphyseal fractures 160
complex fractures 43, 89, 167
compression injuries
  major trauma 173
  paediatric patients 163–4
  pelvis and hip 41–3, 46–8
computed tomography angiography (CTA) 1
  chest 119, 121–2
  pelvis and hips 40
computed tomography (CT)
  abdomen 123, 127, 129, 131–3, 135–51
  ankles and feet 60, 65
  cervical spine 93–4, 97–9
  chest 111–13, 115, 117–22
  emergency radiology 135–51, 167
  face 85–6, 88–91
  hands and wrists 11, 12, 18–19
  head 71, 76, 79–84
  knees 49, 52–5
  major trauma 171–6
  paediatric patients 167
  pelvis and hips 39, 40–1, 43–4
  shoulders 33, 35–7
  thoracic and lumbar spine 104, 107
  window levels and widths 135
  see also multidetector computed tomography
computed tomography pulmonary angiography (CTPA) 121–2
condylar head/neck fractures 87–8
cone beam computed tomography (CBCT) 85, 90–1
congenital dislocation of the hip (CDH) 48
congenital vertebral anomalies 105
contrast-enhanced computed tomography (CECT) 137, 149
contre coup injuries 77–8
coronal views
  abdomen 131, 133, 146
  major trauma 174
cortical contusions 77–8
costal cartilage 125
costrophrenic recesses 175
coxa magna 164
CRITOE/CRITOL acronym 22–3, 164
Crohn's disease 143–4
crush fractures 14, 66–7, 70
CSF *see* cerebrospinal fluid
CT *see* computed tomography
CTA *see* computed tomography angiography
CTPA *see* computed tomography pulmonary angiography
cuboid fractures 66
cuneiform fractures 66

DAI *see* diffuse axonal injury
deep cerebral injury 77
deep vein thrombosis (DVT) 152, 154–5
Delbet classification 46
Denis's three column model 110
dens fractures 101
dense calcaneal apophyses 5
dentoalveolar fractures 87–8
depressed fractures 6
dermoids 126
diaphragm 115–16, 117, 175
diaphyseal fractures 160
Die punch fracture 18
diffuse axonal injury (DAI) 77–8
digital radiography 1
disability 173–4, 176
dislocations
  ankles and feet 63–5
  elbows 24, 27–8
  hands and wrists 14, 15–17, 19–21
  knees 54–7
  pelvis and hips 47–8
  shoulders 30–5
  see also fracture dislocations
distal femur injuries 51
distal fibula injuries 161, 163
distal humerus injuries 162
distal radius injuries 17–18, 162
distal tibia injuries 162–3
diverticulitis 124, 132–3, 140–1
Dolan's lines 86
Doppler ultrasound 157–8
dorsal talar fractures 62
dural spaces 75–6, 83
DVT *see* deep vein thrombosis

ECG *see* electrocardiography
ectopic pregnancy
  abdomen 132, 134
  emergency radiology 150
  emergency ultrasound 156–8
effusions
  emergency ultrasound 154–6
  major trauma 175
  paediatric patients 166
elbows 22–9
  ABCs systematic assessment 23–6, 28

anatomy 22–3
injuries 26–9
paediatric patients 164
paedriatric patients 22–3
electrocardiography (ECG) 175
emergency radiology
ABCs systematic assessment 138
abdominal aortic aneurysms 149
abdominal CT protocols 137–8
acute abdominal pain 135–51
appendicitis 139–40
choleocystitis 142–3
colitis/enteritis 143–4
CT features of conditions 138–9
definition of acute abdomen 135
diverticulitis 140–1
gastrointestinal haemorrhage 149–50
indications for acute abdominal CT 135–6
paediatric patients 159–70
pancreatitis 140–2
tuberculosis 144–5
urolithiasis 147–9
emergency ultrasound 152–8
emphysema 115, 116
empyema 155, 158
endotracheal intubation 113–14
enteritis 143–4
epicondyle ossification 5
epiploic appendagitis 150–1
exposure 175
extra-axial compartment 75–6
extracapsular fractures 45–6
extradural haematoma 76
extraluminal air 124, 128, 134
extraperitoneal bladder rupture 43–4
eyes 9, 76, 83

face 9, 85–92
ABCs systematic assessment 85–7, 92
anatomy 85
blowout fractures 90–1
injuries 87–92
LeFort injuries 88–9
mandibular fractures 87–8
meningitis 84
orbital injuries 89–90
sinuses and soft tissues 91–2
upper third facial fractures 91
zygomatic complex fractures 89
faeculant fluids 138, 146
falciform ligament 129
fall onto an outstretched hand (FOOSH)
elbows 22
hands and wrists 11, 17–18
paediatric patients 160
FAST *see* focused assessment with sonography for trauma
fat pad sign 25–6
fat planes 127, 134
feet
ABCs systematic assessment 59–62, 70
anatomy 59
injuries 66–70
femoral capital epiphysis 164–5
femoral condylar fractures 52–3
femoral neck fractures 45–6
fibular injuries 53–4
flexion distraction fractures 67
flexion teardrop fractures 97–8
floating shoulder 36
fluid collections 138
focused assessment with sonography for trauma (FAST) 152, 156, 172–3
foetuses 156–8
FOOSH *see* fall onto an outstretched hand
forearms 164
foreign bodies
abdomen 126–7, 134
chest 116
emergency ultrasound 156–7
paediatric patients 168
fracture dislocations 4
ankles and feet 66, 69
elbows 27–9
hands and wrists 16
frog's leg lateral views 165–6
full examination 175

Galeazzi fractures
elbows 28–9
hands and wrists 18–19
paediatric patients 164
gallstones
abdomen 126, 132
emergency radiology 143
emergency ultrasound 154
Gamekeeper's thumb 17
Garden's classification 46–7
gastrointestinal haemorrhage 149–50
gastrointestinal tract (GIT) 139, 145
GCS *see* Glasgow coma scale
genitourinary tract 145
GHJ *see* glenohumeral joint
GIT *see* gastrointestinal tract
Glasgow coma scale (GCS) 77–8, 173–4
glenohumeral joint (GHJ) 30–3
greenstick fractures 17, 160–1
growth plate fractures 63–4

haemarthrosis 32
haematoma formation 6
abdomen 131–2, 138, 150–1
chest 116
head 76
major trauma 174–5
paediatric patients 167
thoracic and lumbar spine 107, 109
haemopneumothorax 114
haemorrhage
abdomen 127, 131–2, 142, 149–50
major trauma 173–5
paediatric patients 166
pelvis and hips 43
haemorrhagic contusions 73–82
hands
ABCs systematic assessment 11–14, 21
anatomy 11
injuries 14–17
hangman's fracture 97–8
Harris ring 97–8
Hawkins classification 64
head 71–84
ABCs systematic assessment 71–7
brain injuries 73–6, 77–8
cerebrospinal fluid 72, 75–6, 83
dural spaces 75–6
eyes 76, 83
high density lesions 74–6, 82
hydrocephalus 75
hypertensive haemorrhage 81–2
injuries 77–84
intraparenchymal haemorrhage 80–2
low density lesions 73–4
major trauma 174–5
mass effect 74–5
meningitis 83–4
paediatric patients 167
primary brain injury 77–8
review areas 76–7, 84
stroke 78–80
subarachnoid haemorrhage 82–3
see also face
hemidiaphragm 115–16
hemivertebrae 105
hernias 126–7, 134, 145
hidden blood loss 173–4
high density lesions 74–6, 82
hila 113, 115
Hill–Sachs fractures 32, 34
hips
ABCs systematic assessment 44–5, 48
anatomy 38
injuries 45–8
paediatric patients 164–7
Hutchinson fracture 18–19
hydrocephalus 75
hydronephrosis 154–5
hyperflexion injuries
cervical spine 95
thoracic and lumbar spine 106
hypertensive haemorrhage 81–2
hypoxic brain injury 73–4

IBD *see* inflammatory bowel disease
idiopathic coxa vera 48
IF *see* internal fixation
infections
emergency radiology 138, 143–4
paediatric patients 168–9
inflammation 138
inflammatory bowel disease (IBD) 143
inguinal hernias 126
Insall Salvati ratio 52
insufficiency fractures 68
intercostal drains 114–15, 117
internal fixation (IF) 18
intracapsular fractures 45–6
intramural venous gas 147–8
intraparenchymal haemorrhage 80–2
intraperitoneal air 119, 124, 128–30, 134, 139
intra-uterine cysts 156
intravenous (IV) contrast 71, 83
ischaemia 143
ischaemic stroke 78–80
ischial tuberosity 165–6
isotope uptake 60
IV *see* intravenous

Jefferson fractures 101
Jersey finger 14–15
Judet–Letournel classification 46–7
juvenile Tillaux fractures 63

Klippel–Feil disorder 102
knee dislocation 57
knees 49–58
  ABCs systematic assessment 50–1, 58
  anatomy 49–50
  injuries 51–8

lacerations 119
large bowel dilatation 128
lateral collateral ligament (LCL) 49, 56, 58
lateral compression injuries 41
lateral condylar fractures 26
lateral malleolus 61–2
lateral views
  ankles and feet 66–7, 69
  cervical spine 94–9
  elbows 23–6, 29
  face 85–6
  hands and wrists 12, 15, 19, 21
  knees 50–2, 54–7
  paediatric patients 165–6
  pelvis and hips 45
  thoracic and lumbar spine 105–6, 108
LCL *see* lateral collateral ligament
lead pipe fractures 160–1
LeFort injuries 88–9
ligaments
  knees 49, 56–8
  pelvis and hips 40
  shoulders 36
  thoracic and lumbar spine 109–10
lightbulb sign 33–4
limbus vertebrae 105
lipohaemoarthrosis 3
Lisfranc fracture dislocations 66, 69
low density lesions 73–4
lumbar spine 104–10
  ABCs systematic assessment 108–10
  anatomy 104–6
  emergency radiology 145
  imaging considerations 107
  injury classification 110
  injury mechanisms 106–7
lunate dislocations 21
lung parenchyma 113
lungs 113, 117–18
  see also chest
luxatio erecta 34
lymph nodes 145
lymphadenopathy 115

McGrigor's line 86
magnetic resonance imaging (MRI) 8
  abdomen 123, 136
  ankles and feet 60
  cervical spine 93–4
  elbows 25
  hands and wrists 11, 12, 17, 19–20
  head 80
  knees 49
  paediatric patients 164, 166
  pelvis and hips 44
  thoracic and lumbar spine 105, 107
Maisonneuve fractures 4, 62–3
major trauma 171–6
  ABCDE of trauma 171–2, 175
  ABCs systematic assessment 176
  adjuncts to primary survey 175
  advanced trauma life support 171–6
  interpretation of primary survey images 175–6
  primary survey 171–5
  resuscitation 175
malignancies
  abdomen 125, 127–8, 134, 146–7
  emergency ultrasound 156
  head 73, 80
  multidetector computed tomography 3, 7
  paediatric patients 169
  thoracic and lumbar spine 107
Mallet finger 14
mandibular fractures 87–8
mass effect 74–5
match perfusion deficit 80–1
MCL *see* medial cruciate ligament
MDCT *see* multidetector computed tomography
mean transit time (MTT) 80–1
medial cruciate ligament (MCL) 49, 56
medial epicondylar fractures 26
mediastinum 113, 115
meningitis 83–4
mesenteric adenitis 150–1
mesenteric venous gas 147–8
metacarpal injuries 15, 163
metaphyseal corner fractures 167–8
metastases 3
  abdomen 127, 134
  emergency ultrasound 156
  head 73
  thoracic and lumbar spine 107
metatarsals 66–7, 70
Monteggia fractures 4, 7
  elbows 28–9
  hands and wrists 18
  paediatric patients 164
motor vehicle accidents
  chest 119–20
  knee 52, 56
  pelvis and hips 38
  thoracic and lumbar spine 106–7
MPR *see* multiplanar reconstruction
MRI *see* magnetic resonance imaging
MTT *see* mean transit time
multidetector computed tomography (MDCT) 1–8
  chest 112
  emergency radiology 135–6
  face 85–6
  head 71
  as initial modality of choice 1–8
  major trauma 171, 172, 176
  Rules of twos 1, 2–8
multiplanar reconstructions (MPR) 1
  face 85, 86, 88–9
  head 71
  pelvis and hips 39, 40
multiple fractures 43, 89, 167
myeloma 107

NAI *see* non-accidental injury
nasogastric intubation 115
navicular fractures 66
necrotising pancreatitis 142
NECT *see* non-enhanced computed tomography
neonates 168–9
neurological examination 173–4, 176
neurological injuries 105–6
non-accidental injury (NAI) 7–8, 166–8
non-enhanced computed tomography (NECT) 137, 142, 147, 149
non-haemorrhagic contusions 73
notch views 50, 54

oblique fractures 2
oblique views
  ankles and feet 59–60, 67, 69
  hands and wrists 15
  knees 50
  shoulders 30–1
occipitomental views 85–7, 89–91
odontoid peg fractures 101
olecranon fractures 26–7
omental infarction 150–1
open mouth odontoid views 100–2
open reduction 18
OPG *see* orthopantomography
orbital injuries 89–90
orthopantomography (OPG) 87–8
ossification centres
  ankles and feet 59, 61
  elbows 24
  knees 49
  paediatric patients 164
osteochondral fractures 64, 66
osteochondritis dissecans 53–4
osteomyelitis 166
osteoporosis 107
OTTAWA rules 59, 60
ovarian cysts 154–5

PA *see* posteroanterior
PACS *see* picture archiving and communication systems
paediatric patients
  acute abdominal pain 169–70
  anatomy 160
  chest emergencies 168–9
  definitions and classification 159
  elbows 22–3
  emergency radiology 159–70
  fractures 159–66
  hands and wrists 17
  mechanical and physiological differences 160
  non-accidental injury 166–8
  pelvis and hips 44–5
  physeal fractures 160–4
  renal tract emergencies 169
Paget's disease 107
pancreatic calcifications 125
pancreatitis 131–2, 140–2
panoramic radiography 87
patella dislocations 54–6
patella fractures 54–5
patellofemoral joint (PFJ) 49
PCL *see* posterior cruciate ligament
pelvic inflammatory disease 150–1
pelvis
  ABCs systematic assessment 38–41, 48
  anatomy 38
  injuries 41–4
penetrating injuries 121
perforated diverticulitis 124, 132–3

pericardial effusions 154, 156
peripheral skeleton 9
peritoneum 145
Perthes disease 164–5
PFFD *see* proximal femoral focal deficiency
PFJ *see* patellofemoral joint
phalangeal fractures
  ankles and feet 68
  hands and wrists 14
  paediatric patients 162
phleboliths 125, 148–9
physeal fractures 160–4
picture archiving and communication systems (PACS) 1, 135, 138, 171
pilocytic astrocytoma 73–4
pilon fractures 63
PIPJ *see* proximal interphalangeal joint
pleura 116, 117, 175
pleural effusions 154–6
pleural empyema 168–9
Pneumatosis coli 129
pneumocephalus 72
pneumocytosis 121
pneumomediastinum 117, 118–19
pneumonia 121, 168
pneumoperitoneum 119, 124, 128–30, 134, 139
pneumothorax
  chest 114, 116, 118
  major trauma 175
  paediatric patients 168
posterior cruciate ligament (PCL) 49, 56–7
posterior dislocations 32–4
posterior malleolus 61
posteroanterior (PA) views
  chest 111–13
  hands and wrists 12, 16
primary brain injury 77–8
prostate cancer 127
proximal femoral focal deficiency (PFFD) 48
proximal humeral fractures 36
proximal interphalangeal joint (PIPJ) 2
proximal tibia injuries 53–4
pseudoaneurysms 119–20, 142, 157–8
pseudocysts 142
pseudo-dislocations 32
pseudomembranous colitis 143–4
pubic symphysis diastases 43
pulled elbow 28–9
pulmonary contusions 114, 119
pulmonary embolism 121–2
pulmonary oedema 121
pulmonary vasculature 113, 115, 117

quadriceps mechanism 49, 56

radial head dislocations 27, 29
radial head fractures 26–7
radiocapitellar line (RCL) 24–5
rectus sheath haematoma 150–1
renal failure 154
renal tract calculi 132–3, 147–9, 154–5, 169
renal tract emergencies 169
resuscitation 175
ribs
  chest 116, 120–1
  emergency ultrasound 158
  major trauma 175
  paediatric patients 168
Rigler's sign 129
Ro2 *see* Rules of twos
road traffic accidents *see* motor vehicle accidents
Rolandos 16
Rules of twos (Ro2) 1, 2–8

sacroiliac joints (SIJ) 40
sagittal views 174
SAH *see* subarachnoid haemorrhage
sail sign 25
Salter–Harris classification 3
  ankles and feet 63
  hands and wrists 17–18
  paediatric patients 160–4
  pelvis and hips 45
sarcoidosis 115
scaphoid injuries 18–20
scapholunate dislocations 20
scapular fractures 35–6
scintigraphy 164
SCIWORA *see* spinal cord injuries without radiographic abnormality
SCJ *see* sternoclavicular joint
second opinions 7–8, 176
septic arthritis 7, 165–6
shaft fractures 14
shear force fractures 161
shoulders 30–7
  ABCs systematic assessment 30–2, 37
  anatomy 30
  injuries 32–7
sigmoid cancer 125
sigmoid volvulus 128, 147
SIJ *see* sacroiliac joints
simple fluids 138
sinuses 91–2
Skier's thumb 17
skull X ray (SXR) 1, 6–7, 71, 167
skyline views 50
slipped upper femoral epiphysis (SUFE) 164–6
small bowel dilatation 127–8
Smith's fracture 18
soft tissues 7, 9
  abdomen 134
  ankles and feet 62, 70
  cervical spine 99, 100–2
  chest 116
  elbows 22, 24–6, 28
  emergency ultrasound 157–8
  face 91–2
  hands and wrists 14, 21
  head 72
  knees 50
  major trauma 175–6
  pelvis and hips 40, 43–5, 48
  shoulders 32, 37
  thoracic and lumbar spine 108–10
spinal cord injuries without radiographic abnormality (SCIWORA) 93
spiral fractures 167
sprains 62
SSSC *see* superior shoulder suspensory complex
sternoclavicular joints (SCJ) 30, 34–6, 117
stress fractures
  ankles and feet 66, 70
  knees 54–5
stroke 78–80
subarachnoid haemorrhage (SAH) 82–3
subdural haematoma 76
subhepatic air 129
subluxations
  ankles and feet 62, 64–5, 67
  cervical spine 95–6
  hands and wrists 16
SUFE *see* slipped upper femoral epiphysis
superior shoulder suspensory complex (SSSC) 36
supracondylar fractures 26, 51–2
surgical emphysema 115, 116
SXR *see* skull X ray

talar dome 61–2, 64, 66
talar neck fractures 64, 66
tarsometatarsal joints 66
TB *see* tuberculosis
teardrop fractures 97–8
teeth 126
tendons 14–15, 49
TFCC *see* triangular fibrocartilage complex
thoracic spine 104–10
  ABCs systematic assessment 108–10
  anatomy 104–6
  imaging considerations 107
  injury classification 110
  injury mechanisms 106–7
three column model 110
Thurston–Holland fragment 161
tibial plateau fractures 53–4
tibial stress fractures 54–5
time to peak (TTP) 80–1
toddler's fracture 166–7
Torus fractures 17, 160, 162
transscaphoid perilunate dislocations 21
transverse fractures 162–3
traumatic aortic injury 119–20
triangular fibrocartilage complex (TFCC) 17–18
trimalleolar fractures 63
triplane fractures 63, 65
triquetral fractures 19–20
trough lines 34
TTP *see* time to peak
tuberculosis (TB) 144–5
tuberosity fractures 32, 36
tubo-ovarian abscesses 150–1
tunnel views 50, 54

ulcerative colitis 143
ulnar injuries 17–18, 29
ultrasound (US)
  abdomen 123, 130, 132–3, 150
  ankles and feet 60
  chest 112
  emergency radiology 150
  emergency ultrasound 152–8
  hands and wrists 17
  major trauma 172–3
  paediatric patients 165–6
  pelvis and hips 45
Unicopula sign 129
upper third facial fractures 91
urinary tract infection (UTI) 169
urolithiasis 147–9
UTI *see* urinary tract infection

V/Q scan *see* ventilation–perfusion scintigraphy
vasogenic oedema 73–5

venous catheters 114
ventilation 172–3
ventilation–perfusion scintigraphy (V/Q scan) 122
vertical compression injuries 42
vertical shear (VS) injuries 42–3
viral lung infections 168–9
volar plate avulsion 14–15
volvulus 128, 147
VS *see* vertical shear

wrists
  ABCs systematic assessment 11–14, 21
  anatomy 11
  injuries 17–21
  paediatric patients 160

Y views 33
Young's classification 41

zygomatic complex fractures 89

CURRENT TITLES

ABC of Sexually Transmitted Infections

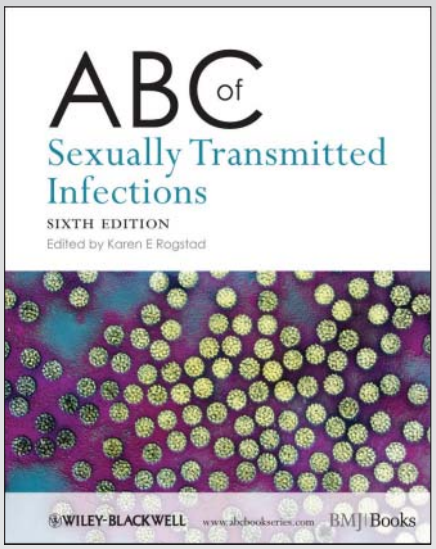
6TH EDITION

Karen E. Rogstad
Sheffield Teaching Hospitals NHS Foundation Trust, Sheffield

With sexually transmitted infections (STIs) a major cause of morbidity and mortality throughout the world, the new edition of *ABC of Sexually Transmitted Infections* is a much-needed introduction and reference guide. This sixth edition:

- Includes the latest guidance on the prevalence, prevention and treatment of STIs, screening programmes and new testing methods
- Features new chapters on service modernization and new care providers, high risk and special needs groups, systemic manifestations, and sexually transmitted infections in resource-poor settings
- Covers contraception in depth and reflects the increasing integration of STI and contraceptive services
- Is ideal for those providing community based STI diagnosis and management such as GPs, primary care physicians, pharmacists and contraceptive service providers. Those in the voluntary sector, junior doctors, medical students, and nurses working in community or specialist services will also find it a valuable resource

APRIL 2011 | 9781405198165 | 168 PAGES | £26.95/US$42.95/€34.90/AU$52.95



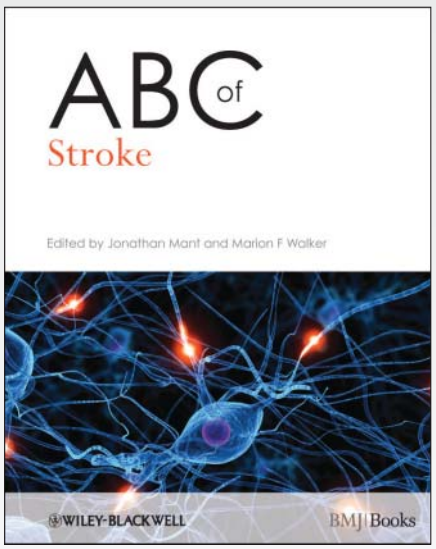
ABC of Stroke

Jonathan Mant & Marion F. Walker
UK Stroke Research Network and Addenbrooke's Hospital, University of Cambridge; UK Stroke Research Network and University of Nottingham

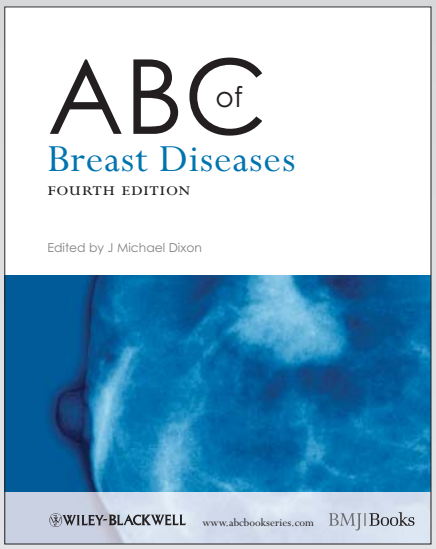
Stroke is the most common cause of adult disability and is of increasing importance within ageing populations. This practical guide to stroke:

- Covers the entire patient journey, from prevention through to long-term support
- Includes primary prevention and management of risk factors for stroke and secondary prevention including pharmaceutical, lifestyle and surgical intervention
- Addresses the general principles of stroke rehabilitation as well as mobility, communication and psychological problems, stroke in younger people and long-term support for stroke survivors and their carers
- Is invaluable to all aspects of stroke for health care professionals and is of particular relevance to GPs, junior doctors, nurses and therapists working with stroke patients and their careers

MARCH 2011 | 9781405167901 | 72 PAGES | £20.95/US$32.95/€26.90/AU$39.95



NEW TITLES



ABC of Breast Diseases

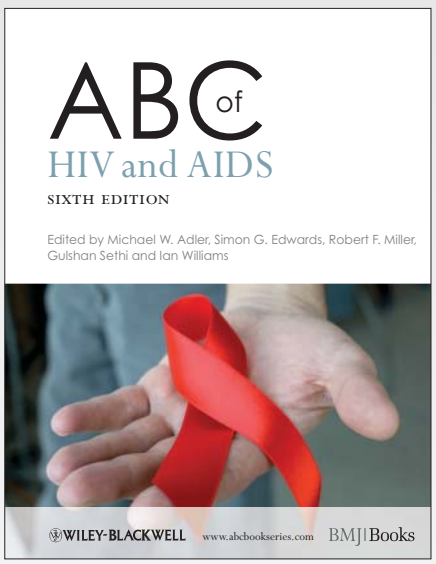
4TH EDITION

J. Michael Dixon
Western General Hospital, Edinburgh, UK

Breast diseases are common and often encountered by health professionals in primary care. While the incidence of breast cancer is increasing, earlier detection and improved treatments are helping to reduce breast cancer mortality. The *ABC of Breast Diseases, 4th Edition*:

- Provides comprehensive guidance to the assessment of symptoms, how to manage common breast conditions and guidelines on referral
- Covers congenital problems, breast infection and mastalgia, before addressing the epidemiology, prevention, screening and diagnosis of breast cancer and outlines the treatment and management options for breast cancer within different groups
- Includes new chapters on the genetics, prevention, management of high risk women and the psychological aspects of breast diseases
- Is ideal for GPs, family physicians, practice nurses and breast care nurses as well as for surgeons and oncologists both in training and recently qualified as well as medical students

AUGUST 2012 | 9781444337969 | 168 PAGES | £27.99/US$46.95/€35.90/AU$52.95



ABC of HIV and AIDS

6TH EDITION

Michael W. Adler, Simon G. Edwards, Robert F. Miller, Gulshan Sethi & Ian Williams
University College London Medical School; Mortimer Market Centre, London; University College London; St Thomas' Hospital, London Medical School; University College London Medical School

Since the previous edition, big advances have been made in treatment, knowledge of the disease and epidemiology. The problem of AIDS in developing countries has become a major political and humanitarian issue.

- Edited by the Director of the Department for Sexually Transmitted Diseases, *ABC of HIV and AIDS, 6th Edition* is an authoritative guide to the epidemiology, incidence, and most up to date management of HIV and AIDS
- Reflects the constantly changing knowledge of the disease and its manifestations, new developments in drug and non-drug management, sociological and political issues
- Includes 6 new chapters on conditions associated with AIDS and further concentration on the community effects of the disease, and the situation of women with AIDS
- Ideal for all levels of health care workers caring for HIV and AIDS patients

JUNE 2012 | 9781405157001 | 144 PAGES | £24.99/US$49.95/€32.90/AU$47.95

NEW TITLES

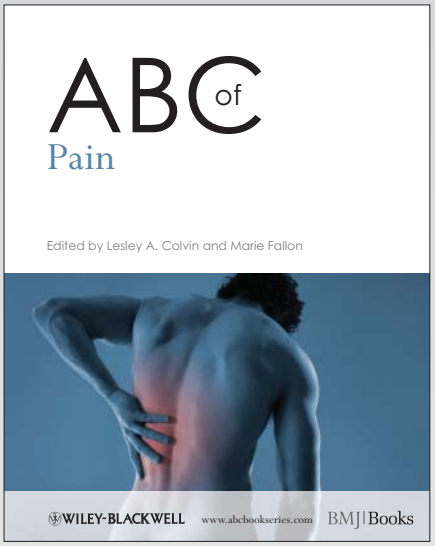
ABC of Pain

Lesley A. Colvin & Marie Fallon
Western General Hospital, Edinburgh; University of Edinburgh

Pain is a common presentation and this brand new title focuses on the pain management issues most often encountered in primary care. *ABC of Pain*:

- Covers all the chronic pain presentations in primary care right through to tertiary and palliative care and includes guidance on pain management in special groups such as pregnancy, children, the elderly and the terminally ill
- Includes new findings on the effectiveness of interventions and the progression to acute pain and appropriate pharmacological management
- Features pain assessment, epidemiology and the evidence base in a truly comprehensive reference
- Provides a global perspective with an international list of expert contributors

JUNE 2012 | 9781405176217 | 128 PAGES | £24.99/US$44.95/€32.90/AU$47.95



ABC of Urology

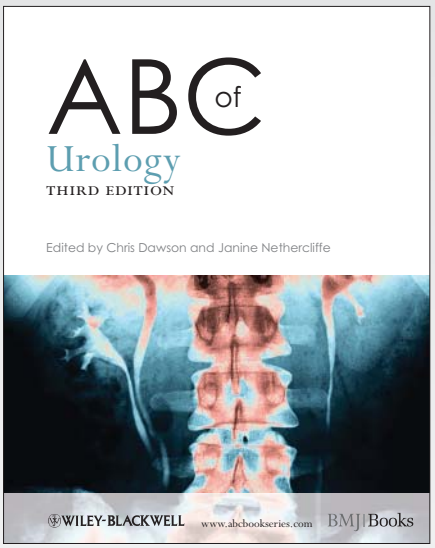
3RD EDITION

Chris Dawson & Janine Nethercliffe
Fitzwilliam Hospital, Peterborough; Edith Cavell Hospital, Peterborough

Urological conditions are common, accounting for up to one third of all surgical admissions to hospital. Outside of hospital care urological problems are a common reason for patients needing to see their GP.

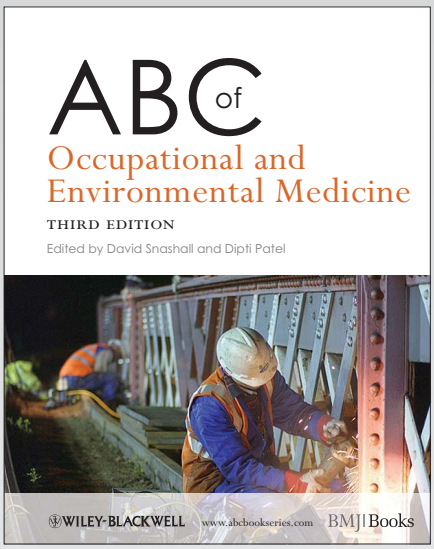
- *ABC of Urology, 3rd Edition* provides a comprehensive overview of urology
- Focuses on the diagnosis and management of the most common urological conditions
- Features 4 additional chapters: improved coverage of renal and testis cancer in separate chapters and new chapters on management of haematuria, laparoscopy, trauma and new urological advances
- Ideal for GPs and trainee GPs, and is useful for junior doctors undergoing surgical training, while medical students and nurses undertaking a urological placement as part of their training programme will find this edition indispensable

MARCH 2012 | 9780470657171 | 88 PAGES | £23.99/US$37.95/€30.90/AU$47.95



For more information on any of these books, please visit the ABC website at **www.abcbookseries.com**

COMING SOON



ABC of Occupational and Environmental Medicine

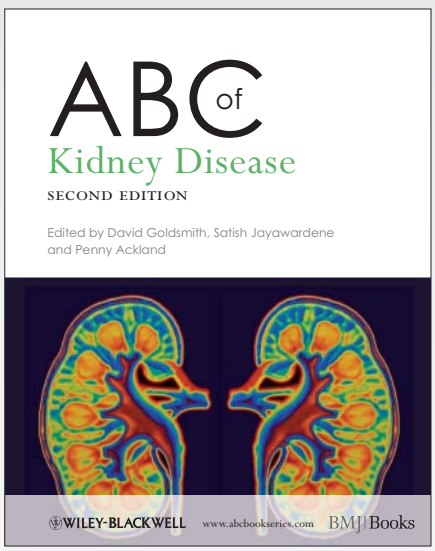
3RD EDITION

David Snashall & Dipti Patel
Guy's & St. Thomas' Hospital, London; Medical Advisory Service for Travellers Abroad (MASTA)

Since the publication of last edition, there have been huge changes in the world of occupational health. It has become firmly a part of international public health, and in Britain there is now a National Director for Work and Health. This fully updated new edition embraces these changes and:

- Provides comprehensive guidance on current occupational and environmental health practice and legislation
- Concentrates on the newer kinds of occupational disease, for example 'RSI', pesticide poisoning and electromagnetic radiation, where exposure and effects are difficult to understand
- Places an emphasis on work, health and well-being, and the public health benefits of work, the value of work, disabled people at work, the aging workforce, and vocational rehabilitation
- Includes chapters on the health effects of climate change and of occupational health and safety in relation to migration and terrorism

NOVEMBER 2012 | 9781444338171 | 168 PAGES | £27.99/US$44.95/€38.90/AU$52.95



ABC of Kidney Disease

2ND EDITION

David Goldsmith, Satish Jayawardene & Penny Ackland
Guy's & St. Thomas' Hospital, London; King's College Hospital, London; Melbourne Grove Medical Practice, London

Nephrology is sometimes considered a complicated and specialized topic and the illustrative ABC format will help GPs quickly and easily assimilate the information needed. *ABC of Kidney Disease, 2nd Edition*:

- Is a practical guide to the most common renal diseases to enable non-renal health care workers to screen, identify, treat and refer renal patients appropriately and to provide the best possible care
- Covers organizational aspects of renal disease management, dialysis and transplantation
- Provides an explanatory glossary of renal terms, guidance on anaemia management and information on drug prescribing and interactions
- Has been fully revised in accordance with new guidelines

OCTOBER 2012 | 9780470672044 | 112 PAGES | £27.99/US$44.95/€35.90/AU$52.95

ALSO AVAILABLE

ABC of Adolescence
Russell Viner
2005 | 9780727915740 | 56 PAGES
£26.99 / US$41.95 / €34.90 / AU$52.95

ABC of Antithrombotic Therapy
Gregory Y. H. Lip & Andrew D. Blann
2003 | 9780727917713 | 67 PAGES
£26.50 / US$41.95 / €34.90 / AU$52.95

ABC of Arterial and Venous Disease, 2nd Edition
Richard Donnelly & Nick J. M. London
2009 | 9781405178891 | 120 PAGES
£31.50 / US$54.95 / €40.90 / AU$59.95

ABC of Asthma, 6th Edition
John Rees, Dipak Kanabar & Shriti Pattani
2009 | 9781405185967 | 104 PAGES
£26.99 / US$41.95 / €34.90 / AU$52.95

ABC of Burns
Shehan Hettiaratchy, Remo Papini & Peter Dziewulski
2004 | 9780727917874 | 56 PAGES
£26.50 / US$41.95 / €34.90 / AU$52.95

ABC of Child Protection, 4th Edition
Roy Meadow, Jacqueline Mok & Donna Rosenberg
2007 | 9780727918178 | 120 PAGES
£35.50 / US$59.95 / €45.90 / AU$67.95

ABC of Clinical Electrocardiography, 2nd Edition
Francis Morris, William J. Brady & John Camm
2008 | 9781405170642 | 112 PAGES
£34.50 / US$57.95 / €44.90 / AU$67.95

ABC of Clinical Genetics, 3rd Edition
Helen M. Kingston
2002 | 9780727916273 | 120 PAGES
£34.50 / US$57.95 / €44.90 / AU$67.95

ABC of Clinical Haematology, 3rd Edition
Drew Provan
2007 | 9781405153539 | 112 PAGES
£34.50 / US$59.95 / €44.90 / AU$67.95

ABC of Clinical Leadership
Tim Swanwick & Judy McKimm
2010 | 9781405198172 | 88 PAGES
£20.95 / US$32.95 / €26.90 / AU$39.95

ABC of Complementary Medicine, 2nd Edition
Catherine Zollman, Andrew J. Vickers & Janet Richardson
2008 | 9781405136570 | 64 PAGES
£28.95 / US$47.95 / €37.90 / AU$54.95

ABC of COPD, 2nd Edition
Graeme P. Currie
2010 | 9781444333886 | 88 PAGES
£23.95 / US$37.95 / €30.90 / AU$47.95

ABC of Dermatology, 5th Edition
Paul K. Buxton & Rachael Morris-Jones
2009 | 9781405170659 | 224 PAGES
£34.50 / US$58.95 / €44.90 / AU$67.95

ABC of Diabetes, 6th Edition
Tim Holt & Sudhesh Kumar
2007 | 9781405177849 | 112 PAGES
£31.50 / US$52.95 / €40.90 / AU$59.95

ABC of Eating Disorders
Jane Morris
2008 | 9780727918437 | 80 PAGES
£26.50 / US$41.95 / €34.90 / AU$52.95

ABC of Emergency Differential Diagnosis
Francis Morris & Alan Fletcher
2009 | 9781405170635 | 96 PAGES
£31.50 / US$55.95 / €40.90 / AU$59.95

ABC of Geriatric Medicine
Nicola Cooper, Kirsty Forrest & Graham Mulley
2009 | 9781405169424 | 88 PAGES
£26.50 / US$44.95 / €34.90 / AU$52.95

ABC of Headache
Anne MacGregor & Alison Frith
2008 | 9781405170666 | 88 PAGES
£23.95 / US$41.95 / €30.90 / AU$47.95

ABC of Heart Failure, 2nd Edition
Russell C. Davis, Michael K. Davis & Gregory Y. H. Lip
2006 | 9780727916440 | 72 PAGES
£26.50 / US$41.95 / €34.90 / AU$52.95

ABC of Imaging in Trauma
Leonard J. King & David C. Wherry
2008 | 9781405183321 | 144 PAGES
£31.50 / US$50.95 / €40.90 / AU$59.95

ABC of Interventional Cardiology, 2nd Edition
Ever D. Grech
2010 | 9781405170673 | 120 PAGES
£25.95 / US$40.95 / €33.90 / AU$49.95

ABC of Learning and Teaching in Medicine, 2nd Edition
Peter Cantillon & Diana Wood
2009 | 9781405185974 | 96 PAGES
£22.99 / US$35.95 / €29.90 / AU$44.95

ABC of Liver, Pancreas and Gall Bladder
Ian Beckingham
1905 | 9780727915313 | 64 PAGES
£24.95 / US$39.95 / €32.90 / AU$47.95

ABC of Lung Cancer
Ian Hunt, Martin M. Muers & Tom Treasure
2009 | 9781405146524 | 64 PAGES
£25.95 / US$41.95 / €33.90 / AU$49.95

ABC of Medical Law
Lorraine Corfield, Ingrid Granne & William Latimer-Sayer
2009 | 9781405176286 | 64 PAGES
£24.95 / US$39.95 / €32.90 / AU$47.95

ABC of Mental Health, 2nd Edition
Teifion Davies & Tom Craig
2009 | 9780727916396 | 128 PAGES
£32.50 / US$52.95 / €41.90 / AU$62.95

ABC of Obesity
Naveed Sattar & Mike Lean
2007 | 9781405136747 | 64 PAGES
£24.99 / US$39.99 / €32.90 / AU$47.95

ABC of One to Seven, 5th Edition
Bernard Valman
2009 | 9781405181051 | 168 PAGES
£32.50 / US$52.95 / €41.90 / AU$62.95

ABC of Palliative Care, 2nd Edition
Marie Fallon & Geoffrey Hanks
2006 | 9781405130790 | 96 PAGES
£30.50 / US$52.95 / €39.90 / AU$57.95

ABC of Patient Safety
John Sandars & Gary Cook
2007 | 9781405156929 | 64 PAGES
£28.50 / US$46.99 / €36.90 / AU$54.95

ABC of Practical Procedures
Tim Nutbeam & Ron Daniels
2009 | 9781405185950 | 144 PAGES
£31.50 / US$50.95 / €40.90 / AU$59.95

ABC of Preterm Birth
William McGuire & Peter Fowlie
2005 | 9780727917638 | 56 PAGES
£26.50 / US$41.95 / €34.90 / AU$52.95

ABC of Psychological Medicine
Richard Mayou, Michael Sharpe & Alan Carson
2003 | 9780727915566 | 72 PAGES
£26.99 / US$41.95 / €34.90 / AU$52.95

ABC of Rheumatology, 4th Edition
Ade Adebajo
2009 | 9781405170680 | 192 PAGES
£31.95 / US$50.95 / €41.90 / AU$62.95

ABC of Sepsis
Ron Daniels & Tim Nutbeam
2009 | 9781405181945 | 104 PAGES
£31.50 / US$52.95 / €40.90 / AU$59.95

ABC of Sexual Health, 2nd Edition
John Tomlinson
2004 | 9780727917591 | 96 PAGES
£31.50 / US$52.95 / €40.90 / AU$59.95

ABC of Skin Cancer
Sajjad Rajpar & Jerry Marsden
2008 | 9781405162197 | 80 PAGES
£26.50 / US$47.95 / €34.90 / AU$52.95

ABC of Spinal Disorders
Andrew Clarke, Alwyn Jones & Michael O'Malley
2009 | 9781405170697 | 72 PAGES
£24.95 / US$39.95 / €32.90 / AU$47.95

ABC of Sports and Exercise Medicine, 3rd Edition
Gregory Whyte, Mark Harries & Clyde Williams
2005 | 9780727918130 | 136 PAGES
£34.95 / US$62.95 / €44.90 / AU$67.95

ABC of Subfertility
Peter Braude & Alison Taylor
2005 | 9780727915344 | 64 PAGES
£24.95 / US$39.95 / €32.90 / AU$47.95

ABC of the First Year, 6th Edition
Bernard Valman & Roslyn Thomas
2009 | 9781405180375 | 136 PAGES
£31.50 / US$55.95 / €40.90 / AU$59.95

ABC of the Upper Gastrointestinal Tract
Robert Logan, Adam Harris & J. J. Misiewicz
2002 | 9780727912664 | 54 PAGES
£26.50 / US$41.95 / €34.90 / AU$52.95

ABC of Transfusion, 4th Edition
Marcela Contreras
2009 | 9781405156462 | 128 PAGES
£31.50 / US$55.95 / €40.90 / AU$59.95

ABC of Tubes, Drains, Lines and Frames
Adam Brooks, Peter F. Mahoney & Brian Rowlands
2008 | 9781405160148 | 88 PAGES
£26.50 / US$41.95 / €34.90 / AU$52.95